Investigating a role for heterotrimeric G-proteins in activating TGFβ in Asthma

Robert James Middlewick

Division of Respiratory Medicine

Thesis submitted for a degree of Doctor of Philosophy
July 2020

Abstract

Asthma is a chronic inflammatory disease of the airways, affecting 5.4 million people in the UK. Asthma pathology is characterised by airway hyper-responsiveness, bronchoconstriction, and airway remodelling. Airway remodelling is particularly prominent in severe asthma and describes structural changes within the airways including, ASM hyperplasia and hypertrophy, subepithelial fibrosis, mucus gland hyperplasia, and angiogenesis. The pleiotropic cytokine TGFβ is plays a central role in the development of all airway remodelling characteristics and is found to have increased activation in asthmatics versus non-asthmatics. Previous studies in ASM cells has shown that the integrin αvβ5 and the actin cytoskeleton is essential for TGFβ activation. Moreover, the heterotrimeric G-proteins $G_{\alpha q/11}$ have been implicated in TGFβ activation in murine embryonic fibroblasts and epithelial cells. However, the class of heterotrimeric G-protein required for TGFβ activation in ASM has not been established. The hypothesis of this thesis is that the heterotrimeric G-proteins $G_{\alpha q/11}$ are required for TGFβ activation in ASM cells.

The methodology of this thesis uses the GPCR agonist lysophosphatidic acid (LPA) and cyclical mechanical stretch as a stimulus to activate TGFβ *in vitro*. TGFβ activation has been primarily measured through western blotting of phospho-Smad2 (pSmad2). Inhibiting heterotrimeric G-protein activation has been carried out using a small molecule inhibitor of $G_{\alpha q/11/14}$, YM-254890, and siRNA.

The results in this thesis demonstrate, for the first time, that $G_{\alpha q/11}$ are not required for either LPA- or stretch-induced TGFβ activation in ASM cells. The serine/threonine kinase, Rho kinase (ROCKI/II), has been shown as central to LPA- and stretch-induced TGFβ activation in ASM cells. Moreover, activation of the small G-protein RhoA has

been shown for the first time to be regulated $G_{\alpha 12/13}$, but not $G_{\alpha q/11}$, in response to LPA in ASM cells. However, inhibition $G_{\alpha 12/13}$ by siRNA had no effect on LPA-induced pSmad2, therefore implying that LPA-induced TGFβ activation may require ROCKI/II, but not RhoA. Finally, inhibition of both $G_{\alpha q/11}$ and $G_{\alpha 12}$ did not reduce LPA-induced TGFβ activation, however, the role of $G_{\alpha 13}$ cannot be discounted due to incomplete knockdown.

Collectively, these data disprove the hypothesis that the heterotrimeric G-proteins $G_{\alpha q/11}$ are required for TGFβ activation in ASM cells. Moreover, they show that LPA- and stretch-induced TGFβ activation in ASM cells does not require either $G_{\alpha q/11}$ or $G_{\alpha 12}$ signalling. The fascinating possibility that ROCKI/II, but not RhoA, is required for LPA-induced TGFβ in ASM cells requires further investigation. If this hypothesis proves to be true it could unlock new opportunities for drug development to reduce airway remodelling in severe asthma.

Acknowledgements

I would like to thank AsthmaUK for funding my PhD scholarship and hope that my research has been a valuable contribution to the field.

A massive thank you to Stephanie who has made the past 4 years a joy and, without whom, I may well have not reached the end. Our frequent visits to the many pubs and microbreweries of Nottingham certainly made the challenging times easier to forget. Not to mention the epic holidays we planned around conferences in California, Vancouver, and Lisbon.

I will be eternally grateful for having such supportive parents who inspire me to be best me. Your wisdom and perspective is always helpful in the face of challenging situations. And a regular talking therapy with Mum about our respective PhD gripes has been a frequent occurrence. I feel very lucky to have you both!

A big thank you to my supervisor Amanda Tatler for teaching me in the lab and supporting my ideas, whilst keeping my research on track. I greatly appreciate you proof-reading my thesis – not the most exciting task! I would also like to thank Gisli for funding conference visits, which have been a unique opportunity and contributed to huge personal growth.

Throughout my PhD I have ensured that my experience was enriched with more than just research. I have enjoyed some fantastic opportunities to compete in many cross country events with the athletics club and learn to climb with the climbing club. These experiences are only as good as the people whom I've shared them with, so thanks to all of you.

Conferences

Robert J. Middlewick, Amanda L. Tatler and Gisli Jenkins.

Investigating the role of the G-proteins GNAQ/11 in contraction-induced airway smooth muscle in asthma

Accepted for American thoracic society 2018 (poster), San Diego, CA, USA.

Robert J. Middlewick, Dominick Shaw, Amanda L. Tatler, and Gisli Jenkins.

'Investigating the role of the g-proteins G_q and G_{11} in airway smooth muscle cell TGFβ activation in asthma'

Accepted for British Association for Lung Research 2018 (prize abstract presentation), Birmingham, UK. PhD prize abstract travel award, £100.

Robert J. Middlewick, Dominick Shaw, Amanda L. Tatler, and Gisli Jenkins.

'Investigating the role of the g-proteins G_q and G_{11} in airway smooth muscle cell TGFβ activation in asthma'

Accepted for European Respiratory Society Lung 2019 (poster), Estoril, Portugal. Young Investigator Travel Award €500.

Robert J. Middlewick, Dominick Shaw, Gisli Jenkins, and Amanda L. Tatler.

'Investigating the role of the G-proteins G_q and G_{11} in airway smooth muscle cell TGFβ in Asthma'

Young Investigator Meeting 2019 (presentation), Sydney, NSW, Australia –School of Medicine Travel Award, £450.

Publications

Jopeth Ramis, **Robert Middlewick**, Francesco Pappalardo, Jennifer T Cairns, Iain D Stewart, Alison E John, Shams-un Nisa Naveed, Ramaswamy Krishnan, Suzanne Miller, Dominick E Shaw, Christopher Brightling, Dean Sheppard, Xiaozhu Huang, Lee Buttery, Felicity Rose, Gisli Jenkins, Simon R Johnson, Amanda L Tatler

'LOXL2 Mediates Airway Smooth Muscle Cells Extracellular Matrix Stiffness and Drives Asthmatic Airway Remodelling'

Under review in the Journal of Allergy and Clinical Immunology.

Robert J. Middlewick, Dominick Shaw, Gisli Jenkins, and Amanda L. Tatler.

'Investigating the role of the G-proteins G_q and G_{11} in airway smooth muscle cell TGFβ in Asthma'

Manuscript in preparation.

Abbreviations

AC	Adenylyl cyclase
AHR	Airway hyper-responsiveness
ALK1	Activin receptor-like kinase 1
ALK5	Activin receptor-like kinase 5
ASM	Airway smooth muscle
BAL	Bronchoalveolar lavage
Ca^{2+}	Calcium
cAMP	Cyclic adenosine monophosphate
DAG	Diacylglyceral
DAMP	Damage-associated molecular pattern
DMSO	Dimethyl sulfoxide
EAR	Early asthmatic response
ECM	Extracellular matrix
EGFR	Epidermal growth factor
FcεRI	High-affinity IgE receptor
FEV_1	Forced expiratory volume 1
GAP	GTPase-activating protein
GDP	Guanine diphosphate
GEF	Guanine nucleotide exchange factor
GM-CSF	Granulocyte-macrophage colony-stimulating factor
GPCR	G-protein coupled receptor
GTP	Guanine triphosphate
HDM	House dust mite
IgE	Immunoglobulin E
IgG	Immunoglobulin G
IL-13	Interleukin-13
IL-17	Interleukin-17
IL-2	Interleukin-2
IL-4	Interleukin-4
IL-5	Interleukin-5
IL-6	Interleukin-6
IL-8	Interleukin-8
IP_3	Inositol 1, 4, 5-triphosphate
LAP	Latent associated peptide
LAR	Late asthmatic response
LARG	Leukemia-associated RhoGEF
LLC	Large latent complex
LPA	Lysophosphatidic acid
LTBP	Latent TGFβ binding protein
MLC	Myosin light chain
MLCK	Myosin light chain kinase
MLCP	Myosin light chain phosphatase
MMP	Matrix metallopeptidase 1
OVA	Ovalbumin
PAI1	Plasminogen activator inhibitor-1
PAMP	Pathogen-associated molecular pattern
PAR1	Protease activated receptor 1
PDGF	Platelet derived growth factor

PIP_2	Phosphatidylinositol-4,5-bisphosphate
PKA	Protein kinase A
PKC	Protein kinase C
pSmad2	Phospho-Smad2
ROCKI/II	Rho-associated protein kinase I/II
S1P	Sphingosine-1-phosphate
T_c	T-cytotoxic cell
TGFβ	Transforming growth factor-beta
T_H	T-helper cell
T_H1	T-helper 1
T_H2	T-helper 2
TIMPS	Tissue inhibitors of metallopeptidases
TNFα	Tumour necrosis factor alpha
T_{reg}	T-regulatory cell
tSmad	Total Smad2/3
VCAM-1	Vascular cell adhesion molecule 1
β_2-AR	β_2-adrenergic receptor

1 Chapter 1: Introduction

1.1 Asthma

Asthma is a chronic inflammatory disease of the airways, resulting in 185 people to be admitted to hospital every day in the UK because of exacerbation (2). Asthma pathology is characterised by airway hyper-responsiveness, bronchoconstriction, and airway remodelling. There are 5.4 million people in the UK who suffer from asthma with 1.1 million children and 4.3 million adults (2). Asthma is more prevalent in developed countries, however the gap between countries is narrowing as it plateaus in high income countries and rises in low and middle income countries due to lifestyle and environmental changes such as a rise in pollution (3). Worldwide there are an estimated 300 million people with asthma and this number is expected to rise by more than 100 million by 2025. In the UK 1 in 12 adults and 1 in 11 children suffer from asthma equating to a total of 5.5 million individuals (AsthmaUK). There are presently no cures for the disease, however a combination of an inhaled short- or long-β_2-adrenergic agonist and corticosteroid can control the disease in many patients. Approximately 10% of patients with asthma have a severe form of the disease that is refractory to corticosteroid treatment, resulting in frequent and uncontrolled exacerbation that lead to a long term reduction in lung function due to narrowing of the airway.

Classically asthma has been characterised into two distinct types. Allergic (atopic) asthma occurs due to sensitisation to inhaled allergens such as house dust mite (HDM), animal dander, pollen and fungal spores, and can be detected by a positive skin prick test or IgE reactivity to these allergens (4). Atopic asthma is the predominant form seen in children and accounts for roughly half of adults with asthma. Non-allergic (non-atopic) asthma is not

triggered by a specific allergen and has no obvious involvement with the adaptive immune system (4). These patients are often resistant to steroid treatment and often suffer from more severe symptoms. Defining asthma as atopic or non-atopic is now seen as an oversimplification and it has been accepted that many factors contribute to varying degrees, resulting in a very heterogeneous disease where subsets that share commonalities are referred to as endotypes (5).

1.1.1 Sensitisation

Airway hyper responsiveness to inhaled allergens and pollutants present in the atmosphere is a key hallmark of asthma, particularly atopic asthma. Epithelial cells line the airway and are the first cells to come into contact with inhaled allergens. Dendritic cells migrate to the epithelial cell surface where they phagocytose the antigen. The antigen is broken down into short peptide fragments and presented on the dendritic cell surface as an antigen-major histocompatibility complex (MHC). The antigen-MHC is presented to naïve T helper cells (T_h), also known as $CD4^+$ cells, which differentiate into Type 1 helper (T_h1) or Type 2 helper (T_h2) cells. Increased IL-4 in the lung of asthmatic patients tips the balance of T_h cell differentiation toward T_h2 cells (6). T_h2 effector cells include B lymphocytes which produce antigen-specific IgE antibodies that bind to the cell surface of mast cells, basophils, B lymphocytes, and eosinophils. This process of sensitisation results in the presence of immune cells that become activated, irrationally, in response to inhaled allergens.

1.1.2 Early and Late Asthmatic response

Allergens that an asthma patient has been sensitised to can trigger an 'exacerbation' when inhaled, characterised by airway obstruction and a drop in forced expiratory volume in 1 second (FEV_1). The response to an inhaled allergen can be broken into an early asthmatic response (EAR) and a late asthmatic response (LAR).

Inhaled allergens bind to, and cross-link, IgE on the surface of mast cells and basophils. Subsequent degranulation of mast cells releases intracellular stores of histamine, tryptase, chemotactic factors, and activates signalling pathways that synthesise signalling lipids such as prostaglandins (PG). These mediators are responsible for initiating constriction of the bronchial airways (bronchoconstriction), stimulating mucus secretion, increasing permeability and dilation of the pulmonary blood vessels. EAR develops within 10-15 minutes of allergen inhalation, peaks at 30 minutes and resolves by 1-3 hours (7).

The LAR is characterised as an eosinophilic inflammatory response that typically occurs 4 to 8 hours after the initial allergen exposure and results in bronchoconstriction. LAR is the result of an influx of active eosinophils and CD4+ T_H cells (8, 9). Moreover, transfer of T_H cells from ovalbumin sensitised mice, a model of asthma, into control mice elicited a LAR response (10).

1.2 Airway Inflammation

1.2.1 Mast Cells

Mast cells are a type of granulocyte originating from hematopoietic stem and are typically found in tissues exposed to the external environment. They play an important role in the inflammatory response seen in asthma. Within mast cells are granules containing heparin, proteases including chymase and tryptase, histamine, IL-4, IL-5, IL-6, and tumour necrosis factor (TNFα) (11, 12). They are stimulated by allergens, physical injury and pathogens by recognising damage-associated molecular patterns (DAMPS) and pathogen associated molecular patterns (PAMPS) respectively. In healthy patients mast cells are typically found surrounding blood vessels, however in asthmatic patients they migrate into airway structures. In the asthmatic airway mast cells are increased in the airway epithelium and mucous glands, but are predominantly found in airway smooth muscle (13). Bronchial biopsy of patients with asthma, eosinophilic bronchitis, and healthy controls found mast cells to be significantly higher in the smooth muscle of asthma patients than either control group (14). Moreover, an increase in mast cells is seen in the distal airways in histological sections from asthma patients versus healthy controls, with the greatest increase found in smooth muscle and mucous glands (15). Coculture of mast cells with ASM cells has been shown to increase TGFβ1 expression in ASM, caused by release of tryptase. This results in increased α-smooth muscle actin (αSMA) and cell contractility and has been suggested to switch ASM cells to a more contractile phenotype (16). Further, biopsy of the asthmatic bronchial mucosa shows αSMA staining intensity to correlate to the number of mast cells within or adjacent to smooth muscle bundles (16).

Mice that have mast cells genetically knocked out do not exhibit LAR. However, transfer of mast cells into these mice or intranasal administration of TNFα restores the LAR (17). Mast cells express the high affinity IgE receptor FcεRI. Upon binding of IgE, degranulation of mast cells occurs rapidly and releases histamine, serotonin, proteoglycans and proteases such as tryptase. This contributes to the EAR. Synthesis of cytokines and chemokines occurs which are released hours after the initial IgE binding, resulting in the LAR (18). Moreover, a humanized anti-IgE antibody, omalizumab, administered to patients with moderate-to-severe or severe asthma, attenuated inflammatory markers including IL-2, IL-4, IL5 and IL-13 (19).

In summary, mast cells migrate to the airway smooth muscle where they play a key role in mediating both the early and late asthmatic response in allergic asthma.

1.2.2 T-lymphocytes

T cells are a type of lymphocyte that have a T cell receptor on their surface and mature in the thymus. They can be divided in four subgroups; cytotoxic T cells (T_C), helper T cells (T_H), memory T cells, and regulatory T cells (T_{reg}). T_c cells are also known as CD8+ due to the presence of this glycoprotein on their cell surface. They bind to infected or damaged cells to induce apoptosis via antigen associated to MHC class I that is expressed on all nucleated cells. T_H cells are also known as CD4+ T cells and are involved in the adaptive immune system. They play a central role in activation of T_C cells and in B cell antibody class switching. T_H cell activation occurs upon antigen presentation by MHC class II molecules present on the surface of antigen presenting cells (APCs), such as dendritic cells, macrophages, and B cells. Once activated, naïve T_H cells begin to

proliferate by releasing IL-2 and will polarise into either T_H1 or T_H2 cells. The cytokine environment determines the polarisation of a T_H cell. It is accepted that IL-4 induces T_H2 polarisation once a threshold has been reached (20). In contrast, T_H1 polarisation is induced by IL-12 and IL-18, which are predominantly released by dendritic cells and macrophages (21).

There are several subtypes of T_H cells grouped by the variety of cytokines and chemokines secreted. T_H1 cells are involved in cell mediated immunity and secretes the cytokines interferon-γ (IFN-γ), interleukin-2 (IL-2), and tumour necrosis factor-β (TNF-β) (22). On the other hand, T_H2 secrete interleukin-4 (IL-4), interleukin-5 (IL-5), interleukin-6 (IL-6), interleukin-9 (IL-9), interleukin-10 (IL-10), and interleukin-13 (IL-) (23, 24). GM-CSF and tumour necrosis factor-α (TNF-α) are cytokines secreted by both T_H1 and T_H2 cells. Asthma is considered to be a T_H2 disease. Genetic depletion of CD4+ T cells ablates key asthma features, in contrast transfer of T_H2 cells from OVA sensitised mice in null mice resulted in induction of asthma features (25, 26).

Memory T cells are long lasting antigen specific cells that can circulate throughout the body or reside in tissues that are exposed to the environment and are able respond rapidly to repeated exposure of antigens (27). T_{reg} cells, also known as suppressor T cells, can develop in the thymus or be induced peripherally. Briefly, in the lung T_{reg} cells function to suppress immune response to antigens that may be continually inhaled and will be discussed in more detail later.

1.2.3 Eosinophilic Asthma

'Asthma' is a blanket term that describes an inflammatory disease of the airway that causes symptoms such as shortness of breath, airflow obstruction, and wheezing. Asthma can be clustered into 5

phenotypic groups based on clinical characteristics (28). Eosinophilic asthma is viewed as a T_H2 disorder, defined when induced sputum eosinophil count is greater than 2% of the total cell count (29). Eosinophils contain an array of pre-synthesised mediators in secondary granules that are thought to be implicated in asthma pathogenesis. Many cytotoxic mediators are contained within secondary granules, including eosinophil peroxidase (EPO), major basic protein (MBP), and eosinophil cationic protein (ECP), which are able to puncture the cell membrane, ultimately inducing cell lysis (30). Eosinophils are also a source of many pro-inflammatory cytokines including IL-4, IL-5, IL-6, IL-8, GM-CSF, and TNFα (31). Eosinophils stimulated with IFN-γ were able to induce apoptosis in cultured epithelial cells, an effect that was inhibited by pre-treatment with an anti-TNFα antibody (32). The release of mediators from eosinophils causes damage to the epithelium, a key feature of airway remodelling in asthma that will be discussed in more detail later. Moreover, mast cells are able to be reactivated, and release histamine, by a combination of MBP and eosinophil sonicate, suggesting a role for eosinophils contributing to the LAR (33).

T_H2 cells play an essential role in recruitment of eosinophils to the lung. Eosinophils migrate in response to cytokines, chemokines, and adhesion molecules. The cytokines IL-4 and IL-5 are released by T_H2 cells and are involved in IgE production and allergic sensitisation, and eosinophil survival respectively (23). IL-5 is an eosinophil chemoattractant. Levels of IL-5 have been correlated with eosinophil count in the BAL of both topic and atopic asthma (34). Vascular cell adhesion molecule-1 (VCAM-1) is an adhesion molecule that is essential for eosinophil tethering and rolling during recruitment to the lung. CD4+ deficient mice subjected to OVA sensitisation and challenge are protected against lung eosinophilia because of their

inability to upregulate VCAM-1, and therefore prevent eosinophil migration (35). Moreover, addition of recombinant IL-13 to murine airways induces AHR and influx of eosinophils in BAL (24). IL-13, released by T_H2 cells, binds to the IL-4 receptor. Both ablation of IL-13 and blockade of the IL-4 receptor reverse AHR in a murine model of allergic asthma, however this effect was independent of airway eosinophilia (24). Goblet cell metaplasia is a process where epithelial cells transdifferentiate to produce mucus that blocks the airway lumen. The T_H2 cytokines IL-4 and IL-13 are primarily responsible for goblet cell metaplasia and will be discussed in more detail later (23, 24, 36).

A study of 42 patients with mild to moderate asthma found two distinct subtypes of asthma, classified as T_H2^{hi} and T_H2^{lo}. These groups were differentiated by expression of IL-5 and IL-33, which was significantly higher in T_H2^{hi} versus T_H2^{lo} groups (36). The T_H2^{hi} group had a significantly higher eosinophil count in both peripheral blood and BAL. Moreover, airway hyper-responsiveness in T_H2^{hi} group was significantly worst.

Clinical trials have been carried out using drugs designed to block T_H2 cytokine signalling. Dupilumab is an inhibitor of the IL-4 receptor, thus blocking IL-4 and IL-13 signalling. Patients with moderate to severe asthma that presented with increased blood eosinophil count were treated with dupilumab. Treatment resulted in an improvement in lung function and reduced exacerbation frequency (37). IL-5 has been targeted directly by the development of mepolizumab. Asthma patients presenting with frequent exacerbations and eosinophilic inflammation had a significantly reduced exacerbation rate and increased lung function after treatment with mepolizumab (38, 39). The national institute for health and care excellence (NICE) have approved the use of

mepolizumab as an add-on therapy for patients with severe refractory eosinophilic asthma.

In summary, T_H2 cell polarisation is required for the recruitment of eosinophils to the airways in asthma. Eosinophil activation may play a role in the LAR, and recent clinical trials targeting T_H2 cytokine signalling have been successful in reducing the frequency of exacerbation in patients with eosinophilic asthma.

1.2.4 Neutrophilic Asthma

A subset of asthma patients have a high neutrophil count and are described as having 'neutrophilic asthma'. Reversible airflow obstruction in this subset of asthma is often incomplete and associated with corticosteroid resistance. Neutrophilic asthma has been shown to have a 30% prevalence in studies analysing bronchial biopsies and induced sputum samples (40, 41).

Immunostaining of bronchial biopsies have identified markers of the IL-17 pathway to be present in neutrophilic asthma. A 3-fold increase in IL-17F+ positive cells was observed in patients with neutrophil-high asthma (40). Increased expression of IL-17A, IL-17F, IL-22, and IL-23 have also been identified within the neutrophilic asthma subset (40). IL-17 is increased in the airways of severe asthmatics and has been correlated to neutrophil count and airway hyper-responsiveness (42). Moreover, treatment of murine tracheal rings and lung slices with IL-17A enhanced smooth muscle contraction. In human tracheal smooth muscle cells this was shown to occur because of an upregulation of ROCKII and increased phosphorylation of myosin light chain kinase (43). IL-17RA or IL-17A deficient mice have significantly reduced neutrophil recruitment to the lung after allergen challenge (44). Further, identification of antigen specific IL-

17 T_H2 in a murine model of asthma showed that there was an increased influx of inflammatory cells, and exacerbated features of asthma, compared to classical T_H2 cells (45). Additionally, adoptive transfer of T_H17, the primary source of IL-17A and IL-17F, into mice subjected to OVA challenge increased recruitment of neutrophils (46).

Phenotypic analysis of adults and children with acute asthma showed that asthma was typically eosinophilic in children and neutrophilic in adults (47). Moreover, patients with neutrophilic asthma also have eosinophils present within the mucosa. This raises the possibility that neutrophilic asthma may arise in patients with progressive severe asthma. A clinical trial has used the anti-IL-17 monoclonal antibody brodalumab, which inhibits both IL-17A and IL-17F, in asthmatics (48). The trial failed with no overall benefit to the asthma cohort, however, this study did not select patients based on the presence of IL-17, but rather on clinical status. These studies identify the IL-17 pathway as a key feature of neutrophilic asthma and is associated with increased airway hyper-responsiveness.

1.3 Airway Remodelling

Airway remodelling broadly describes the structural changes that occur within the small and large airways of asthmatic patients. Common features include epithelial damage, angiogenesis, mucous gland hyperplasia, ASM hypertrophy and hyperplasia, and subepithelial fibrosis. Airway remodelling is associated with an accelerated loss of lung function that is greater in asthmatic patients when compared to healthy patients (49, 50). Moreover, there has been an association of asthma severity with airway remodelling (51). There is a consensus that airway remodelling is a secondary event to inflammation (52). Overexpression mouse models of the T_H2 cytokines IL-4, IL-5, IL-9, and IL-13 result in spontaneous airway inflammation, airway hyper-responsiveness, increased mucus secretion, and airway remodelling (53-56). Cytokines IL-4 and IL-5 play a key role in eosinophil infiltration into the lung and have been discussed in detail above. The effects of IL-9 in the asthmatic lung require the presence of IL-13 (57). However, IL-13 does directly affect structural changes in the lung, including goblet cell metaplasia, by acting directly on epithelial cells (58). The pleiotropic cytokine transforming growth factor-beta (TGFβ) also plays a central role in airway remodelling in asthma. This chapter will discuss the features of airway remodelling, and the mechanistic process that drives them in asthma.

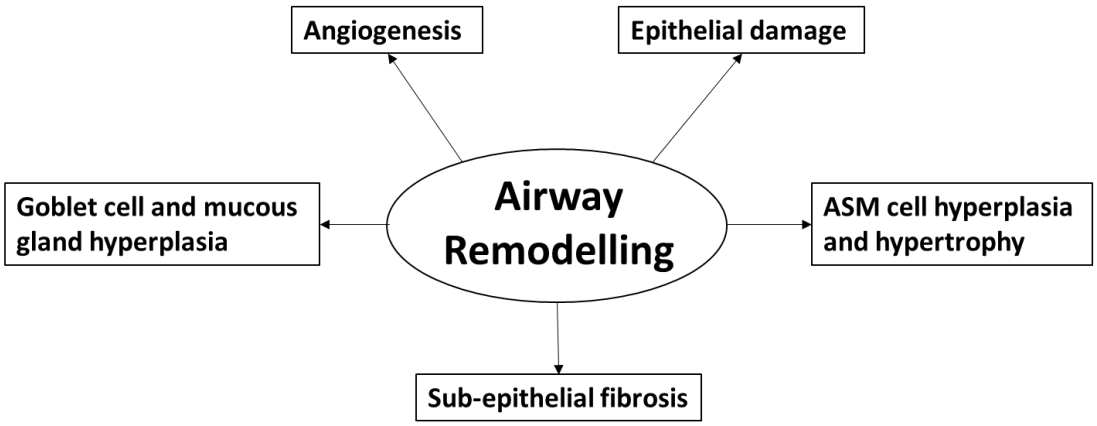

Figure 1.1. The key features of airway remodelling in asthma.

1.3.1 Airway Epithelium

The epithelial layer acts as a barrier between the external environment and the internal structure of the airways. It is, therefore, frequently in contact with inhaled foreign bodies. The epithelium plays an essential role in maintaining healthy airways but in asthma the integrity of the epithelium is disrupted. This is known as epithelial shedding, a process that is widely accepted as an early, or initial, step in asthma pathogenesis (52). Moreover, biopsies of asthmatic bronchoscopy demonstrate that there is significant loss of epithelium when compared to the controls (59). In turn, the degree of epithelial shedding has been associated with airway reactivity (60). Susceptibility to epithelial shedding has been linked with a reduction of E-cadherin in the epithelium of asthmatics, which can be induced by house dust mites (61, 62). Immunostaining of the epithelial damage marker, epidermal growth factor receptor (EGFR), is increased in bronchial biopsies of asthmatics (63). TGFβ is able to initiate epithelial cell apoptosis and promote epithelial mesenchymal transition in the airway epithelium of asthmatic patients (64, 65). Damage to the airway epithelium in asthma is accompanied by reduced ability to regenerative capability (66). Consequently,

damage to the epithelium increases exposure in inhaled agents, airway hyper-responsiveness, and sensitivity to oxidants (67). An increase in mucous is observed in the airway of asthmatics, due to goblet cell and mucous gland hyperplasia. Increased mucous production reduced the lumen area and is prominent in fatal asthma (68).

1.3.2 Subepithelial Fibrosis

The subepithelial layer is formed of ECM proteins including collagens, fibronectin, tenascin, and proteoglycan. Subepithelial fibrosis describes the process of basement membrane thickening and reduced elasticity of the airways due to deposition of fibrous proteins below the epithelium. Although subepithelial fibrosis has been reported in all severities of asthma, there is an association between asthma severity and thickness of the basement membrane (69, 70). An increase in collagen I, III and VII, fibronectin, lumican, and tenascin are seen in the asthmatic airway, most significant in individuals with severe asthma (71-73). Transcription of these genes can be induced by TGFβ, which is found at elevated levels within the airway of asthmatic patients (74).

Deposition of the extracellular matrix (ECM) is primarily controlled by fibroblasts and myofibroblasts (75). In fibrotic airways fibroblasts can polarise to myofibroblasts and have a greater presence in the airways of asthmatic versus healthy patients and in uncontrolled versus controlled asthmatics (76-78). TGFβ promotes fibroblast to myofibroblasts differentiation and proliferation by inducing release of fibroblast growth factor-2 (FGF-2) (79, 80). The number of activated fibroblasts and myofibroblasts are increased in the airways post allergen challenge, suggesting that exacerbation increases ECM deposition (81). Moreover, *in vivo* the OVA model of asthma showed

that repeated exacerbation increased airway resistance associated with collagen deposition (82). TGFβ also induces expression of matrix metalloproteinases (MMPs) and tissue inhibitors of metalloproteinases (TIMPs), which are essential regulators of ECM structure (83). Ultimately subepithelial fibrosis induces structural changes in the lung that make breathing more difficult for a severe asthma by contributing to airway narrowing and resistance (84).

1.3.3 Airway Smooth Muscle Hyperplasia & Hypertrophy

The ASM mass in the large and small asthmatic airways is greater than healthy patients. It has been associated with disease duration and severity (85, 86), and is attributed to both hyperplasia and hypertrophy, which are in turn associated with an increase in ECM (87-90). This contributes to stiffness of the airways as well as narrowing and persistent airway obstruction. Moreover, the larger ASM bundle undergo more forceful contractions during exacerbation and therefore increases the likelihood of complete occlusion of the airways.

The relative contribution of hypertrophy and hyperplasia to the ASM bundle is a matter of debate and can vary depending on the location of the airway. Hypertrophy is a natural process that occurs when muscle is put under repeated stress, however hypertrophy has been observed in children with asthma, suggesting that there is a pathologic process occurring rather than a homeostatic one (89). The evidence of hypertrophy is limited because there are more opportunities to introduce experimental artefact and cell size is more difficult to quantify. Measurement of ASM cell size in biopsies of patients with asthma have shown them to be larger than control patients (87, 89). Conversely, a study of ASM in biopsies of patients with mild to moderate asthma found ASM cell number was 2-fold

higher compared to control patients and there was no evidence of hypertrophy or gene expression changes (88). Moreover, cells cultured from explants of asthmatic lungs have a faster proliferation rate than those from healthy controls (91). In the asthmatic airway there are a plethora of inflammatory cytokines that modulate cell activity, some of which induce ASM cell hypertrophy, including angiotensin and TGFβ (92, 93). Many of these also promote cell proliferation, including TGFβ, tryptase, sphingosine-1-phosphate (S1P) (94-96).

In addition to hyperplasia and hypertrophy, cell migration has been implicated in enlarged ASM mass. There is evidence that ASM cells can migrate in response to platelet derived growth factor (PDGF) and TGFβ in culture, however this is yet to be shown in human asthma (97). Myofibroblasts are contractile cells that are responsible for ECM deposition and have been found to migrate to the airways after allergen challenge, where it has been suggested that they could transdifferentiate to ASM cells, although this has not yet been proven (81, 98). Fibrocytes are mesenchymal precursors that circulate in the peripheral blood. In asthma there is not only an increase in circulating fibrocytes, but also an increase in the number of fibrocytes within the ASM bundle (99, 100). Moreover, fibrocytes have been shown to migrate to the airway of asthma patients after allergen challenge where they are able to adopt a contractile phenotype (101). These highlight the mechanisms, including hypertrophy, hyperplasia, and migration, that contribute to an overall increase in ASM cell mass within the airways of asthmatic patients.

1.3.4 Angiogenesis

Angiogenesis describes the process of forming new blood vessels, a process involving the migration, growth and differentiation of endothelial cells. Increased vascularisation both in terms of the number and area covered has been observed in the airway wall in fatal asthma (102). Analysis of biopsies from the asthmatic airway identified that both the number and size of blood vessels are increased compared to healthy controls (103, 104). Angiogenesis however, is not limited to patients with severe fatal asthma. Biopsies from patients with mild asthma showed that both the number and size of the blood vessels were increased when compared to healthy controls (105).

Angiogenesis is stimulated by inflammatory mediators such as vascular endothelial growth factor (VEGF) and plasminogen activator inhibitor-1 (PAI1). VEGF is a potent activator of endothelial cell growth and vascular permeability (106). The number of VEGF positive cells within the airway has been correlated to vascular area (107). VEGF is increased in the airways of asthmatics and can be secreted by a range of cells, including eosinophils and macrophages, fibroblasts, and ASM (108). The T_H2 cytokines IL-4, IL-5, IL-13 and TGFβ enhance VEGF production by fibroblasts and ASM cells (109, 110). VEGF can also upregulate the expression of metalloproteinase-9 (MMP-9), which plays a critical role in ECM turnover, suggesting angiogenesis can directly alter the ECM (111). Moreover, *PAI1* is one of the genes that is regulated by TGFβ and contributes to airway remodelling (112). Overall, angiogenesis contributes to reduced airway lumen size due to oedema from permeable blood vessels, and enhanced supply of inflammatory mediators.

1.3.5 Goblet cell and mucous gland hyperplasia

There is clear evidence of goblet cell and mucous gland hyperplasia in asthmatic biopsies, most prominent in cases of fatal asthma (68, 113). The consequence of mucous gland hyperplasia is that more mucous is secreted into the airway of asthmatics. Not only is there an increase in the amount of mucous but mucociliary clearance is also impaired in asthmatics due to a damaged epithelium (114). Mucins are the major component of mucous. In human patients MUC5AC is the primary expressed mucin, and is found to be higher in asthmatic patients versus healthy patients (115). MUC5AC is thought to impair mucociliary clearance by tethering mucous to epithelial cells, thus increasing the probability of airway plugging (116). TGFβ2 has been shown to induce synthesis of mucins in airway epithelial cells (117). Mice subjected to the OVA model of asthma have increased goblet cells and mucous production, which is attenuated by an anti-TGFβ antibody (118). There is limited evidence behind mechanism of goblet cell hyperplasia in asthma. However, it is clear that mucous production is increased and clearance is reduced in the airways of asthmatic patients. Consequently, the lumen area is reduced increasing the risk of a fatal asthma attack and airway plugging.

1.4 Airway Smooth Muscle

ASM cells are spindle shaped mesenchymal cells that play an important structural role within the lung and collectively form a contractile bundle. They are described as having a "hill and valley" formation when fully confluent in tissue culture (119). As described in section 1.1.3 airway smooth muscle mass is greatly increased in the lungs of asthmatic patients. This is critical because airway hyper-responsiveness to external stimuli is a key characteristic of asthma and ASM cell contraction results in bronchoconstriction during acute exacerbation. Smooth muscle cells also contribute to the inflammatory milieu by secreting cytokines, growth factors, and inflammatory mediators. Moreover, ASM cells exhibit phenotype plasticity allowing them to switch between contractile and secretory phenotypes in response to mitogens and changes to the ECM (120-122)

1.4.1 ASM Cell Contraction

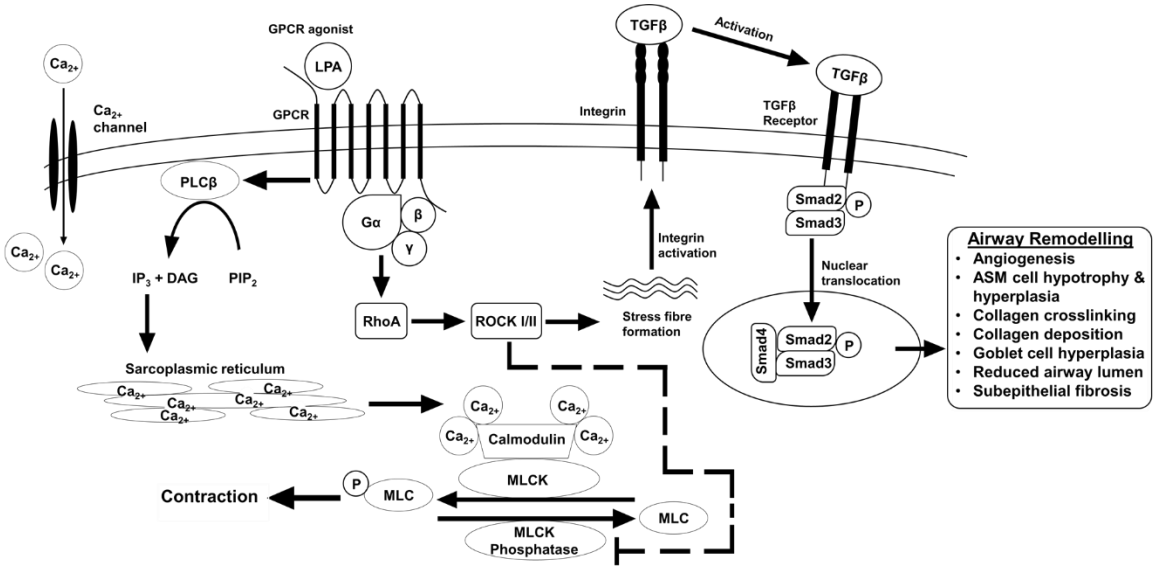

Figure 1.2 Overview of signalling pathways that induce smooth muscle cell contraction.

There are two distinct pathways that are involved in ASM cell contraction, which I will refer to as calcium-dependent and calcium-independent. It has been suggested that calcium-dependent cells contraction is rapid, whereas calcium-independent contraction is longer and sustained (123). The first step of transducing extracellular stimuli to cellular contraction requires a heterotrimeric G-protein coupled receptor (GPCR). They are composed of α, β, and γ subunits, where β and γ (βγ) are perpetually bound. Upon ligand binding there is a conformational change, prompting GDP to GTP exchange in the α subunit and therefore releasing βγ dimer.

In the calcium-dependent pathway, all four members of the $G_{\alpha q}$ family bind directly to PLCβ on the cytosolic side of the cell membrane (124). Activated PLCβ hydrolyses phosphatidylinositol-4,5-bisphosphate (PIP_2) to inositol 1,4,5-triphosphate (IP_3) and diacylglycerol (DAG), which both play independent roles in smooth muscle contraction. IP_3 binds to the IP_3 receptor on the sarcoplasmic reticulum, opening Ca^{2+} channels and resulting in efflux of Ca^{2+} from the sarcoplasmic reticulum into the cytosol. Intracellular Ca^{2+} binds to calmodulin inducing a conformational change that in turn allows it to bind and activate myosin light chain kinase (MLCK). Phosphorylation of Ser20 of the regulatory MLC by MLCK results in myosin cross bridge cycling and cellular contraction. DAG, on the other hand, binds to the serine/threonine kinase PKC along with Ca^{2+} and directly phosphorylates MLCK (125).

The calcium-independent pathway involves activation of the small GTPase RhoA. The heterotrimeric G-proteins $G_{\alpha 12}$ and $G_{\alpha 13}$ have classically been linked to RhoA and involved in stress fibre formation, however recent evidence has also linked $G_{\alpha q}$ and $G_{\alpha 11}$ to RhoA activation (126-128). RhoGEFs (Rho guanine nucleotide exchange factors) induce exchange of GDP for GTP in RhoA, resulting in

activation and allowing it to bind its effectors ROCKI/II, which are serine/threonine kinases (129). ROCKI/II phosphorylates the myosin-binding subunit of myosin light chain phosphatase (MLCP) at Thr696 and Thr853, inactivating its phosphatase activity and preventing interaction with MLC (130). This results in sustained contraction and induces calcium sensitivity. ROCKI/II also play a role in stress fibre formation. Stress fibres are composed of 10-30 actin filaments, cross-linked by α-actinin, and bind to focal adhesions that anchor the cytoskeleton to the ECM (131). Stress fibres can transmit intracellular force to the focal adhesions, which subsequently activate mechanosensitive proteins such as talin and integrins (132). This is of particular importance in airway remodelling because the αvβ5 integrin activates TGFβ (133). ROCKI/II promote stress fibre formation by phosphorylating the actin binding kinases, LIM kinases 1 and 2, which in turn phosphorylate and inactivate the actin-depolymerising factor cofilin (134). Inhibition of ROCKI/II causes stress fibres and focal adhesions to disassemble in fibroblasts (123). The result of ROCKI/II activation is that actin dynamics are tipped in favour of assembly and stable actin stress fibres form.

The contractile apparatus of ASM are composed of thick myosin filaments and thin actin filaments. Contraction occurs when the actin and myosin filaments slide across each other by the well described ‘sliding filament mechanism’. Phosphorylation of the MLC by MLCK leads to a conformational change in the myosin head and induces ATPase activity in the myosin head. Subsequently the myosin head binds to the thin actin filaments forming a cross-bridge and inducing cross-bridge cycling. Termination of ASM contraction requires dephosphorylation of MLC, which is carried out by MLCP. A study looking at the content of MLCK in ASM bundles from human patients

found that it was increased in asthmatics, suggesting that this could contribute to airway hyper-responsiveness and contractility (135).

Blocking Ca^{2+} channels has been trialled as a treatment for asthma to prevent exacerbation and ASM contraction. Trials using diltiazem, nifedipine, and verapamil, found that exercise-induced bronchospasm was inhibited, however they did not inhibit contraction induced by external stimuli and were limited by potency and side effects (136). Current bronchodilator drugs such as salbutamol and formoterol target β_2-receptors that activate cAMP and subsequently protein kinase A (PKA), which reduces cytosolic Ca^{2+} and directly activates MLCP (137). There is however, a population of severe asthmatics, which constitute 10% of the total asthmatic population, whom do not respond to β_2-agonists and suffer from frequent and uncontrolled exacerbation.

In summary, two distinct mechanisms of ASM cell contraction have been described, both of which induce contraction with slightly different outcomes. Despite being distinct there is cross-talk between these pathways at the point of MLC regulation, with the calcium-dependent pathway activating MLCK and promoting contraction and the calcium-independent pathway inhibiting MLCP activity thus preventing negative regulation of contraction. In asthma there is particular interest in the calcium-independent pathway because of the link between RhoA and TGFβ activation that will be discussed later.

1.5 Heterotrimeric G-proteins

G-protein coupled receptors (GPCRs), also known as seven transmembrane receptors, are the largest and most diverse family of membrane receptors found in eukaryotic cells (138). GPCRs are coupled to heterotrimeric G-proteins, composed of Gα and βγ subunits, which bind to a pocket on the cytosolic side of the receptor. The Gα subunit contains a GTP binding pocket and has inherently low GTPase activity. The βγ subunits are permanently coupled and do not disassociate from one another. When GDP is bound the Gα and βγ form an inactive trimer; upon exchange of GDP for GTP, βγ disassociate from the Gα subunit to initiate signalling.

Upon ligand binding to the receptor there is a conformational change in the transmembrane helices 3 and 6 which alter the shape of the binding pocket in which the G-protein trimer is coupled (139). This induces the exchange of GDP to GTP in the Gα subunit. Gα<GTP> dissociates from the βγ dimer becoming catalytically active to induce its target signalling pathways. Heterotrimeric G-proteins are divided into 4 classes and are based on sequence homology of the catalytically active Gα subunit; $G_{\alpha s}$, $G_{\alpha i/o}$, $G_{\alpha q/11}$, $G_{\alpha 12/13}$. The inherent GTPase activity of the Gα subunit is low, therefore GTPase-activating proteins (GAPs) are the primary negative regulators of G-protein signalling, increasing the rate of hydrolysis 50-fold (138).

1.5.1 $G_{\alpha q/11}$ signalling

The $G_{\alpha q/11}$ family comprises 4 alpha subunits; $G_{\alpha q}$, $G_{\alpha 11}$, $G_{\alpha 14}$, $G_{\alpha 16}$. $G_{\alpha q/11}$ are ubiquitously expressed, $G_{\alpha 14}$ is expressed in the lung, liver, and kidney, $G_{\alpha 16}$ is only found in hematopoietic cells. The GPCRs coupled to $G_{\alpha q/11}$ include but are not limited to, the M1, M3, and M5 muscarinic receptors, angiotensin II type 1 receptor, and LPA receptors 1 to 5 (140). Classically, $G_{\alpha q/11}$ activate PLCβ by allosteric

binding causing the releasing of an auto-inhibitory loop and allowing it to catalyse PIP_2 to IP_3 and DAG (141). As discussed in the previous section, this leads to Ca^{2+}-dependent contraction. The α subunit has intrinsic GTPase activity, however PLCβ acts as a GTPase-activating protein (GAP) thereby increasing GTPase activity by more than 50-fold and acting as a negative regulator of $G_{\alpha q/11}$ (142).

More recently, there has been emerging evidence that $G_{\alpha q/11}$ are able to activate more than just PLCβ. One of these targets include p63RhoGEF, known to activate the small G-protein RhoA, and interestingly is also a target of $G_{\alpha 12/13}$ (143). Another target, leukemia-associated RhoGEF (LARG) has also been linked with RhoA activation via $G_{\alpha q}$ (144). Despite both of these heterotrimeric G-protein families being able to activate RhoA, $G_{\alpha q/11}$ has been shown to do so at a lower potency than $G_{\alpha 12/13}$ in mouse embryonic fibroblasts (145). This provides evidence that there is cross-talk between heterotrimeric G-protein signalling pathways that may be regulated based on the compliment of RhoGEFs within certain cell types. Indeed, mechanical ventilation-induced TGFβ activation, thought to involve RhoA, in the murine lung is abolished when epithelial $G_{\alpha q/11}$ is genetically absent (127). $G_{\alpha q/11}$ are also able to activate MAPK and ERK signalling pathways in both a PLCβ-independent and PLCβ-dependent manner. In epithelial cells ERK signalling has been shown to activate inflammatory molecules, including IL-8, which increased ASM cell proliferation and may contribute to ASM hypertrophy (146).

1.5.2 $G_{\alpha 12/13}$ signalling

$G_{\alpha 12/13}$ are expressed ubiquitously. GPCR receptors coupled to $G_{\alpha 12/13}$ include, angiotensin II type 1 receptor, endothelin, S1P, and LPA 1, 2, 4, and 5 receptors (147). Many of these receptors also couple to

$G_{\alpha q/11}$, suggesting that activation of these pathways may occur in tandem. $G_{\alpha 12/13}$ are activated by GPCRs in the same manner described for $G_{\alpha q/11}$. Upon activation of $G_{\alpha 12/13}$ and the G_{α}<GTP> can be bound by the RhoGEFS p115RhoGEF, PDZ-RhoGEF, and LARG (148, 149). These RhoGEFS contain an RH domain that binds to $G_{\alpha 12/13}$ and functions as a GAP, thus enhancing GTP hydrolysis and acting as a negative regulator of signalling. Moreover, they contain a Dbl-homology (DH)/pleckstrin-homology (PH) domain that directly interacts with RhoA and exhibits GEF activity to induce a conformational change resulting in exchange of GDP to GTP (150). RhoGEF localisation to the plasma membrane is thought to be regulated by the PH and RH domains thus ensuring close proximity to the heterotrimeric G-proteins (151). Activated RhoA phosphorylates its primary effector ROCKI/II, which in turn inhibits MLCP, promoting contraction. Studies on vascular smooth muscle cells have shown that upon treatment with a range of vasoconstrictors there is a dual role for $G_{\alpha q/11}$ and $G_{\alpha 12/13}$ coupling to GPCRs and regulating phosphorylation of MLC and thus smooth muscle tone (152). A fourth RhoGEF is known to interact with $G_{\alpha 12/13}$, A-kinase anchor protein 13 (AKAP13), however this protein differs from the other three because it does not exhibit GAP activity to stimulate hydrolysis of GTP (153). In a rat model of asthma, repeated allergen exposure was shown to increase the abundance of $G_{\alpha 12}$ and $G_{\alpha 13}$ protein (154).

1.5.3 $G_{\alpha s}$ and $G_{\alpha i}$ signalling

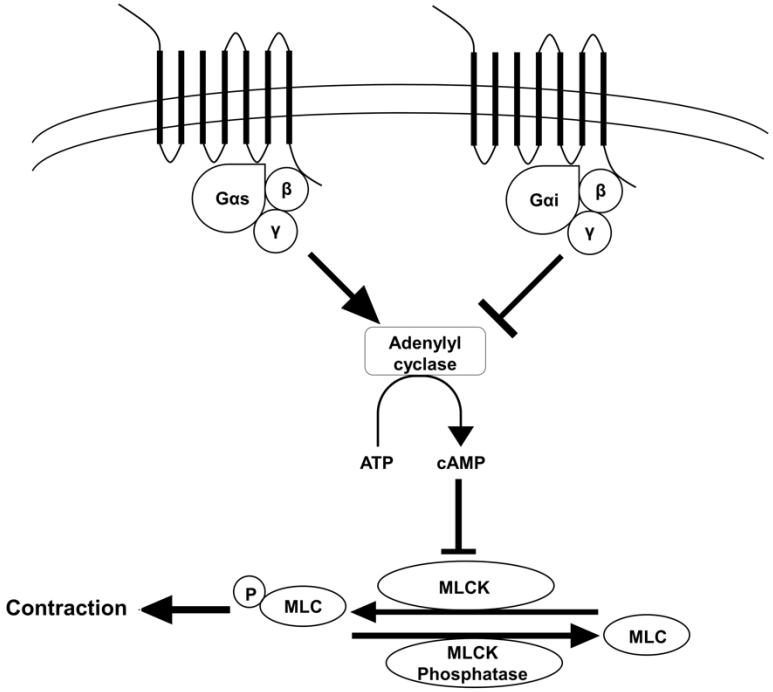

Figure 1.3 Overview of $G_{\alpha s}$ and $G_{\alpha i}$ signalling.

Signalling of $G_{\alpha s}$- and $G_{\alpha i}$-linked GPCRs revolve around regulating the enzyme adenylyl cyclase (AC). Upon activation of a $G_{\alpha s}$-coupled receptor, GDP is exchanged for GTP and the catalytically active G_{α} subunit dissociates from the $G_{\beta\gamma}$ subunit, increasing AC activity. In contrast, $G_{\alpha i}$ antagonises this system by inhibiting AC activity. There are nine AC isoforms that are widely distributed across tissues of the body (155). It functions to catalyse the conversion of ATP into the secondary messenger cyclic adenosine monophosphate (cAMP). An increase in intracellular cAMP results in the activation of protein kinase A (PKA), which inhibits MLCK and therefore blocks smooth muscle contraction (156). In ASM cells PKA has been shown to promote bronchodilation, thus asthma management strategies have sought to exploit this pathway (157).

The most common asthma management medications are inhaled β_2-adrenoceptor (β_2-AR) agonists (158). They function by acting on the

$G_{\alpha s}$-linked β_2-AR, which activates AC and increases intracellular cAMP, resulting in PKA activation and bronchodilation. They are primarily used to relieve acute exacerbation and to manage asthma in combination with inhaled corticosteroids, however, 10% of asthmatics do not respond to treatment (158). Crosstalk between $G_{\alpha s}$ and $G_{\alpha i}$ has been shown in cultured human ASM cells. After prolonged treatment of ASM cells with a β_2-AR agonist, PKA is able to activate $G_{\alpha i}$-$\beta\gamma$ signalling, which in turn activates the cAMP hydrolysing enzymes PDE4 (159). This mechanism has been attributed with β_2-AR agonist insensitivity.

In a rat model of airway hyper-responsiveness, induced by repeated allergen exposure, $G_{\alpha i3}$ was found to have increased expression in bronchial smooth muscle cells (160). Moreover, transgenic mice overexpressing $G_{\alpha i2}$ were found to have reduced contractile responses after methacholine challenge (161). However, the role of $G_{\alpha i}$ in asthma has not been fully established.

1.6 Transforming Growth Factor β

TGFβ is a pleiotropic cytokine that is found in abundance within the ECM. It plays an essential role in homeostatic regulation of inflammation, tissue repair, and cell proliferation. There is a large body of evidence that describes its role in fibrosis and airway remodelling within the airways. The features of airway remodelling, subepithelial fibrosis, epithelial damage, ASM hyperplasia and hypertrophy, goblet cell hyperplasia, and angiogenesis have been described in section 1.3. Although TGFβ is central to these processes, abolition of its signalling pathway is not a viable treatment option due to its pleiotropic nature. At lower concentrations TGFβ acts as a suppressor of inflammation, however in a fibrotic diseased state TGFβ activation increases to a pathologic levels and promotes airway fibrosis. The process of airway remodelling may act homeostatic response to protect against particular features of asthma such as airway hyper-responsiveness (AHR). A murine OVA model of asthma resulted in an increase in total TGFβ and fibrosis, which was reduced with an anti-TGFβ antibody but this also increased AHR (162). Moreover, overexpression of active TGFβ1 in rat airways results in an increase in fibrotic markers, including ECM deposition, fibronectin, and myofibroblasts (163).

1.6.1 TGF-β Synthesis and Structure

Transforming growth factor beta (TGFβ) is a pleiotropic cytokine that belongs to the transforming growth factor superfamily, which is composed of at last 30 signalling molecules including the activin and inhibins, bone morphogenetic proteins, and the TGFβ subfamily; TGFβ1, TGFβ2, and TGFβ3. The three TGFβ isoforms share 64-85% sequence homology and are expressed in most cell types in humans, however TGFβ1 is the most abundant (164).

TGFβ is synthesised as a pro-hormone composed of a short C-terminal sequence that forms the active TGFβ molecule, a long N-terminal that forms the latency-associated peptide (LAP), and a signal sequence (165). The pro-hormone is cleaved in the Golgi complex by the endopeptidase furin, separating C-terminal TGFβ and N-terminal LAP domains (166). Individual LAP and TGFβ monomers form homodimers via disulphide bonds. Both of these homodimers associate by another disulphide bond forming a complex referred to as the small latent complex (SLC). The LAP undergoes folding so that it envelops active TGFβ, preventing TGFβ from interacting with its receptors. Latent TGFβ binding protein (LTBP) binds to the SLC via disulphide bonds between cysteine residues on TGFβ and LTBP, forming a molecule known as the large latent complex (LLC) (166). TGFβ is secreted from most cells as the LLC. LTBP is a 120-240kDa protein glycoprotein that regulates the bioavailability of TGFβ by tethering it to the ECM where latent TGFβ is stored (167). Latent TGFβ can therefore be stored in abundance within the ECM. Liberation of the active TGFβ homodimer can be carried out by proteases such as plasmin, MMP-2 and MMP-9, reactive oxygen species, or integrins (133, 168, 169).

1.6.2 TGFβ Activation

TGFβ is secreted from cells and stored in the ECM. Its activation is the rate limiting step to its bioavailability (170). A number of methods of liberating the active TGFβ molecule from its LAP have been described including, acidification, alkalisation, high temperature, and reactive oxygen species (171, 172). However, very few mechanisms have been shown to have relevance *in vivo*. Some key mechanisms of TGFβ are described in more detail here, with particular focus on integrin-mediated TGFβ activation.

1.6.2.1 Integrin mediated TGF-β Activation

TGFβ activation occurs when the active molecule is liberated from the LAP, allowing it to bind to its receptor. One method of liberation, crucially relevant to this thesis, occurs upon binding of an integrin. Integrins are mechanosensitive cell surface proteins composed of α and β subunits that bind to components of the ECM including fibronectin, collagen, and laminin, and also interact with other cells. There are five integrins that can activate TGFβ; αvβ1, αvβ3, αvβ5, αvβ6, and αvβ8 (133, 173-176).

Integrins undergo conformational change upon sensing force. When inactive they remain in a 'closed' conformation that sterically prevents the head domain from interacting with its target RGD sequence. Upon feeling force the integrin lengthens into an 'open' conformation allowing the binding head to interact with various targets. The force that activates integrins can be from both external or internal signals, so called 'outside-in' and 'inside-out' signalling. Internal force leading to integrin activation can be generated by reorganisation of the actin cytoskeleton. This occurs during cellular contraction induced by binding of agonists such as LPA and methacholine. Integrins are predominantly found at focal adhesion sites where the cytoskeleton is linked to the ECM via multiple structural proteins including talin and vinculin (177). The large mechanosensitive protein talin binds to the cytoskeletal tail of integrin, which is linked to the actin cytoskeleton via the crosslinking protein vinculin (178). Mature TGFβ is enveloped by the LAP that renders it inactive. The LAP of TGFβ1 and TGFβ3, but not TGFβ2, contains an RGD sequence that is a target of integrin. Therefore, integrin is able to with the RGD sequence of LAP to induce a

conformational change and liberate mature TGFβ, allowing it to interact with cell surface receptors.

Processes such as cellular contraction in response to GPCR agonists via the Ca^{2+}-dependent and Ca^{2+}-independent pathways described in section 1.4.1 result in cytoskeletal reorganisation. This induces the formation of focal adhesion complexes, leading to talin binding to the cytoplasmic tail of integrin and its subsequent activation. In severe asthma, this mechanism of TGFβ activation is prominent because patients suffer from frequent and uncontrolled exacerbation therefore exerting force throughout the airways.

ASM cells from asthmatics activate more TGFβ than those from non-asthmatics in response to methacholine and LPA (133). Cultured ASM cells treated with anti-β5 antibody inhibited methacholine and LPA-induced TGFβ, demonstrating that the αvβ5 integrin is responsible for TGFβ activation in ASM cells (133). Moreover, mutations in the talin binding portion of the cytoplasmic tail of β5 abolished TGFβ activation, confirming that talin is essential for integrin mediated TGFβ activation (133). The actin assembly inhibitor, cytochalasin D, also prevents contraction-induced TGFβ activation because integrin cannot be activated without being linked to the cytoskeleton. Airway remodelling observed in the OVA model of asthma is completely abolished *in vivo* upon application of an RGDS peptide that blocks the binding site of integrins, thus preventing integrin mediated TGFβ activation (179). Moreover, transgenic mice with a mutation in the RGD sequence to RGE in the LAP shared characteristics of TGFβ null mice despite normal levels of TGFβ synthesis (180). ECM matrix stiffness has also been implicated in TGFβ activation. In myofibroblasts, αvβ5-mediated TGFβ activation was found to increase by in increasing ECM stiffness or tension (173).

In contrast to ASM cells, epithelial cells activate TGFβ via the αvβ6 integrin (181). Initially the GPCR agonist thrombin has been shown to activate αvβ6 and TGFβ by binding to the PAR1 receptor (175). Agonist-induced TGFβ activation in epithelial cells was shown to induce cytoskeletal reorganisation via RhoA and ROCKI/II (128). Moreover, LPA-induced TGFβ activation was inhibited by siRNA knockdown of $G_{\alpha q/11}$ but not $G_{\alpha 12/13}$ or $G_{\alpha i}$ (128). Interestingly, total TGFβ within the murine lung is increased after high-pressure forced ventilation, but this effect is abrogated upon epithelial knockout of $G_{\alpha q/11}$ (127). These studies suggest that GPCR agonist induced TGFβ activation occurs via a $G_{\alpha q/11}$ RhoA-integrin pathway in epithelial cells.

TGFβ activation can also occur via mechanical signalling without addition of an agonist. The mechanosensitive nature of integrin and talin allows TGFβ activation in response to force, such as matrix stiffness and mechanical stretch (182-184). There is evidence that TGFβ gene expression is increased in response to 12% cyclical stretch in ASM cells, which required RhoA and ROCKI/II (183). It is not clear however, whether stretch directly results in TGFβ activation. A study of cyclical stretch on vascular smooth muscle cells showed secretion of TGFβ was inhibited by the angiotensin receptor inhibitor, saralasin (185). This implies that stretch induces the release of autocrine factors that act on cell surface receptors in induce TGFβ release. Release and activation of TGFβ in response to stretch causes the release of ECM components including fibronectin and collagen (182, 185). The implication in asthma is that uncontrolled exacerbation increases mechanical force within the lung, resulting in activation of TGFβ and promoting airway remodelling.

1.6.2.2 Proteolytic TGFβ Activation

Proteolytic activation of TGFβ has been described to occur through the serine protease and metalloproteases plasmin and MMP-2 and MMP-9 (168, 186). They play a role in ECM degradation, and TGFβ plays a key role in maintaining and stimulating ECM production, thus, this method of TGFβ activation may play a key role in ECM turnover (187). Proteases can cleave the LAP, thus liberating the active TGFβ molecule from the ECM, allowing it to bind to its receptor (188). However, thus far this mechanism has only been demonstrated to activate TGFβ *in vitro*.

1.6.2.3 Thrombospondin-1 (TSP1) Activation of TGFβ

The homotrimer thrombospondin-1 is part of the thrombospondin family of large glycoproteins. It plays a variety of roles in processes including, cell adhesion, angiogenesis, platelet aggregation, and cell proliferation (189). TSP1 is expressed in tissues of the kidneys, aorta, skeletal muscle fibres, and the lung (190). Its expression has been shown to increase in response to injury and has been implicated in wound healing (191). TGFβ can secreted from activated platelets in an inactive LLC. However, TGFβ can be secreted in its active form and has been shown to do so in complex with TSP1, thus suggesting that TSP1 can activate TGFβ (192). Moreover, TSP1 has also been shown to activate TGFβ secreted by endothelial cells (193).

The mechanism by which TSP1 is able to activate TGFβ does not involve liberation of the active TGFβ molecule from the LAP. Rather, TSP1 interacts with the LAP, inducing conformational change that exposes the active TGFβ molecule and allows it to interact with its receptor whilst still attached to the LAP (194). TSP1-null mice show a slight overlap with TGFβ-null mice with increased inflammation, thus suggesting that this mechanism of TGFβ activation is relevant *in vivo* (195). However, TSP1 is not solely required for TGFβ

activation as there was still residual staining of active TGFβ in TSP1-null mice, and TSP1 does not activate all latent TGFβ *in vitro* (193, 195).

1.6.3 TGF-β Receptors and Signalling Pathway

The TGFβ superfamily signal through heterotrimeric complexes of serine/threonine kinase cell surface receptors, known as type I and type II receptors. There are five type I receptors and seven type II receptors that associate in different combinations to specifically bind to each ligand of the TGFβ superfamily (196). The three TGFβ isoforms of TGFβ bind to the type I receptors, ALK1, ALK5, and TGFβRI and to the type II receptor TGFβRII. There is also a type III receptor, TGFβRIII, which binds to TGFβ but is thought to present TGFβ to TGFβRII as opposed to direct involvement in signalling. Both TGFβ1 and TGFβ3 bind to TGFβRII with high affinity, whereas TGFβ2 binds with low affinity and required the assistance of TGFβRIII for signalling (197).

Activation of these receptors by TGFβ requires binding of the dimeric ligand to two type I and two type II receptors. Initially, TGFβ binds to the constitutively active type II receptor kinase, TGFβRII, which phosphorylates the GS domain of the type I receptor kinase, resulting in activation of type I receptor kinase activity (196). The phosphorylation targets of TGFβRI are members of the Smad signalling family. Smads directly transduce signals from the TGFβ superfamily into the nucleus to regulate transcriptional activity. There are five receptor regulated Smads that are phosphorylated by type I receptors; Smad1, Smad2, Smad3, Smad5, and Smad8. Scaffolding proteins such as Smad anchor for receptor activation (SARA) link Smads to the receptor complex, enabling efficient phosphorylation (198). TGFβ binding to its receptor results in the

phosphorylation of Smad2 and Smad3, which oligomerise to form a Smad2/3 complex. The Smad2/3 complex bind to the co-Smad, Smad4, forming a heterotrimer. Smad4 undergoes constitutive nuclear import and is actively exported. Upon forming a complex with Smad2/3 the whole complex localises to the nucleus and nuclear export is inhibited, resulting in accumulation of the Smad2/3/4 complex within the nucleus (199). Both Smad3 and Smad4 are able to bind to Smad-binding elements (SBEs) and promoter regions of target genes to regulate transcription (200).

TGFβ signalling is terminated through signalling of inhibitory Smads. Smad7 acts as a negative regulator by sterically inhibiting the kinase domain of TGFβRI, thus preventing phosphorylation of Smad2 and Smad3 (201). Moreover, Smad7 recruits phosphatases to desphosphorylate TGFβRI and ubiquitin ligases to signal for receptor degredation (202, 203). Smad2/3 are also dephosphorylated by phosphatases within the nucleus that halt transcriptional regulation and promote nuclear export (204).

1.6.4 Biological functions of TGFβ

TGFβ is found in most cell types and plays a number of diverse roles within the body. These vary from prenatal organ development to inflammatory regulation. As such, knockout of any TGFβ isoforms results in increased embryonic lethality. Interestingly, there is little phenotypic overlap between mice null of each TGFβ isoform, suggesting that there is no redundancy in their respective signalling pathways.

There is significant embryonic lethality associated with TGFβ1 knockout because transgenic mice with this mutation give birth to half the expected offspring (205). This is due to defective haematopoiesis and endothelial differentiation within the embryo resulting in impaired vasculogenesis (206). TGFβ1 knockout mice

display a progressive wasting syndrome 2 weeks after birth, weighing half that of their healthy littermates at time of death at around 3 to 5 weeks old (205). These mice were found to have an influx of inflammatory cells, including lymphocytes and macrophages, in the lungs and heart, which ultimately resulted in organ failure and death (207).

Two-thirds of TGFβ2 knockout mice die shortly before or during birth and the rest suffer from developmental defects and only survive for a few minutes (208). Developmental defects are seen in the heart, skull, eye, inner ear, skeletal malformations and cleft palate (208). Lung development was not affected, however the structure of the large airways was compromised.

A crucial role for TGFβ3 in development of the lung has been demonstrated. TGFβ3 null mice typically die within 20 hours of birth due to defective lung development. This was particularly evident in the terminal airspaces where alveoli failed to develop properly and there was observable intrapulmonary haemorrhage in addition to an increased number of mesenchymal cells (209). These mice also had a cleft palate due to failure of the epithelium to bind to the mesenchyme, suggesting that TGFβ3 plays a vital role in interaction of these cell types (209, 210).

These studies in transgenic mice highlight the differing roles of the three TGFβ isoforms. TGFβ1 is a vital regulator of immune response as well as heart development and vasculogenesis. TGFβ2 is essential for development of an array of organs and skeletal structure. TGFβ3 also plays a role in development, which is specifically focussed within the lungs.

1.6.5 TGFβ in asthma

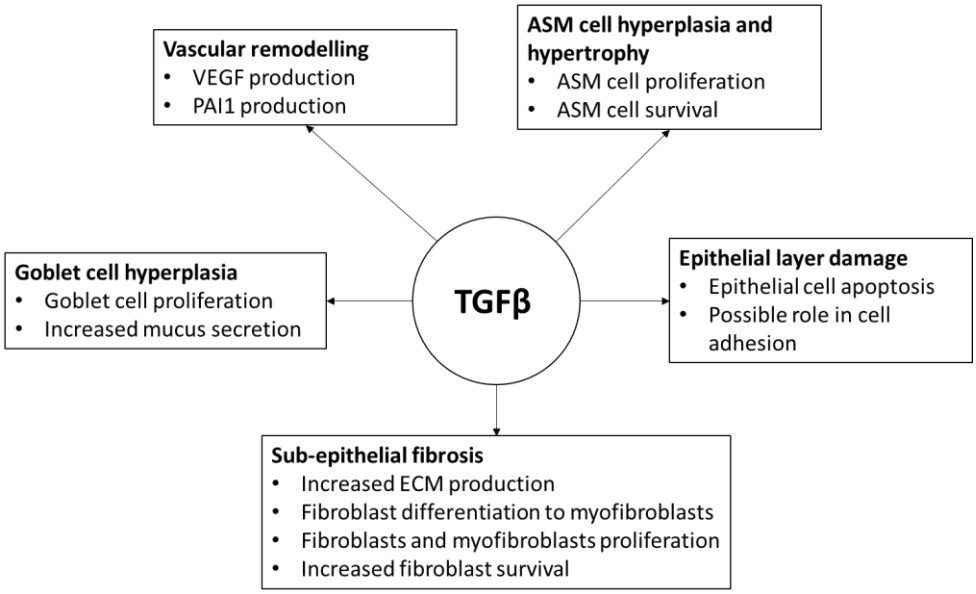

Figure 1.4. Summary of the effects of TGFβ within the airways that contribute to airway remodelling in asthma, taken from Makinde et al. (1).

TGFβ plays a central role in asthma pathogenesis, in particular promoting airway remodelling (see overview in figure 4.1). An increase in TGFβ1 and TGFβ2 is observed in the bronchoalveolar lavage (BAL) fluid of asthmatics (74). Allergen challenge of asthmatic patients resulted in an increase in TGFβ1 24 hours post-challenge as part of the late asthmatic response (211). The amount of TGFβ1 within the submucosa was both higher in asthmatics than healthy individuals and associated with asthma severity (212, 213). Furthermore, an increase in phospho-Smad2 has been observed in bronchial biopsies from asthmatic patients, indicating that there is more TGFβ is being activated (214). A study in mice that underwent the OVA model of asthma have increased ECM deposition, ASM cell proliferation, and mucus production, all of which were reduced by treatment with an anti-TGFβ antibody (118). These studies demonstrate that TGFβ is increased in the airways of asthmatic

patients and that it is activating its signalling pathway via phosho-Smad2. It is also clear that TGFβ1 is the primary TGFβ isoform of interest in asthma because it activated genes involved in airway remodelling, including PAI1, collagen, VEGF, and fibronectin (215). Evidence for the role of TGFβ2 in asthma is more limited, however it has been demonstrated to increase the expression of mucin in epithelial cells from asthmatic patients, which a major component of mucous (117). There is little evidence for the role of TGFβ3 in asthma, which plays a key role in lung development.

TGFβ1 is expressed in nearly all cell types within the lungs including the epithelium, fibroblasts, ASM cells, vascular smooth muscle cells (216-219). The primary source of TGFβ within the lung of asthmatic patients has been shown to be eosinophils, which are recruited to the airways by the milieu of proinflammatory chemokines (212). IL-5 promotes eosinophil survival and is elevated in the asthmatic airway. Treating asthmatic patients with the anti-IL-5 antibody, mepolizumab, reduced lung eosinophilia, TGFβ1 expression and concentration in the BAL fluid, and reduced deposition of some ECM components (220). Moreover, IL-5 null mice subjected to OVA challenge for 3 months had reduced TGFβ and total lung collagen compared to wildtype controls (221). Despite the reduction of eosinophils and ECM synthesis seen when administering mepolizumab, there was no reduction in airway hyper-responsiveness in response to allergens. Consequently, severe asthmatics who have frequent and uncontrolled exacerbations are still able to activate TGFβ through many other cell types within the lung.

One of the most obvious features of airway remodelling in asthma is subepithelial fibrosis, to which TGFβ contributes greatly. The subepithelial layer is formed of ECM proteins including collagens,

fibronectin, tenascin, and proteoglycan. In asthma it becomes thickened and stiffer due to an increase in deposition of ECM, including collagen and fibronectin (69). The main source of ECM deposition is mesenchymal cells, in particular myofibroblasts. As highlighted in section 1.3, TGFβ promotes fibroblast to myofibroblasts transition and proliferation (79). Moreover, TGFβ can induce MMP and TIMP expression, which play an essential role in ECM turnover (83, 222). Mice administered with TGFβ1 had increased collagen I and III mRNA, and a significant increase in total lung collagen (223). Moreover, TGFβ is able to induce fibronectin synthesis in ASM via the integrin αvβ5 (224). Subjecting vascular smooth muscle cells to mechanical stretch induces collagen and fibronectin synthesis as well as MMP2 activity (182). A similar stretch protocol on ASM cells yielded an increase in TGFβ expression (183). It is likely that the force generated within the lung during exacerbation contributes to TGFβ activation, and therefore airway remodelling, due to the mechanosensitive nature of TGFβ-activating integrins.

When observing airway remodelling in the asthmatic lung there is a clear increase in the amount of ASM cells. This results in thick bands of ASM that are able to contract with a greater force. Coupled to the other features of airway remodelling, this increases the risk of an exacerbation completely occluding the airways. ASM cells have been shown to activate TGFβ by the integrin αvβ5. Treating mice subjected to the OVA model of asthma with an anti-αvβ5 antibody prevented thickening of the ASM layer seen in isotype control mice (133). Moreover, αvβ5 knockout mice subjected to the *A. fumigatus* model of asthma had reduced thickening of the ASM layer (133). Despite the reduction in ASM thickness, blocking αvβ5 lead to an increase in

inflammatory cells observed in the BAL fluid, highlighting the pleiotropic role of TGFβ (133).

In culture, activation of mitogen-activated protein kinases (MAPKs) by TGFβ has been shown to induce ASM cell proliferation(225). TGFβ has also been shown to promote ASM cells to synthesise ECM proteins. Cultured ASM cells are able to secrete and activate TGFβ, which binds to its receptor on the ASM cell surface to activate synthesis of collagen I (226). Connective tissue growth factor (CTGF) induces synthesis of collagen I and fibronectin in fibroblasts (227). TGFβ is able to induce synthesis and release of CTGF from ASM cells, an effect which is greater in cells taken from asthmatics in comparison to healthy controls (228, 229). CTGF is also able to act on ASM to promote synthesis of the ECM proteins collagen I and fibronectin (230). Overall the structure of the ASM layer in the airways of asthmatic patients is clinically different to healthy patients and contributes to airway remodelling.

Vascular remodelling is a feature of airway remodelling. There are more blood vessels in bronchial mucosa of asthmatics and these vessels are more permeable (107). VEGF is a strong inducer of endothelial cell growth and vascular permeability (106). In the asthmatic airways there is a correlation between the number of VEGF positive cells and vascular area (107). TGFβ is able to augment VEGF synthesis in human ASM cells and fibroblasts via the Smad signalling cascade (231, 232).

There is an increase in the amount of mucous in the airways of asthmatic patients that is particularly prominent in fatal asthma (233). This is due to an increase in the number of goblet cells and size of mucous glands. TGFβ2 has been shown to induce synthesis of mucins, a major component of mucous, in airway epithelial cells (117). Treatment of mice subjected to the OVA asthma model with

an anti-TGFβ antibody reduced mucous production in the airway (118). In a severely remodelled airway where the lumen diameter is already reduced, mucous overproduction can plug the airway and increase the likelihood of a fatal asthma attack.

The epithelial layer is damaged in asthmatic patients due to a process known as epithelial shedding (234). This leaves underlying cells exposed to inhaled particles and allergens that can induce an exacerbation. Analysis of bronchial biopsies has demonstrated a correlation between epithelial damage and airway hyper-responsiveness (60). TGFβ is able to have both an apoptotic and antiapoptotic effect on cells depending on the cellular context and phase of the cell cycle (64). A pro-apoptotic effect of TGFβ is seen in cultured human epithelial cells when it signals through a non-Smad pathway mediated by MAPK (64). Another mechanism of epithelial wall degradation is through EMT. TGFβ induces EMT in epithelial cells through its canonical Smad signalling pathway, an effect which is greater in cells from asthmatic patients (65). This implies that epithelial cells in asthmatics are primed for EMT. Overall, the combination of TGFβ promoting apoptosis and EMT results in degradation of the epithelial barrier and increased AHR.

1.7 Summary

Asthma is an inflammatory disease with high prevalence. An estimated 10% of asthmatics suffer from a severe form of the disease, which is characterised by frequent and uncontrolled exacerbations. These patients present clinical features including subepithelial fibrosis, ASM hypertrophy and hyperplasia, angiogenesis, epithelial damage, and goblet cell hyperplasia, collectively known as airway remodelling.

The pleiotropic cytokine TGFβ is central to airway remodelling and is found activated more in the airways of asthmatic patients than healthy patients. It is therefore important to determine the signalling pathway that results in TGFβ activation to identify new therapeutic targets that prevent airway remodelling. Within the inflammatory milieu of the asthmatic lung there are many agonists of heterotrimeric G-protein coupled receptors (GPCR), which are key to inducing exacerbation and airway hyper-responsiveness. In murine embryonic fibroblasts and epithelial cells, the heterotrimeric G-protein family $G_{\alpha q/11}$ and small G-protein RhoA is required for TGFβ activation. In ASM cells the integrin αVβ5 is required for LPA- and methacholine-induced TGFβ activation. However, the precise signalling pathway that leads to TGFβ activation in ASM cells, the primary contractile cells of the airway, is not known. This thesis, therefore, attempts to delineate the signalling pathway that induces TGFβ activation in response to cyclical mechanical stretch and the GPCR agonist LPA.

1.8 Hypothesis and Aims

The overall aim of this thesis was to test the hypothesis that the heterotrimeric G-protein family $G_{\alpha q/11}$ are required for TGFβ activation in ASM cells *in vitro*. This was broken down into three aims:

1. Develop a new cell-based model to study G-protein signalling in ASM cells.
2. Determine whether $G_{\alpha q/11}$ are required for LPA-induced TGFβ activation.
3. Determine whether $G_{\alpha q/11}$ are required for cyclical mechanical stretch-induced TGFβ activation.

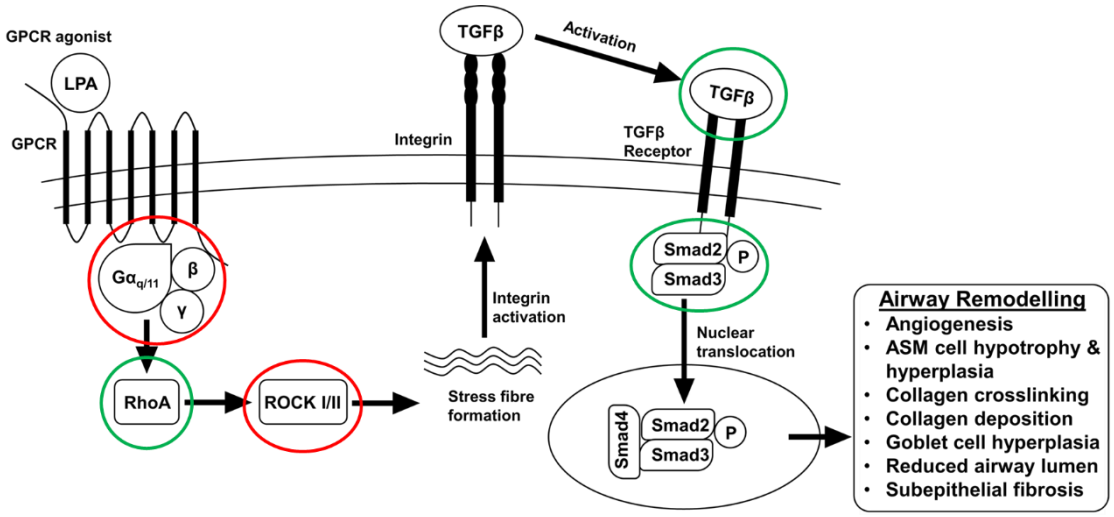

Figure 1.5 Hypothesised pathway leading to TGFβ activation in ASM cells. Red circles represent molecules in the pathway that were inhibited. Green circle represent primary endpoints used throughout this thesis.

To answer this broad hypothesis, it was broken down into smaller stages. At each step, a stimulus was applied to human ASM cells in the form of the GPCR agonist LPA, or cyclical mechanical stretch. The primary endpoint measured to determine TGFβ activation throughout this thesis was phosphorylation of Smad2 (pSmad2).

The pathway that leads to TGFβ activation was interrogated at various points. To determine whether there was a role for GPCRs in TGFβ activation, the heterotrimeric $G_{\alpha q/11}$ were targeted through a combination of genetic and molecular approaches. This part of the pathway has not been defined in ASM cells. There is a small body of evidence that demonstrated the role of RhoA and its effector ROCKI/II are involved in TGFβ activation in other cell types. It was important, therefore, to assess the possible role of these signalling proteins. ROCKI/II was targeted directly using a small molecule inhibitor. RhoA activation was targeted indirectly by inhibition of heterotrimeric G-proteins.

As this thesis progressed it became clear that RhoA was regulated by another family of heterotrimeric G-proteins, $G_{\alpha 12/13}$. The possible role of $G_{\alpha 12/13}$ in TGFβ activation was explored in the final chapter of this thesis.

2 Chapter 2: Materials and Methods

2.1 Cell Culture

2.1.1 Human Airway Smooth Muscle Cells

Primary human airway smooth muscle (HASM) cells were supplied by Professor Simon Johnson, Nottingham respiratory research unit, University of Nottingham, UK, or, Professor Dominic Shaw, NIHR Biomedical Research Centre, University of Nottingham, UK. Staining for α-smooth muscle actin was carried out by the biomedical research unit to confirm that cells were mesenchymal. They were cultured at passage 5 or 6 in Dulbecco's modified Eagles medium (DMEM) (Sigma-Aldrich) supplemented with 10% foetal calf serum (FCS) (Harlan UK) and 4mM L-glutamine at 37°C, 5% CO_2 in a humidified incubator. The medium was changed every 2-3 days until cells were 100% confluent for experiments. Cells were growth arrested for 24 hours prior to experiments in serum free DMEM, 4mM L-glutamine.

ASM cells were collected by Simon Johnson with approval from the Nottingham Research Ethics Committee (12/EM/0199). Cells were grown from bronchial biopsies that were dissected to separate ASM bundles before being expanded in primary culture. Asthmatic patients were asked to cease taking inhaled medication, including short/long acting β_2-agonists and inhalers for 48 hours prior to the first visit. Patients were defined as mild/moderate asthmatics through the following criteria (235):

Inclusion criteria for patients with asthma

- 18-65 years of age
- Physician diagnosed asthma
- Post bronchodilator FEV1>80% predicted
- Asthma phenotype fitting criteria for methacholine challenge
- Able to give informed consent

Exclusion criteria for patients with asthma

- Participation in a clinical drug trial within 3 months
- Pregnant or breast feeding

- Any other chronic respiratory condition
- Smoker within the last year or previous smoking history of >10 pack years
- History of life threatening exacerbation of asthma
- Use of >1000mcg inhaled corticosteroid / day
- Exacerbation of asthma within the last 6 weeks
- Use of oral steroids, theophylline or leukotriene antagonists with the last 6 weeks
- Any severe systemic illness (malignancy, diabetes, tuberculosis)
- Inability to give informed consent
- Known Cerebral or Aortic Aneurysm
- Recent myocardial infarction
- Recent eye surgery

Inclusion criteria for healthy subjects

- 18-65 years of age
- Non-smoker or less than 10 pack year smoking history
- Post bronchodilator FEV1>80% predicted normal value
- No known respiratory illness
- Able to give informed consent

Exclusion criteria for healthy subjects

- Diagnosis of asthma or any other respiratory disease
- Smoker within the last year or previous smoking history of >10 pack years
- Respiratory infection within the last 6 weeks (e.g. pneumonia, bronchitis)
- Use of oral steroids, theophylline, or leukotriene antagonists within the last 6 weeks
- Any severe systemic illness (e.g. malignancy, diabetes, tuberculosis)
- Inability to give informed consent
- Pregnant or breast feeding
- Known Cerebral or Aortic Aneurysm
- Recent myocardial infarction
- Recent eye surgery

Cells collected by Professor Dominick Shaw were under ethical approval (11/EM/0062). Cells were grown from bronchial biopsies that were dissected to separate ASM bundles before being expanded in primary culture. Patients were defined as having moderate to severe asthma by the following criteria (236):

Inclusion Criteria

- Male or female aged between 18 and 80 years old
- Clinical diagnosis of refractory asthma

- Symptomatic despite receiving treatment at step 4 of the BTS asthma guidelines: evidence of poor asthma control in terms of regular night-time awakening (>2/week) or more than four puffs of relief medication/day (>twice/week) requiring repeated (two or more per year) courses of oral corticosteroids despite treatment with high-dose inhaled corticosteroids (≥1000μg beclomethasone or equivalent) and treatment with, or a previous unsuccessful trial of, a long-acting beta-agonist or leukotriene antagonist

Exclusion Criteria

- Pregnant females
- Inadequate contraception or lactation
- Antibiotic course within the last 6 weeks
- Smoking history in excess of 20 pack years
- Clinical diagnosis of allergic bronchopulmonary aspergillosis
- Bronchiectasis
- Abnormal liver function tests
- History of liver disease
- Medication known to interact with azithromycin (e.g., ciclosporin, digoxin, ergot derivatives, terfenadine, warfarin, antacids, and ritonavir)

2.1.2 Transformed Mink Lung Epithelial Cells

Transformed Mink Lung Epithelial Cells (TMLC) express the TGFβ responsive portion of the *PAI1* promoter that drives a luciferase gene and a neomycin resistance gene (237). They were a kind gift from Professor Dan Rifkin, NYC. TMLC were grown in DMEM, 10% FCS, 4mM L-glutamine, and 25μg/ml G418.

2.1.3 Murine Tracheal Smooth Muscle Cells

$G_q^{fl/fl}G_{11}^{-/-}$ mice were a kind gift from Professor Stefan Offermanns, Max-Planck-Institute for Heart and Lung Research, Germany (238). Mice were bred under project and personal licence authorised under the Animals in Scientific Procedures Act 1986. Tissue collection was ethically approved by the Animal Welfare Ethical Review Board (ethics number 000078).

Mice were a mix of male and female aged between 6 and 8 weeks before being humanely killed following Schedule 1 procedures of the

Animal (Scientific Procedures) Act 1986. Animals were sacrificed by overdose of sodium pentobarbital that was given by intraperitoneal injection. Lungs were dissected from the mice by first cutting through the rib cage to expose the lungs before the trachea was cut as high as possible and lungs removed. Lungs were transferred to Dulbecco's modified Eagles medium (DMEM) (Sigma-Aldrich) supplemented with 10% FCS (Harlan UK) and 4mM L-glutamine, 200µg/ml streptomycin, 5µg/ml amphotericin B.

To isolate tracheal smooth muscle cells, a 6-well plate was scratched using a scalpel to help the trachea to stick to the plate. The trachea was then removed from the lungs and cut into quarters using a scalpel. Sections of trachea were stuck onto the tissue culture plate ensuring the lumen side of the airway was facing down and the ringed cartilage facing up. The trachea was incubated in the same media described above at 37°C, 5% CO_2. Media was changed every 3 days until colonies of cells appeared in the wells. Once the well was 50% confluent, cells were trypsinised and transferred to a T25 cell culture flask. These cells were deemed passage 1. Cells were stored in liquid nitrogen in 90% FCS plus 10% dimethyl sulfoxide (DMSO) at $5x10^5$cell/ml for future use.

2.2 Co-Culture Assay

2.2.1 Principle

The co-culture assay was designed so that TGFβ activated by HASM cells could be quantified. When TGFβ is activated it will bind to the TGFβ receptor on the surface of the TMLC. The *PAI1* promoter then drives luciferase transcription and translation. The bioluminescence from luciferase can be measured in relative light forming units (RLFU). To ensure that the quantity of luciferase is proportional to active TGFβ a standard curve was produced by treating TMLCs alone with known quantities of TGFβ. The results from the experiment were

only used if RLFU was within the linear range of the standard curve. This is a specific method of measuring active TGFβ, however it is indirect. It is possible to calculate the amount of TGFβ within a sample using the standard curve, but there is a high level of variability and noise within the system due to the steep gradient of the standard curve, therefore relative increase in TGFβ was calculated to normalise noise between experiments. The advantage of this method is that only active TGFβ is measured and it is relatively fast and simple in comparison to measuring phospho-Smad2, another common measure of TGFβ activation.

2.2.2 Method

HASM cells were seeded in a 96-well tissue culture plate, at $2x10^5$cells/ml in a volume of 50µl and allowed to bind to the plate overnight. Cells were growth arrested for 24 hours prior to experiments. Immediately before the experiment, 50µl TMLCs were added to the wells at $1x10^6$cell/ml, final well volume 200µl. The conditions were carried out in triplicate, on both HASM cells plus TMLC and TMLC alone. A standard curve was generated by stimulating TMLCs alone with recombinant TGFβ1(R&D Systems) at 0, 250, 500, 1000pg/ml. Eighteen hours post stimulation cells were washed with PBS and lysed with 50µl luciferase lysis buffer (Promega). The plate was frozen at -20°C for at least 1 hour to aid cell lysis. Lysate was transferred to a white opaque 96 well plate and luminescence was measured by an Omega FLUOstar® plate reader that was set to inject 50µl luciferase assay reagent from the Promega luciferase assay system kit. Luminescence was measure in relative light forming units (RLFU) and values were determined to be within the linear portion of the TGFβ standard curve. RLFU values generated from TMLC wells alone was subtracted from the HASM plus TMLC

value to remove TGFβ independent luminescence. Data was normalised to relative change by using the following formular:

Relative inhibition = (Sample RLFU - Positive Control RLFU) / Positive control RLFU

If there is inhibition this gives a negative value i.e. if there is 50% inhibition, relative fold change will be -0.5. To graphically represent this value the following formula was applied:

Inhibition = 1 – Relative inhibition

Therefore the positive control sample will always equal 1, and if there is 50% inhibition a sample value will equal 0.5.

2.3 Western Blotting

2.3.1 Principle

Western blotting is a technique that is used to separate proteins by molecular weight. Cells are lysed in ice cold lysis buffer and kept at a maximum of 4°C throughout preparation to minimise protein degradation. Cell lysates are run through a sodium dodecyl sulphate polyacrylamide gel electrophoresis (SDS-PAGE) gel by applying an electric current that repels negatively charged proteins to the positive end of the gel by electrostatic repulsion. Smaller proteins migrate further through the gel, whereas larger proteins do not travel as far, thus, proteins are separated based on size. The protein is transferred to a polyvinylidene fluoride (PVDF) membrane via an electric current. Proteins can then be detected by addition of an antibody that targets a protein-specific antigen. The molecular weight can be determined by comparing how far the protein ran through the gel to a molecular ladder, which is also run through the

gel and has coloured bands that stop at different points based on their molecular weight.

2.3.2 Cell Lysis

Cell medium was removed and cells washed with ice-cold PBS. Cells were lysed in 100µl cell lysis buffer and the plate was scraped before being put in the freezer at -80°C for at least 1 hour to aid lysis. Lysate was transferred to a pre-chilled eppendorf tube and centrifuged at 16,000xg for 10 minutes to remove cell debris. Protein concentration was determined by BCA assay.

2.3.3 BCA Assay and Sample Preparation

The BCA assay (Thermofisher) uses set protein concentrations ranging from 100µg/ml to 2000µg/ml to generate a standard curve. Protein lysate samples were loaded in a 96-well plate with the standard curve. Protein detection reagent was then added to the wells and the plate incubated at 37°C for 20 minutes. Protein concentration determined by measuring absorbance at 562nm. The standard curve was used to determine the protein concentration in each sample to ensure that an equal concentration of protein could be loaded into the western blot gel. Each sample was mixed with 4x Laemmli buffer at a ratio of 3:1, and boiled for 5 minutes.

2.3.4 Running the Western Blot

Gel casting apparatus were set up according to manufacturer's protocol (BioRad). A 10% resolving gel was prepared in the laboratory by adding 6.66ml 30% Bis/acrylamide, 5.2ml buffer 1, 7.92 distilled water. The stacking gel was prepared by adding 1.3ml 30% Bis/acrylamide, 2.5ml buffer 2, and 6.1ml distilled water. The gel was added to the apparatus and allowed to set before the resolving gel was applied on top with a comb insert. Once set, the gel was put into the tank and comb removed. The compartment and tank was filled with 1x running buffer (see appendix). Rainbow™

protein marker (Sigma-Aldrich) was added to the first lane followed by samples. The gel was run at 150V until the lowest molecular weight band had reached the bottom of the gel (approximately 1 hour).

Protein transfer was carried out by first soaking a PVDF membrane in methanol for 30 seconds and washing with tap water. Sponge, filter paper, and the PVDF membrane were left in transfer buffer to soak. The SDS-PAGE gel was removed from the apparatus and placed in transfer buffer (see appendix). In a transfer cassette a sponge was laid on the red side followed by filter paper, membrane, gel, filter paper and another sponge. A roller was used to ensure that no air bubbles were left between the membrane and gel. The cassette was placed in a transfer tank with the gel closest to the negative electrode. Voltage was applied at 100mV for 50 minutes with the tank standing in ice, to transfer the protein from the gel and into the PVDF membrane. Following transfer, the membrane was stained with Ponceau's stain (BioRad) to ensure protein transfer and washed with Tris-Buffered Saline, 0.1% Tween® (TBST) 2 x 5 minute (see appendix).

2.3.5 Protein Detection

To reduce non-specific binding of antibodies the membrane was blocked in 5% non-fat milk (BioRad) for 1 hour at room temperature. Primary antibody (described for each experiment within the figure legends, see appendix for code and concentration) was diluted in 5% bovine serum albumin (BSA) TBST and left on the membrane overnight at 4°C. The membrane was washed in TBST 2 x 5 minutes. Secondary antibody goat anti-rabbit (Agilent, E0432) was diluted in 5% non-fat milk and incubated with the membrane for 2 hours at room temperature. To remove any non-specific secondary antibody binding the membrane was washed 5 x 5 minutes in TBST. For

protein detection, the membrane was blotted dry and placed on cling film, equal parts of Clarity™ ECL solution (BioRad) was applied to the membrane for 30 seconds. A second piece of cling film sandwiched the membrane and was placed into a cassette along with Hyperfilm ECL, in the dark room. Developed bands were compared to the Rainbow™ marker to determine molecular weight. GAPDH or Smad2/3 were as a loading control. Note that western blots towards the end of this thesis were developed using a LI-COR C-DiGit® Blot Scanner.

2.4 siRNA Transfection

2.4.1 Principle

Transfection is the process of introducing nucleic acids into a cell. The method described here uses a lipid reagent that merges with the cell membrane, releasing its contents into the cell. A lipid vector was used to carry siRNA, which is a short strand of nucleic acids that have a complimentary sequence to the mRNA of a gene that is to be silenced. The siRNA strand binds to free mRNA within the cell, preventing mRNA translation and therefore synthesis of the target protein. This method of gene silencing is only temporary, but is a simple and effective way to transiently knock down proteins of interest. The effectiveness of transfection can be measured at the RNA level by quantitative polymerase chain reaction (QPCR) and at the protein level by western blot. At the RNA level, knockdown of a genes expression can typically be seen between 24 and 72 hours post-transfection. Whereas knockdown at the protein level can be far more variable depending how rapid protein turnover is, for example the expression of very stable proteins that are turned over slowly will take longer to reduce that proteins that are rapidly turned over within a cell.

2.4.2 Transfection

Cells were plated at a density of $1.2x10^5$cells/ml in a volume of 1ml in a 6 well plate to ensure 40% confluency at the time of transfection. In separate tubes, 8µl lipofectamine 2000 (Sigma-Aldrich) (1µl per 100µl final volume of Opti-MEM)was added to 400µl Opti-MEM media (Thermofisher), and 60nM of siRNA was added to 400µl of Opti-MEM. For each experiment, a non-targeting control siRNA was used as a negative control to ensure that siRNA delivery was not effecting our target gene. A transfection reagent control labelled 'mock transfected' was also carried out for each experiment, containing only lipofectamine, to ensure that the vehicle was not having any obscure effect. The siRNA and lipofectamine were then combined to allow the lipofectamine to engulf siRNA strands within a lipid vesicle, and incubated at room temperature for 20 minutes. Growth media was removed from the cells and the transfection mixture was overlaid on cells for 4 hours. The mixture was then removed, cells washed with PBS, and growth media added to cells allowing expansion prior to experiments. Both, QPCR and protein expression, were measured to determine whether the target gene had been knocked down.

Note: when multiple siRNA sequences were used, they were pooled together following exactly the same protocol i.e. 60nM $G_{\alpha q}$ + 60nM $G_{\alpha 11}$ in 400µl Opti-MEM, mixed with 8µl of lipofectamine 2000 in 400µl of Opti-MEM.

2.5 Quantitative Polymerase Chain Reaction QPCR

2.5.1 Principles

Quantitative polymerase chain reaction (QPCR) is used to quantify specific sequences of cDNA that are derived from mRNA via reverse

transcription polymerase chain reaction (RT-PCR). QPCR is the process of amplifying DNA within a sample using a thermocycler, where a fluorescent dye, such as SYBR Green, intercalates with double stranded DNA (dsDNA) product and the fluorescence intensity is measured after each amplification cycle. As the dye intercalates with dsDNA, fluorescence is directly proportional to the amount of DNA product. A single gene can be targeted by designing specific primer sequences that bind to the 3' and 5' end of a gene product. A stable and ubiquitously expressed endogenous control gene (housekeeping gene), such as β-2-microglobulin, is also amplified within the same sample to minimise variability. Gene expression is then calculated versus the housekeeping gene.

To ensure that a single DNA sequence has been amplified the PCR dissociation curve is analysed. The dissociation curve is a graph that shows fluorescence intensity on the Y-axis and melting temperature on the X-axis. A single peak is present if there has been amplification of a single DNA sequence. A non-targeting control (NTC) well of water is also run alongside samples. The dissociation curve of the NTC should be a flat line, indicating that there has been no amplified gene product or show a very small double peak that indicates primer dimer formation that can occur when there is no DNA sample present in a well. Once satisfied that a single gene product has been amplified the expression versus the housekeeper can be calculated (239).

2.5.2 Cell Lysis and RNA Isolation

RNA isolation was carried out using a NucleoSpin RNA II kit (Macherey Nagel). Cells were washed with PBS and lysed using 350µl RAI lysis buffer supplemented with β-mercaptoethanol (10µl/ml). Lysate was transferred to the homogenisation column and centrifuged at 11,000xg for 1 minute. The column was discarded and

350µl 70% ethanol was mixed with the flow-through. This was added to the NucleoSpin filter column and centrifuged at 11,000xg for 30 seconds to bind RNA to the column. Flow-through was discarded and 350µl membrane desalting buffer was added to the column to remove unwanted salts, and centrifuged at 11,000xg for 30 seconds. DNase mixture was prepared by adding 90µl DNase I reaction buffer to 10µl DNase I per sample. 95µl of this mixture was applied to the column for 15 minutes at room temperature to remove any DNA. The membrane was washed with 200µl RA2 buffer and centrifuged at 11,000xg for 30 seconds. A final 2 washes were completed using 600µl RA3 buffer and centrifuging at 11,000xg for 30 seconds and then 2 minutes to completely dry the membrane. The RNA was eluted from the column by adding 40µl nuclease-free water to the column and incubating for 10 minutes at room temperature before centrifuging at 11,000xg for 2 minutes. RNA was stored at -80°C. RNA concentration and purity was measured using spectrophotometry using a nanodrop to ensure that isolated RNA was at sufficient purity and concentration to be reverse transcribed.

Concentration:

RNA (µg/µl) = OD260nm x RNA extinction coefficient x dilution factor

Purity:

A ratio of OD 260nm:280nm between 1.8 - 2 was used for PCR reaction.

2.5.3 Reverse Transcription and Polymerase Chain Reaction

To anneal the primer to template RNA a mixture containing 0.5µg Oligo $d(T)_{20}$, 1µl dNTP mixture (10mM each), 6µl nuclease free water was added to 5µl isolated RNA. The mixture was heated to 65°C for 5 minutes on a PCR machine and then incubated on ice for at least 1

minute. A reverse transcription reaction mixture was prepared containing 4µl 5x SuperScript IV buffer, 1µl 100mM DTT, 25 units of RNasin™, and 1µl SuperScript IV, per sample. 7µl of this mixture was added to each well and incubated at 55°C for 10 minutes. Once the reaction was completed cDNA was stored at -20°C.

2.5.4 QPCR Method

Takara SYBR Premix Ex Taq mastermix containing SYBR green was combined with 2µl of cDNA and specific primers (see appendix for primer sequences), making a total volume of 20µl. A no template control containing no cDNA was carried out. All conditions were measured in duplicates. QPCR was carried out in the thermocycler Mx3000P® by Stratagene under the following conditions: 95˚C for 2 minutes, then 35 cycles of 95˚C for 1 minute, 60˚C for 1 minute, 72˚C for 1 minute, and 72˚C for 5 minutes. The point at which PCR product is detected is determined by the fluorescent dye breaching a determined threshold. The cycle number at which this occurs is called cycle threshold (Ct). A Ct value is given to both the gene of interest and housekeeping gene, β2-microglobulin (β2-M). Data was normalised by subtracting the Ct of β2-M from the target gene. Control samples were then subtracted from all data points giving ΔΔCt. Relative gene expression was then determined by the following calculation:

Relative expression (fold increase) $= 2 - \Delta\Delta Ct$

2.6 Lentivirus Production and Transduction

2.6.1 Principles

Lentivirus' are derived from human immunodeficiency virus (HIV-1) and can be used as a gene delivery vector that has the ability to infect both dividing and non-dividing cells. The lentivirus traverses the plasma membrane by endocytosis and can interact with nuclear

import apparatus to enter the nucleus. Lentiviruses integrate genetic material into the host genome for stable and long-term expression. The components to produce lentivirus are split across 3 plasmids and are replication incompetent for safe use in the laboratory. These plasmids consist of a lentiviral transfer plasmid, packaging plasmid, and envelope plasmid. The lentiviral transfer plasmid contains the gene of interest surrounded by long terminal repeat sequences, which allow the plasmid sequence to be incorporated into the host genome. The packaging and envelope plasmids encode components of the viral capsid. To produce an active lentivirus, all three plasmids are combined in 'packaging cells', usually HEK T293 cells. Active virus is then released into the media, where is can be harvested and applied to target cells. Lentiviruses interact with the host cell membrane and release viral RNA. Often, lentiviruses also carry the proteins reverse transcriptase and integrase. Once the genetic material is in the cell the RNA is reverse transcribed into cDNA and then integrated into the host genome by integrase. The gene will then be stably expressed in the host cell.

2.6.2 Plasmid Amplification

The three lentiviral plasmids were a kind gift from Professor Maddy Parsons, Kings College London, UK. The plasmids arrived in blotting paper, and therefore required amplification. They were eluted in dH_20 and the concentration was determined by measuring the A_{260} and A_{320} on the nanodrop. The following formula determines the DNA concentration:

Concentration (µg/ml) = (A_{260} - A_{320}) x dilution factor x 50µg/ml

DNA yield (µg) = DNA concentration x sample volume

Each plasmid contained an ampicillin resistance gene to allow positive selection of transformed bacterial colonies. One Shot™

Stbl3™ Chemically Competent *E. coli* (Thermofisher) were thawed on ice before addition and gentle mixing of 100pg of plasmid. The vial of *E. coli* and plasmid DNA was incubated on ice for 30 minutes before undergoing heat shock for 45 seconds in a 42°C water bath. The vial was immediately placed on ice for 2 minutes, after heat shock. Next, 250µL of pre-warmed super optimal broth with catabolite repression (S.O.C) media (Thermofisher) was added to the vial. Vials were placed in a horizontal shaker at 225rpm at 37°C for 1 hour. Both 25µL and 100µL of transformed *E. coli* were spread on agar plates containing 100µg/ml Ampicillin to positively select transformed bacterial colonies. Plates were incubated overnight at 37°C, 5% CO_2. Individual colonies were scraped from the agar plate and added to 25ml of warm nutrient broth (Sigma-aldrich) containing 100µg/ml ampicillin. The mixture was placed in a 37°C shaker at 220rpm for 8 hours. This mixture was then added to 100ml of nutrient broth and incubated in a 37°C shaker at 220rpm overnight.

2.6.3 Plasmid Midiprep

The midiprep was conducted using the Qiagen® Kit (cat. 12143). The bacterial culture was centrifuged at 6000xg for 15 minutes at 4°C to form a large pellet and discard excess broth. The pellet was resuspended in 4ml of buffer P1. Next, 4ml of buffer P2 was gently added to the mixture and inverted 5-6 times, then incubated for 5 minutes at room temperature to lyse the *E. coli*. Next, 4ml of P3 buffer was added and mixed vigorously before being incubated on ice for 15 minutes to precipitate DNA, proteins, and cell debris. After incubation, the micture was centrifuged at 20000xg for 15 minutes at 4°C. The supernatant, containing plasmid, was removed and the pellet discarded. The QIAGEN-tip 100 was equilibrated by applying 4ml of QBT buffer until all of the buffer had run through the tip by gravity. Next, the supernatant was added to the tip in order to collect

the plasmid within the resin. Once the supernatant had passed through the tip, a wash step was carried out to remove any contaminants by applying 2x10ml of QC buffer. DNA was then eluted from the resin in 5ml of QF buffer, and collected in a 15ml tube. Precipitation of DNA was achieved by adding 10ml of 100% ethanol and mixing. The solution was then aliquoted into eppendorfs and placed in a 4°C centrifuge at 10000xg for 10 minutes. The ethanol was then tipped off and left upside down to dry, leaving only a pellet of DNA. Next, 1ml of 70% ethanol was added to wash away any salts remaining in the DNA pellet. The sample was then centrifuged at room temperature, 10000xg for 3 minutes. The ethanol was then pipetted off and the remaining ethanol was left to evaporate overnight. Finally, the pellets were resuspended in 30µl dH_2O and combined before measuring DNA purity and concentration on the nanodrop (described above).

To ensure that the plasmids had been copied without base-pair errors, they were sent for Sanger sequencing. Due to the large size of the plasmids, 9kbp, only the active portion of the plasmid was sequenced. Sanger sequencing requires a primer, DNA polymerase, normal deoxynucleotidetriphosphates (dNTP) and di-deoxynucleotidetriphosphates (ddNTP) that are modified to have a specific fluorescent dye attached based on the dNTP present. This allows the precise sequence of the plasmid to be determined by measuring the colour of the fluorescent dye.

2.6.4 Lentivirus Production - FuGENE® HD

Human embryonic kidney (HEK) cells were used to package the lentiviral plasmids. They were grown in a T25 flask until 70% confluent. In an eppendorf, 2.85µg transfer plasmid, 0.7µg packaging plasmid, and 2.15µg envelope plasmid were mixed in 600µl of Opti-MEM reduced serum media (Thermofisher). In a

separate eppendorf, 17.1µl FuGENE® HD, a nonliposomal transfection reagent, was mixed with 600µl Opti-MEM. The contents of these eppendorfs were then mixed and left at room temperature for 15 minutes to allow of the DNA and transfection reagent to combine. Next, media was aspirated from HEK cells and washed with PBS. The plasmid transfection mixture was incubated overnight. The transfection mix was then aspirated and replaced with antibiotic free growth medium for 48 hours. After 48 hours the media, containing lentivirus, was harvested and centrifuged at 1000xg for 3 minutes to pellet cell debris.

2.6.5 Lentivirus production – Polyethylenimine (PEI)

Another method of lentivirus production used in this thesis involved the use of PEI (Sigma-Aldrich) as a transfection reagent, instead of FuGENE® HD. PEI was prepared by dissolving in dH_2O to achieve a final concentration of 1mg/ml and adjusting to pH 7 using HCL. It was then filtered by a 0.22µm filter to remove insoluble material. HEK cells were grown to 70% confluency. A total of 20µg of plasmid DNA was added to 150µl Opti-MEM reduced serum media (Thermofisher) (10µg transfer plasmid, 3.3µg packaging plasmid, and 6.7µg envelope plasmid). The volume of PEI added to the tube varied between a ratio of 1:1, 2:1, or 3:1 PEI to DNA. The mixture was incubated at room temperature to allow negatively charged DNA to associate with positively charged PEI. Next, half of the growth media was removed from HEK cells and this Opti-MEM, DNA, and PEI mixture was added to the HEK cells for 48 hours. After 48 hours the media, containing lentivirus, was harvested and centrifuged at 1000xg for 3 minutes to pellet cell debris.

2.6.6 Lentivirus detection

Lenti-X GoStix (Takarabio) are a rapid qualitative tool determine successful packaging of lentivirus. The Lenti-X GoStix measure the

lentiviral capsid protein p24, but do not show whether the lentivirus is active, only that it has been successfully packaged.

20µl of supernatant was added to the Lenti-X GoStix well. Next, 3 drops of Chase Buffer were added to the well and bands were left to develop for 10 minutes. There is an internal control band always develops and a sample band that develops if p24 is detected in the sample. If the sample band and control band are of similar intensity, it indicates your sample has more than $5x10^5$ IFU/ml (infectious units per ml).

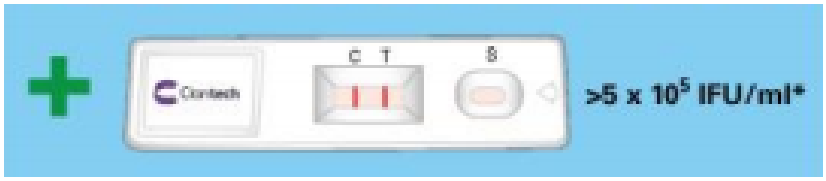

Image taken from Lenti-X GoStix (Takarabio) protocol.

2.6.7 Lentivirus Transduction

Target cells were seeded at a density of $1.5x10^5$cells/ml to achieve 70% confluency. Lentiviral media was added to the target cells so that is comprised either 25%, 50%, 75%, or 100% of the total volume of growth media depending on the lentiviral titer. Lentiviruses have a negatively charged membrane, thus they are repelled from the surface of target cells. To overcome this, the cationic polymer, polybrene (Sigma-Aldrich) 8µg/ml, was added to the growth media to neutralise the negatively charged cell membrane. This allows the lentivirus to interact with the cell membrane and insert its RNA into the host cell. The target gene is then reverse transcribed by reverse transcriptase before being integrated into the host genome by integrase. Cells were incubated with the lentiviral media for 3 days.

2.6.8 Positive Selection of Cells Transfected with Lentivirus

The target genes in this thesis included a puromycin resistance gene to allow positive selection of transduced cells. First, a kill curve was produced by treating target cells with an ascending concentration of puromycin up to 8000ng/ml. Each concentration of puromycin was carried out in triplicate wells. Cells were incubated with puromycin for 3 days until cell viability was assessed via 3-[4,5-dimethylthiazol-2-yl]-2,5-diphenyltetrazolium bromide (MTT) (Sigma-Aldrich) assay. Cells were incubated at 37˚C, 5% CO_2 for 30 minutes with 0.5mg/ml. Next, media was aspirated and cells washed with PBS before the addition of 50µl DMSO. Absorbance at 550nm was measured on an Omega FLUOstar® plate reader.

Once cells had been incubated with lentivirus, transduced cells were positively selected. The lowest concentration of puromycin (Sigma-Aldrich) that killed all cells after 3 days, as determined by the kill curve, was used. Cells were incubated with this concentration of puromycin in growth media for 3 days.

2.6.9 Counting GFP positive cells

Cells transduced with lentivirus containing a *GFP* gene were counted to determine transduction efficiency. Four random areas of the 6-well plate were selected and marked with a dot. A light microscope was aligned with the dot at X100 magnification. Both, the total number of cells, and GFP positive cells, within the field of view were manually counted. Cells were deemed GFP positive if they were green. The total number of cells and GFP positive cells in each area were added together and the following formula was used to determine transfection efficiency:

Transfection efficiency = (GFP positive cell no./Total cell no.) x 100

2.7 Cyclical Mechanical Cell Stretching

2.7.1 Principle

This process has been designed to replicate breathing where constant contraction and cell elongation occurs and uses the Flexcell® FX-5000™ Tension System. Contrary to active contraction, cell stretching is a process whereby cells elongate passively. Cells were cultured on a flexible membrane that can be placed on a fixed post. A vacuum pump is used to pull the flexible membrane over the post which results in equibiaxial cell stretching. Both the frequency and amplitude of stretching can be changed so that it can replicate breathing in difference species. Tidal breathing in mice occurs at a frequency of 1Hz, whereas humans do so at 0.3Hz. The percentage of elongation can also be changed by the user from 5% to 25% elongation, allowing replication of tidal breathing or of deep inhalation.

2.7.2 Methods

Cells were plated at $2x10^5$cells/ml to achieve 100% confluency on collagen I coated BioFlex® six-well plates and serum starved 24 hours prior to stretching. Collagen I coated plates were used because previous work from a member of our laboratory found that cells don't adhere to uncoated plates after a long stretching regimen. All cells were plated on duplicate collagen I coated BioFlex® plates so that one could be stretched and another left unstretched to use as a control. Lubricant was applied to the fixed post of the Flexcell® to allow the membrane to stretch freely. The plates were placed on the Flexcell® posts and put in a cell culture incubator. A piece of Perspex was placed on top of the plates to ensure that they did not moved while undergoing a stretching regimen. Unstretched plates were placed in the incubator separately. A program was run with a

specified frequency and percentage of elongation over a period of time ranging between 4 and 48 hours.

2.8 RhoA G-LISA Activation Assay

2.8.1 Principles

The RhoA G-LISA® (Cytoskeleton) is an enzyme-linked immunoabsorbent assay (ELISA) designed to detect activated RhoA (RhoA<GTP>). The kit contains a RhoA<GTP>-binding protein linked to the 96 well plate, which binds RhoA<GTP> while RhoA<GDP> is removed during wash steps. A positive control containing concentrated RhoA is included in the assay to ensure that the assay is detecting the protein. A negative control with only lysis buffer is used as a blank, and samples that had not been stimulated with LPA were used to show baseline RhoA activation in ASM cells. In each sample, RhoA activation is determined by comparing activated versus non-activated lysates. It is essential to keep all samples ice-cold until they are added to the ELISA plate to prevent hydrolysis of GTP to GDP. This assay does not determine the concentration of activated RhoA, but shows whether RhoA is activated, or not, and allows relative activation to be compared between sample conditions.

2.8.2 Method

Cells in 6-well plates were stimulated with LPA (Sigma-Aldrich) for 3 minutes. At 3 minutes, cells were washed with ice-cold PBS and 80µl lysis buffer added to wells. Lysate was transferred to pre-chilled eppendorf tubes and centrifuged at 10,000xg for 1 minute. 2 x 5µl lysate was transferred to a 96-well plate for protein quantification, while remaining lysate snap-frozen in liquid nitrogen.

To determine protein concentration 295µl Precision Red was added to 5µl sample lysate and incubated at room temperature for 3 minutes. Absorbance was measured at 600nm. The value was multiplied by 7.5 to give protein concentration. All samples were equalised to a concentration between 0.4-2mg/ml.

RhoA G-LISA strips were activated by adding 100µl ice-cold dH_2O. A positive control was prepared by adding 12µl reconstituted RhoA protein to 48µl lysis buffer and 60µl binding buffer. A blank was made up of 60µl lysis buffer and 60µl binding buffer. Samples were equalised immediately before the ELISA by adding ice cold lysis buffer. Samples were then prepared by adding 60µl ice-cold binding buffer and 60µl sample lysate to a chilled eppendorf and vortexed for 5s. A volume of 50µl was added to the ELISA plate in duplicate and placed on a cold orbital shaker set to 400rpm at 4°C for 30 minutes. The ELISA plate was then washed twice before adding 200µl of antigen presenting buffer for 2 minutes. The ELISA plate was washed 3 times before 50µl anti-RhoA antibody, previously diluted 1/250, was added and left to incubate for 45 minutes on an orbital shaker set at 400rpm at room temperature. The plate was then washed 3 times before a secondary HRP labelled antibody, previously diluted 1/62.5, and incubated on an orbital shaker at 400rpm for 45 minutes at room temperature. Detection reagent was prepared by mixing equal volumes of solution A and B. The ELISA plate was then washed 3 times and 50µl detection reagent was added per well and incubated at 37°C for 12 minutes. To stop the reaction 50µl stop solution was added and the results were collected by reading the absorbance of each well at 490nm.

2.9 Statistics

Data is expressed as median ±interquartile range (IQR) unless otherwise stated. Statistical analysis of two groups used a Mann-

Whitney U test because this is a non-parametric test and the number of replicates in most experiments were low. With low replicate numbers it is not possible to determine if data is parametric. The Mann-Whitney U test ranks data points into groups for comparison and does not take into account the size of the change, only whether there is a change or not. A limitation is that there cannot be a p value 0.05 with three replicates, no matter how large the effect size is.

For multiple comparison tests a one-way Kruskal-Wallis ANOVA was used. This test compares the means of three or more groups and determines whether there is a difference between two or more group means. It does not, however, determine which groups have a difference. This requires a follow up test. In this thesis a Dunnetts test was used because it compares all of the group means with a control mean.

A one-sample t-test was used once during this thesis because the data had been processed so that the control was equal to 1 and all groups were relative to the control. The test compares the mean of all groups with a single sample. This test requires approximately normal distribution and no significant outliers.

An unpaired t-test has been used in this thesis to compare a groups containing six cell lines. This test assumes normal distribution and compares the means of two groups to determine whether there is a significant difference. Unlike the Mann-Whitney U test, the t-test takes into account the size of the difference between two groups.

3 Chapter 3 Optimisation of lentivirus production and transduction

3.1 Rationale

Asthma is a chronic inflammatory disease of the airways. Asthma pathology is characterised by airway hyper-responsiveness, bronchoconstriction, and airway remodelling. 5.4 million people in the UK suffer from asthma with 1.1 million children and 4.3 million adults (Asthma UK). 10% of asthma patients suffer from severe asthma and do not respond to available treatments. This results in frequent and uncontrolled asthma attacks that trigger structural changes within the airway, known as airway remodelling.

Airway remodelling is a term that describes the structural changes seen in the asthmatic lung, including subepithelial fibrosis, ASM hypertrophy and hyperplasia, loss of epithelial integrity, angiogenesis, and goblet cell hyperplasia (240). These structural changes increase airway resistance and therefore reduce lung function (241). TGFβ is a pleiotropic cytokine that is central to airway remodelling in asthma (223, 242). TGFβ is able to induce epithelial apoptosis and epithelial-mesenchymal transition (65, 243). Subepithelial fibrosis describes thickening and fibrosis of the airways caused by deposition of excess ECM such as collagens, fibronectin, and proteoglycans (73, 223, 244). Differentiation of fibroblasts to myofibroblasts, the primary source of excess ECM deposition in the asthmatic airway, is induced by TGFβ (78, 79). Increased ASM mass is a key feature of airway remodelling in severe asthma, resulting in stronger contractions of the airways during exacerbation. TGFβ induces ASM cell proliferation and migration, resulting in increased ASM mass (242). Both goblet cell hyperplasia and angiogenesis have been linked to the effects of TGFβ in the asthmatic airways (117, 231).

Determining the precise activation pathway of TGFβ is therefore important to identify potential treatment strategies to prevent airway remodelling. In mice, knockout of $G_{\alpha q/11}$ in the alveolar epithelium prevented a force-induced increase in TGFβ activation (127). In human epithelial cells, $G_{\alpha q}$ is required for LPA-induced TGFβ (128). This has led to the hypothesis that the heterotrimeric G-proteins $G_{\alpha q/11}$ are required for TGFβ activation in ASM cells.

One of the methods of testing this was to genetically knockdown $G_{\alpha q/11}$ and there are multiple methods available to achieve genetic knockdown. This could be done by using transient gene knockdown of mRNA by using targeted siRNA. This has the advantage of being a relatively quick method genetic manipulation and can functionally reduce the mRNA and protein target. However, it is difficult to achieve complete protein knockout within the cell, the effect is transient, and siRNA is most effective in dividing cells (245).

Clustered regularly interspaced short palindromic repeats (CRISPR) is a genome editing technique adapted from the defence mechanism of bacteria against bacteriophage (246). When bacteria are infected with bacteriophage they capture DNA fragments from the bacteriophage and create CRISPR arrays. Upon infection of the same, or similar virus, the bacteria use the CRISPR array to transcribe RNA that is complementary to the bacteriophage DNA, which it binds to and signals DNase enzymes to cut the DNA thus disabling the virus (247). CRISPR is frequently used to knockdown gene expression and is described as a cheap and easy method to employ. An RNA guide sequence is designed that binds to the target DNA and endonuclease. The enzyme then cuts the DNA at the target and the DNA is repaired, deleting the target gene. There are challenges achieving complete knockout with CRISPR, for example it can have off-target effects due to binding to sequences that are not perfectly complimentary with 3-

5 base pair mismatches, resulting in mutations in unwanted genes (248). The guide RNA sequence can greatly affect the cleavage capability of the target gene. Guide RNA that forms strong secondary structures have a reduced ability to cleave the target gene, thus, a panel of guide RNA should be tested in a cleavage assay to determine efficacy before being introduced into the target cell (249).

Lentivirus are derived from human immunodeficiency virus (HIV-1) and can be used as a gene delivery vector that has the ability to infect both dividing and non-dividing cells (250). This is possible because the virus traverses the plasma membrane by endocytosis and can interact with nuclear import apparatus to enter the nucleus (251). An advantage of using lentivirus as a gene delivery vector is that they can integrate genetic material into the host genome for stable and long-term expression (252, 253). The components to produce lentivirus are split across 3 plasmids and are replication incompetent to increase safety. These plasmids consist of a lentiviral transfer plasmid, packaging plasmid, and envelope plasmid (254). The lentiviral transfer plasmid contains the gene of interest surrounded by long terminal repeat sequences, which allow the plasmid sequence to be incorporated into the host genome. The packaging and envelope plasmids encode components of the viral capsid. To produce an active lentivirus, all three plasmids are combined in 'packaging cells', usually HEK T293 cells (255). Lentivirus is then produced and released into the media, which can be used to transfect target cells.

Our laboratory had acquired $G_q^{fl/fl}G_{11}^{-/-}$ mice from Professor Stefan Offermanns, Max-Planck-Institute for Heart and Lung Research, Germany. These mice had a 'floxed' $G_{\alpha q}$ gene and $G_{\alpha 11}$ knocked out. The term floxing refers to a gene that has been sandwiched between two *Lox P* sites. These can be recombined by Cre recombinase, a

tyrosine recombinase enzyme from bacteriophage. The result of Cre recombination of *Lox P* sites is deletion of the sandwiched gene, thus creating a stable genetic knockdown of the target gene, in this case $G_{\alpha q}$. ASM cells from the $G_q^{fl/fl}G_{11}^{-/-}$ mice were isolated from the tracheae. This was done by sacrificing the mice in order to remove the tracheae, dissecting it into quadrants, and sticking them down to a tissue culture plate. The cells were then expanded to create stocks for lentiviral transfection. The principle of this chapter was to transfect the $G_q^{fl/fl}G_{11}^{-/-}$ ASM cells with lentivirus containing a Cre-recombinase plasmid to generate a cell with a stable $G_{\alpha q/11}$ knock down.

3.2 Aims

Generate lentivirus containing a plasmid encoding Cre-recombinase. Transfect murine $G_q^{fl/fl}G_{11}^{-/-}$ ASM cells with lentivirus to generate a cell line with stable knockdown of $G_{\alpha q/11}$.

3.3 Results

3.3.1 Amplifying plasmid stocks and generating puromycin resistant lentivirus

The lentiviral transfer, packaging, and envelope plasmids were a gift from Professor Maddy Parsons, Kings College London. The transfer plasmid encoded *Cre*, which would induce removal of $G_{\alpha q}$, and a puromycin resistance gene to allow positive selection of transduced cells. A small quantity was delivered and therefore needed to be amplified to create a stock. Competent *E. coli* were transformed with each plasmid individually and left to grow overnight. Transformed *E. coli* were harvested the following day and a Qiagen midiprep kit was used to isolate the amplified plasmid stocks (figure 3.1A). Next, murine $G_q^{fl/fl}G_{11}^{-/-}$ ASM cells were cultured and exposed to an increasing concentration of puromycin for 3 days. An MTT assay was conducted to assess cell viability and generate a kill curve (figure 3.1B). There was a linear reduction in cell death from no puromycin to 1000ng/ml where maximum cell death was reached. There was a plateau from 1000ng/ml to 8000ng/ml. Therefore 1000ng/ml puromycin was the optimum concentration to use for positive selection of cell transduced with puromycin resistance.

A

Plasmid Name	Plasmid Stock (ng/µL)
pMDG	383
p8.91	414
pLKO Cre	353

B

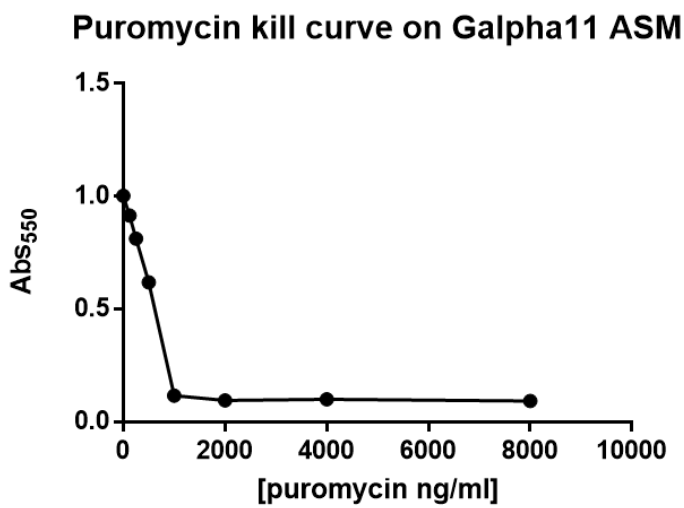

Figure 3.1. The transfer plasmid pLKO Cre, envelope plasmid p8.91, packaging plasmid pMDG were amplified to generate a stock, A. Murine $G_q^{fl/fl}G_{11}^{-/-}$ ASM cells were treated with an increasing concentration of puromycin for 3 days and cell viability was determined by an MTT assay, (n=1) B. Data points represent the mean of 3 internal replicates.

Next, I sought to produce active lentivirus that could be used to transduce the murine $G_q^{fl/fl}G_{11}^{-/-}$ ASM cells. This would incorporate Cre recombinase into the host genome and generate a double knockout of $G_{\alpha q}$ and $G_{\alpha 11}$. First, 2.85µg transfer plasmid, 0.7µg packaging plasmid, and 2.15µg envelope plasmid were combined in with FuGENE® HD transfection reagent in a flask containing the packaging cells HEK T293 for transfection. The virus was produced and released into the media which was collected after 48 hours (figure 3.2A). To confirm that lentivirus had been produced, the supernatant was applied to Lenti-X GoStix, which confirmed the presence of the structural virus capsid protein p24 (data not shown). Supernatant was aliquoted and stored at -80°C for further use.

Transduction was initially attempted in wild-type murine embryonic fibroblasts (WT MEFs) because they are easier to transfect than primary cells and therefore represented a good cell type to validate whether the lentivirus was viable. The DNA to be delivered into the host cells included *Cre recombinase* and a puromycin resistance gene. Lentiviral media from frozen stock was mixed with normal growth media to make up 25%, 50%, or 75% of the total media. Media was then applied to WT MEFs, grown to 100% confluence, in a 6-well tissue culture plate and incubated for 3 days to allow transduction to take place. After 3 days, lentiviral media was replaced with normal growth media containing 1000ng/ml of puromycin, as determined by the kill curve (figure 3.1B), and incubated for 3 days for positive selection to take place. However, no cells survived positive selection indicating that transduction did not take place (no data shown). This could have been due to low yield of lentivirus in the packaging step, or due to lentivirus losing viability. Next, lentiviral transduction was repeated in WT MEFs. *Cre* expression was measured as an endpoint to determine whether gene

transduction was successful and the lentivirus was viable. Fresh lentiviral media was used directly from packaging cells instead of using frozen lentiviral media as described above. Lentivirus-containing supernatant was diluted in normal media to make up 25%, 50%, or 75% of the total media volume and applied to WT MEFs for 6, 8 or 52 hours (figure 3.2B). *Cre* was measured by QPCR in WT MEFs to determine whether the lentivirus had successfully incorporated into the host genome. The positive control was a sample of whole lung protein collected from mice that had *Cre* expression restricted to epithelial cells. *Cre* expression was observed in all samples that were exposed to lentivirus regardless of the percentage of lentiviral supernatant applied or the exposure time (figure 3.2C). *Cre* expression in the WT MEFs that were exposed to 75% lentiviral supernatant for 52 hours was highest with expression 40-fold higher than the control. *Cre* expression in samples that were exposed to lentivirus for 6 hours show a percentage-dependent increase, with 25% and 50% lentiviral media having 6-fold and 10-fold *Cre* expression respectively versus the positive control.

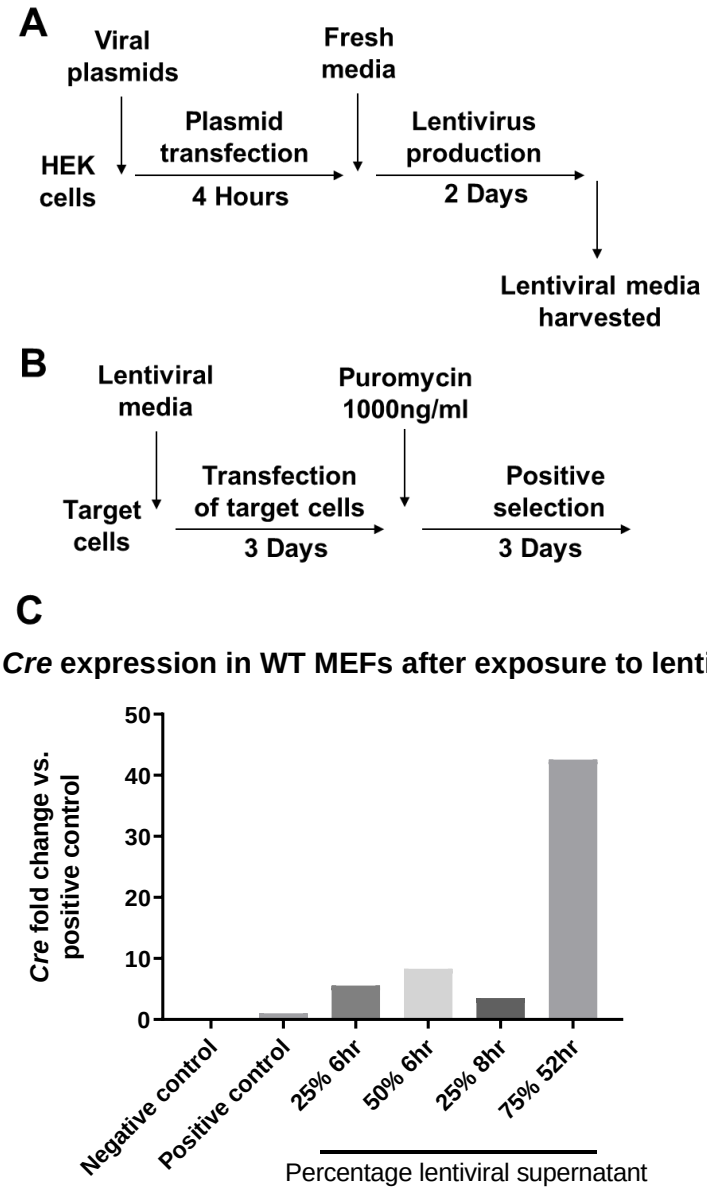

Figure 3.2. The process of producing lentivirus using packaging cells, A. The process of transducing target cells with lentivirus, B. WT MEFs were treated with different percentages of lentiviral supernatant for 6, 8, or 52 hours and *Cre* expression was measured by QPCR, (n=1 experiment) C.

Due to successful transduction of *Cre* in WT MEFs using fresh media, transduction of WT MEFs and positive selection was carried out. Fresh lentiviral media comprising 25%, 50%, 75%, or 100% of the total growth media was applied to WT MEFs, grown to 100% confluence, in a 6-well plate. WT MEFs were incubated with lentiviral media for 3 days. Lentiviral media was then replaced with fresh growth media containing 1000ng/ml puromycin for positive selection of transduced cells. After 3 days there were 3 small colonies of cells in the well containing 100% lentiviral media, however they did not expand (data not shown).

3.3.2 Transduction of cells using a transfer plasmid containing GFP

Lentiviral transduction of WT MEFs with Cre was successful. Next, I wanted to transduce $G_q^{fl/fl}G_{11}^{-/-}$ ASM cells with *Cre* and puromycin resistance, and positively select transduced cells to generate a double knockout of $G_{\alpha q}$ and $G_{\alpha 11}$. The experimental methods discussed in the previous section were repeated on $G_q^{fl/fl}G_{11}^{-/-}$ ASM cells, however all of the cells died upon addition of puromycin because transduction did not occur (no data not shown).

At this point 2 things were changed to improve transduction and efficiency and analysis:

1. A lentiviral plasmid encoding GFP instead of a puromycin resistance was used to allow visual identification of transduction and,
2. The transfection reagent FuGENE® HD was swapped with polyethylenimine (PEI) to improve transfection of packaging cells and lentivirus yield.

Lentivirus was produced in packaging cells that had been transfected using a PEI to DNA ratio of either 3:1, 2:1, or 1:1. GFP positive packaging cells were observed when harvesting supernatant, indicating that lentiviral production had been successful. Supernatant from the three conditions was transferred to the target HEK T293 cells for 48 hours. Four random areas of the tissue culture plate were selected for counting of GFP positive cells and percentage transfection calculated (figure 3.3A). There was a small PEI to DNA ratio-dependent increase in GFP positive cells. The highest transduction percentage was 42% at a 3:1 PEI to DNA ratio with the lowest at 24% from 1:1 PEI to DNA.

Next, I repeated the experiment targeting $G_q^{fl/fl}$ $G_{11}^{-/-}$ murine ASM cells with lentivirus (figure 3.3B). There was small ratio-dependent

increase in GFP positive cells, however the transduction percentage was very small. A PEI to DNA ratio of 3:1 elicited the highest transfection percentage of 6%, compared to 1% in cells that were treated with supernatant from 1:1 DNA to PEI. Proportionally the ratio-dependent increase in transduction was similar between WT MEFS and $G_q^{fl/fl}G_{11}^{-/-}$ murine ASM cells however the total efficiency was approximately 90% lower. Due to the low transfection efficiency in the primary $G_q^{fl/fl}G_{11}^{-/-}$ murine ASM cells the lentivirus experiments were stopped.

A

HEK T293 transfected with lentiviral supernatant on 30th Nov 17						
Packaging cell PEI ratio	3:1		2:1		1:1	
Area	Total Cells counted	GFP positive cells	Total Cells counted	GFP positive cells	Total Cells counted	GFP positive cells
1	82	28	85	47	192	54
2	105	51	153	27	177	13
3	79	21	91	25	82	19
4	179	82	187	64	159	143
Total	611	255	630	206	746	148
Transfection %	42%		32%		24%	

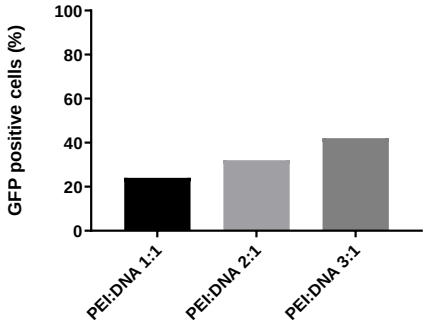

B

$Cre^+/G_q^{fl/fl}G_{11}^{-/-}$ murine ASM cells transfected with lentiviral supernatant on 29th Jan 18						
Packaging cell PEI ratio	3:1		2:1		1:1	
Area	Total Cells counted	GFP positive cells	Total Cells counted	GFP positive cells	Total Cells counted	GFP positive cells
1	60	2	35	2	45	0
2	51	11	61	4	30	0
3	30	0	81	3	35	1
4	81	1	60	0	37	1
Total	222	14	237	9	147	2
Transfection %	6%		4%		1%	

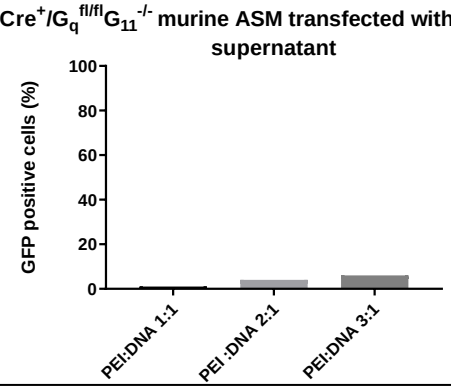

Figure 3.3. Lentiviral supernatant from packaging cells transduced with a PEI:DNA ratio of 1:1, 2:1, and 3:1 was used to transduce HEKS and $G_q^{fl/fl}G_{11}^{-/-}$ murine ASM cells with lentivirus, A+B. GFP positive cells were counted from 4 random areas using a fluorescent microscope. HEK T293 cells had a ratio-dependent increase in transduction, maximal at 42% (n=1 experiment), A. $G_q^{fl/fl}G_{11}^{-/-}$ murine ASM cells also showed a ratio-dependent increase in transduction, maximal at 6% (n=1 experiment), B.

3.4 Discussion

TGFβ plays a key role in fibrotic disease and has been identified as central to airway remodelling in asthma. Previous work has highlighted that $G_{\alpha q}$ and RhoA are required for LPA-induced TGFβ activation in mouse embryonic fibroblasts (128). Knockout of epithelial $G_{\alpha q}$ and $G_{\alpha 11}$ in mice inhibited force-induced increase in total lung TGFβ (127). These studies suggest that $G_{\alpha q}$ and $G_{\alpha 11}$ might be important for TGFβ activation in asthma. The aim of this thesis was to determine whether $G_{\alpha q}$ and $G_{\alpha 11}$ were required for LPA and stretch induced TGFβ activation in ASM cells.

Transgenic mice with a double knockout of $G_{\alpha q}$ and $G_{\alpha 11}$ die at embryonic day 11, and mice with only one allele of either $G_{\alpha q}$ or $G_{\alpha 11}$ die shortly after birth with cardiac malformation and craniofacial defects (256). This chapter set out to produce a primary ASM cell line with stable genetic knockdown of $G_{\alpha q}$ and $G_{\alpha 11}$. Using a stable genetic knockdown has significant advantages in comparison to transient genetic knockdown; there is complete knockout of the gene and protein, experimental time courses are not limited by transient knockdown, and the cell line could be kept as a tool for future use.

Lentiviruses are a subtype of retroviruses and can have long incubation periods. Perhaps the most well-known lentivirus is Human Immunodeficiency Virus (HIV). Lentiviral vectors are efficient gene delivery tools that induce long-term gene expression. They are able to traverse the plasma membrane due to the envelope protein VSV-G and enter the host cell nucleus by interacting with nuclear import complexes (251). An advantage using lentivirus as a gene delivery tool is that it can transduce both dividing and non-dividing cells (252). They are designed to be replication deficient so once they integrate into the host genome they become inactive.

To acquire the ASM cells $G_q^{fl/fl}G_{11}^{-/-}$ mice were sacrificed and ASM cells from the tracheae were harvested. These mice were $G_{\alpha q}$ floxed and $G_{\alpha 11}$ null. Floxing is a mechanism whereby *LoxP* promotor sites are introduced to flank a target gene. These sites are recognised by Cre recombinase, a tyrosine recombinase enzyme, and recombined thus removing the target gene. My aim was to generate a lentivirus containing *Cre* and a puromycin resistance gene that could transfect the $G_q^{fl/fl}G_{11}^{-/-}$ ASM cells to knockout $G_{\alpha q}$ and $G_{\alpha 11}$. Transfected cells would undergo positive selection by incubation with puromycin.

First, I amplified the plasmid stocks that had been received as a gift from Professor Maddy Parsons, Kings College London. To achieve this, *E. coli* were transformed with the transfer, envelope, and packaging plasmids. Plasmid concentrations were measured by using a nanodrop, which showed that there was a sufficient concentration to store them as a stock for lentivirus generation (figure 3.1).

To produce active lentivirus, the transfer, packaging, and envelope plasmids had to be combined in a packaging cell. Typically HEK T293 cells are used for lentiviral packaging because they are easy to transfect and grow rapidly (255). Commercially available FuGENE® was the transfection reagent used in experiments that were producing lentivirus containing *Cre* and puromycin resistance. To confirm that lentivirus had been produced, the supernatant was applied to Lenti-X GoStix, which confirmed the presence of the structural virus capsid protein p24 (data not shown). This indicated that lentiviral production had been successful. However, directly measuring p24 often overestimates the quantity of active lentivirus because it measures total p24 within a sample regardless of whether it is in an active viral capsid (257). Another method for measuring lentivirus is to measure viral RNA using qPCR targeting specific viral structural genes, however this also tends to overestimate active virus

(257). Lentivirus can be measured using functional assays that measure effects of the virus in target cells. Examples include, using antibiotic resistance and measuring the number of cell colonies that survive, or measuring the target gene by qPCR in target cells (257).

Initially, I transduced WT MEFs because they are fast growing and easy to transduce (254). Lentiviral media taken from frozen stocks, produced as described above, were diluted in media so that lentiviral media constituted 25%, 50%, or 75% of the total volume. After three days of incubation with lentivirus, media was replaced with fresh media containing 1000ng/ml of puromycin for positive selection of transduced cells. However, no cells survived, suggesting that there was no transduction. It is important to note that this experiment used frozen lentiviral media, which was intended to standardise experiments and allow consistent replication. Lentivirus, however, is difficult to store and rapidly degrades. A single freeze-thaw cycle has been shown to reduce infection efficiency by 33% (258). Moreover, lentivirus infection efficiency reduces exponentially every 1.4 days when stored at 4°C (258). Thus, it was decided that all further experiments would be carried out using fresh lentiviral media that did not require storing.

Next, fresh lentivirus media was diluted in normal media to make up 25%, 50%, or 75% of the total volume. I measured *Cre* expression by qPCR in WT MEFs that had been incubated with lentivirus to confirm that viable lentivirus was able to integrate into the cell genome. *Cre* was expressed in all cells that were exposed to lentiviral media. The percentage of lentiviral supernatant that WT MEFs were incubated with appeared to affect the *Cre* expression (figure 3.2C). WT MEFs treated for 4 hours with media composed of 50% lentiviral supernatant had a 4-fold increase in *Cre* expression compared 25% media. This fits with previous work that demonstrated incubating

cells with higher concentrations of lentivirus increases transduction (259). WT MEFs treated with 75% lentiviral supernatant for 52 hours had a 30-fold increase in *Cre* expression. Previous studies have shown that increased incubation time of lentivirus with target cells results in increased transduction efficiency (259). However, it is not possible to say whether more cells had been transfected with *Cre* because the lentivirus may have incorporated *Cre* multiple times into a single cell. The positive control used in this experiment used whole lung lysate from mice that expressed *Cre* in epithelial cells. This may explain why *Cre* in the samples were comparably high when compared to the positive control because the epithelial cells will have made up a small proportion of the whole lung lysate. These results confirmed that viable lentivirus was produced and able to transduce into the target gene into cells.

Expression of *Cre* had been observed in all WT MEFs incubated with fresh lentiviral media. This indicated that transduction was taking place. Next, I wanted to determine whether I could positively select WT MEFs that had been transduced. Again, cells were treated with fresh lentiviral media constituting 20%, 50%, 75%, or 100% of the total volume of media. There were a few small colonies of WT MEFs that survived three days of positive selection, however they did not expand. It is possible that the sheer amount of cell death that occurred due to low transduction efficiency resulted in the release of large quantities of anti-proliferative molecules, such as IL-1 and nitric oxide, thus preventing expansion of positively selected cells (260). This result was in contrast a previous experiment where no WT MEFs survived positive selection after incubation with frozen lentiviral media. However, it is important to note that there was a 100% lentiviral media condition added to this experiment.

To generate a stable cell line with $G_{\alpha q}$ and $G_{\alpha 11}$ knocked out I replicated transduction described above in $G_q^{fl/fl}G_{11}^{-/-}$ murine ASM cells. Incubation was left for 3 days before adding 1000ng/ml puromycin for positive selection. No cells survived puromycin insult indicating that transfection was unsuccessful (no data available). To overcome the lack of transduction in primary cells and optimise transduction I changed 2 things:

1. I acquired a transfer plasmid containing a GFP sequence to allow visualisation and rapid identification of transfected cells using a fluorescent microscope.
2. I changed my transfection reagent from FuGENE® HD to polyethylenimine (PEI) in order maximise transfection of packaging cells and therefore lentiviral concentration.

During the packaging and production of lentivirus I used PEI to plasmid DNA ratios of 1:1, 2:1, and 3:1. PEI is a highly branched polymer that condenses DNA to form positively charged particles (261). These are able to bind to the negatively charged cell surface and be endocytosed into the cell (262). HEK T293 cells were used for optimisation because they are easy to transduce, and incubated with 100% lentiviral supernatant. Random areas of the plate were selected to count GFP positive cells by microscopy to calculate transduction efficiency. There was a ratio-dependent increase in GFP positive cells. The highest transduction efficiency was 42% in cells with lentiviral supernatant produced with a 3:1 ratio of PEI to DNA. This was 2-fold higher than cells transduced with lentiviral supernatant from a PEI to DNA ratio of 1:1, which had a transfection efficiency of 24%. However, when this was replicated in $G_q^{fl/fl}G_{11}^{-/-}$ murine ASM cells transduction efficiency was far lower. Lentiviral supernatant produced with a PEI to DNA ratio of 3:1 elicited 6% transduction efficiency and a 1:1 ratio gave 1% efficiency.

Proportionally, the increase of transduction efficiency seen when changing the PEI to DNA ratio was similar in $G_q^{fl/fl}G_{11}^{-/-}$ murine ASM cells and HEK T293 cells, however the transduction efficiency was around 90% lower. The low transduction efficiency seen in $G_q^{fl/fl}G_{11}^{-/-}$ murine ASM cells transduced with GFP provides an explanation to the unsuccessful antibiotic selection. It suggests that either there was no transduction of the target gene or, transduction efficiency was far too low for a colony of cells to survive.

Retroviruses have a short half-life and the distance they can travel is limited to a few hundred microns by Brownian motion (263). In the past, methods such as flow-through transduction have been used to enhance transduction and overcome this physical restraint (264). More recently it was noted that both the cell surface and virus are negatively charged, creating electrostatic repulsion (265). The cationic polymer, polybrene, increases viral absorption into the cell by neutralising charge repulsion between the negatively charged cell surface and virus (265, 266). Polybrene was used in all of the experiments in this thesis to enhance lentiviral transduction, however transduction efficiency remained low. Transduction of any cell type can be challenging, however this is particularly true when transducing primary cells. This is evidenced in this thesis with the difference between HEK T293 cells and $G_q^{fl/fl}G_{11}^{-/-}$ murine ASM cells.

The low efficiency of transduction is likely to be the result of low lentivirus yield, thus reducing the likelihood of interaction and absorption of lentivirus into the ASM cells. Lentivirus can be concentrated by using ultracentrifugation at a relative centrifugal force (RCF) of 90,000xg for 1 hour (267). A more accessible method of concentrating lentivirus has been demonstrated using an RCF of 10,000xg for 4 hours with a 20% glucose gradient, and resulted in a 3-fold increase in transduction compared to un-concentrated

lentivirus (258). This particular method was not attempted, however if I were to try to carry out lentivirus transduction in the future I would. It would increase the concentration of lentiviral particles in supernatant and a smaller volume could be used thus allowing more particles to reach the cell surface before becoming inactive.

Another modern approach to gene editing is CRISPR-cas9. This process requires the design of RNA with a guide sequence that binds to the target gene and Cas9 enzyme. The enzyme then cuts the DNA at the target and the DNA is repaired, deleting the target gene. This method of gene editing is often described as easy and cheap. However, complete knockout isn't always achievable with CRISPR and it can have off-target effects due to mutations within the DNA (248). Analysis of knockout at the protein level using 4 guide RNAs per gene showed that CRISPR can be highly variable depending on the guide RNA sequence (268). A recent publication has used CRISPR to knockout $G_{\alpha q}$ and $G_{\alpha 11}$ in HEK T923 cells highlighting that this method can be successfully employed to analyse the role of GPCRs (269). Ultimately, lentivirus was the gene delivery tool that was used due to the availability of $G_q^{fl/fl}G_{11}^{-/-}$ mice where there was an opportunity to generate a cell line that had permanent and stable knockout of $G_{\alpha q}$ and $G_{\alpha 11}$.

In this chapter a series of steps have been carried out from amplifying individual lentivirus plasmids to transducing primary cells. Lentivirus production and lentiviral transduction have been improved throughout this chapter using PEI. Transduction of lentivirus into WT MEFs to induce *Cre* expression was successful, however there were challenges translating this into murine ASM cells. It was a similar story with transduction of GFP which was achieved in HEK T293 cells, but was minimal in murine ASM cells.

4 Chapter 4: Investigating the role of $G_{\alpha q/11}$ and RhoA in LPA-induced TGFβ activation in airway smooth muscle cells

4.1 Rationale

LPA is a water-soluble phospholipid present in all tissues of the body. LPA acts on five G-protein coupled receptors, LPA_1-LPA_5, and can regulate multiple cellular functions including proliferation, survival, growth, migration, and angiogenesis [see review (270)]. LPA_1 and LPA_2 couple to $G_{\alpha i/0}$, $G_{\alpha q/11}$, and $G_{\alpha 12/13}$, LPA_3 couples to $G_{\alpha i/0}$, $G_{\alpha q/11}$, not $G_{\alpha 12/13}$, and LPA_4 and LPA_5 couple to $G_{\alpha q/11}$, $G_{\alpha 12/13}$, and $G_{\alpha s}$ (271).

There have been studies in humans with allergic asthma showing LPA in the BAL increased in response to allergen challenge (272). Moreover, allergen challenge increases the concentration of autotaxin, an enzyme that synthesises LPA, in BAL of human asthmatic patients (273). Although the specific role of LPA in asthma is unknown, there have been suggestions that it could be involved in epithelial-barrier repair (272). Intranasal inhalation of LPA in healthy mice resulted in an increase in the murine homologue of IL-8, via PKC/NF-kappaB signalling, suggesting a role in airway inflammation (274). Moreover, inhibition of the LPA_2 receptor in a HDM model of asthma reduced airway inflammation and IL-4 and IL-5 concentration within the lung (275, 276). These studies suggest that LPA is a positive regulator of inflammation *in vivo*. LPA is present within many tissues, and is typically found at concentrations of 0.1μM in the blood plasma and 10μM in the serum (277).

In addition to its effect on airway inflammation, LPA enhances contraction and inhibits the relaxation of isolated tracheal rings (278), suggesting a potential role in asthmatic bronchoconstriction. Actin reorganisation occurs in human ASM cells treated with LPA. This

effect was prevented by a C3 exoenzyme that inhibits RhoA activation, and by a double siRNA knockdown of $G_{\alpha q}$ and $G_{\alpha i\text{-}2}$ (279).

LPA is known to activate TGFβ by altering actin dynamics via the small GTPase RhoA (280, 281). RhoA regulates Rho-kinase I/II (ROCKI/II), a serine/threonine kinase (282). The kinase activity of ROCKI/II is rendered inactive due to autoinhibitory intramolecular folding. Activation of RhoA occurs when a RhoGEF promotes exchange of GDP for GTP allowing it to bind to the Rho binding domain of ROCKI/II, which disrupts its autoinhibitory folding and thus activating its serine/threonine kinase activity (283). Both stress fibre formation and cell contractility are regulated by ROCKI/II. Stress fibres form when ROCKI/II phosphorylates LIM kinase, which in turn phosphorylates and therefore inhibits cofilin, an actin depolymerisation protein (figure 4.1) (284). Stress fibres cause integrins to cluster at the cell surface, forming large protein structures that connect the cell cytoskeleton to the ECM, called focal adhesions. Talin and integrin are mechanosensitive proteins found within focal adhesion complexes. Talin binds to the cytoplasmic portion of integrin in response to force, causing integrin to form an 'open' active structure. When active, integrin exposes its binding domain, which recognises an RGD motif found in the latent associated peptide that keeps TGFβ biologically inactive (285). LPA-induced TGFβ activation occurs via a RhoA-integrin αvβ6 pathway in bronchial epithelial cells (281). In contrast, the integrin αvβ5 is required for LPA and methacholine-induced TGFβ activation in airway smooth muscle cells (133).

As discussed in section 1.5.5 TGFβ plays a central role in the structural changes within the asthmatic airway, collectively known as airway remodelling. TGFβ has been shown induce epithelial apoptosis and epithelial-mesenchymal transition (65, 243), subepithelial

fibrosis (73, 223, 244), differentiation of fibroblasts to myofibroblasts (78, 79), increased ASM mass ASM cell proliferation and migration, resulting in increased ASM mass and strong airway contraction upon exacerbation (242). Furthermore, both goblet cell hyperplasia and angiogenesis have been linked to the effects of TGFβ in the asthmatic airways (117, 231).

Smooth muscle cell contraction occurs through two mechanisms. One mechanism occurs via phospholipase C (PLC), a membrane associated enzyme that catalyses the hydrolysis of phosphatidylinositol 4,5-bisphosphate (PIP_2) to diacyl glycerol (DAG) and inositol 1,4,5-trisphosphate (IP_3). IP_3 binds to calcium channels in the sarcoplasmic reticulum, causing an efflux of calcium into the cytosol. Calcium binds to calmodulin, which then binds to and activates myosin light-chain kinase (MLCK). Phosphorylated MLC induces cross-bridge cycling and contraction. Myosin light chain phosphatase (MLCP) acts as a 'brake' to contraction by dephosphorylating MLC. ROCKI/II is able to phosphorylate and inhibit MLCP via the RhoA/ROCK pathway, thus resulting in sustained contraction.

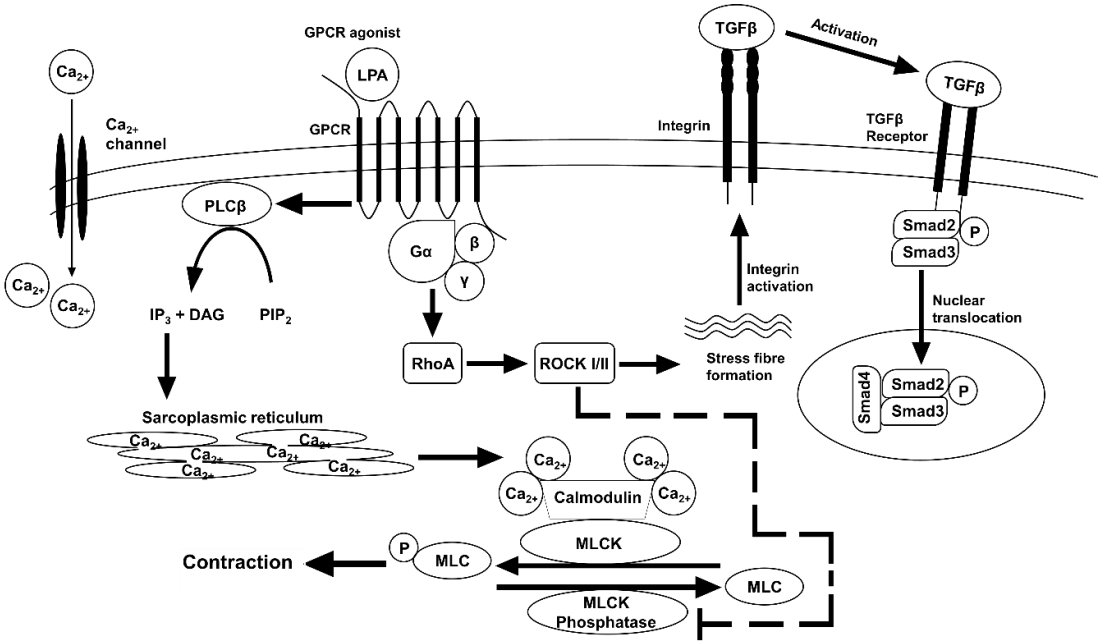

Figure 4.1. Diagram of the calcium-dependent and calcium-independent contraction pathways in ASM cells.

G-protein coupled receptors (GPCRs) are seven transmembrane receptors that couple with heterotrimeric G-proteins. GPCRs undergo conformational change upon ligand binding, allowing them to act as a GEF and bind an associated G-protein. GDP is exchanged for GTP in the G_{α} subunit causing dissociation of G_{α} from $G_{\beta\gamma}$ and allowing them to modulate intracellular signalling. There are four G-protein sub-classes, $G_{\alpha s}$, $G_{\alpha i/o}$, $G_{\alpha q/11}$, $G_{\alpha 12/13,}$ distinguished by sequence homology. While GCPRs tend to bind a particular class of G-proteins, they are capable of activating multiple classes. Moreover, ligand binding to a GPCR may activate multiple G-proteins, allowing for diverse array of downstream signalling events.

Traditionally, $G_{\alpha q/11}$ have been associated with initiating calcium-contraction signalling via PLCβ in smooth muscle cells, described above. On the other hand, $G_{\alpha 12/13}$ activate RhoA and therefore induce stress fibre formation. However, $G_{\alpha q}$ has been shown to activate TGFβ via a RhoA-integrin αvβ6 pathway in bronchial epithelial cells (128, 286). Moreover, mice with epithelial $G_{\alpha q/11}$ knockout had reduced

total TGFβ concentration in lung homogenate and were protected against TGFβ activation in response to high stretch ventilation (287). This suggests that downstream signalling pathways of G-proteins is cell type specific. The sub-class of G-protein that is required for TGFβ activation in ASM cells in currently unknown.

4.2 Aims

The G-protein class required for integrin-mediated TGFβ activation in ASM cells is not established. This chapter investigates whether $G_{\alpha q/11}$ and RhoA are required for LPA-induced TGFβ activation in ASM cells.

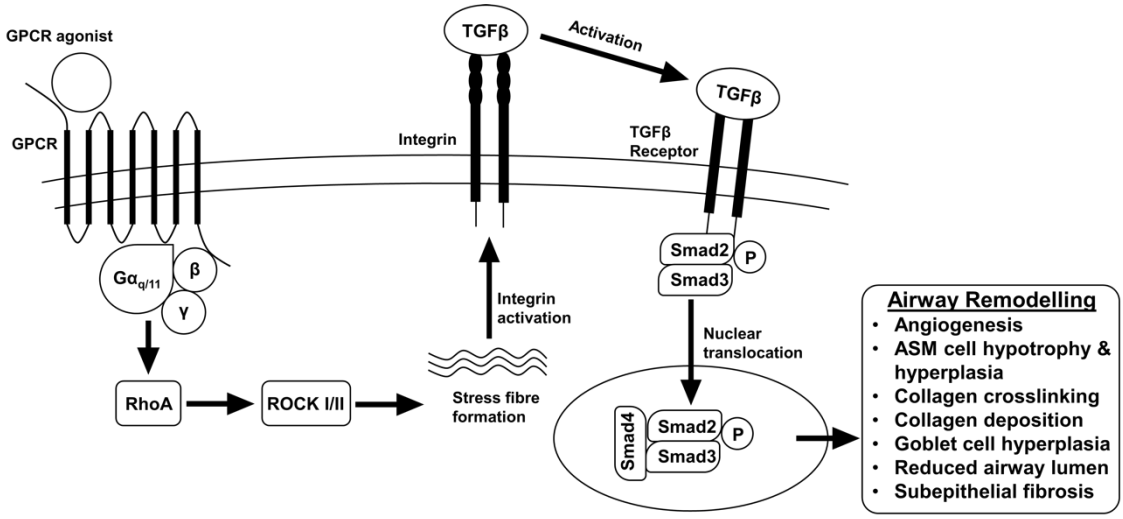

Figure 4.2 Hypothesised pathway leading to TGFβ activation in ASM cells.

4.3 Results

4.3.1 LPA activates RhoA and the TGFβ pathway in ASM cells

Before beginning to determine the role of the G-proteins $G_{\alpha q/11}$ on the TGFβ activation pathway in ASM cells, LPA concentration responses were carried out to confirm that the cells would activate the TGFβ in response to LPA. First, a coculture experiment where TMLC cells containing a plasmid encoding the TGFβ responsive portion of the *PAI1* promotor driving luciferase synthesis, were added to cultured ASM cells (133). This provided an indirect readout of TGFβ activation, proportional to bioluminescence. Raw bioluminescence was normalised to the no LPA control so data is shown as fold change versus control. Both asthmatic and non-asthmatic ASM cells responded in a concentration-dependent manner to LPA (figure 4.3). Asthmatic, but not non-asthmatic cells, had significantly increased TGFβ activation at 100μM LPA. The median magnitude of change was similar between non-asthmatic and asthmatic cells, however there was more variability in asthmatic cells and the fold-change was slightly higher at 1μM and 10μM LPA.

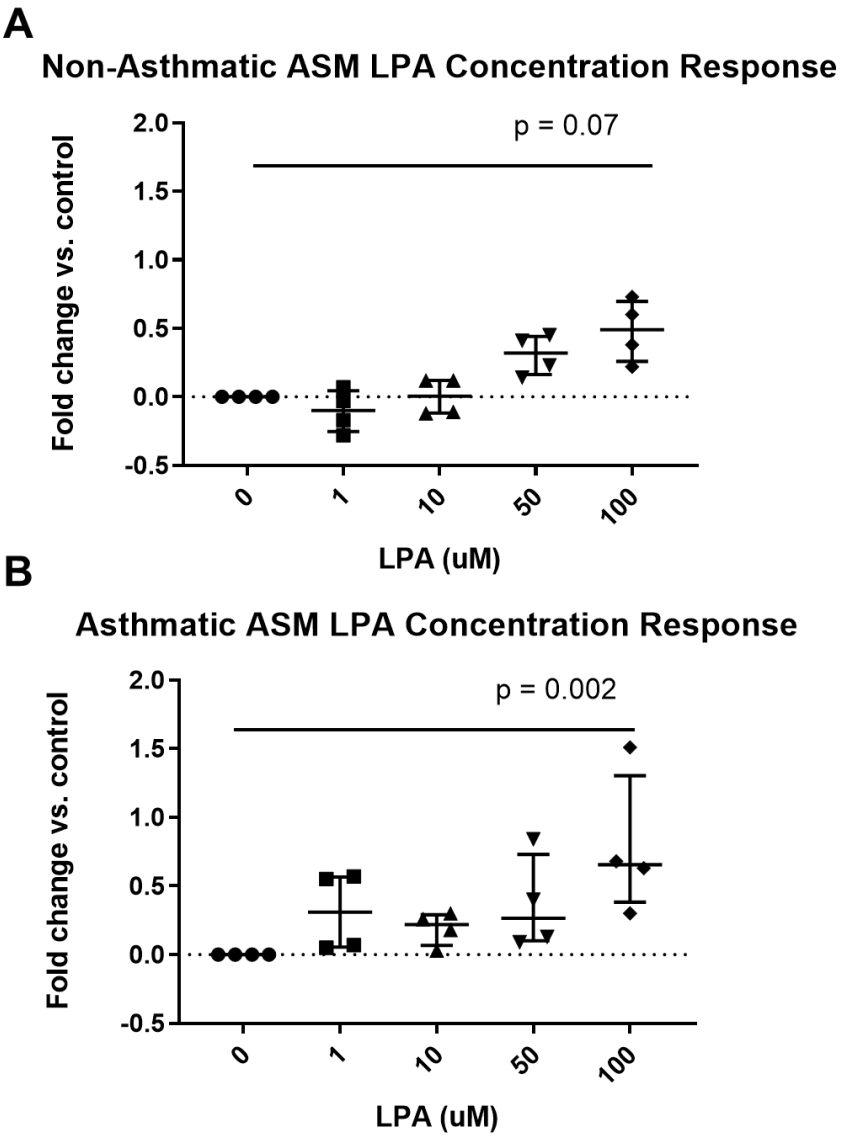

Figure 4.3. Human ASM cells were cultured in 96 well plates and TMLC cells were added to each well immediately prior to the experiment. Human ASM cells (n=4 cell lines) and TMLC co-culture were stimulated with a concentration range of LPA and incubated for 18 hours. Cells were lysed and bioluminescence measured by spectrophotometry. Bioluminescence, and therefore TGFβ activity, increased in a concentration-dependent fashion in response to LPA in both non-asthmatic and asthmatic ASM cells, A+B. Data expressed as the median fold change versus 0μM LPA control ± IQR. Statistical test is a Kruskal-Wallis one-way ANOVA.

As the coculture assay measured TGFβ activation indirectly via a luciferase readout a direct measurement of TGFβ activation was used to validate the coculture data. Phosphorylation of Smad2/3 complex is the first signalling event that occurs downstream of TGFβ receptor (see section 1.5 in the introduction), thus pSmad2 can be measured by western blot and Smad2/3 can be used as the loading control. Increasing concentrations of LPA were added to cultured ASM cells and incubated for 4 hours whereupon the cells were lysed and pSmad2 measured by western blot. The pSmad2 signal, measured by densitometry, increased in a concentration-dependent fashion in response to LPA addition which was maximal and significant at 100μM (figure 4.4). The lowest concentration of LPA to elicit a consistent response across four separate cell lines was 25uM, however the pSmad2 signal was variable. Taken together both of these experiments show that LPA activated TGFβ in ASM cells. Due to the consistent and strong pSmad2 signal using 100μM LPA, this concentration was used for future experiments.

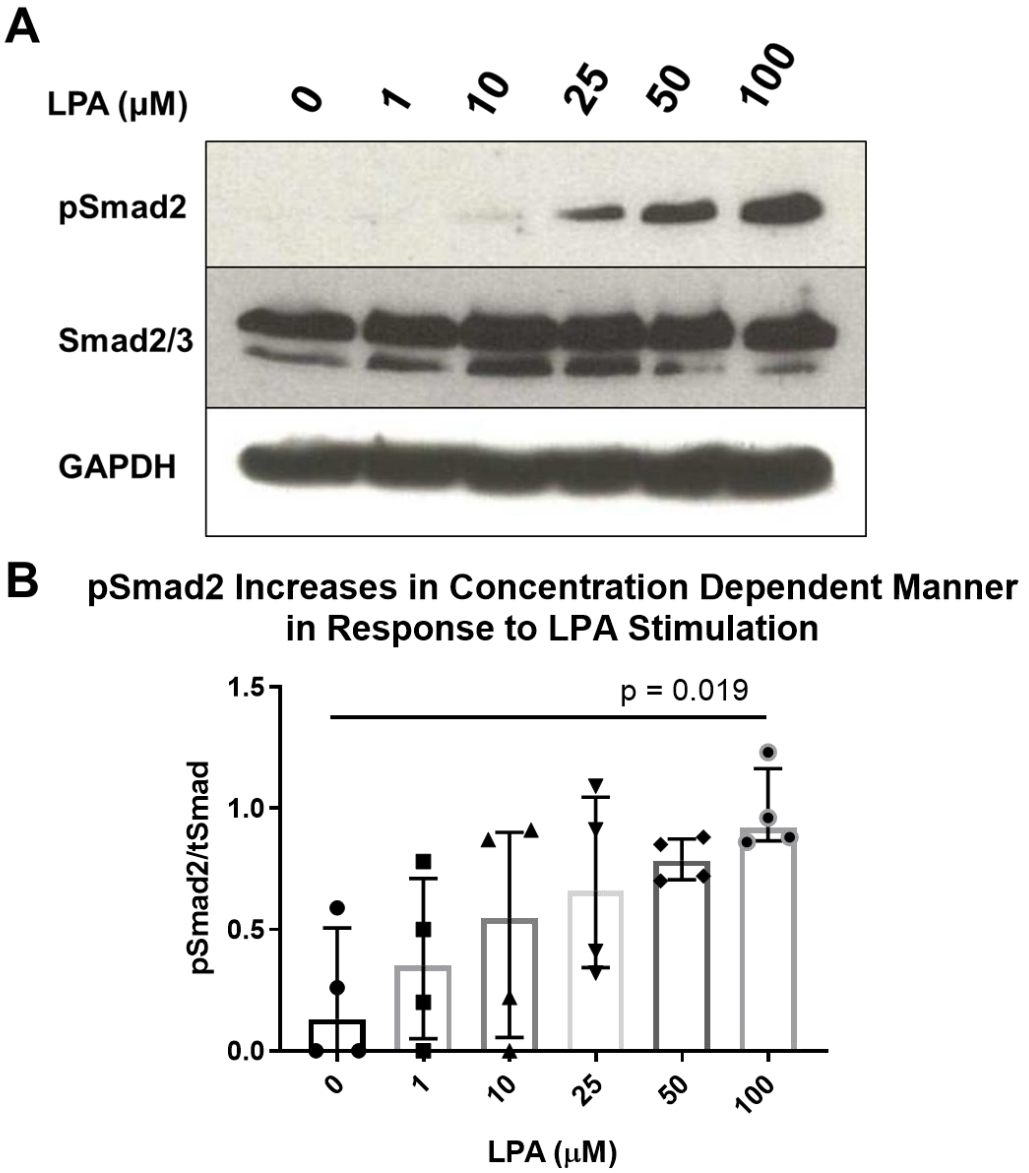

Figure 4.4. Human ASM cells were stimulated with a concentration range of LPA for 4 hours. Cells lysates were harvested and a western blot performed to detect pSmad2, A. LPA increased pSmad2 in a concentration-dependent fashion, maximal at 100μM. Densitometry of repeat experiments in different asthmatic donor cell lines is shown as median pSmad2 over Smad2/3 ± IQR (n=4 cell lines), B. Statistical test is a Kruskal Wallis one-way ANOVA.

Previously this group has shown that LPA-induced TGFβ activation required activation of RhoA in epithelial cells (281). RhoA is a small GTPase that is primarily involved in cytoskeletal reorganisation and acts upon its effector ROCKI and II, a serine threonine kinase that phosphorylates myosin light chain kinase, inducing stress fibre and focal adhesion formation. Here I measured active RhoA by ELISA in ASM cells treated with LPA to determine whether RhoA was activated in response to LPA in ASM cells.

First, to determine the optimum time point that RhoA becomes activated in response to LPA, a time course of active RhoA was carried out. ASM cells were treated with 100μM LPA between 0 and 30 minutes with intervals that were recommended by the manufacturers' protocol. The reaction kinetics of GDP to GTP exchange and subsequent GTP hydrolysis occur rapidly with an immediate increase in active RhoA at minute 1, peaking at minute 3 and decreasing to baseline at minute 30 (figure 4.5a). After determining the optimum time point to measure RhoA activation, experiments were performed to assess RhoA activation in response to 10 and 100uM LPA (figure 4.5b). This was carried out to ensure that LPA directly increased RhoA activation. LPA at 10μM induced an increase in active RhoA that was 2-fold higher than basally active RhoA. Absorbance increased from 0.4 to 0.5 when comparing 10μM and 100μM LPA stimulation indicating an increase in RhoA activation of approximately 20%. This demonstrates concentration-dependent activation of RhoA in response to LPA; 100μM was used for future experiments to ensure consistency with the pSmad2 western blots.

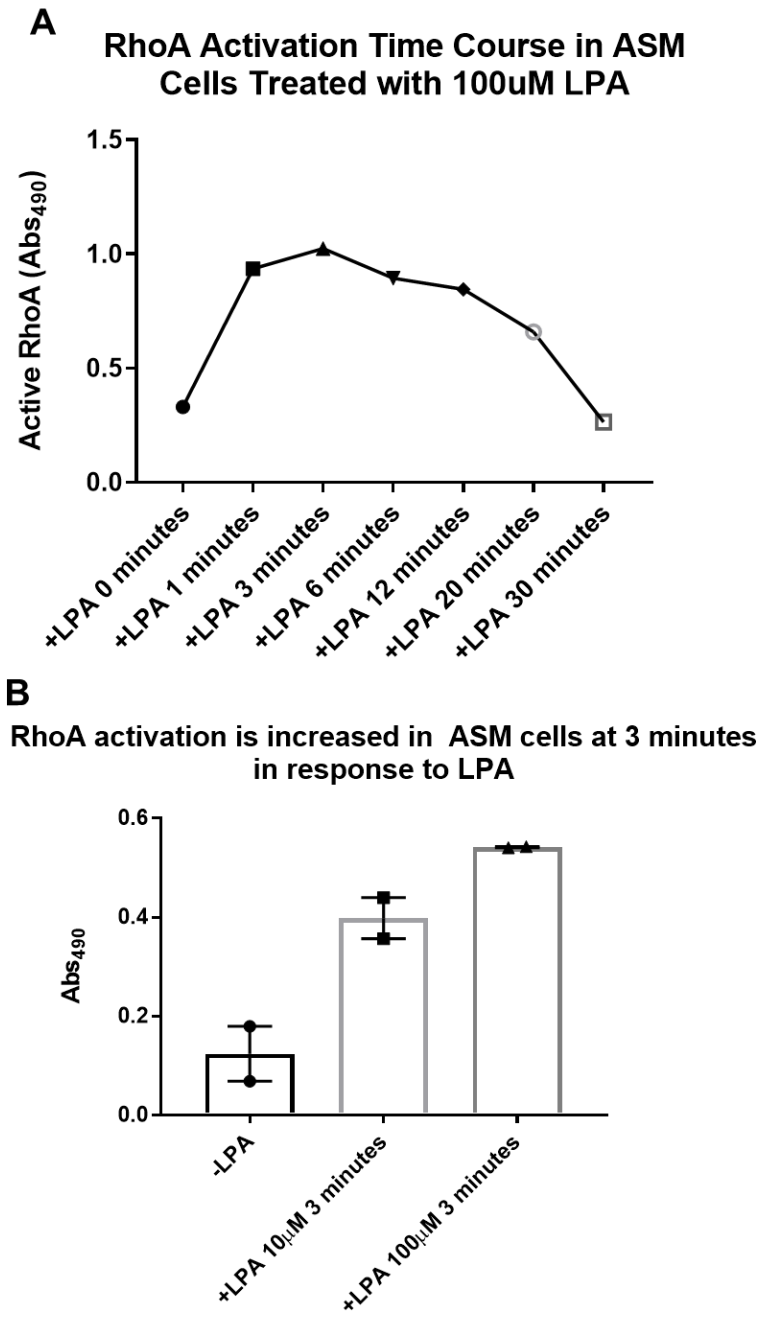

Figure 4.5. Human asthmatic ASM cells were stimulated with 100μM LPA and active RhoA was measured by ELISA between 1 and 30 minutes (n=1 experiment), A. RhoA activation occurred rapidly, peaking at minute 3 and decreasing over time until minute 30. Human asthmatic ASM cells were then stimulated with either 10 or 100μM LPA and active RhoA measured at minute 3 by ELISA (n=2 experiments, same cell line), B. Data is expressed as median absorbance ± IQR.

In summary, this section has shown that RhoA and TGFβ is activated in an LPA concentration-dependent fashion in ASM cells. TGFβ activation has been shown both indirectly by luciferase synthesis in coculture with TMLC cells and directly by measuring pSmad2 by western blot. Lastly, RhoA activation occurred in response to LPA in ASM cells at 3 minutes and is concentration dependent.

4.3.2 Small molecule inhibition of the $G_{\alpha q/11/14}$ does not inhibit TGFβ or RhoA activation in ASM cells

To determine whether $G_{\alpha q/11}$ were required for LPA-dependent TGFβ activation, a small molecule inhibitor of $G_{\alpha q/11/14}$ was used, YM-254890 (Wako Chemicals). YM-254890 is a cyclic dipsipeptide isolated from *Chromobacterium* sp. QS3666 that is membrane permeable and prevents the Gα subunit from exchanging GDP for GTP, thereby rendering the G-protein in its inactive state. It as a reported IC_{50} of 0.1-0.2μM (288). ASM cells were cultured and TMLC were added immediately prior to the experiment. Cells were pre-incubated with a concentration range of YM-254890 for 45 minutes prior to 100μM LPA addition. Bioluminescence was measured as an indirect readout of TGFβ activation after 18 hours (Figure 4.6a). The LPA positive control was norlised to 1 so data is plotted as relative change versus 1, which is represented as a dotted line. As with previous experiments LPA increased TGFβ versus media alone. YM-254890 reduced LPA-induced TGFβ concentration-dependently with maximal inhibition achieved at 10nM with a p value of 0.056. The difference in effect size between 10nM and 100nM YM-254890 was negligible despite non-significant and significant respectively. TGFβ activation remained 1.5-fold higher in cells treated with 10nM YM-254890 when compared to cells treated with media alone. To ensure that the inhibitor did not affect the TMLC cells, the concentration range of YM-254890 was also applied to TMLC cells alone (figure 4.6b). There was a significant reduction in LPA-induced luciferase in TMLC treated with YM-254890, however it was not concentration-dependent. This indicates that there is a non-specific inhibitory effect of YM-254890 on TMLC, therefore validation in ASM cells in monoculture was required.

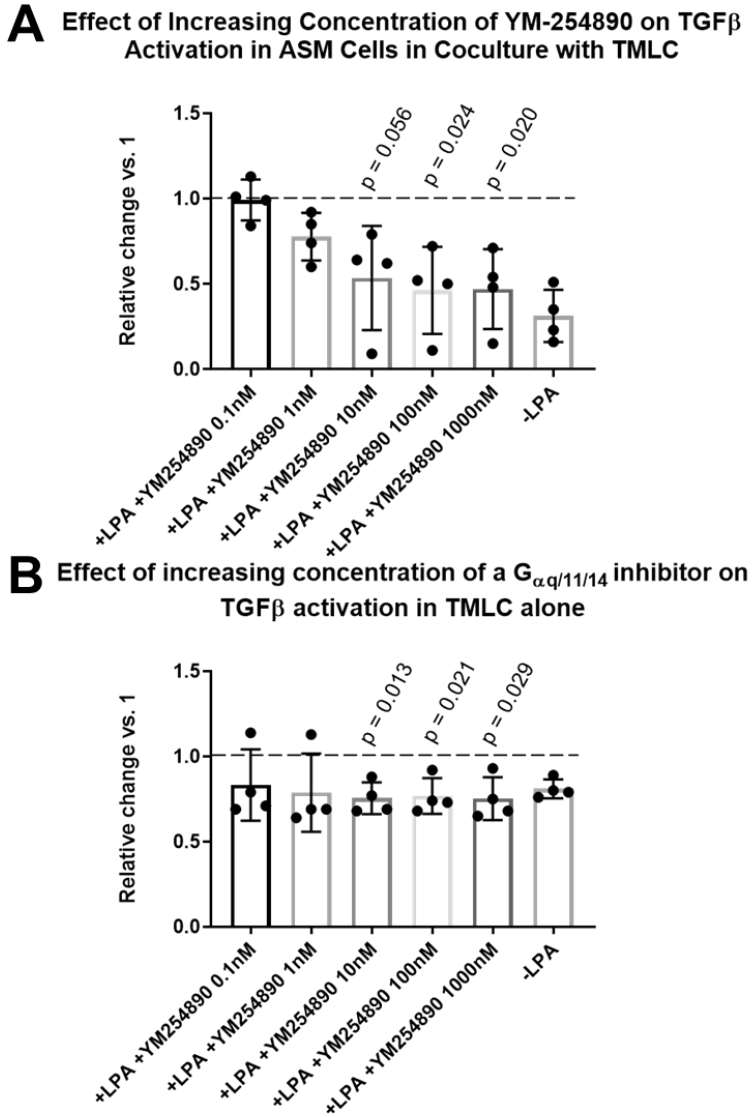

Figure 4.6. Human asthmatic ASM cells were cultured in 96 well plates and TMLC cells were added to each well immediately prior to the experiment. Cells were pre-treated with YM-254890 45 minutes prior to 100μM LPA addition. Cells were lysed and bioluminescence measured by spectrophotometry. The LPA positive control has been normalised to 1 (dotted line) and plotted values are the relative difference versus 1. There was a YM-254890 concentration-dependent decrease in LPA-induced bioluminescence in ASM cells co-cultured with TMLC (n=4 cell lines), A. There was a significant but not dose-dependent effect of YM-254890 on TMLC alone (n=4 experiments), B. Data expressed as the mean fold change versus 0μM LPA control ± SEM. Statistical testing used a one sample t test.

To validate inhibition of TGFβ activation demonstrated in the ASM-TMLC coculture a second readout of TGFβ activity was used, *PAI1* expression. TGFβ can induce transcription of *PAI1* and therefore be used as an indirect measure of TGFβ activation. ASM cells were pre-treated with 10nM of the $G_{\alpha q/11/14}$ inhibitor YM-254890 because this was the lowest concentration that reduced TGFβ activation in the ASM-TMLC coculture (figure 4.7). LPA treatment significantly increased *PAI1* expression by 4-fold versus the no LPA control. The inhibitor did not reduce LPA-induced *PAI1* (figure 4.6). *PAI1* is a quick endpoint that can indicate TGFβ activation, however, it is an indirect measure of TGFβ activity that is not specific to TGFβ signalling.

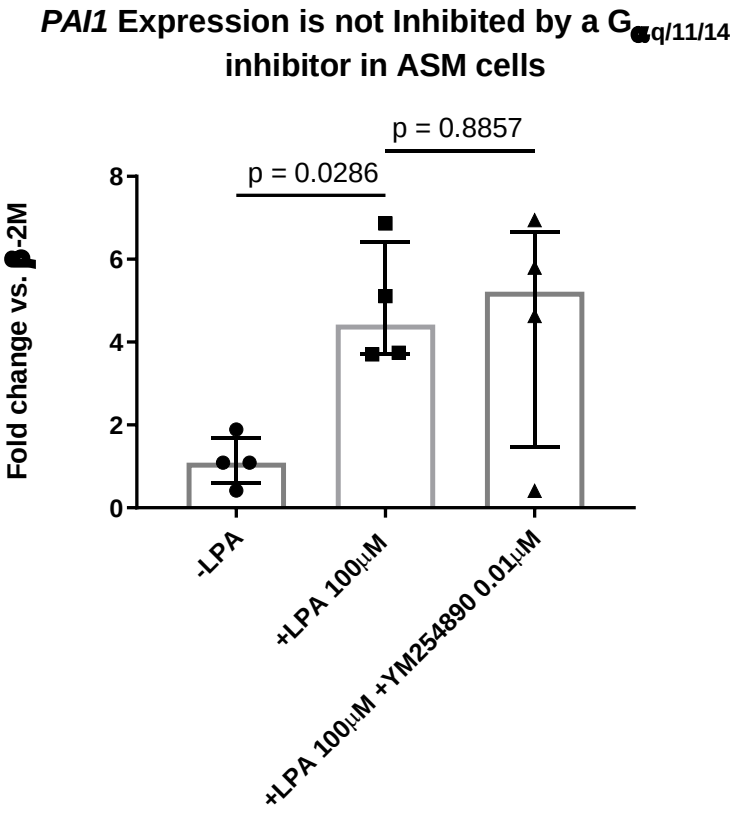

Figure 4.7. Human ASM cells were pre-treated with YM-254890 prior to 100μM LPA addition. PAI1 mRNA expression was measured 4 hours after LPA treatment, (n=4). LPA significantly increased PAI1 expression, however this was not inhibited by YM-254890. Data expressed as the median fold change versus β-2M ± IQR. Statistical tests are Mann-Whitney U.

Next, a pSmad2 western blot was carried out to validate the coculture assay and *PAI1* QPCR because it is a direct and specific measure of TGFβ pathway activation. A monoculture of human ASM cells were pre-incubated with a concentration range of YM-254890 45 minutes prior to 100μM LPA addition (figure 4.8a+b). Densitometry of pSmad2 over the Smad2/3 loading control was used to quantify repeat western blots. There was a significant increase in pSmad2 in response to LPA, with a similar effect size seen in the ASM-TMLC coculture and *PAI1* QPCR assay. However, in contrast to the coculture there was no reduction in pSmad2 at any concentration of YM-254890. This result was similar to the *PAI1* QPCR carried out in a monoculture of ASM cells where there was no inhibition of LPA-induced *PAI1* expression.

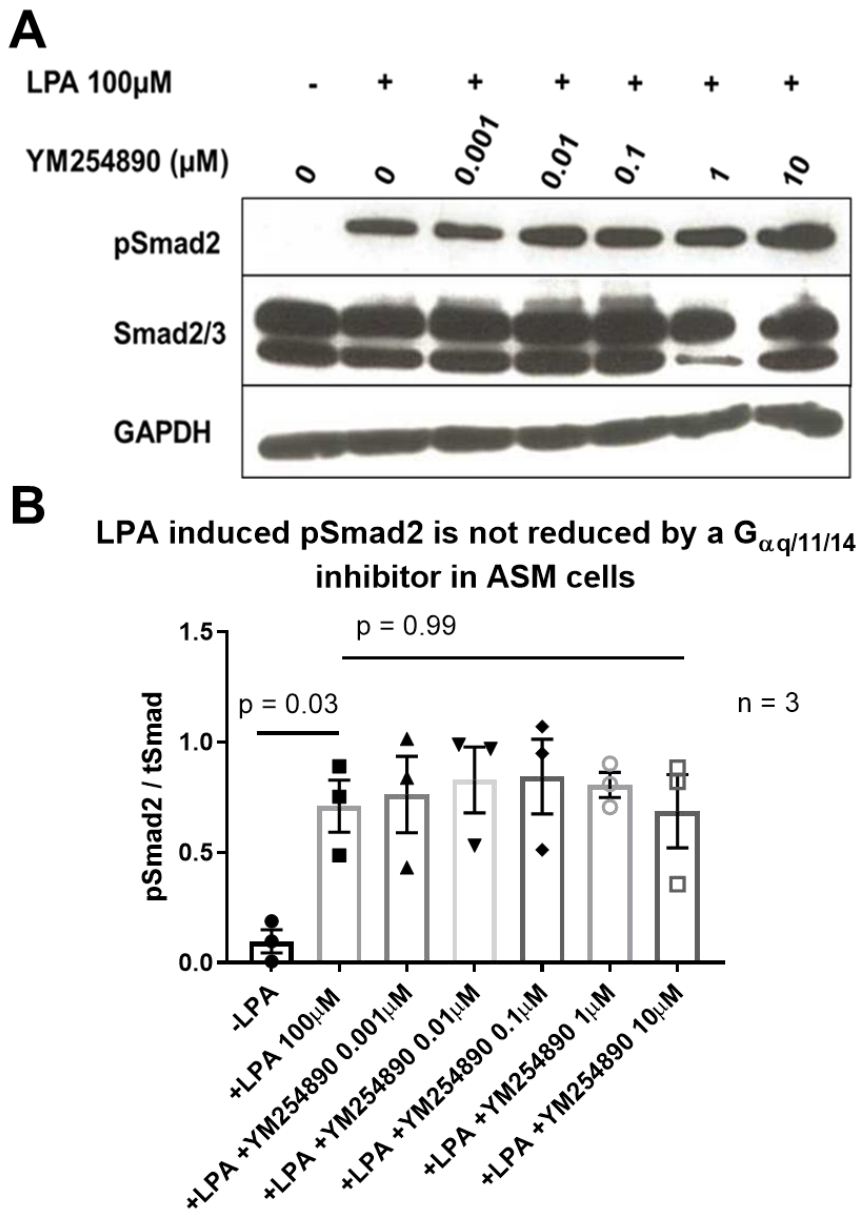

Figure 4.8. Human asthmatic ASM cells, pre-treated with YM-254890 were stimulated with 100μM LPA for 4 hours. Cells lysates were harvested and a western blot was run to detect pSmad2, A. Densitometry of repeat experiments is shown as mean pSmad2 over Smad2/3 ± SEM (n=3 cell lines), B. There was no reduction in LPA-induced pSmad2 at any concentration of YM-254890. Statistical test is Dunnett's ordinary One-Way ANOVA.

RhoA has previously been shown to be essential for TGFβ activation in epithelial cells and is activated after 3 minutes of LPA treatment in ASM cells (figure 4.5). Next, I wanted to determine whether inhibiting $G_{\alpha q/11}$ would inhibit LPA-induced RhoA activation. ASM cells were pre-treated with a concentration range of the $G_{\alpha q/11/14}$ inhibitor YM-254890 for 45 minutes before the addition of 100μM LPA. Active RhoA was measured after 3 minutes by ELISA and presented as percentage absorbance versus the +LPA control (figure 4.9). There was a significant increase in active RhoA in response to LPA that was 3-fold higher than the no LPA control, however there was no effect of YM-254890 on RhoA activation at any concentration suggesting that $G_{\alpha q/11/14}$ do not play a role in LPA-induced RhoA activation.

In summary, this section aimed to determine whether the heterotrimeric G-proteins $G_{\alpha q/11}$ were required for LPA-induced TGFβ activation in ASM cells. This was tested using the small molecule inhibitor of $G_{\alpha q/11/14}$, YM-254890. These data show that when ASM cells were cultured alone, pSmad2, *PAI1* expression, and RhoA activation was not inhibited by YM-254890, suggesting that $G_{\alpha q/11}$ are not required for TGFβ activation. This was in contrast to when ASM cells were cocultured with TMLC, which showed that TGFβ activation reduced at 10nM YM-254890. It was therefore important to use another method of inhibiting $G_{\alpha q/11}$ to validate these data, which was done using siRNA and will be presented in the next section.

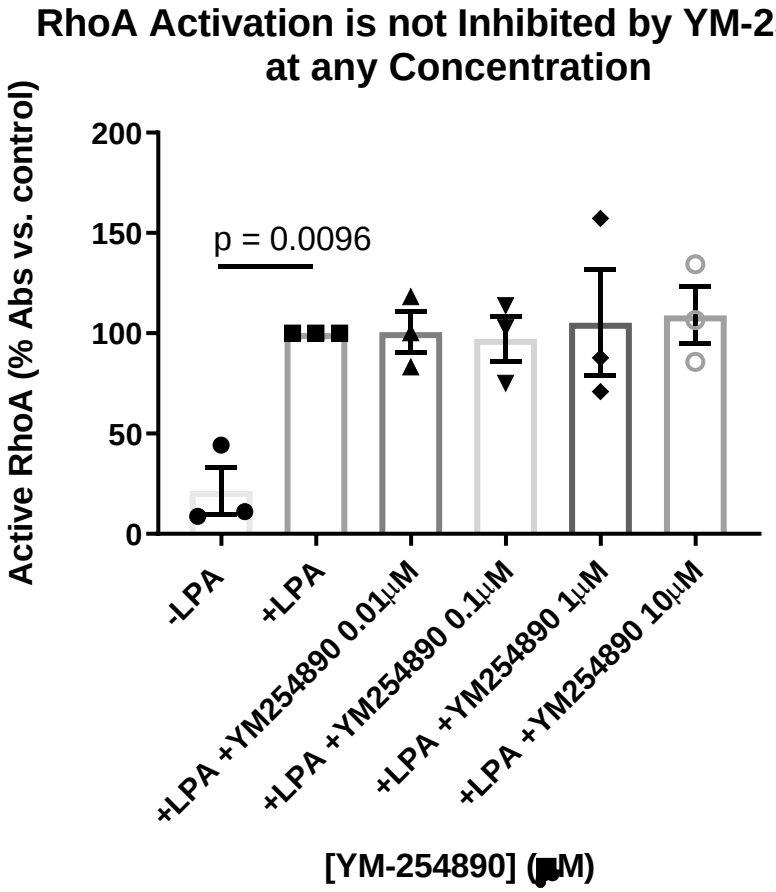

Figure 4.9. Human asthmatic ASM cells, pre-treated with YM-254890 were stimulated with 100μM LPA for 3 minutes. Cells lysates were harvested and active RhoA measured by ELISA (n=3, same cell line). Data shown as mean percentage absorbance versus +LPA ± SEM. Statistical test is a Dunnett's One-Way ANOVA.

4.3.3 Knockdown of $G_{\alpha q/11}$ by siRNA does not inhibit RhoA or TGFβ activation in ASM cells

To further investigate a role for Gq/11 in LPA-induced TGFb activation and validate the $G_{\alpha q/11/14}$ inhibitor data transient siRNA knockdown of the $G_{\alpha q}$ and $G_{\alpha 11}$ subunits in ASM cells was carried out. Initially ASM cells were transfected with a negative control siRNA, $G_{\alpha q}$ and $G_{\alpha 11}$ siRNA, or mock transfected with lipofectamine transfection reagent. $G_{\alpha q}$ and $G_{\alpha 11}$ mRNA was measured 24, 48, and 72 hours post transfection to ensure that the siRNA knocked down its target. Gene expression is normalised to the housekeeping gene β-2M and data is shown as fold change versus control siRNA. Both $G_{\alpha q}$ and $G_{\alpha 11}$ mRNA was significantly reduced by approximately 95% down at all time points compared to both mock transfected and control siRNA transfected cells (figure 4.10). This demonstrated that the siRNA was reducing expression of its target mRNA.

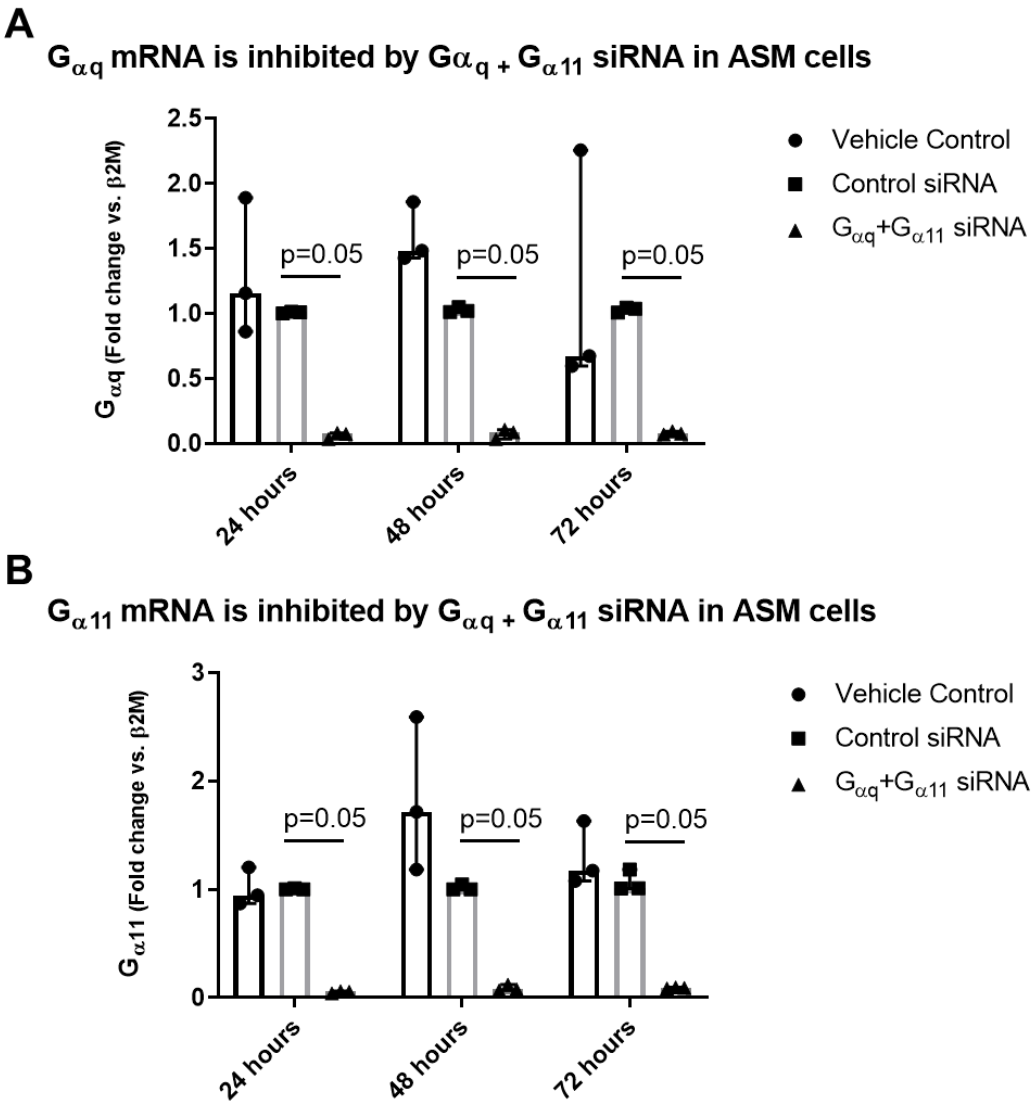

Figure 4.10. Human ASM cells were either, mock transfected, transfected with control siRNA, or siRNA targeting $G_{\alpha q}$ and $G_{\alpha 11}$. Cell lysates were harvested and mRNA expression measured by QPCR (n=3). Normalisation of QPCR data was done against the housekeeping gene β-2M and presented as median ± IQR. Statistical test used was a Mann-Whitney U.

Next, protein knockdown was determined to ensure that siRNA knockdown of $G_{\alpha q}$ and $G_{\alpha 11}$ mRNA resulted in a reduction at the protein level. Protein knockdown of $G_{\alpha q}$ was measured by western blot and showed greatest reduction at 72 hours post-transfection (appendix 1). To determine whether $G_{\alpha q}$ and $G_{\alpha 11}$ knockdown had an effect on LPA-induced TGFβ activation, ASM cells were treated with 100μM LPA for 4 hours, 72 hours post-transfection. For each experiment $G_{\alpha q}$ and $G_{\alpha 11}$ protein was measured by western blot and quantified by densitometry to ensure that there was sufficient protein knockdown. Both $G_{\alpha q}$ and $G_{\alpha 11}$ were significantly, but not completely, knocked down by siRNA at the protein level in each experiment (figure 4.11 A & B). There was approximately 80% knockdown of $G_{\alpha q}$ protein and 95% knockdown of $G_{\alpha 11}$ protein.

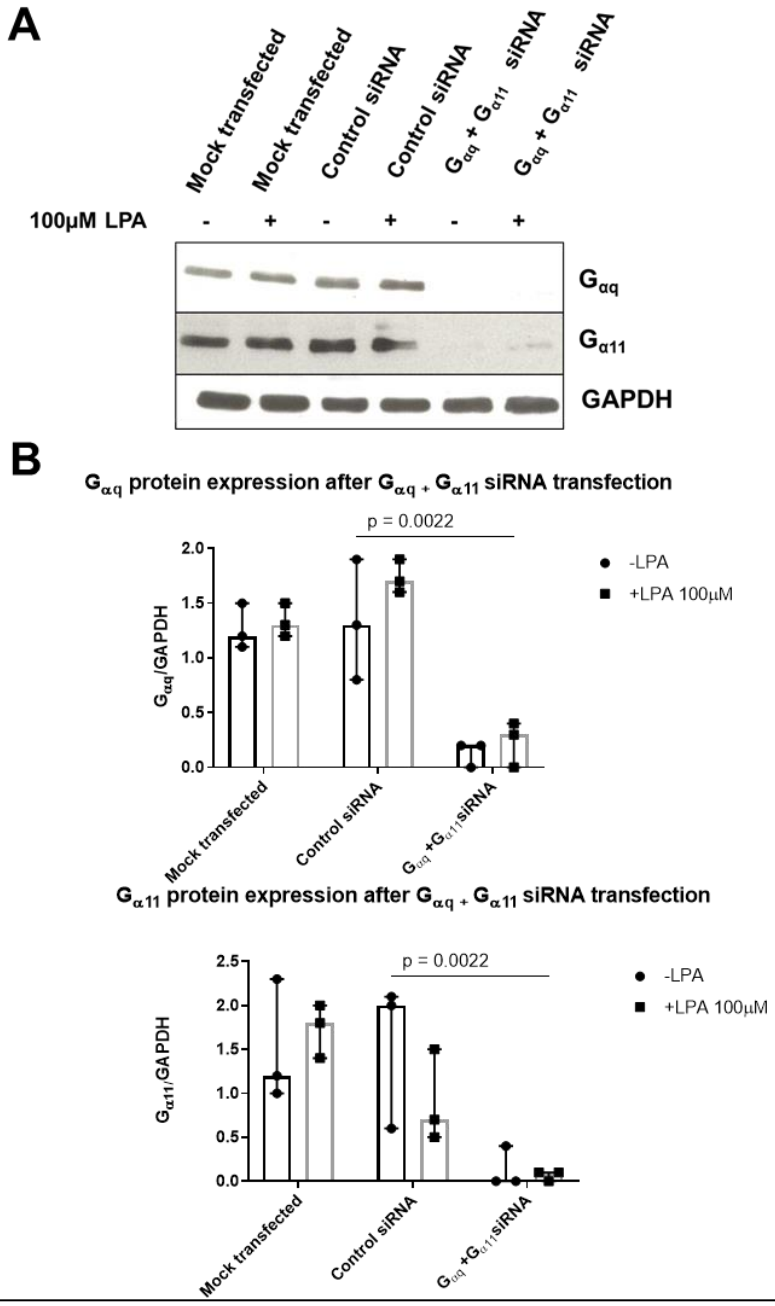

Figure 4.11. Human asthmatic ASM cells mock transfected, transfected with control siRNA, or transfected with $G_{\alpha q}$ and $G_{\alpha 11}$ siRNA for 72 hours (n=3 cell lines). Representative western blot showing $G_{\alpha q}$ and $G_{\alpha 11}$ protein in lysates from siRNA transfection experiments, A. There was significant knockdown of both $G_{\alpha q}$ and $G_{\alpha 11}$ in all experiments (n=3 cell lines) shown by densitometry, B. Data is presented as median ± IQR. Statistical test used was a Mann-Whitney U of control siRNA and $G_{\alpha q}$ + $G_{\alpha 11}$ siRNA groups.

Once protein knockdown of $G_{\alpha q}$ and $G_{\alpha 11}$ was determined, the ratio of pSmad2 to Smad2/3 was measured using densitometry of western blots to assess activation of the TGFβ pathway. LPA induced an increase in pSmad2 in all conditions when compared to each no LPA control (figure 4.12 A & B). In cells mock transfected with lipofectamine and control siRNA there was no detectible basal pSmad2. Knockdown of $G_{\alpha q}$ and $G_{\alpha 11}$ did not reduce LPA-induced pSmad2 and actually increased pSmad2 in cells that were either untreated or treated with 100μM LPA. This increase was not significant, however there was a large effect size that was 2-fold higher than LPA-induced pSmad2 in mock transfected and control siRNA transfected cells. Basal pSmad2 was detectible in ASM cells treated with $G_{\alpha q}$ and $G_{\alpha 11}$ siRNA, however this was approximately 80% lower than pSmad2 in control cells treated with LPA.

These data validate the data shown in the previous section which showed a $G_{\alpha q/11/14}$ inhibitor did not reduce LPA-induced pSmad2, *PAI1* expression, or RhoA activation. Taken as whole the data that has been presented so far shows that $G_{\alpha q/11}$ are not required for LPA-induced TGFβ activation or RhoA activation in ASM cells.

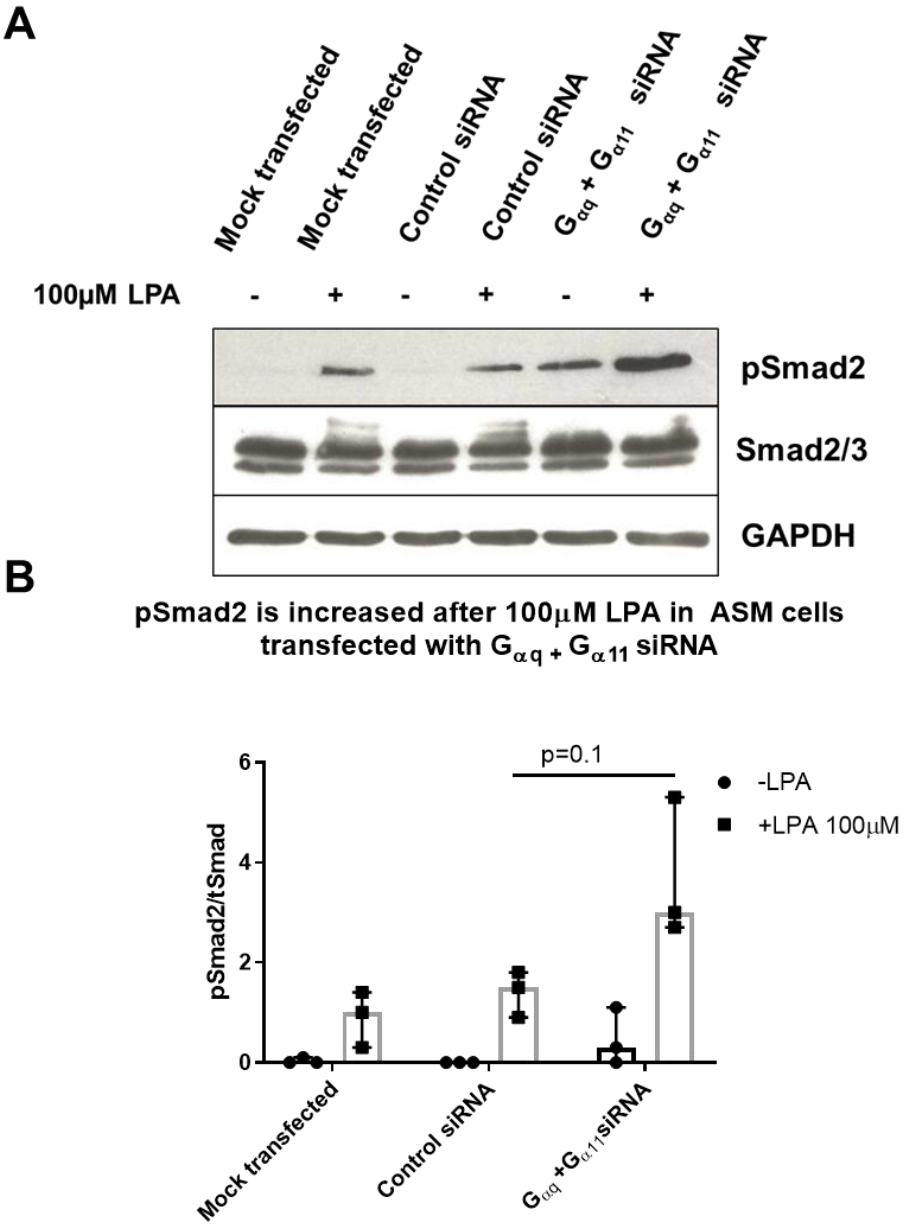

Figure 4.12. Human asthmatic ASM cells mock transfected, transfected with control siRNA, or transfected with $G_{\alpha q}$ and $G_{\alpha 11}$ siRNA for 72 hours (n=3 cell lines). Cells were treated with 100μM LPA for 4 hours after transfection. Representative western blot showing pSmad2 and Smad2/3, A. Densitometry shows that there was an LPA-induced increase in pSmad2 and this was not reduced in ASM cells treated with $G_{\alpha q}$ and $G_{\alpha 11}$ siRNA, B. Data is expressed as median ± IQR. Statistical test is a Mann-Whitney U.

Next, I wanted to validate previous data in this chapter showing a $G_{\alpha q/11/14}$ inhibitor did not inhibit LPA-induced RhoA activation. ASM cells were treated with control, or $G_{\alpha q}$ and $G_{\alpha 11}$ siRNA, and RhoA activation was measured by ELISA (figure 4.13). Active RhoA was increased in both controls at 3 minutes after treatment with LPA. Treating ASM with $G_{\alpha q}$ and $G_{\alpha 11}$ siRNA resulted in a small non-significant reduction in RhoA activation from an absorbance of 0.18 to 0.13. However, the confidence interval was large and overlapped with the siRNA control group. This suggests that $G_{\alpha q/11}$ may play a small role in RhoA activation but they are not the primary regulator.

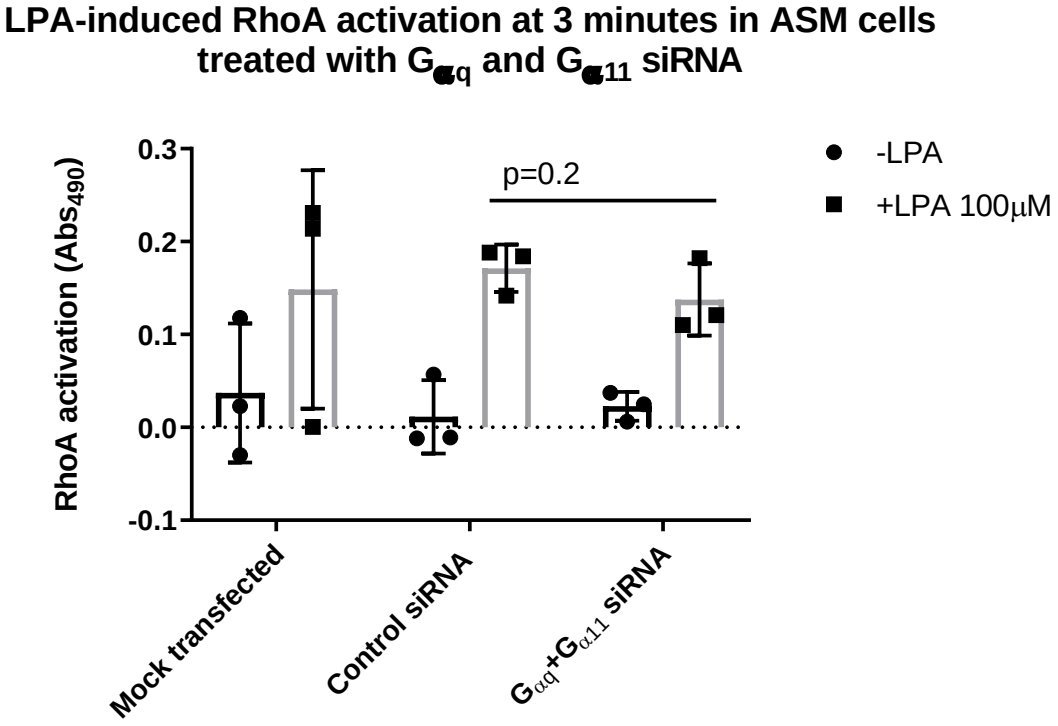

Figure 4.13. Human asthmatic ASM cells mock transfected, transfected with control siRNA, or $G_{\alpha q}$ and $G_{\alpha 11}$ siRNA, siRNA for 72 hours (n=3 cell lines). Cells were treated with 100μM LPA for 3 minutes after siRNA transfection and active RhoA measured by ELISA. Data is presented as median ± IQR. Statistical test is a Mann-Whitney U.

4.3.4 ROCKI/II inhibition blocks LPA-induced TGFβ activation

RhoA is required for TGFβ activation in epithelial cells through induction of cytoskeletal reorganisation. In ASM cells, cytoskeletal reorganisation activates TGFβ by integrin αVβ5 however a role for the RhoA pathway in ASM has not previously been demonstrated. To ensure the RhoA pathway was involved in LPA-induced TGFβ activation, its effectors ROCKI/II serine-threonine kinases were inhibited using the small molecule inhibitor Y27623 (Tocris). Previous studies have used 5μM or 10μM concentrations of this inhibitor, however, the reported IC_{50} to inhibit contraction of rabbit aortic strips was reported between 0.3-1μM (289, 290). Human ASM cells were pre-treated with 5μM or 10μM of a ROCKI/II inhibitor for 30 minutes before addition of 100μM LPA for 4 hours. LPA-induced pSmad2 was measured by densitometry of western blots. There was inhibition of pSmad2 by the ROCKI/II inhibitor Y27623 at 10μM, although this was not significant the effect size was large with a reduction in pSmad2 that was 4-fold lower than ASM cells treated with LPA alone (figure 4.14). The reduction in pSmad2 was concentration-dependent between 5μM and 10μM of the ROCKI/II inhibitor. These data suggest that the RhoA-ROCKI/II pathway is required for TGFβ activation in ASM cells.

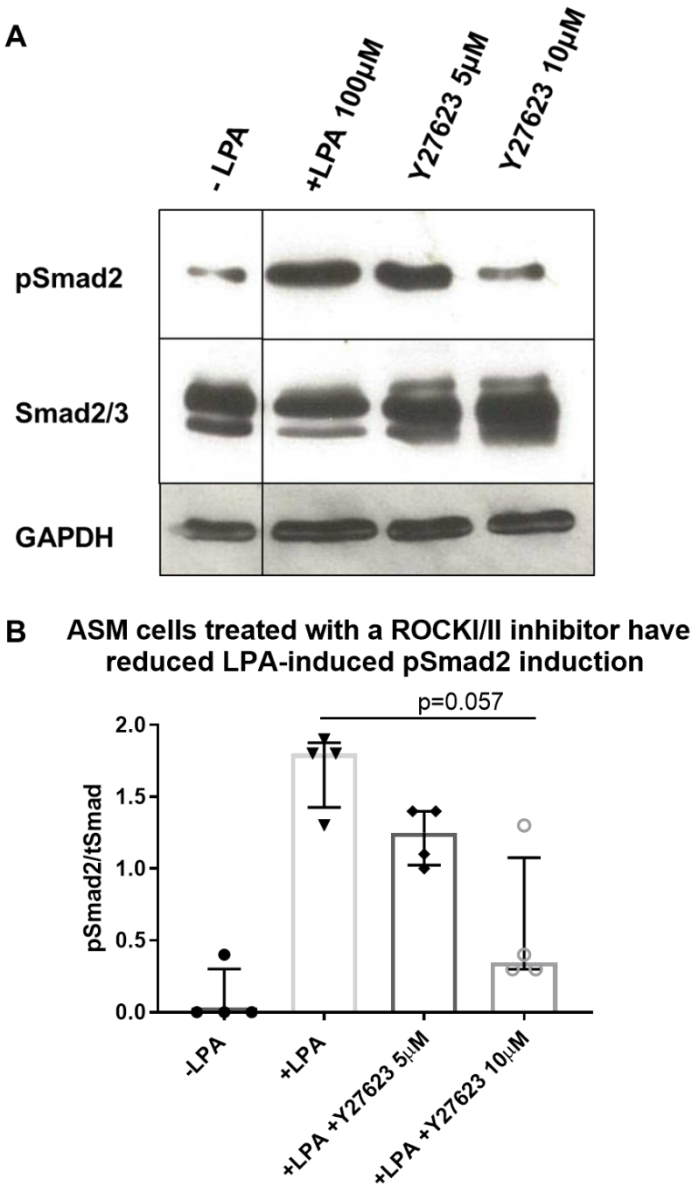

Figure 4.14. Human asthmatic ASM cells were pre-treated with the ROCKI/II inhibitor Y27623 for 30 minutes before addition of 100μM LPA for 4 hours. pSmad2 measured by western blot and quantified by densitometry (n=4 cell lines). LPA-induced pSmad2 was inhibited at 10μM Y27623. Data is expressed as median ± IQR. Statistical analysis used a Mann-Whitney U test.

4.4 Discussion

In the lung of patients suffering with severe asthma there are extensive structural changes within the airways. These structural changes are termed as airway remodelling and include subepithelial fibrosis, ASM hyperplasia and hypertrophy, epithelial damage, goblet cell hyperplasia, and angiogenesis (1). The pleiotropic cytokine TGFβ plays central role in airway remodelling. It is therefore important to understand the precise signalling pathway that activates TGFβ in ASM cells.

The aim of this chapter was to test the hypothesis that the heterotrimeric G-proteins $G_{\alpha q/11}$ are required for LPA-induced TGFβ activation in ASM cells. In the murine lung, high pressure forced ventilation was shown to increase total TGFβ in the lung and was abrogated by epithelial knockout of $G_{\alpha q}$ and $G_{\alpha 11}$ (127). Further, LPA-induced TGFβ activation in murine embryonic fibroblasts is dependent on integrin β6, RhoA, and $G_{\alpha q}$ (128). In ASM cells, the integrin αvβ5 is required for TGFβ activation and a polymorphism in the cytoplasmic domain of β5 abrogates LPA-induced TGFβ activation (133). However, the role of GPCRs in ASM cell TGFβ activation has not been explored. LPA was used as an agonist because its receptors are upstream of $G_{\alpha q/11}$, $G_{\alpha 12/13}$, $G_{\alpha s}$, and $G_{\alpha i/o\ (271)}$. Moreover, LPA is increased in the BAL of asthmatic patients after allergen challenge and has been used to elicit a pSmad2 signal in murine embryonic fibroblasts (128, 272).

All of the experiments described in this chapter, except the comparison of non-asthmatic and asthmatic cells, were carried out in asthmatic ASM cells. There were two reasons for this; first, in order to show inhibition of TGFβ I wanted the maximum TGFβ signal, and asthmatic ASM cells have been shown to activate more TGFβ than non-asthmatic ASM cells (133). The second was to ensure that

analysis of the TGFβ signalling pathway was relevant in cells taken from asthmatic patients because asthmatic cells behave differently to non-asthmatic cells. A comparison between asthmatic patients and allergic rhinitis patients given inhaled bronchoconstrictors showed that only asthmatics suffered exaggerated airway narrowing (291).

Initially, this chapter set out to show that LPA could activate elements of TGFβ signalling including, TGFβ activation, TGFβ signalling by pSmad2, and RhoA activation. Consistent with previous work both active TGFβ, shown by TMLC coculture, and pSmad2 were increased in ASM cells in a concentration-dependent manner in response to LPA treatment (128, 133). Asthmatic cells showed a slightly higher fold-increase of luciferase, indicating active TGFβ, when treated with LPA in coculture compared to non-asthmatic cells. Previous work has shown that asthmatic ASM cells activate more TGFβ than non-asthmatic cells in response to both LPA and methacholine (133). Throughout the rest of this chapter 100μM of LPA was because it gave a strong and consistent pSmad2 signal. Although this is higher than the physiological range, 0.1-10μM, the limited sensitivity of the assay required a higher concentration of LPA to amplify the system to allow efficient interrogation of the signalling pathway (277).

In epithelial cells, RhoA and integrin αvβ6 are central to TGFβ activation (128, 175). RhoA and its effector ROCKI/II play an important role in actin polymerisation and contraction in response to agonists in smooth muscle cells (292, 293). Data in this chapter shows that RhoA activation occurs rapidly, peaking at 3 minutes, in response to LPA in ASM cells. Taken collectively these data show that LPA activates the TGFβ pathway and RhoA in ASM cells. LPA has been shown to induce smooth muscle contraction and RhoA activation, but

it is not known whether RhoA is required for TGFβ activation in ASM cells (293, 294).

After demonstrating that LPA induced TGFβ activation I sought to inhibit TGFβ activation by inhibiting $G_{\alpha q/11}$. This family of heterotrimeric G-proteins have been shown to be involved in LPA-induced TGFβ activation in murine embryonic fibroblasts (128). The $G_{\alpha q/11/14}$ inhibitor, YM-254890, significantly blocked LPA-induced TGFβ activation in a coculture of ASM cells and TMLC with an effect size of approximately 50%. A small significant reduction in luciferase activity was seen in TMLC cells treated with LPA and $G_{\alpha q/11/14}$ inhibitor, suggesting that the inhibitor was effecting the TMLC, however the reduction was not concentration-dependent. This suggested that inhibiting $G_{\alpha q/11/14}$ abrogates LPA-induced TGFβ activation. Next, I measured LPA-induced *PAI1* expression in a monoculture of ASM cells. *PAI1* mRNA can be used as an indirect measure of TGFβ activation because it is regulated, although not exclusively, by the TGFβ signalling (133). A concentration of 10nM of the $G_{\alpha q/11/14}$ inhibitor was selected because this concentration significantly inhibited TGFβ activation in an ASM-TMLC coculture. However, the $G_{\alpha q/11/14}$ inhibitor had no effect on LPA-induced *PAI1* expression. Both of these experiments used indirect measures of TGFβ activation. The coculture assay used the TMLC reporter cell line, measuring *PAI1* driven luciferase activity. Whereas *PAI1* mRNA expression was measured in a monoculture of ASM cells. Moreover, *PAI1* is regulated by TGFβ and Wnt/β-catenin signalling, and is therefore not a specific or direct measure of TGFβ activation (295). Thus, it was important to use a specific and direct measure of TGFβ activation to determine whether $G_{\alpha q/11}$ were required for LPA-induced TGFβ activation.

Measuring pSmad2 is the most specific indicator of TGFβ activation because phosphorylation of Smad2 is the first signalling event after activation of the TGFβ receptor. Therefore, pSmad2 was measured by western blot to validate either the ASM-TMLC coculture or *PAI1* expression data. Interestingly, LPA-induced pSmad2 was not inhibited at any concentration of the $G_{\alpha q/11/14}$ inhibitor. This result was the same as when measuring LPA-induced *PAI1* expression. However, it was in contrast to the ASM-TMLC coculture, which showed that luciferase, and therefore TGFβ activation, was inhibited by the $G_{\alpha q/11/14}$ inhibitor. The reason for the difference between the ASM-TMLC coculture data and the *PAI1* mRNA and pSmad2 data is difficult to pinpoint. To date there have been no studies that have measured TGFβ activation using both a TMLC coculture assay and pSmad2 western blot. The coculture provides an indirect measure of active TGFβ via luciferase. In contrast, phosphorylation of Smad2 is the first signalling event after TGFβ receptor binding. Measuring pSmad2 is therefore a more specific indicator of TGFβ activation than the coculture assay. Additionally, both pSmad2 and *PAI1* expression were measured in a monoculture of ASM cells, thus removing any effects of interaction between the ASM cells and TMLC. Additionally, there was a small inhibitory effect of the $G_{\alpha q/11/14}$ inhibitor on TMLC alone, although the effect size was small it is likely that this contributed to the inhibitory effect seen.

Due to the discrepancy between these experiments, siRNA knockdown of $G_{\alpha q}$ and $G_{\alpha 11}$ was carried out to validate either the ASM-TMLC coculture assay or pSmad2 western blot. Knockdown of $G_{\alpha q}$ and $G_{\alpha 11}$ protein was achieved at 72 hours and ASM cells were treated with 100μM LPA. Knockdown of $G_{\alpha q}$ and $G_{\alpha 11}$ did not reduce LPA-induced pSmad2 in ASM cells, in fact pSmad2 was increased in comparison to the siRNA control transfection. The increase in

pSmad2 was 2-fold compared to ASM cells transfected with control siRNA. Genetic knockdown can have indirect effects on other G-protein family members. In HeLa cells, both $G_{\alpha i1}$ and $G_{\alpha 12}$ expression was increased in cells that had undergone siRNA knockdown of $G_{\alpha q/11}$ (296). Thus, the increase in pSmad2 after $G_{\alpha q/11}$ knockdown may be due to an increase in expression of other heterotrimeric G-proteins. These data show that pSmad2 is not inhibited by the $G_{\alpha q/11/14}$ inhibitor nor $G_{\alpha q/11}$ siRNA transfection and suggest that $G_{\alpha q/11}$ are not required for LPA-induced TGFβ activation. This is in contrast to epithelial cells and murine embryonic fibroblasts where $G_{\alpha q/11}$ have been shown to be involved stretch and LPA mediated in TGFβ activation respectively (127, 128).

In epithelial cells, it is accepted that there is a G_q-RhoA-integrin β6 pathway required for LPA-induced TGFβ activation (127, 128). The GTPase RhoA and its effector ROCKI/II, a serine/threonine kinase responsible for cytoskeletal organisation, are central to integrin-β6 mediated TGFβ activation in epithelial cells (175). ROCKI/II increases smooth muscle cell contractility and stress fibre formation by inhibiting myosin light chain phosphatase, therefore maintaining myosin light chain phosphorylation and activation (130). ROCKI also activates a range of proteins involved in cytoskeletal regulation, including LIM kinase which stabilises actin filaments (283). In ASM cells, LPA-induced TGFβ activation has been shown to occur via integrin αvβ5, however the pathway leading to integrin activation has not been described. For the first time ROCKI/II has been shown to be required, although not exclusively, for LPA-induced pSmad2 activation in ASM cells. This might suggest that RhoA is also likely to be involved in this TGFβ pathway in ASM cells because ROCKI/II is the primary effector of RhoA (282, 297). However, RhoA does not exclusively control ROCKI/II activation and RhoA independent

pathways have been described. Arachidonic acid is able to activate ROCKI/II by binding to its auto-inhibitory PH domain and induce contraction of smooth muscle fibres (298). Moreover, ROCKI activation can also be induced by phosphoinositide-dependent kinase-1 (PDK1) binding in competition with its negative regulator RhoE (299).

So far this chapter has shown that the RhoA effectors ROCKI/II, but not $G_{\alpha q/11}$, are required for LPA-induced TGFβ activation in ASM cells. This suggested that RhoA activation was unlikely to be regulated by $G_{\alpha q/11}$, however it was important to rule this out. A study in HEK T293 cells has shown that $G_{\alpha q}$ is able to activate RhoA, however the majority of studies show that $G_{\alpha 12/13}$ are primarily responsible for RhoA activation (300-302). In this thesis, active RhoA was measured by ELISA after 3 minutes of incubation with LPA. No reduction in active RhoA was observed at any concentration of the $G_{\alpha q/11/14}$. There was a small non-significant reduction in LPA-induced RhoA after treatment with siRNA targeting $G_{\alpha q/11}$. However, there was large confidence interval that overlapped with the control siRNA group, therefore suggesting that $G_{\alpha q/11}$ were not the primary heterotrimeric G-proteins that regulated RhoA in ASM cells. This finding is in contrast to work in murine embryonic fibroblasts, which showed that LPA-induced TGFβ activation required RhoA and $G_{\alpha q}$ (128).

A family of guanine nucleotide exchange factors (RhoGEFs) are required to catalyse GDP to GTP exchange in RhoA. They transduce the signals from active heterotrimeric G-proteins to RhoA (303). The RhoGEF family is diverse and many have a single GTPase target making them essential signal transducers between GPCRs. Moreover, regulation of RhoGEFs has been suggested to occur via spatiotemporal mechanisms and subcellular localisation (304). At present, five RhoGEFs have been shown to link heterotrimeric G-

protein signalling to RhoA activation; p115-RhoGEF, PDZ-RhoGEF, LARG, p63-RhoGEF, and AKAP13 (148, 149, 301).

Traditionally, the primary effector of $G_{\alpha q/11}$ in smooth muscle cells is PLCβ which catalyses PIP_2 to IP_3 and DAG, leading to increased cytosolic calcium, which in turn results in phosphorylation of the myosin light chain and cell contraction (305). More recently however, p63RhoGEF was identified as a specific link between the $G_{\alpha q/11}$ angiotensin 1 receptor and RhoA in vascular smooth muscle cells isolated from rat aorta (306). Moreover, sphingosine-1-phosphate has been shown to activate RhoA through a combination of $G_{\alpha q}$ and $G_{\alpha 12/13}$ in vascular smooth muscle cells isolated from rat aorta (307). However, classical research has shown p115-RhoGEF, PDZ-RhoGEF, and leukaemia-associated RhoGEF (LARG) to specifically associate with $G_{\alpha 12/13}$ and activate RhoA (148, 303, 308). Analysing expression of RhoGEFs in ASM cells was not within the scope of this thesis, however it could indicate which heterotrimeric G-proteins are coupled to RhoA.

In conclusion, this chapter has demonstrated that $G_{\alpha q/11}$ are not required for LPA-induced TGFβ or RhoA activation in ASM cells. Moreover, for the first time, this chapter has shown ROCKI/II are required for LPA-induced TGFβ activation. These data disprove the hypothesis that $G_{\alpha q/11}$ are required for LPA-induced TGFβ activation in ASM cells. Moreover, it suggests that RhoA is likely to be required for LPA-induced TGFβ activation. The question remains, which heterotrimeric G-proteins are upstream of RhoA and TGFβ activation. Research described above suggests that $G_{\alpha 12/13}$ are most frequently linked to RhoA activation through p115-RhoGEF, PDZ-RhoGEF, and LARG, therefore this hypothesis will be tested in chapter 6 (148, 303, 308).

5 Chapter 5: Investigating the role of G-proteins in cyclical mechanical stretch-induced TGFβ activation in ASM cells

5.1 Rationale

The lung is a dynamic organ that is constantly undergoing cycles of stretch and constriction due to the changes in air pressure that are experienced during breathing. This contributes to the unique, ever-changing microenvironment within the lung. All cells within the lung are subjected to different forces throughout the breathing cycle. The asthmatic lung is exposed to more force due to the excessive contraction of a thickened ASM band (90). Moreover, the airways of asthmatic patients are stiffer because of the structural changes that occur during the process of airway remodelling (240). These structural changes increase airway resistance and therefore increase the amount of strain that individual cells are exposed to during normal breathing (241).

It is well known that cells contain mechanosensitive proteins that initiate cellular signalling in response to force. These forces can be generated internally through reorganisation of the actin cytoskeleton during contraction. Alternatively, they can be generated through changes in the extracellular environment through remodelling of the ECM. These responses lead to a change of gene expression within the cell. Cyclical stretch of cardiac fibroblasts results in an increase in total protein synthesis, including TGFβ, in comparison to unstretched cells (309). Hepatic stellate cells also increase both mRNA and TGFβ release in response to stretch, an effect that is abrogated when RhoA is inhibited (310). ASM and vascular smooth muscle cells have been shown to increase TGFβ1 expression in response to cyclical mechanical stretch (183, 311). Moreover, an increase in mRNA for collagen I and IV, and fibronectin was observed

(311). These studies demonstrate that TGFβ and ECM components mRNA expression can be upregulated in response to cyclical mechanical stretch. Not only is total TGFβ expression and protein upregulated in response to stretch, TGFβ activation is also increased. Fibrotic lung strips taken from a rat and subjected to tensile force showed an increase in active TGFβ1 liberated from extracellular stores and an increase in phospho-Smad2, a specific measure of TGFβ signalling (312).

As discussed in section 1.5.5 TGFβ plays a central role in the structural changes within the asthmatic airway, collectively known as airway remodelling. TGFβ has been shown induce epithelial apoptosis and epithelial-mesenchymal transition (65, 243), subepithelial fibrosis (73, 223, 244), differentiation of fibroblasts to myofibroblasts (78, 79), increased ASM mass ASM cell proliferation and migration, resulting in increased ASM mass and strong airway contraction upon exacerbation (242). Furthermore, both goblet cell hyperplasia and angiogenesis have been linked to the effects of TGFβ in the asthmatic airways (117, 231).

The mechanism of stretch-induced TGFβ activation is not entirely clear. Tensile force-induced TGFβ activation in a fibrotic lung strip was attenuated by an integrin αv subunit inhibitor and a ROCKI/II inhibitor (312). Similarly, cyclical stretch-induced TGFβ activation in hepatic stellate cells was blocked by a RhoA inhibitor (310). These studies suggests that RhoA/ROCKI/II are central to stretch-induced activation of TGFβ1. Further, a study on human ASM cells showed that cyclical mechanical stretch-induced TGFβ1 expression and secretion was abrogated by inhibitors of RhoA, ROCKI/II, PI3K, PTK, and MEKI/II (183). It went on to highlight that the transcription factor AP-1 was involved in cyclical mechanical stretch-induced TGFβ1 transcription. Conversely, some studies have suggested that

mechanical stretch itself is not responsible for TGFβ1 expression, but stretch induces the release of factors that bind to receptors on the cell surface to induce TGFβ expression. A study on vascular smooth muscle cells showed that cyclical mechanical stretch-induced TGFβ1 expression and secretion was inhibited by the angiotensin II receptor inhibitor, saralasin (185). This study suggested that angiotensin II was acting in a paracrine manner to induce TGFβ1 activation and release. TGFβ1 itself acts as a paracrine factor, being expressed and released from cells, binding to its tyrosine kinase receptor and induces gene expression changes such as collagen III synthesis (185, 313).

If cyclical mechanical stretch induces the release of paracrine factors that stimulate TGFβ activation then it may act via GPCRs. At present, it is not known whether a specific class of heterotrimeric G-protein is involved in stretch-induced TGFβ activation. If angiotensin is acting in a paracrine factor to stimulate TGFβ release in vascular smooth muscle cells then it is highly likely that a heterotrimeric G-protein is involved because the angiotensin receptors couple to $G_{\alpha q/11}$, $G_{\alpha 12/13}$, and $G_{\alpha i/o}$ (314). In cardiac myocytes subjected to pressure overload found that the $G_{\alpha 12/13}$-coupled receptor P2Y6 was required for TGFβ-induced fibrosis in the heart (315). A study in mice showed that forced high pressure ventilation resulted in an increase in total lung TGFβ1, an affect that was abrogated in transgenic mice with epithelial knockout of $G_{\alpha q/11}$ (127). These data suggest that there could be a role for $G_{\alpha q/11}$ or $G_{\alpha 12/13}$ in stretch-induced TGFβ activation in various cell types. The specific class of heterotrimeric G-proteins involved in stretch-induced TGFβ activation has not been studied.

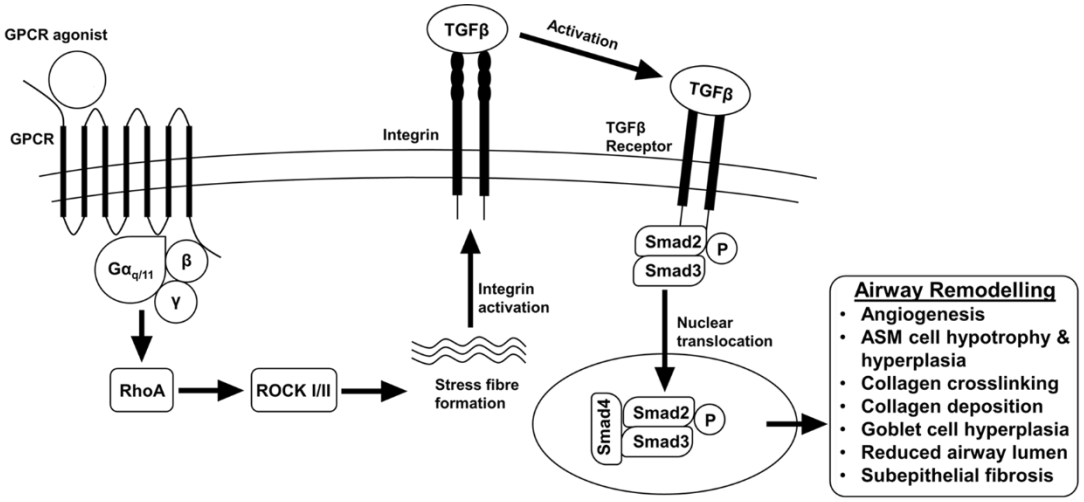

Figure 5.1. Hypothesised pathway leading to TGFβ activation in ASM cells.

5.2 Aims

This chapter investigates whether $G_{\alpha q/11}$ are required for cyclical mechanical stretch-induced TGFβ activation in ASM cells.

5.3 Results

5.3.1 Cyclical mechanical stretch activates TGFβ in both non-asthmatic and asthmatic ASM cells

First, a cyclical mechanical stretch time course was carried out to determine the optimum time point to measure pSmad2. ASM cells isolated from asthmatic patients were stretched at a frequency of 0.3Hz, to replicate normal human breathing, and at an equibiaxial stretch of 15%. Cells were stretched for 4, 8, 24, and 48 hours and pSmad2 measured by western blot. Quantification of western blots was done by measuring the densitometry of pSmad2 over Smad2/3. There was an increase in pSmad2 at all time points except at 48 hours in one experiment (figure 5.2). Statistical testing of the unstretched group versus the stretched group at all time points pooled together shows that stretch induced a significant increase in pSmad2. The largest increase in pSmad2 was a 3-fold increase after 4 hours of stretch. At 8 hours there was only a 1.5 fold increase in pSmad2, and at 24 and 48 hours the increase in pSmad2 because far more variable. For further, experiments 4 hours of stretch was used due to the magnitude and consistency of the pSmad2 signal.

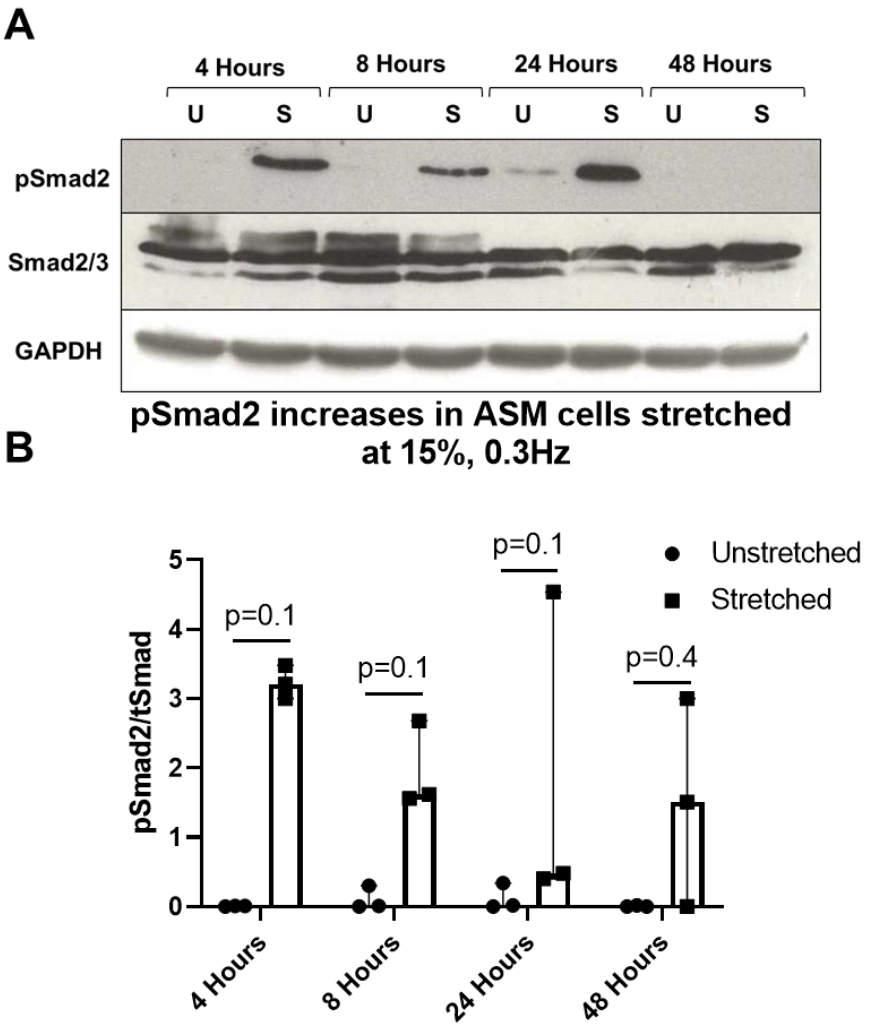

Figure 5.2. Human ASM cells were cultured collagen I coated Flexwell tissue culture plates. Human ASM cells (n=3 cell lines) were stretched at a frequency of 0.3Hz and equibiaxial stretch of 15% for 4, 8, 24, and 48 hours. Stretch induced a significant increase in pSmad2 versus unstretched cells (p=0.0286). Representative western blot of pSmad2, Smad2/3, and GAPDH measured at all time points, A. Densitometry of western blots expressed as median pSmad2/tSmad ± IQR. Statistical test is a Mann-Whitney U.

Next, a comparison of pSmad2 activation between ASM cells isolated from non-asthmatic and asthmatic patients was carried out by western blot. This was done to investigate whether more TGFβ activation might occur in the lung of asthmatic patients while breathing normally. Cells were stretched at a frequency of 0.3Hz and equibiaxial stretch of 15%. Quantification of western blots was done by measuring the densitometry of pSmad2 over Smad2/3. Stretch induced a significant increase in pSmad2 in both groups (figure 5.3). Non-asthmatic cells saw a 1.5-fold increase in pSmad2, whereas asthmatic cells exhibited a 2.5-fold increase. The increase in pSmad2 in asthmatic cells was similar to the increase seen at 4 hours in the previous time course experiment (figure 5.2), however pSmad2 in non-asthmatic cells was 50% lower. Although there was not a significant difference between the two groups after stretch there is clearly a trend to more pSmad2 in asthmatic stretched cells. The mean pSmad2 increase in asthmatic ASM cells was 50% higher than the non-asthmatic group. It is likely that to see a statistical difference between the two stretched groups there would need to be a high sample size because of the large standard error of mean. However, this data does show that there is more stretch-induced pSmad2 in asthmatic versus non-asthmatic ASM cells despite the variability between individual data points.

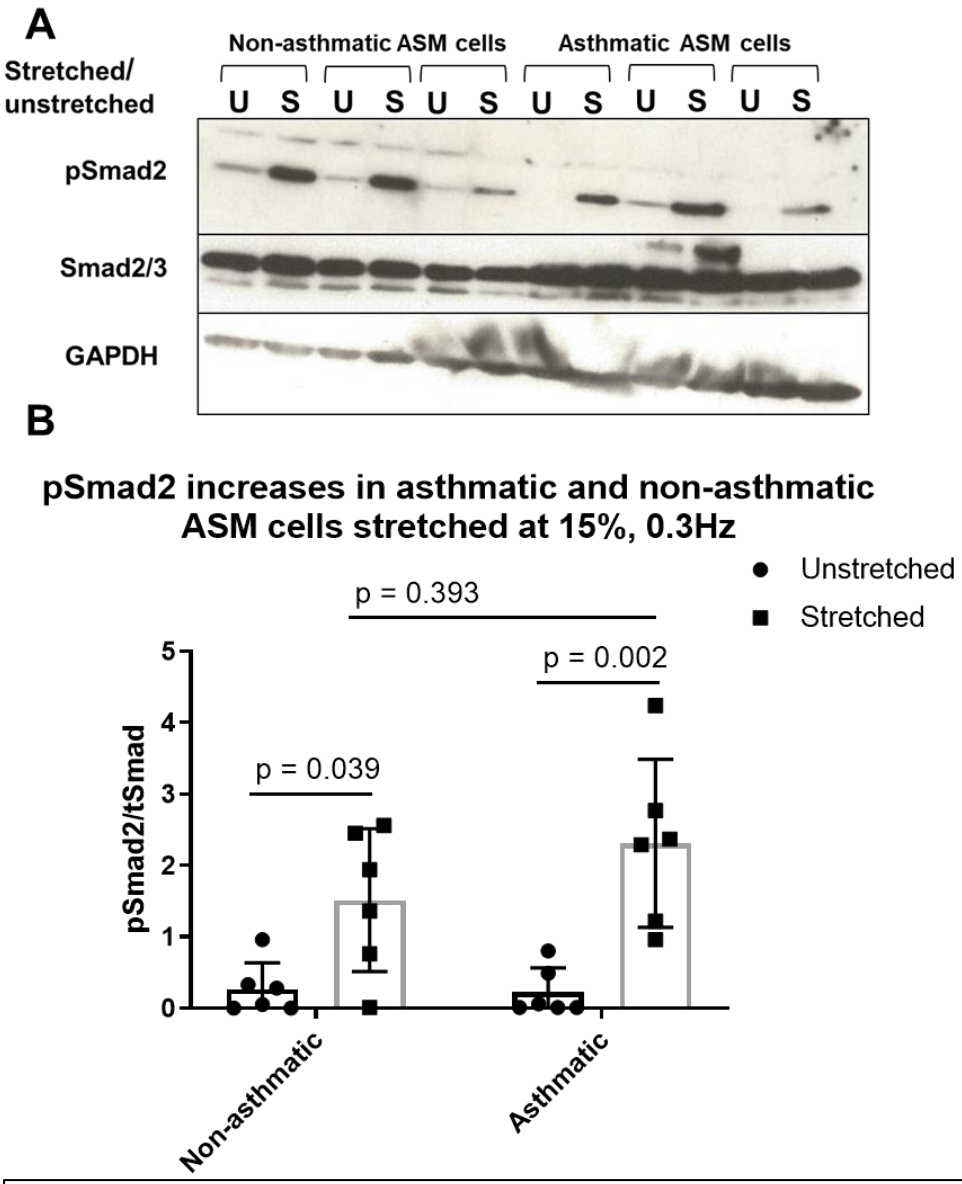

Figure 5.3. Human ASM cells were cultured collagen I coated Flexwell tissue culture plates. Human non-asthmatic ASM cells (n=6 cell lines) and asthmatic cells (n=6 cell lines) were stretched at a frequency of 0.3Hz and equibiaxial stretch of 15% for 4 hours. Stretch induced a significant increase in pSmad2 in both groups. There was a small non-significant difference in pSmad2 between both groups with asthmatic ASM cells inducing more pSmad2. Representative western blot of pSmad2, Smad2/3 and GAPDH A. Densitometry of western blots expressed as mean pSmad2/tSmad ± SEM. Statistical test is t-test.

5.3.2 The role of $G_{\alpha q/11}$ in stretch-induced pSmad2 in ASM cells

To determine whether $G_{\alpha q/11}$ were required for stretch-induced TGFβ siRNA knockdown of $G_{\alpha q}$ and $G_{\alpha 11}$ was carried out in the same manner as in chapter 4. Cells were treated with the transfection vehicle, negative control siRNA, or $G_{\alpha q}$ and $G_{\alpha 11}$ siRNA. Experiments were carried out 72 hours post-transfection. Knockdown of $G_{\alpha q}$ and $G_{\alpha 11}$ was determined for each experiment by western blot and calculating the ratio of $G_{\alpha q}$ or $G_{\alpha 11}$ to GAPDH using densitometry (figure 5.4). There was significant knockdown of both $G_{\alpha q}$ and $G_{\alpha 11}$ protein when comparing the negative control transfected group against the $G_{\alpha q}$ and $G_{\alpha 11}$ transfected groups. Stretch had no effect on the efficiency of $G_{\alpha q}$ and $G_{\alpha 11}$ knockdown. The knockdown observed was similar to that achieved in chapter 4, which was significant but not complete.

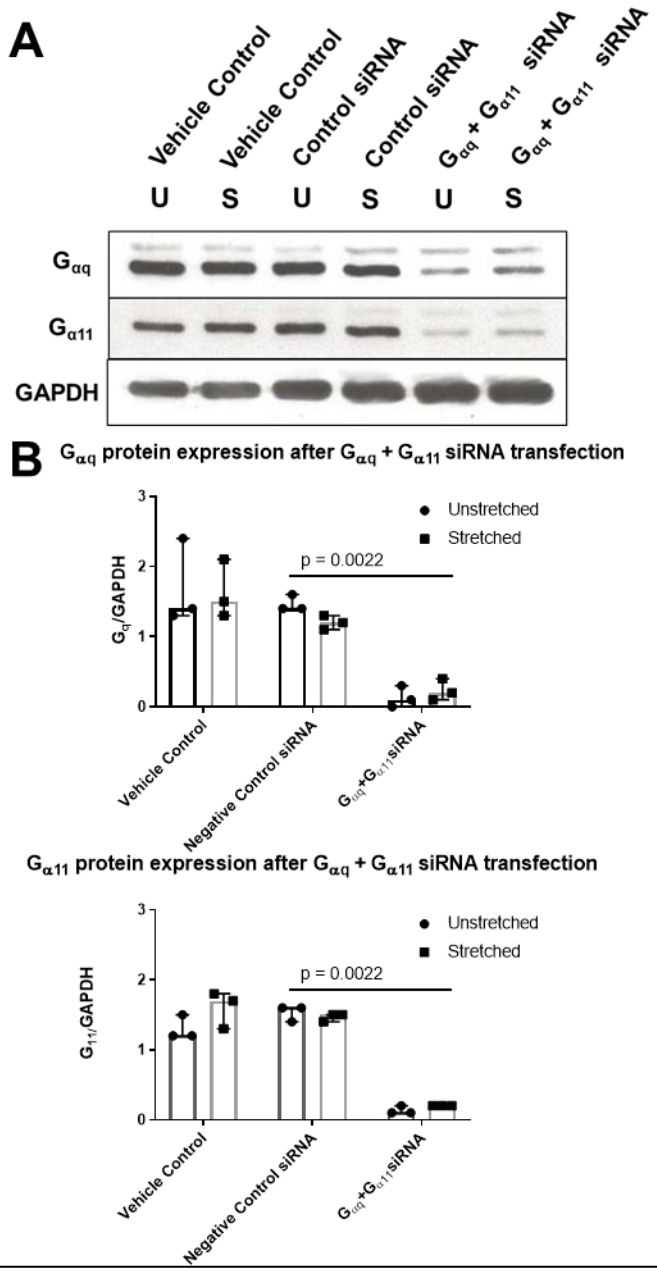

Figure 5.4. Human ASM cells were cultured collagen I coated Flexwell tissue culture plates. Human asthmatic cells were treated with siRNA targeting $G_{\alpha q}$ and $G_{\alpha 11}$ (n=3 cell lines). Cells were stretched, 72 hours after transfection, at a frequency of 0.3Hz and equibiaxial stretch of 115% for 4 hours. Representative western blot showing $G_{\alpha q}$ and $G_{\alpha 11}$ protein in lysates from siRNA transfection experiments, A. There was significant knockdown of both $G_{\alpha q}$ and $G_{\alpha 11}$ in all experiments (n=3 cell lines) shown by densitometry, B. Data is presented as median ± IQR. Statistical test used was a Mann-Whitney U of control siRNA and $G_{\alpha q}$ + $G_{\alpha 11}$ siRNA groups.

Once knockdown of $G_{\alpha q}$ and $G_{\alpha 11}$ was determined by western blot, activation of TGFβ was determined by measuring pSmad2. A western blot was carried out to determine whether pSmad2, the first signalling event after TGFβ receptor activation, was activated in response to cyclical mechanical stretch in ASM cells. Cells were stretched for 4 hours, 72 hours post siRNA transfection. Cyclical mechanical stretch induced an increase in pSmad2 in the transfection vehicle control, siRNA control and $G_{\alpha q}$ and $G_{\alpha 11}$ groups (figure 5.5). There was also a noticeable increase in basal pSmad2 in unstretched ASM cells treated with $G_{\alpha q}$ and $G_{\alpha 11}$ siRNA. Contrary to the hypothesis that knockdown of $G_{\alpha q}$ and $G_{\alpha 11}$ would inhibit cyclical mechanical stretch-induced pSmad2, there was actually a non-significant 2-fold increase in pSmad2 in the $G_{\alpha q}$ and $G_{\alpha 11}$ siRNA group versus the control siRNA group. Moreover, this result mirrors the effect of LPA-induced pSmad2 in ASM cells treated with $G_{\alpha q}$ and $G_{\alpha 11}$ in Chapter 4.

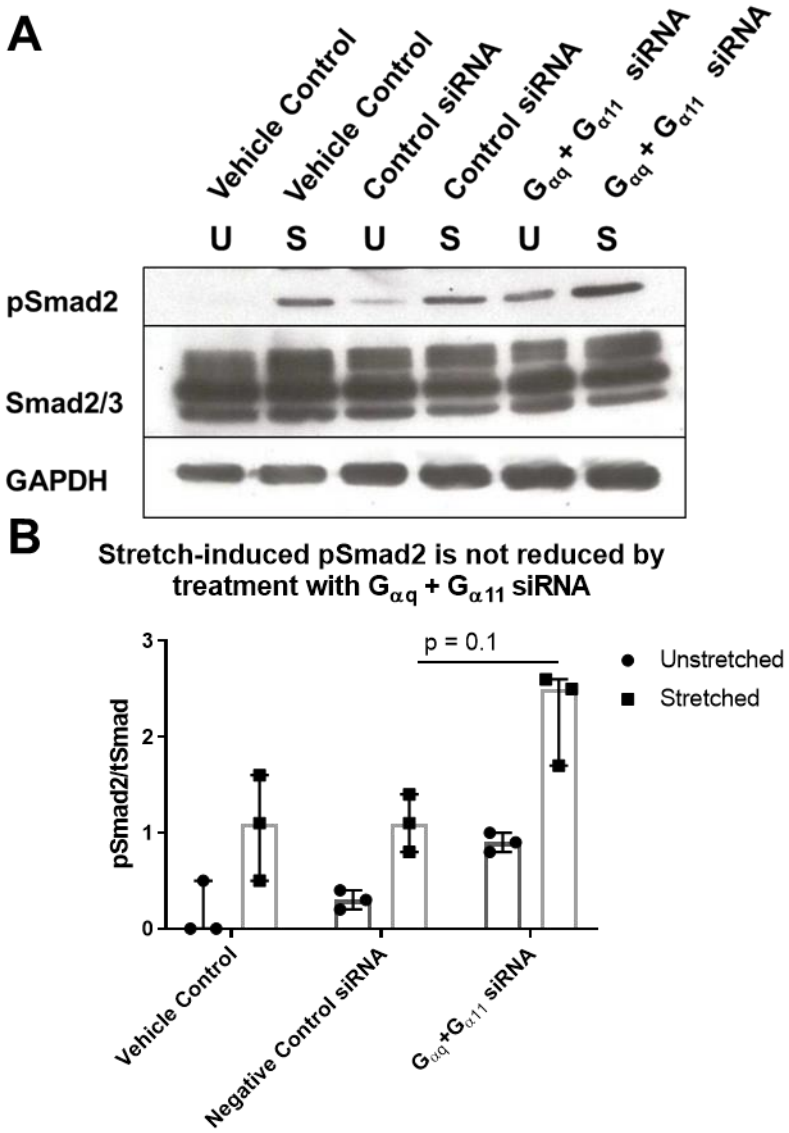

Figure 5.5. Human ASM cells were cultured collagen I coated Flexwell tissue culture plates. Human asthmatic cells were treated with siRNA targeting $G_{\alpha q}$ and $G_{\alpha 11}$ (n=3 cell lines). Cells were stretched, 72 hours after transfection, at a frequency of 0.3Hz and equibiaxial stretch of 15% for 4 hours. Representative western blot showing pSmad2 and Smad2/3 protein, A. There was no reduction of stretch-induced pSmad2 in ASM cells treated with $G_{\alpha q}$ and $G_{\alpha 11}$ siRNA (n=3 cell lines) shown by densitometry of pSmad2 over Smad2/3, B. Data is presented as median ± IQR. Statistical test used was a Mann-Whitney U of stretched control siRNA versus stretched $G_{\alpha q}$ + $G_{\alpha 11}$ siRNA.

Next, the small molecule inhibitor of $G_{\alpha q/11/14}$ was used to validate data showing cyclical mechanical stretch induced pSmad2 in ASM cells treated with $G_{\alpha q}$ and $G_{\alpha 11}$ siRNA. Asthmatic ASM cells were pre-treated with 10nM of the $G_{\alpha q/11/14}$ inhibitor, YM-254890, for 45 minutes prior to stretch. This concentration was selected because it significantly inhibited LPA-induced TGFβ activation in a coculture of ASM cell and TMLC reporter cell experiment (figure 4.5a). Moreover, this concentration of YM-254890 inhibited stretch-induced pSmad2 in precision cut lung slices (Appendix figure 2). Cells were subjected to 15% stretch for 4 hours at a frequency of 0.3Hz to replicate normal breathing. Levels of pSmad2 were measured by western blot and quantified by densitometry. Cyclical mechanical stretch induced an increase in pSmad2 versus the unstretched controls in both the vehicle control and YM-254890 groups (figure 5.6). The stretch-induced increase in pSmad2 was approximately 3-fold in the vehicle control group and 2-fold in the YM-254890 group compared to their respective unstretched controls. However, the magnitude of stretch-induced pSmad2 in the YM-254890 treated group was around half that of the vehicle control group, suggesting that there was a trend towards inhibition of pSmad2. This is in contrast to experiments that used siRNA to knockdown $G_{\alpha q}$ and $G_{\alpha 11}$ where there was a clear stretch-induced increase in pSmad2.

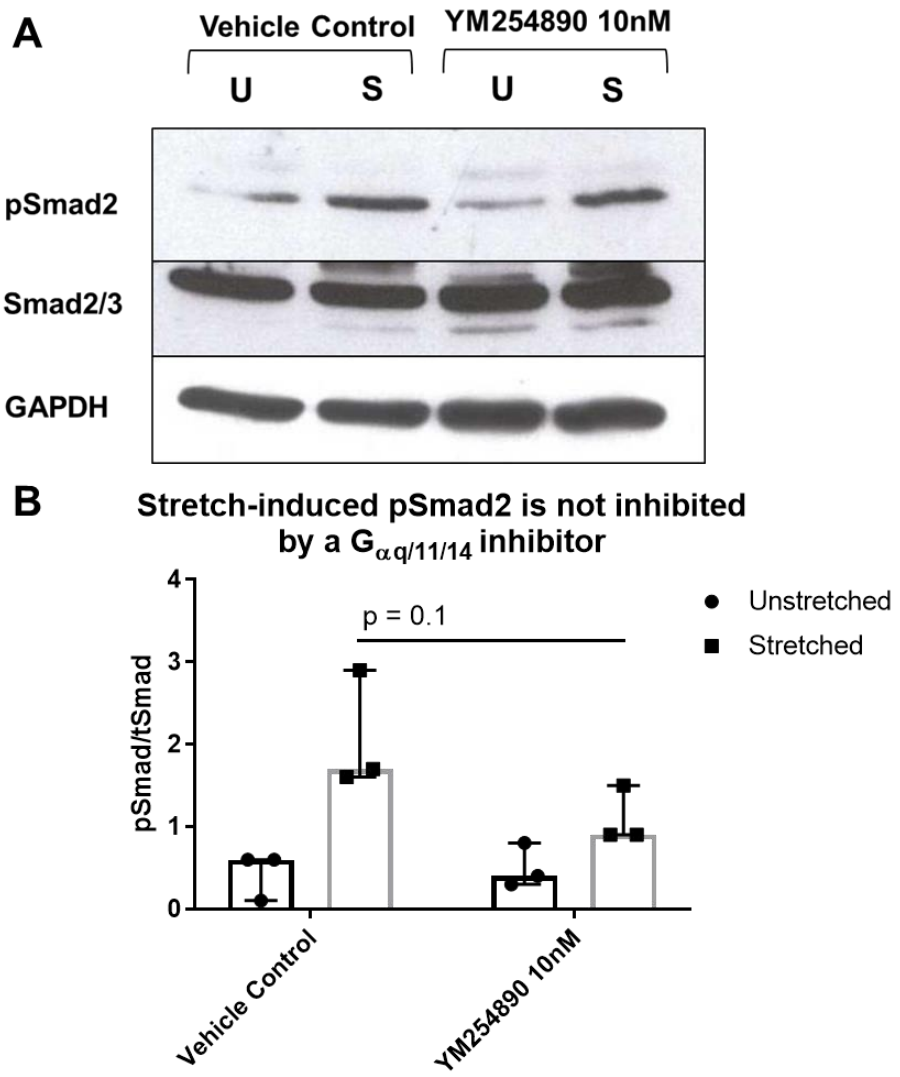

Figure 5.6. Human ASM cells were cultured collagen I coated Flexwell tissue culture plates. Human asthmatic cells were pre-treated with a small molecule inhibitor of $G_{\alpha q/11/14}$ YM-254890 45 minutes prior to stretch (n=3 cell lines). Cells were stretched at a frequency of 0.3Hz and equibiaxial stretch of 15% for 4 hours. Representative western blot showing pSmad2 and Smad2/3 protein, A. There was a reduction in the magnitude of stretch-induced pSmad2 in ASM cells treated with YM-254890 compared to the vehicle control, however there was still a stretch induced increase in pSmad2 in both groups (n=3 cell lines) shown by densitometry of pSmad2 over Smad2/3, B. Data is presented as median ± IQR. Statistical test used was a Mann-Whitney U of the stretched vehicle control group versus stretched YM-254890 group.

5.3.3 Small molecule inhibition of ROCKI/II inhibits cyclical mechanical stretch-induced pSmad2

To determine whether there was a role for the serine/threonine kinase ROCKI/II in cyclical mechanical stretch-induced TGFβ signalling, a small molecule inhibitor was used. A concentration of 10μM was used because this inhibited LPA-induced pSmad2 in asthmatic ASM cells in chapter 4 (figure 4.13). Human asthmatic ASM cells were pre-treated with an inhibitor of ROCKI/II, Y27623, 45 minutes prior to stretch. Cells were subjected to 15% cyclical mechanical stretch for 4 hours at a frequency of 0.3Hz. Western blot was used to measure pSmad2 and densitometry pSmad2 over Smad2/3 determined the relative magnitude of pSmad2. There was a large stretch-induced increase in pSmad2 in the vehicle control group (figure 5.7). Stretch-induced pSmad2 was abrogated by the ROCKI/II inhibitor, Y27623. There was a 50% reduction in the magnitude of pSmad2 in the stretched Y27632 cells compared to the stretched vehicle control, however the confidence intervals were large and it was not significant. The level of pSmad2 was increased in the unstretched Y27623 group compared to the unstretched vehicle control, however it is clear that the stretch-induced pSmad2 was abrogated by Y27623.

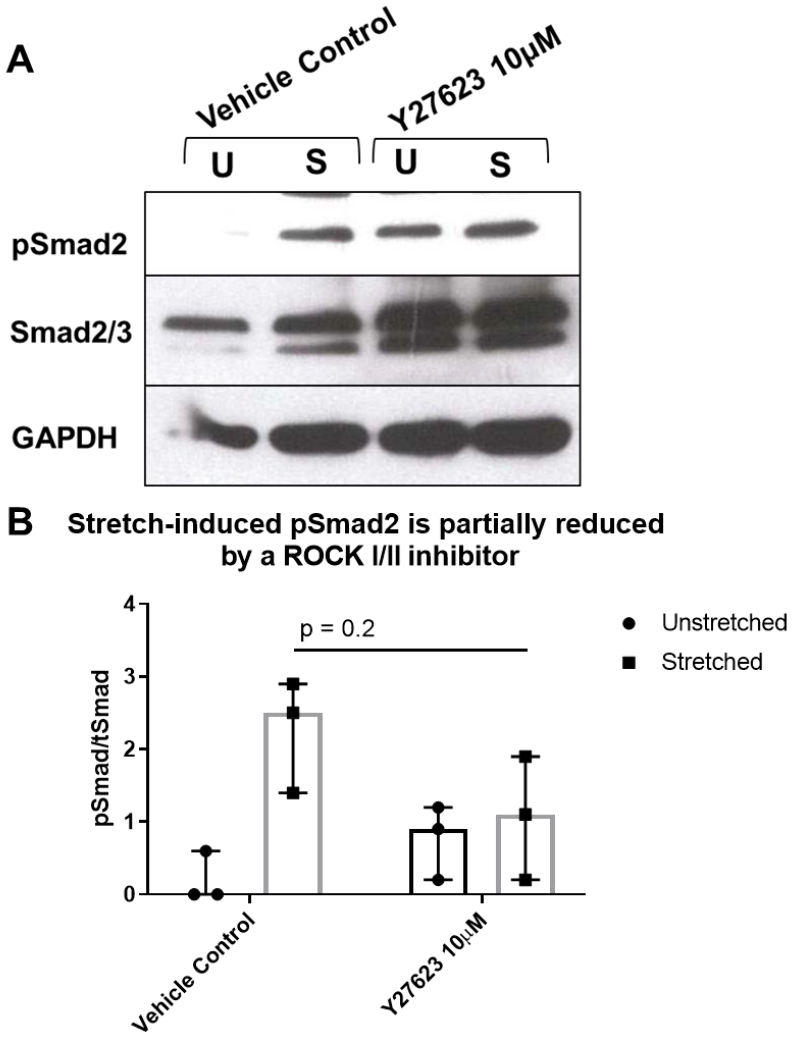

Figure 5.7. Human ASM cells were cultured collagen I coated Flexwell tissue culture plates. Human asthmatic cells were pre-treated with a small molecule inhibitor of ROCKI/II Y27623 45 minutes prior to stretch (n=3 cell lines). Cells were stretched at a frequency of 0.3Hz and equibiaxial stretch of 15% for 4 hours. Representative western blot showing pSmad2, Smad2/3 and GAPDH, A. Stretch-induced pSmad2 was inhibited in the Y27623 group, however the amount of pSmad2 in unstretched cells was also higher in this group (n=3 cell lines) shown by densitometry of pSmad2 over Smad2/3, B. Data is presented as median ± IQR. Statistical test used was a Mann-Whitney U of the stretched vehicle control group versus stretched Y27623 group.

5.4 Discussion

The pleiotropic cytokine TGFβ is known to play a central role in fibrotic diseases and can induce the expression of fibrotic genes that contribute to airway remodelling seen in the airway of severe asthmatic patients. Overexpression of TGFβ and pSmad2 in the asthmatic airways has been linked to subepithelial fibrosis, ASM cell hyperplasia and hypertrophy, epithelial damage, goblet cell hyperplasia, and angiogenesis (1, 211, 214). It is therefore important to fully understand the mechanism by which TGFβ becomes activated in the airways of severe asthmatics, who suffer from frequent exacerbation.

All of the experiments described in this chapter, except the comparison of non-asthmatic and asthmatic cells, were carried out in asthmatic ASM cells. There were two reasons for this; first, in order to show inhibition of TGFβ I wanted the maximum TGFβ signal, and results in this chapter show, for the first time, that asthmatic ASM activate more TGFβ in response to stretch than non-asthmatic ASM cells. The second was to ensure that analysis of the TGFβ signalling pathway was relevant in cells taken from asthmatic patients because asthmatic cells can behave differently to non-asthmatic cells. A comparison between asthmatic patients and allergic rhinitis patients given inhaled bronchoconstrictors showed that only asthmatics suffered exaggerated airway narrowing (291).

The primary statistical test used in this chapter was the Mann-Whitney U. This was used because the majority of experiments used three replicates and therefore cannot be assumed to show normal (Gaussian) distribution. Gaussian distribution assumes that the results will fit in a standard bell-curve (316). A statistical limitation to the Mann-Whitney U test is that it does not measure the magnitude of difference between the means, but rather ranks each

individual data point based on its value. It is therefore impossible to attain statistical 'significance' with three replicates no matter how large the effect size or small the confidence interval.

The lung is a dynamic environment constantly subjected to mechanical forces during breathing. It has been hypothesised that mechanical stress is communicated between different cell types within the airways to induce structural changes (317). Integrins are mechanosensitive cell surface proteins that are able to liberate the active TGFβ molecule by binding to an RGD motif in the LAP of TGFβ. The integrin αvβ5 is responsible for TGFβ liberation in ASM cells, whereas αvβ6 is responsible in epithelial cells (128, 133). In mice subjected to low pressure and high pressure forced ventilation, there was a significant increase in total lung TGFβ1 after high pressure ventilation (127). This effect was abrogated by epithelial knockout of $G_{\alpha q}$ and $G_{\alpha 11}$, but not $G_{\alpha 11}$ alone (127). In cultured ASM cells, stretch has been shown to increase TGFβ1 gene expression via a RhoA/ROCKI/II signalling (183). However, it has not been determined whether a $G_{\alpha q/11}$ play a role stretch-induced TGFβ activation in ASM cells. Nor has pSmad2, the first signalling event after TGFβ receptor activation, been measured in ASM that have undergone a stretching regimen.

Previous work in human ASM cells has shown that TGFβ1 mRNA is increased after 3 hours of uniaxial cyclical mechanical stretch using a Flexcell™. Cells were subjected to 12% stretch at a frequency of 0.3Hz (183). This frequency is experienced during human tidal breathing. Human ASM cells are stretched by 4-5% during tidal breathing and as much as 25%-30% during deep inspiration (318). For the experiments conducted in this thesis, 15% equibiaxial stretch was selected due to previous unpublished work in this laboratory and because other published work typically uses 12% stretch. It is

plausible that 15% stretch represents physiological levels *in vivo* that would be experienced during normal daily activity.

It is known that levels of TGFβ are increased in the BAL fluid and submucosa of asthmatic versus non-asthmatic patients (74, 213). Further, human ASM cells from asthmatic patients treated with LPA induce more TGFβ activation than non-asthmatic ASM cells (133). However, a comparison of asthmatic versus non-asthmatic stretch-induced TGFβ activation in human ASM cells has not been carried out. Measuring pSmad2 by western blot showed that there was more stretch-induced pSmad2, and therefore TGFβ activation, in asthmatic versus healthy ASM cells. The median increase in pSmad2 in asthmatic versus non-asthmatic ASM cells was clear but not significant due to large confidence intervals in both groups. However, a significant difference is likely to have been observed if the experiment carried greater power through more cells lines. More pSmad2 was expected in asthmatic ASM cells in response to stretch based on research that has shown TGFβ activation to be higher in asthmatic cells in response to other stimuli such as LPA and methacholine (133). This finding is important because it demonstrates that asthmatic ASM cells are primed to activate more TGFβ and are therefore induce airway structural changes in comparison to ASM cells from a non-asthmatic airway (133, 161).

At present, it is not clear how mechanical stretch induces TGFβ activation. To date, most studies have linked cell surface receptors to stretch-induced TGFβ. Angiotensin II, a GPCR agonist, is required for cyclical mechanical stretch-induced TGFβ activation in vascular smooth muscle cells (185). Moreover, in mice total lung TGFβ is increased after high pressure forced ventilation and abrogated by epithelial knockout of $G_{\alpha q/11}$ (127). These studies suggest that the mechanical force applied to the cell during stretching induces the

released of a paracrine factor that can act back on the cell to trigger the TGFβ signalling pathway. There have been no *in vitro* studies to determine whether $G_{\alpha q/11}$ are required for stretch induced TGFβ activation in ASM cells.

In this thesis, siRNA was used to knockdown $G_{\alpha q/11}$ prior to cyclical mechanical stretch. There was no reduction in stretch-induced pSmad2 in siRNA treated cells compared with the control groups. In fact, there was a 2-fold increase in pSmad2 in siRNA treated cells compared to the control group. This effect was also observed in chapter 4 when ASM cells were treated with $G_{\alpha q/11}$ siRNA and stimulated with LPA. Conversely, treating ASM cells with small molecule $G_{\alpha q/11/14}$ inhibitor before the stretch regimen reduced the magnitude of stretch-induced pSmad2, but did not abrogate stretch-induced pSmad2. It is interesting that blocking $G_{\alpha q/11}$ by siRNA caused pSmad2 to increase whereas using the small molecule inhibitor caused pSmad2 to decrease. Targeting $G_{\alpha q/11}$ using siRNA knocks down the catalytically active G_{α} subunit, whereas the inhibitor keeps the heterotrimer locked in its inactive state by preventing the exchange of GDP for GTP (288). It is possible that knockdown of the G_{α} subunits by siRNA leaves excess free $G_{\beta\gamma}$ subunits in the cytoplasm. $G_{\beta\gamma}$ primarily function to trigger a negative feedback loop to stop GPCR signalling by activating G-protein coupled receptor kinases, thus it is unlikely that this caused the increase in pSmad2 (319).

The other obvious difference is that the inhibitor also blocks signalling of $G_{\alpha 14}$, the least studied subunit of the $G_{\alpha q}$ family. $G_{\alpha 14}$ has a more restricted expression pattern than the ubiquitously expressed $G_{\alpha q/11}$, but is expressed in the lungs as determined by total organ RNA (320). However, expression of $G_{\alpha 14}$ was not measured in cells used in experiments described in this thesis. Moreover, $G_{\alpha 14}$ is also

able to activate PLCβ through $G_{\alpha q/11}$, some $G_{\alpha i}$, and some $G_{\alpha s}$ coupled receptors (321). PLCβ catalyses the hydrolysis is PIP_2 to IP_3 and DAG, which are secondary messengers that can initiate intracellular calcium signalling and activate PKC. To date, there is no evidence that TGFβ activation is downstream of calcium signalling or PKC signalling, therefore it is unlikely that $G_{\alpha 14}$ is involved in TGFβ activation. However, it is interesting that pSmad2 increased by 50% in ASM treated with $G_{\alpha q/11}$, whereas it decreased by 50% in cells treated with a $G_{\alpha q/11/14}$ inhibitor. This reduction in pSmad2 in the presence of the $G_{\alpha q/11/14}$ could be due to additional inhibition of $G_{\alpha 14}$. Alternatively, genetic manipulation of heterotrimeric G-proteins may have had off-target effects. There is evidence that genetic knockdown of a specific class of heterotrimeric G-protein can lead to an increase in expression of other G-proteins (296). It is therefore possible that knockdown of $G_{\alpha q/11}$ is causing the expression of other G-proteins to increase.

It clear is from both siRNA knockdown of $G_{\alpha q/11}$ and small molecule inhibition of $G_{\alpha q/11/14}$ that stretch continued to induce an increase in pSmad2, and therefore TGFβ activation. These results show that of $G_{\alpha q/11}$ are not required for cyclical mechanical stretch-induced TGFβ activation in human asthmatic ASM cells. This finding is in contrast to data in airway epithelial cells. Increased total lung TGFβ in response to high pressure ventilation in mice was abrogated by the epithelial knockout of both $G_{\alpha q/11}$ (127). These results indicate that either, paracrine factors released upon stretch are acting on receptors that are coupled to different G-protein families in airway epithelial and ASM cells, or mechanical stretch in ASM cells activates TGFβ independently of any GPCR.

Angiotensin and endothelin are released from stretched aorta smooth muscle cells and cardiac fibroblasts respectively, both of which are

GPCR agonists (185, 309). Mechanical strain on human ASM has been shown to induce secretion of the proteases MMP1 and MMP2, the latter of which has been identified as an activator of latent TGFβ (322). ATP is also released from multiple cell types, including human ASM cells, in response to mechanical strain and is associated with inflammation (323). Moreover, prostaglandin is released from ASM cells in response to stretch and its receptors are coupled to $G_{\alpha s}$ and $G_{\alpha i}$ heterotrimeric G-protein families (324). It would have been interesting to determine whether there was secretion of a specific mediator from stretched ASM that induced TGFβ activation. A media transfer experiment was considered, however, TGFβ is upregulated and secreted upon stretch so it would have directly induced pSmad2 and thus not answered the question of whether a secreted mediator or stretch itself induces TGFβ signalling. Mass spectrometry of media from stretched ASM cells could also have been analysed, however, based on previous data described here there are likely to be many secreted factors from stretched ASM cells. This would be an interesting experiment to carry out in the future, particularly if there was data indicating a paracrine mechanism.

In the majority of research analysing the pathway leading to TGFβ activation, the small G-protein RhoA and its effectors ROCKI/II are frequently described as central to its activation. Indeed, inhibition of RhoA or ROCKI/II abrogated uniaxial stretch-induced TGFβ1 expression and secretion in ASM cells (183). Work in this thesis showed that inhibiting ROCKI/II using the small molecule inhibitor Y27623 prevented cyclical mechanical stretch-induced pSmad2, and therefore TGFβ activation. This result supports the current literature showing that Y27623 prevents stretch-induced TGFβ activation in fibrotic lung strips, and TGFβ expression in ASM cells (183, 312). However, in this thesis it is noticeable that Y27623 increased pSmad2

in unstretched control ASM cells, a feature that does not happen in fibrotic lung strips treated with the same concentration of this inhibitor (312). Nor does TGFβ expression or secretion increase in unstretched ASM cells treated with the same concentration of Y27623 (183). This is the first time that pSmad2 has been measured in ASM cells subjected to cyclical mechanical stretch treated with a ROCKI/II inhibitor. It indicates that ROCKI/II is central to the activation of TGFβ in stretched ASM cells, and fits with the current body of work that shows RhoA/ROCKI/II to be central to TGFβ activation from a range of stimuli.

In conclusion, this chapter has highlighted for the first time in human ASM cells that cyclical mechanical stretch can induce TGFβ signalling through pSmad2. Moreover, the heterotrimeric G-protein family $G_{\alpha q/11}$ is not involved in stretch-induced TGFβ activation in human ASM cells. It seems likely from this data and from others that the serine/threonine kinase ROCKI/II is central to TGFβ activation in ASM cells.

6 Chapter 6: Investigating the role of the Gα12/13 in LPA- and stretch-induced TGFβ activation in ASM cells

6.1 Rationale

Asthma is a chronic inflammatory disease of the airways characterised by airway hyper-responsiveness, inflammation, and bronchoconstriction. As a consequence the cells within the airways of asthmatics are subjected to a milieu of inflammatory cytokines and mechanical forces.

Cells are subjected to a large contractile force during bronchoconstriction due to thickening of the ASM band in asthmatic patients (93). Moreover, lungs of asthmatic patients are described as having airway resistance, which describes resistance to air flow generated from friction and stiffening of the lungs (240). The result of these structural changes within the lung is that individual cells within the asthmatic lung are exposed to more strain during breathing (241). Moreover, data in chapter 5 of this thesis has shown that even when cells are subjected to equal strain, asthmatic cells activated more TGFβ than non-asthmatic cells. Thus, a combination of greater strain within the asthmatic airways and cells that are able to activate more TGFβ results in exaggerated TGFβ response ad contributes to airway remodelling (1).

LPA is a water soluble phospholipid that is present in many tissues of the body and is typically found at concentrations of 0.1μM in the blood plasma and 10μM in the serum (277). LPA is increased in the BAL of human subjects after allergen challenge (272). Autotaxin, an enzyme responsible for LPA synthesis, is also increased in the BAL of human subjects after allergen challenge (273). Healthy mice dosed with LPA via intranasal inhalation developed an increase in the murine homologue of IL-8, via PKC/NF-kappaB signalling (274).

Moreover, inhibition of the LPA_2 receptor in a HDM model of asthma reduced airway inflammation and IL-4 and IL-5 concentration within the lung (275, 276). These studies indicate that LPA plays a role in inflammation within the asthmatic airway. However, the role of LPA may not be limited to inflammation. LPA has been demonstrated to induce contraction and inhibit relaxation of isolated tracheal rings, and thus may be one of the many small molecules that induce bronchoconstriction within the asthmatic airway (278).

As discussed in section 1.5.5 TGFβ plays a central role in the structural changes within the asthmatic airway, collectively known as airway remodelling. TGFβ has been shown induce epithelial apoptosis and epithelial-mesenchymal transition (65, 243), subepithelial fibrosis (73, 223, 244), differentiation of fibroblasts to myofibroblasts (78, 79), increased ASM mass ASM cell proliferation and migration, resulting in increased ASM mass and strong airway contraction upon exacerbation (242). Furthermore, both goblet cell hyperplasia and angiogenesis have been linked to the effects of TGFβ in the asthmatic airways (117, 231).

LPA-induced TGFβ has been shown to require the small G-protein RhoA and its effector ROCKI/II in murine embryonic fibroblasts (128). The GPCR, protease activated receptor 1 (PAR1) has been shown to activate TGFβ in the murine lung and was suggested to occur via a RhoA and ROCK dependent mechanism, determined in murine embryonic fibroblasts (175). Fibrotic lung strips subjected to tensile force increase TGFβ activation and pSmad2, the first signalling event in the TGFβ pathway, an effect that was abrogated by an inhibitor of ROCKI/II (312). Further, cyclical mechanical stretch in human ASM cells is able to increase TGFβ1 expression, a process that is inhibited by an inhibitor of RhoA or ROCKI/II (183). Hepatic stellate cells, a mesenchymal cell found in the liver, also

release TGFβ in response to cyclical stretch which is inhibited by transfection with dominant negative RhoA (310). The sum of these studies clearly indicate that the RhoA/ROCKI/II axis is central to TGFβ activation and synthesis in response to both agonist and mechanical stretch stimuli. Indeed, this thesis has shown that inhibition of ROCKI/II abrogated TGFβ-induced pSmad2 in ASM cells stimulated with both LPA and cyclical mechanical stretch.

RhoA is a small G-protein that exchanges GDP for GTP upon activation by a RhoGEF. Its effector ROCKI/II is a serine/threonine kinase that remains inactive due autoinhibitory intramolecular folding, which is disrupted upon binding of RhoA<GTP> (283). ROCKI/II is a regulator of cytoskeleton dynamics, cell contractility, and calcium sensitisation (325). ROCKI/II is able to promote cell contraction through phosphorylation and thus inhibition of myosin light chain phosphatase (MLCP), which prevents MLCP from dephosphorylating MLC (130, 326). Stress fibres are significant contractile structures that are regulated by ROCKI/II (327). Upon activation, ROCKI/II phosphorylates and activates LIM domain kinases, which in turn phosphorylate the actin depolymerising protein cofilin (283). This results in the formation stress fibres composed of actin bundles of 10-30 actin filaments, which are cross linked by several actin crosslinking proteins including α-actinin (328).

Stress fibres are linked to large multiprotein complexes called focal adhesions, which serve to tether the actin cytoskeleton to the ECM. Integrins are mechanosensitive cell surface proteins that cluster at focal adhesion sites. Integrins are linked to the actin cytoskeleton through talin binding to the cytoplasmic portion of integrin, which is in turn cross linked to the actin cytoskeleton by vinculin (133). The extracellular portion of integrin binds to components of the ECM, thus directly linking the cell cytoskeleton to the ECM. Integrins are key

activators of latent TGFβ that recognise the RGD motif in the latent associated peptide and thus liberate the active TGFβ molecule in response to mechanical force (284). In human ASM cells αvβ5 has been shown to activate TGFβ in response to LPA and methacholine, and inhibition of this integrin in a murine OVA model of asthma reduces airway remodelling (133). Moreover, RhoA has been shown to induce ASM contraction by catalysing the assembly of focal adhesions and regulating actin polymerisation (293).

It is clear that the RhoA/ROCKI/II axis is central to TGFβ activation. The heterotrimeric G-protein class upstream of RhoA activation has not been fully established in ASM cells. Knockdown of $G_{\alpha q}$ in murine embryonic fibroblasts abrogated TGFβ activation, which was shown to require both RhoA and ROCKI/II (128). Moreover, knockout of epithelial $G_{\alpha q/11}$ in the murine lung abrogated an increase in total TGFβ in response to forced high pressure ventilation (127). The link between $G_{\alpha q/11}$ and RhoA is by no means clear in all cell types. Many agonists that activate RhoA are also able to activate $G_{\alpha q}$, however $G_{\alpha q/11}$ alone are rarely sufficient to activate RhoA (329). Platelets treated with thromboxane degranulate and undergo shape change that is dependent on RhoA and ROCKKI/II. Knockout of $G_{\alpha q}$ inhibited platelet degranulation, a calcium-dependent process, however shape change was shown to require $G_{\alpha 12/13}$ activation of RhoA and ROCKI/II, and MLC phosphorylation (330). $G_{\alpha 12/13}$, protein was found to be significantly upregulated in the bronchial smooth muscle of rats subjected to repeated antigen exposure (154). Moreover, in $G_{q/11}$ deficient mice, LPA, serotonin, and bradykinin were able to induce stress fibre formation in fibroblasts through $G_{\alpha 13}$ (331). In contrast, stress fibre formation via the muscarinic M_1 receptor required $G_{\alpha q/11}$ (331). These studies suggest that $G_{\alpha 12/13}$ are primarily required for

RhoA activation and RhoA-dependent responses, however it is also apparent that there is some crosstalk between $G_{\alpha q/11}$ and $G_{\alpha 12/13}$.

The point of crosstalk between $G_{\alpha q/11}$ and $G_{\alpha 12/13}$ is not entirely clear, however both of these G-protein families have been shown to have the same targets. Classically, $G_{\alpha q/11}$ were thought to exclusively target PLCβ and trigger calcium signalling and cell contraction. More recently, $G_{\alpha q/11}$ have also been shown also bind p63-RhoGEF and LARG, both of which are able to activate RhoA (143, 144). Similarly, $G_{\alpha 12/13}$ are able to bind p63Rho-GEF, LARG, p115-RhoGEF, and PDZ-RhoGEF (148, 149). This may act as a point of crosstalk between $G_{\alpha q/11}$ and $G_{\alpha 12/13}$, however it has also been shown that $G_{\alpha q/11}$ activates these RhoGEF at a lower potency in comparison to $G_{\alpha 12/13}$, in murine embryonic fibroblasts (145). It is likely that the amount of crosstalk between these pathways varies between cell type.

There is evidence of involvement of another family of heterotrimeric G-proteins, $G_{\alpha i/o}$, in RhoA/ROCK signalling. Actin reorganisation in response to LPA and carbachol in ASM cells was abrogated by inhibition of RhoA (332). Targeting $G_{\alpha i2}$ with siRNA inhibited carbachol-induced reorganisation, whereas both $G_{\alpha i2}$ and $G_{\alpha q}$ siRNA were required to inhibit LPA-induced actin reorganisation (332). These data suggest that LPA can induce actin reorganisation via either $G_{\alpha i2}$ or $G_{\alpha q}$, with RhoA being central to this process. In contrast, overexpression of $G_{\alpha i2}$ in murine ASM cells reduced cell contractility by downregulating PLCβ, the target of $G_{\alpha q/11}$ (161). Moreover, inhibiting $G_{\alpha i2}$ resulted in sensitisation of smooth muscle cells to $G_{\alpha q}$ mediated contraction by upregulating expression of PKCα (161). It was suggested that $G_{\alpha i2}$ upregulation functioned as a protective mechanism to airway hyper-responsiveness.

At present, there is evidence that $G_{\alpha q/11}$ are involved in RhoA mediated TGFβ contraction in murine embryonic fibroblast, in

response to LPA (128). In this thesis, $G_{\alpha q/11}$ have been definitively shown not to be required for LPA-induced RhoA or TGFβ activation, in human ASM cells. There many links between $G_{\alpha 12/13}$ and RhoA activation that have been highlighted, and RhoA is known to be involved in TGFβ activation, therefore this chapter assesses the whether $G_{\alpha 12/13}$ are involved in LPA- and stretch-induced TGFβ activation in ASM cells.

6.2 Aims

Assess whether the heterotrimeric G-proteins $G_{\alpha 12/13}$ are involved in LPA- and stretch-induced RhoA and TGFβ activation in ASM cells.

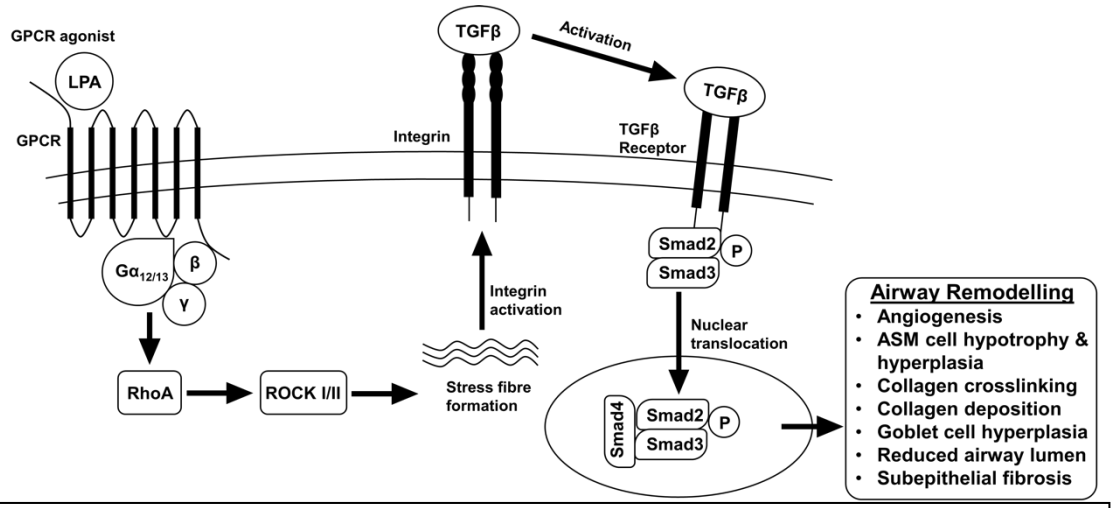

Figure 6.1. Hypothesised pathway leading to TGFβ activation in ASM cells.

6.3 Results

6.3.1 Knockdown of G_{12} and G_{13} mRNA expression using siRNA

Initially, validation of siRNA targeting $G_{\alpha 12}$ and $G_{\alpha 13}$ was carried out to determine that it was working and capable of reducing $G_{\alpha 12}$ and $G_{\alpha 13}$. ASM cells were treated with the transfection reagent alone (vehicle control), control siRNA, or $G_{\alpha 12}$ and $G_{\alpha 13}$ siRNA for 4 hours. QPCR was carried out on cell lysates taken at 24, 48, and 72 hours to quantify both $G_{\alpha 12}$ and $G_{\alpha 13}$ mRNA (figure 6.2). There significant knockdown of $G_{\alpha 12}$ and $G_{\alpha 13}$ mRNA at all time points that was around 95% lower in comparison to the control siRNA group. These data indicated that the siRNA was working efficiently. The 72 hour time point was used in future experiments as this gave a good knockdown in expression and would allow consistency between these experiments and those using siRNA targeting $G_{\alpha q}$ and $G_{\alpha 11}$ (chapter 5).

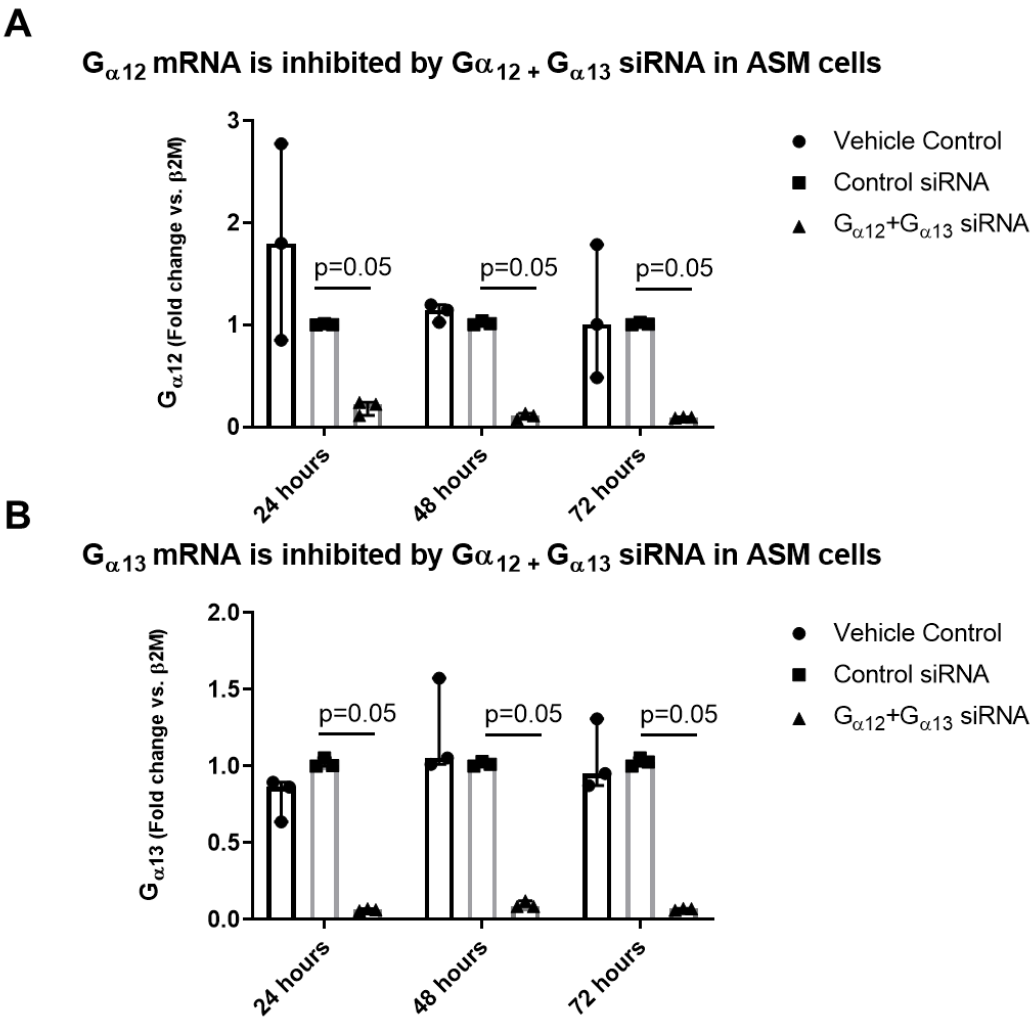

Figure 6.2. Human ASM cells were either, mock transfected, transfected with control siRNA, or siRNA targeting $G_{\alpha 12}$ and $G_{\alpha 13}$. Cell lysates were harvested and mRNA expression measured by QPCR (n=3 cell lines). Normalisation of QPCR data was done against the housekeeping gene β-2M and presented as median ± IQR. Statistical test used was a Mann-Whitney U.

6.3.2 Activation of RhoA is mediated through signalling from $G_{12/13}$ in ASM cells

To determine which heterotrimeric G-proteins were required for RhoA activation, asthmatic ASM were treated with siRNA targeting $G_{\alpha q}$ and $G_{\alpha 11}$ or, $G_{\alpha 12}$ and $G_{\alpha 13}$. The same protocol for siRNA transfection was carried out as previously described in chapter 4 of this thesis. Cells were treated with 100μM LPA, 72 hours post transfection, for 3 minutes and active RhoA was measured by ELISA (figure 6.3). LPA treatment increased active RhoA in the mock transfected, control siRNA, and $G_{\alpha q}$ and $G_{\alpha 11}$ transfected ASM cells, however this was abrogated in cells transfected $G_{\alpha 12}$ and $G_{\alpha 13}$ siRNA. The magnitude of absorbance in cells treated with LPA was around 0.15 for all conditions except when ASM were treated with $G_{\alpha 12}$ and $G_{\alpha 13}$ siRNA, which reduced the absorbance to 0.03. The reduction in LPA-induced RhoA activation seen in ASM cells treated with $G_{\alpha 12}$ and $G_{\alpha 13}$ siRNA was not significant due to the statistical test used, however is likely to be significant if additional replicates were carried out, due to the large effect size and narrow confidence interval. It is notable that there is still a very small increase in LPA-induced RhoA activation in cells treated with $G_{\alpha 12}$ and $G_{\alpha 13}$ siRNA, however this could be due to incomplete protein knockdown or crosstalk from other G-protein families. Taken as a whole this experiment clearly shows that LPA-induced RhoA activation is primarily controlled by the $G_{\alpha 12/13}$ family of heterotrimeric G-proteins.

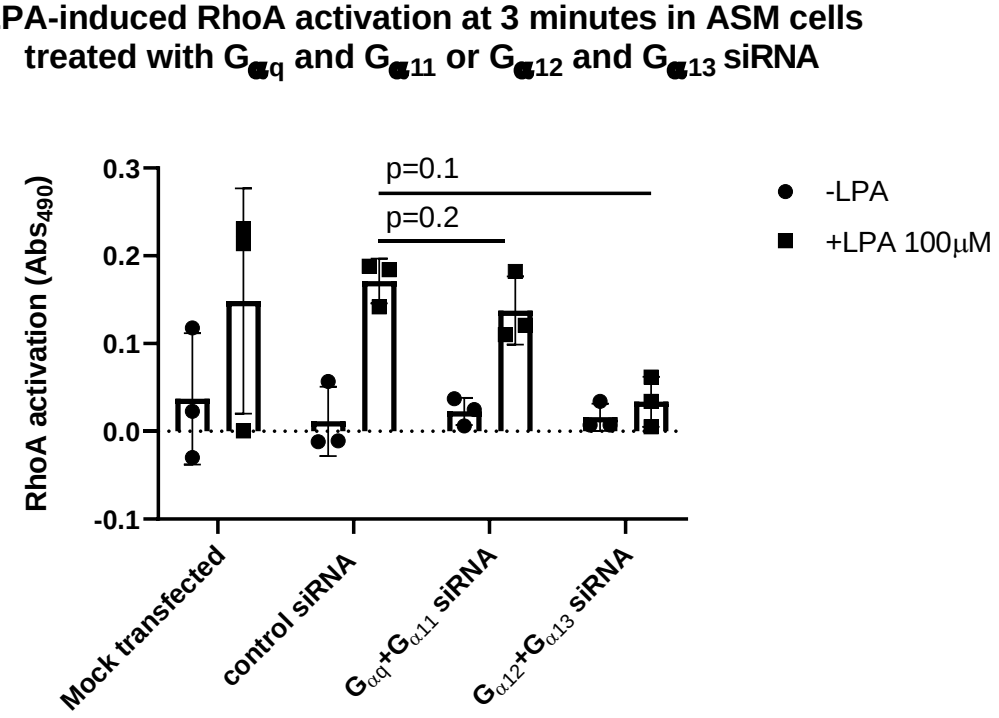

Figure 6.3. *Note: this is the same graph as that shown in figure 4.13, however this graph additionally shows results from $G_{\alpha 12}$ and $G_{\alpha 13}$ siRNA treated cells, which were cropped out in figure 4.13.*

Human asthmatic ASM cells were mock transfected, transfected with control siRNA, $G_{\alpha q}$ and $G_{\alpha 11}$ siRNA, or $G_{\alpha 12}$ and $G_{\alpha 13}$ siRNA for 72 hours (n=3 cell lines). Cells were treated with 100μM LPA for 3 minutes after siRNA transfection and active RhoA measured by ELISA. LPA-induced RhoA activation was blocked by treatment with $G_{\alpha 12}$ and $G_{\alpha 13}$ siRNA. Data is presented as median ± IQR. Statistical test is a Mann-Whitney

6.3.3 LPA-induced pSmad2 is not reduced in ASM cells treated with $G_{\alpha 12}$ and $G_{\alpha 13}$ siRNA

To determine whether $G_{\alpha 12}$ and $G_{\alpha 13}$ knockdown had an effect on LPA-induced TGFβ activation, ASM cells were treated with 100μM LPA for 4 hours, 72 hours post-transfection. For each experiment $G_{\alpha 12}$ and $G_{\alpha 13}$ protein was measured by western blot and quantified by densitometry to ensure that there was sufficient protein knockdown. There was significant knockdown of both $G_{\alpha 12}$ and $G_{\alpha 13}$ protein that was approximately 60% lower than the control siRNA group (figure 6.4). It is also notable that transfection with control siRNA appears to slightly increase $G_{\alpha 12}$ and $G_{\alpha 13}$ protein. These data combined with the functional effect of $G_{\alpha 12}$ and $G_{\alpha 13}$ knockdown on RhoA (figure 6.3) suggest that protein knockdown was sufficient to analyse the role of $G_{\alpha 12}$ and $G_{\alpha 13}$ in LPA-induced pSmad2.

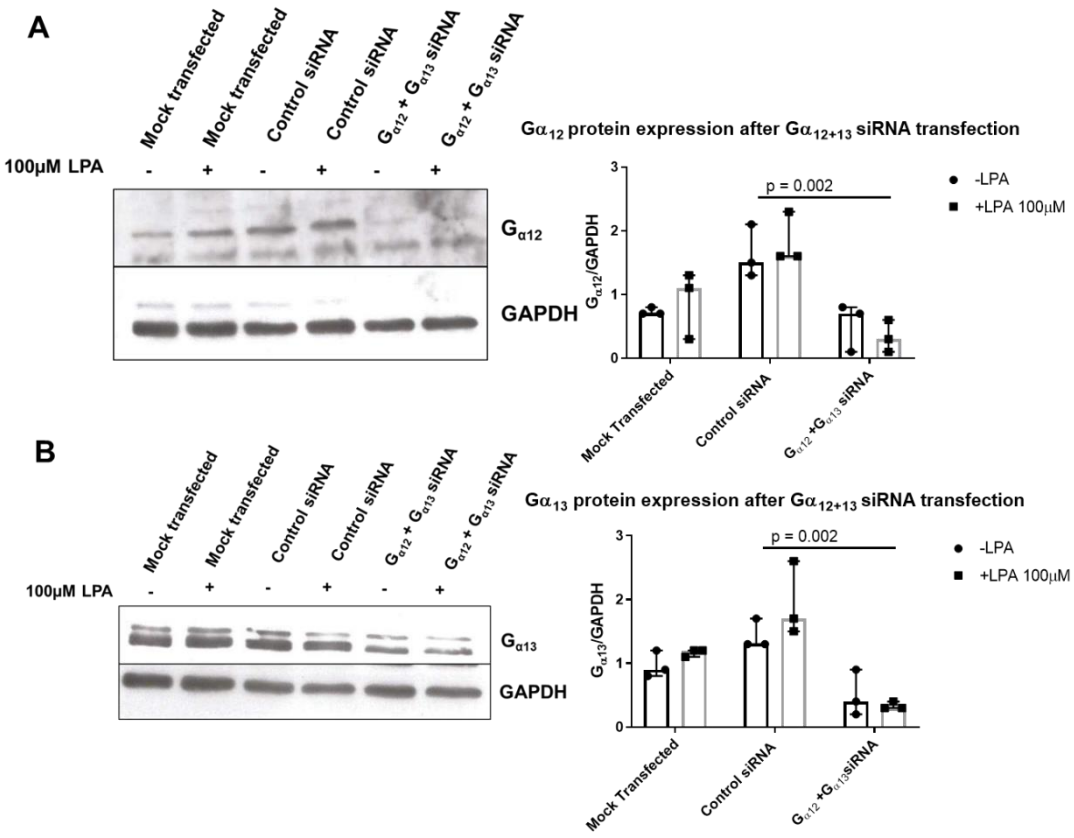

Figure 6.4. Human asthmatic ASM cells mock transfected, transfected with control siRNA, or $G_{\alpha 12}$ and $G_{\alpha 13}$ siRNA for 72 hours (n=3 cell lines). Representative western blots showing $G_{\alpha 12}$ protein and densitometry, A, and G_{13} protein and densitometry, B, from siRNA transfection experiments where ASM cells were treated with LPA. There was significant knockdown of both $G_{\alpha 12}$ and $G_{\alpha 13}$ in all experiments versus the control siRNA group (n=3 cell lines) shown by densitometry. Data is presented as median ± IQR. Statistical test used was a Mann-Whitney U of control siRNA and $G_{\alpha 12}$ + $G_{\alpha 13}$ siRNA groups.

Once knockdown had been determined, asthmatic ASM cells were treated with 100μM LPA for 4 hours, 72 hours post-transfection. The ratio of pSmad2 to Smad2/3 was measured by western blot to determine activation of the TGFβ signalling pathway. Densitometry was used to quantify western blots. LPA induced a strong pSmad2 signal in all conditions that was not inhibited by treatment with $G_{\alpha 12}$ and $G_{\alpha 13}$ siRNA (figure 6.5). The median ratio of pSmad2 to Smad2/3 was around 25-50% lower in both siRNA treated groups versus the mock transfected group, however the siRNA groups have a much wider confidence interval. There was no difference between the control siRNA group and $G_{\alpha 12}$ and $G_{\alpha 13}$ group, which had wide overlapping confidence intervals. These data clearly indicate that siRNA knockdown of $G_{\alpha 12}$ and $G_{\alpha 13}$ does not inhibit LPA-induced pSmad2 in ASM cells.

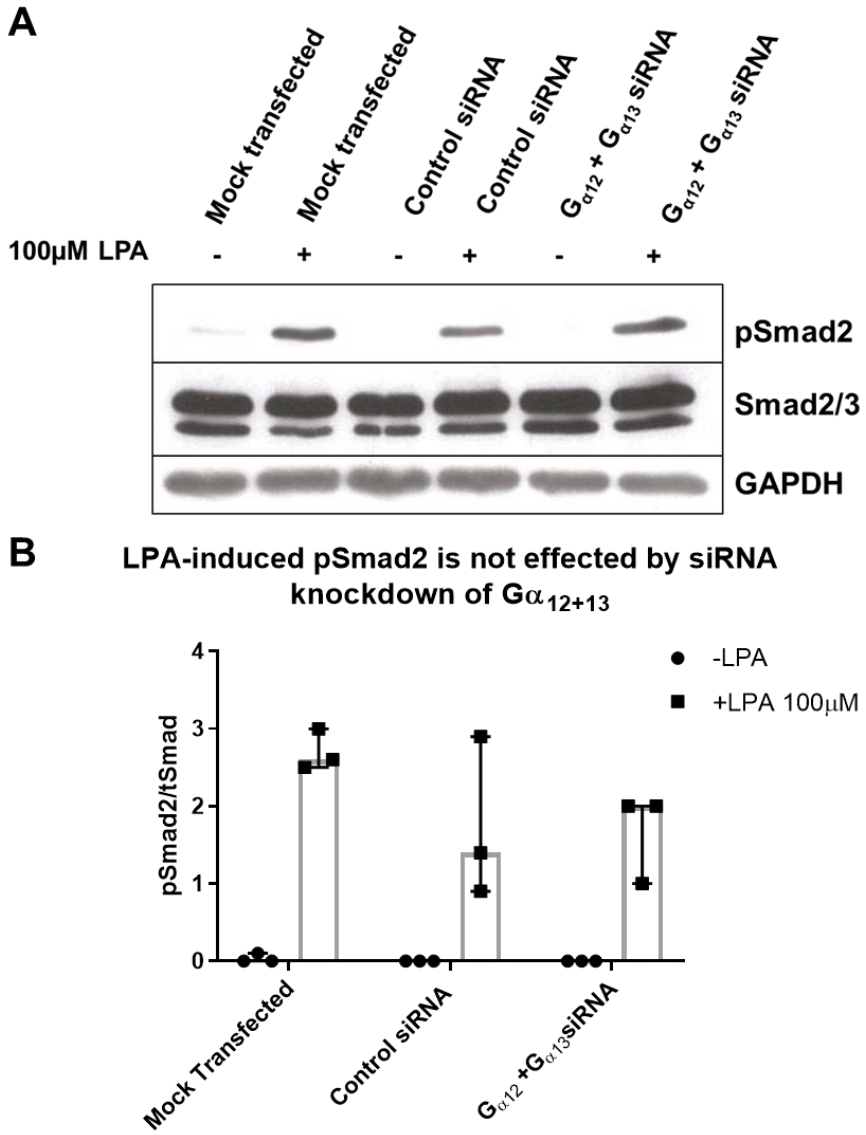

Figure 6.5. Human asthmatic ASM cells mock transfected, transfected with control siRNA, or transfected with $G_{\alpha 12}$ and $G_{\alpha 13}$ siRNA for 72 hours (n=3 cell lines). Cells were treated with 100μM LPA for 4 hours after transfection. Representative western blot showing pSmad2 and Smad2/3, A. Densitometry shows that LPA-induced pSmad2 was not reduced in ASM cells treated with $G_{\alpha 12}$ and $G_{\alpha 13}$ siRNA, B. Data is expressed as median ± IQR.

6.3.4 Cyclical mechanical stretch-induced pSmad2 is not reduced in ASM cells treated with $G_{\alpha 12}$ and $G_{\alpha 13}$ siRNA

Next, the role of $G_{\alpha 12}$ and $G_{\alpha 13}$ in cyclical mechanical stretch-induced TGFβ activation was assessed using siRNA targeting using the same method described above. Human asthmatic ASM cells were subjected to 15% stretch at a frequency of 0.3Hz for 4 hours, 72 hours post-transfection. To ensure that there was protein knockdown at the time of the experiment, both $G_{\alpha 12}$ and $G_{\alpha 13}$ protein was measured by western blot for each experiment and quantified by densitometry. There was approximately 90% knockdown of $G_{\alpha 12}$ in stretched ASM cells and around 70% knockdown in unstretched ASM cells (figure 6.6A). A comparison of all conditions in the control siRNA group versus the $G_{\alpha 12}$ and $G_{\alpha 13}$ siRNA group showed that there was significant knockdown of $G_{\alpha 12}$. Analysis of $G_{\alpha 13}$, however, showed that there was no difference between the control siRNA group and $G_{\alpha 12}$ and $G_{\alpha 13}$ group (figure 6.6B). This indicated that there was no knockdown of $G_{\alpha 13}$.

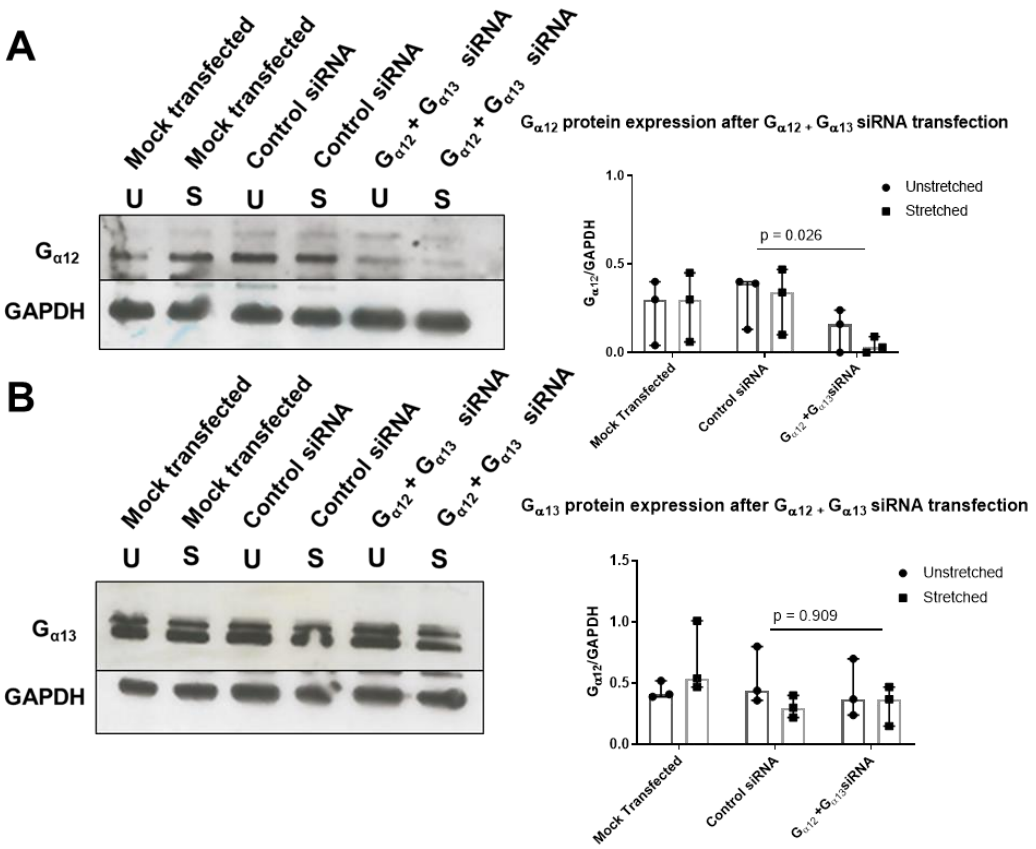

Figure 6.6. Human asthmatic ASM cells mock transfected, transfected with control siRNA, or $G_{\alpha 12}$ and $G_{\alpha 13}$ siRNA for 72 hours (n=3 cell lines). Representative western blots showing $G_{\alpha 12}$ protein and densitometry, A, and G_{13} protein and densitometry, B, from siRNA transfection experiments where ASM cells were subjected to 15% stretch at 0.3Hz for 4 hours. There was significant knockdown of $G_{\alpha 12}$ but not $G_{\alpha 13}$ in all experiments versus the control siRNA group (n=3 cell lines) shown by densitometry. Data is presented as median ± IQR. Statistical test used was a Mann-Whitney U of control siRNA and $G_{\alpha 12}$ + $G_{\alpha 13}$ siRNA groups.

Next, pSmad2 and Smad2/3 were measured by western blot and quantified by densitometry to determine whether there had been activation of the TGFβ signalling pathway (figure 6.7). Stretch induced an increase in pSmad2 in the mock transfected group. Interestingly, siRNA transfection of either control siRNA or $G_{\alpha 12}$ and $G_{\alpha 13}$ siRNA increased basal pSmad2 in unstretched cells, which was also seen in transfected unstretched ASM cells in chapter 5 (figure 5.5), but not in any experiments using LPA. There was no stretch-induced pSmad2 increase in the control group, in part due to an increase in basal pSmad2 in unstretched cells. However, stretch did induce an increase in pSmad2 in the $G_{\alpha 12}$ and $G_{\alpha 13}$ siRNA group, with a median that was 3-fold higher than unstretched cells. This effect was comparable to stretch-induced pSmad2 in $G_{\alpha q}$ and $G_{\alpha 11}$ siRNA treated cells in chapter 5 (figure 5.5). Although the confidence interval is too wide to conclude that siRNA knockdown of $G_{\alpha 12}$ and $G_{\alpha 13}$ results in an increase in stretch-induced pSmad2, it is clear that stretch-induced pSmad2 is not reduced.

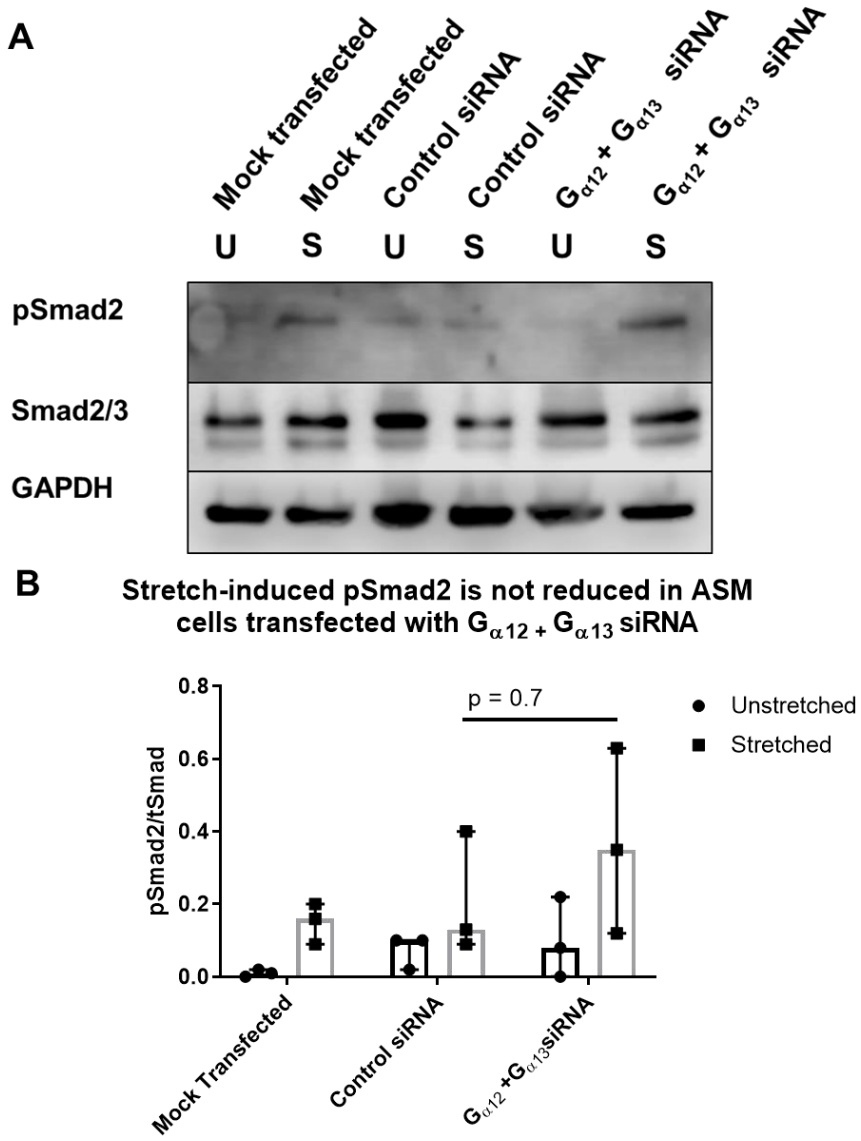

Figure 6.7. Human asthmatic ASM cells mock transfected, transfected with control siRNA, or transfected with $G_{\alpha 12}$ and $G_{\alpha 13}$ siRNA for 72 hours (n=3 cell lines). Cells were subjected to 15% stretch at a frequency of 0.3Hz for 4 hours. Representative western blot showing pSmad2 and Smad2/3, A. Densitometry shows that LPA-induced pSmad2 was not reduced in ASM cells treated with $G_{\alpha 12}$ and $G_{\alpha 13}$ siRNA, B. Data is expressed as median ± IQR.

6.3.5 Quadruple knockdown of $G_{\alpha q}$, $G_{\alpha 11}$, $G_{\alpha 12}$, and $G_{\alpha 13}$ by siRNA does not inhibit LPA-induced pSmad2 in ASM cells

The question remained that if blocking $G_{\alpha q}$ and $G_{\alpha 11}$ or $G_{\alpha 12}$ and $G_{\alpha 13}$ did not block stretch- or LPA-induced pSmad2 in ASM cells, what would happen if all of these G-proteins were knocked down. The same siRNA protocol was followed as described previously in this chapter, but instead used all 4 siRNA oligonucleotides. Human asthmatic ASM cells were treated with LPA for 4 hours, 72 hours after transfection. Initially, western blotting was used to determine efficient protein knockdown for each experiment. There was around 90% knockdown of both $G_{\alpha q}$ and $G_{\alpha 11}$, which was statistically significant when comparing the control siRNA group with the $G_{\alpha q}$, $G_{\alpha 11}$, $G_{\alpha 12}$ and $G_{\alpha 13}$ siRNA group (figure 6.8).

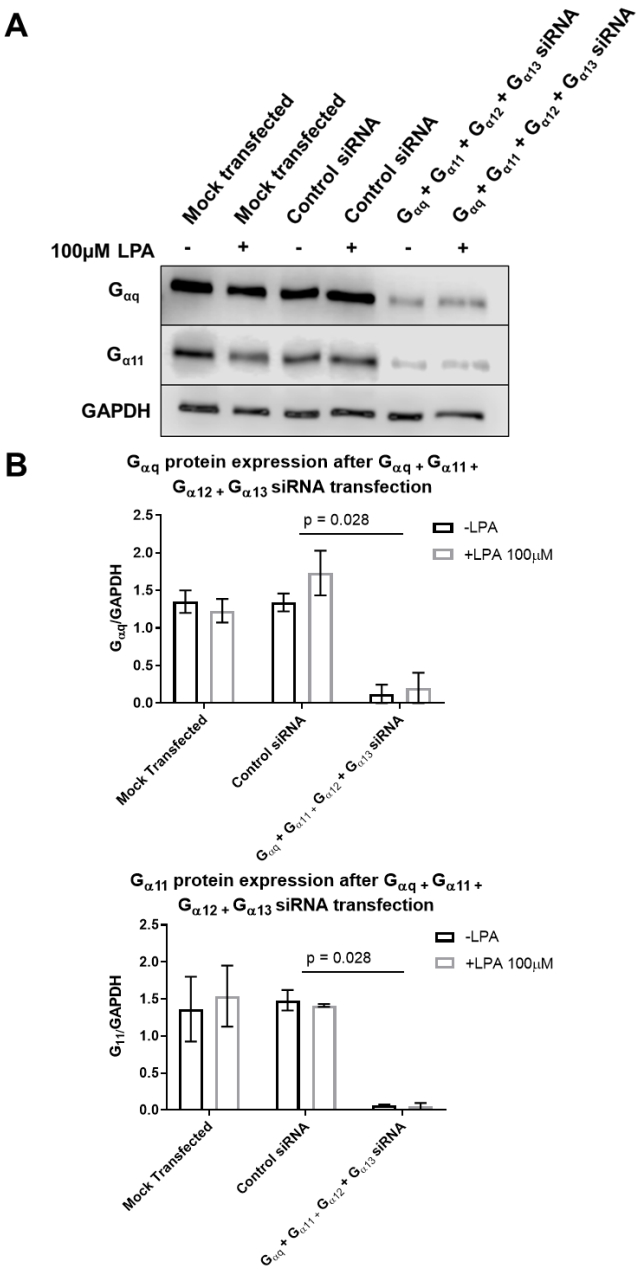

Figure 6.8. Human asthmatic ASM cells mock transfected, transfected with control siRNA or, $G_{\alpha q}$, $G_{\alpha 11}$, $G_{\alpha 12}$ and $G_{\alpha 13}$ siRNA for 72 hours (n=2 cell lines). Representative western blots showing $G_{\alpha q}$ and $G_{\alpha 11}$ protein, A, and densitometry, B. ASM cells were treated with 100μM LPA for 4 hours, 72 hours after siRNA transfection. There was significant knockdown of both $G_{\alpha q}$ and $G_{\alpha 11}$ in all experiments versus the control siRNA group (n=3 cell lines) shown by densitometry. Data is presented as median ± IQR. Statistical test used was a Mann-Whitney U of control siRNA and $G_{\alpha q}$, $G_{\alpha 11}$, $G_{\alpha 12}$ and $G_{\alpha 13}$ siRNA siRNA groups.

$G_{\alpha 12}$ and $G_{\alpha 13}$ protein was also measured to determine knockdown efficiency (figure 6.9). There was efficient knockdown of $G_{\alpha 12}$ of around 90%, however this was not significant because of wider confidence intervals within the control siRNA group. On the other hand, there was no knockdown of $G_{\alpha 13}$ compared to the control siRNA group, similar to what was seen in experiments described above (figure 6.6). These data show that knockdown of $G_{\alpha q}$ and $G_{\alpha 11}$ or $G_{\alpha 12,}$ but not $G_{\alpha 13}$, was efficient.

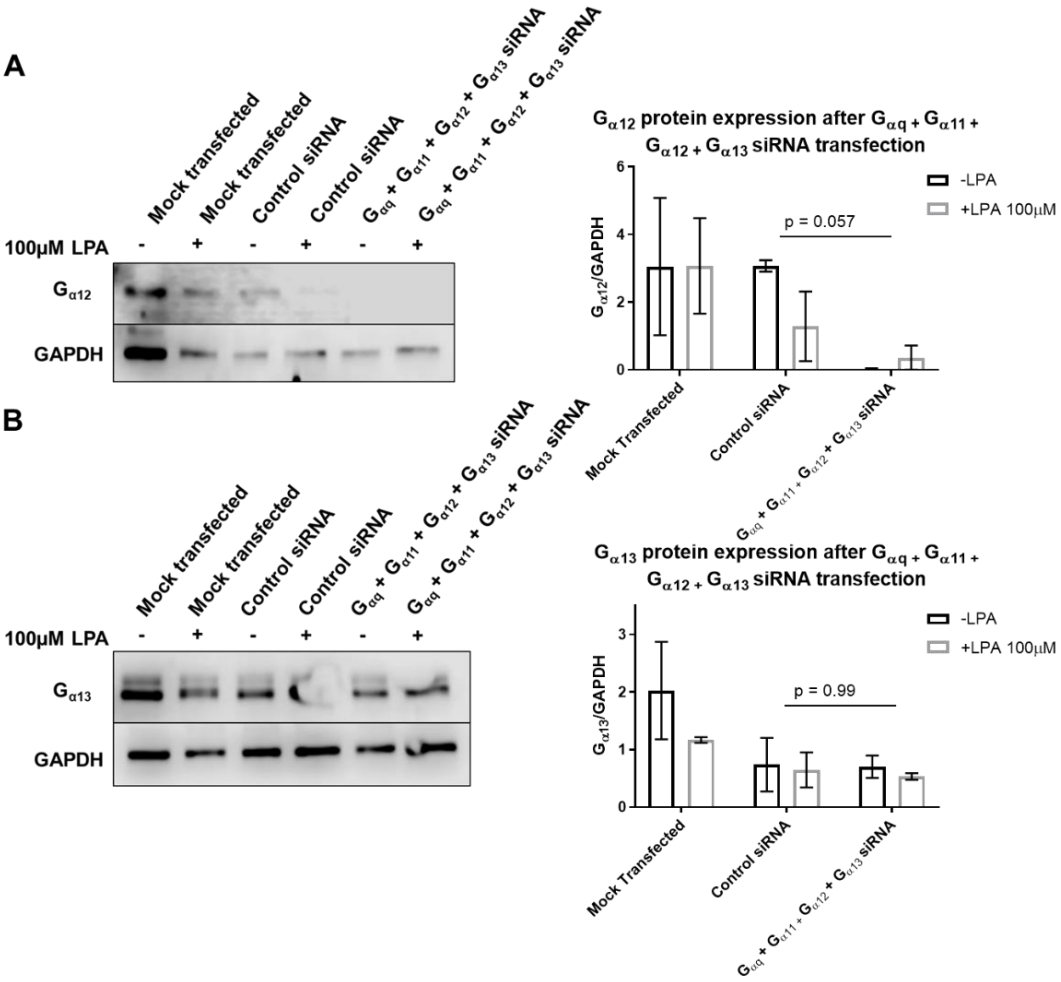

Figure 6.9. Human asthmatic ASM cells mock transfected, transfected with control siRNA, or $G_{\alpha q}$, $G_{\alpha 11}$, $G_{\alpha 12}$ and $G_{\alpha 13}$ siRNA for 72 hours (n=2 cell lines). Representative western blots showing $G_{\alpha 12}$ protein and densitometry, A, and G_{13} protein and densitometry, B, from siRNA transfection experiments where ASM cells were treated with 100μM LPA for 4 hours. There was good but not significant knockdown of $G_{\alpha 12}$ and no knockdown of $G_{\alpha 13}$ in all experiments versus the control siRNA group (n=2 cell lines) shown by densitometry. Data is presented as median ± IQR. Statistical test used was a Mann-Whitney U of control siRNA and $G_{\alpha 12}$ + $G_{\alpha 13}$ siRNA groups.

After determining the efficiency of siRNA knockdown, pSmad2 and Smad2/3 were measured by western blot and quantified by densitometry (figure 6.10). This was to determine TGFβ activation because pSmad2 is the first signalling event in the TGFβ signalling pathway. There was a large induction of pSmad2 in all groups treated with LPA. The median of both siRNA treated groups was around half the mock transfected group, although there were only 2 replicates and a wide confidence interval. There was no difference in LPA-induced pSmad2 in the control siRNA group versus the $G_{\alpha q}$, $G_{\alpha 11}$, $G_{\alpha 12}$, and $G_{\alpha 13}$ siRNA group. Data shown here has a similar trend as that seen in LPA-induced pSmad2 in ASM cells treated with $G_{\alpha 12}$ and $G_{\alpha 13}$ siRNA (figure 6.5). These data suggest that neither $G_{\alpha q}$ and $G_{\alpha 11}$ or $G_{\alpha 12}$ are required for LPA-induced TGFβ activation, however there was no knockdown $G_{\alpha 13}$ therefore it is not possible to conclude whether this protein plays a role or not.

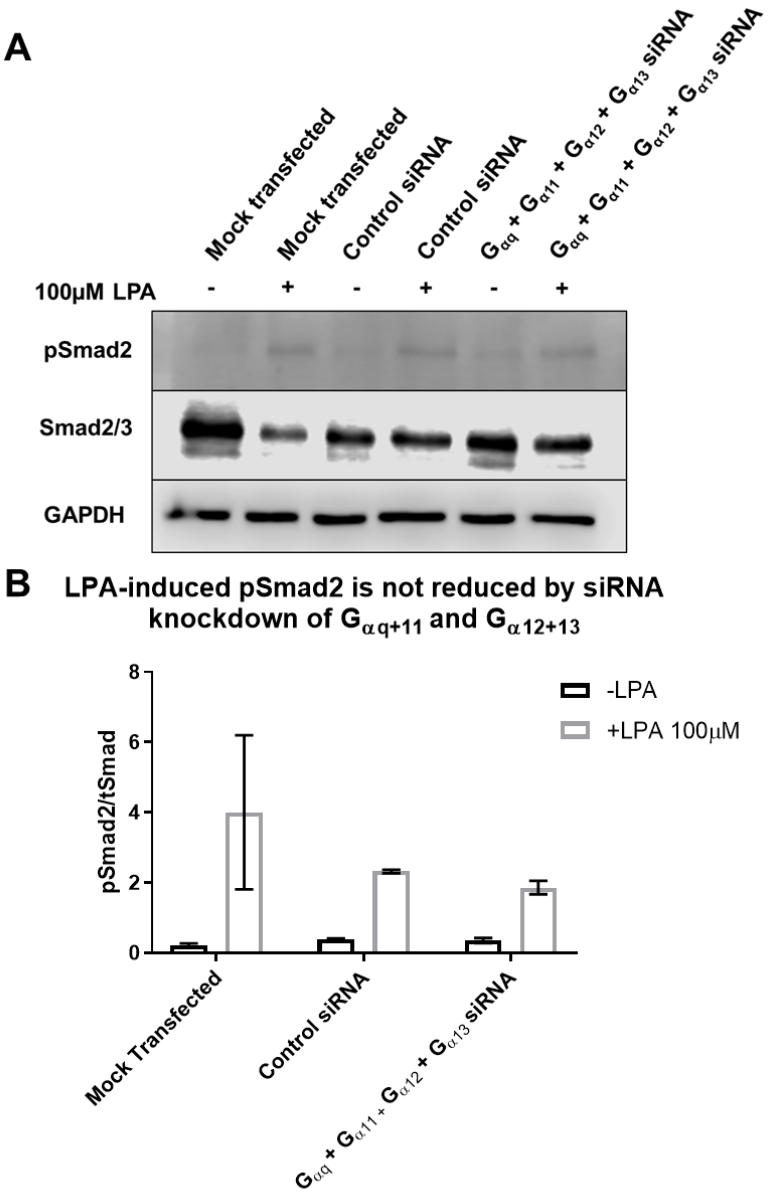

Figure 6.10. Human asthmatic ASM cells mock transfected, transfected with control siRNA, or $G_{\alpha q}$, $G_{\alpha 11}$, $G_{\alpha 12}$ and $G_{\alpha 13}$ siRNA for 72 hours (n=2 cell lines). Cells were treated with 100μM LPA for 4 hours, 72 hours after transfection. Representative western blot showing pSmad2 and Smad2/3, A. Densitometry shows that LPA-induced pSmad2 was not reduced in ASM cells treated with $G_{\alpha q}$, $G_{\alpha 11}$, $G_{\alpha 12}$ and $G_{\alpha 13}$ siRNA, B. Data is expressed as median ± IQR.

6.4 Discussion

The pleiotropic cytokine TGFβ is known to play a central role in fibrotic diseases and can induce the expression of fibrotic genes that contribute to airway remodelling seen in the airway of severe asthmatic patients. Overexpression of TGFβ and pSmad2 in the asthmatic airways has been linked to subepithelial fibrosis, ASM cell hyperplasia and hypertrophy, epithelial damage, goblet cell hyperplasia, and angiogenesis (1, 211, 214). It is therefore important to fully understand the mechanism by which TGFβ becomes activated in the airways of severe asthmatics, who suffer from frequent exacerbation.

In chapter 4 and 5 of this thesis it was clear that the heterotrimeric G-proteins $G_{\alpha q/11}$ do not play a role in either LPA- or stretch-induced TGFβ activation in ASM cells. This is in contrast to findings in murine embryonic fibroblasts that showed $G_{\alpha q}$ to be the G-protein that led to LPA-induced TGFβ activation (128). Moreover, forced ventilation-induced TGFβ secretion in mice was abrogated by epithelial knockdown of $G_{\alpha q/11}$ (127). The heterotrimeric G-protein that transmits extracellular LPA and stretch signals to induction of TGFβ activation in ASM cells has not been analysed.

Research across a range of cell types, looking at both TGFβ synthesis and activation, have identified RhoA and its effector ROCKI/II as central to this pathway (128, 175, 183). In murine embryonic fibroblasts both LPA- and PAR1-induced TGFβ activation was abrogated by an inhibitor of RhoA or ROCKI/II (128, 175). Further, mechanical stretch-induced TGFβ1 expression in ASM cells was abrogated by inhibiting RhoA or ROCKI/II (183). The heterotrimeric G-proteins $G_{\alpha 12/13}$ are found to be upregulated in the bronchial smooth muscle of rats subjected to repeated antigen exposure(154). Moreover, $G_{\alpha 12/13}$ are able to activate RhoA via p115-RhoGEF, PDZ-

RhoGEF, LARG, and p63-RhoGEF (148, 149). In $G_{\alpha q/11}$ deficient mice, LPA was able to induce stress fibre formation, a process associated with RhoA activation, via $G_{\alpha 13}$ (331). These studies indicated that $G_{\alpha 12/13}$ were a good candidate for LPA- and stretch-induced TGFβ activation.

There are currently no commercially available molecular inhibitors of $G_{\alpha 12/13}$, therefore genetic approaches were required to manipulate this pathway. Knockdown of $G_{\alpha 12/13}$ was done by using siRNA, which effectively abolished $G_{\alpha 12/13}$ mRNA at 24, 48, and 72 hours after transfection (figure 6.2). RhoA was the first endpoint to be measured after knockdown of $G_{\alpha 12/13}$. Knockdown of $G_{\alpha q/11}$ was also carried to determine whether there was a dual role for these G-protein families in RhoA activation, or whether regulate distinct pathways. There was a clear drop in LPA-induced RhoA activation at 3 minutes in ASM cells treated with siRNA targeting $G_{\alpha 12/13}$, but not $G_{\alpha q/11}$. The effect of $G_{\alpha 12/13}$ siRNA didn't bring the median RhoA activation to the level of cells that were not treated with LPA. This may have been due to not achieving 100% protein knockdown, or due to $G_{\alpha q/11}$ being able to activate RhoA albeit with far less potency. It isn't possible to state which of these hypotheses are true because protein knockdown wasn't measured during this experiment. It is clear however, that knockdown of $G_{\alpha 12/13}$ had a functional effect on RhoA activation. This is the first time that $G_{\alpha 12/13}$ have been shown to regulate LPA-induced RhoA activation in ASM cells. No previous studies have ascertained which family of heterotrimeric G-proteins regulates RhoA in ASM cells.

Next, pSmad2 was measured to determine whether $G_{\alpha 12/13}$ was required for LPA-induced TGFβ activity in ASM cells. Previous studies have shown that Gαq was required for LPA-induced TGFβ activation in murine embryonic fibroblasts, however it is clear from this thesis

that this is not the case in ASM cells (128). No reduction in LPA-induced pSmad2 was observed in ASM cells treated with siRNA targeting $G_{\alpha 12/13}$. This result was surprising because knockdown of $G_{\alpha 12/13}$ blocked RhoA activation, therefore the hypothesis was that it would also block pSmad2 signalling. Indeed, inhibition of RhoA activation was measured 3 minutes after LPA treatment, whereas pSmad2 was measured after 4 hours of LPA treatment. However, it highly likely that RhoA activation was inhibited for the whole time course because siRNA knockdown is relatively stable and $G_{\alpha 12/13}$ protein levels were significantly reduced. It is also notable that LPA-induced pSmad2 activation was not increased in cells treated with $G_{\alpha 12/13}$ siRNA, which was the case in $G_{\alpha q/11}$ siRNA treated cells in chapter 4. This suggests that knockdown of $G_{\alpha q/11}$ amplifies TGFβ activation, whereas knockdown of $G_{\alpha 12/13}$ does not.

Stretch-induced TGFβ synthesis has been shown to require RhoA and ROCKI/II in ASM cells (183). Indeed, inhibition of ROCKI/II abrogated stretch-induced pSmad2 in chapter 5 of this thesis. However, siRNA knockdown of $G_{\alpha 12/13}$ did not inhibit stretch-induced pSmad2, which in fact increased with a similar trend to that observed upon knockdown of $G_{\alpha q/11}$ in chapter 5. It is clear that knockdown of $G_{\alpha 13}$ in cells undergoing a stretching regimen was not successful. The key difference between the conditions of stretched cells and LPA treated cells is the type of tissue culture plate. Cells undergoing stretch were on a flexible collagen I coated plate, whereas LPA treated cells were on a standard plastic plate. This may have effected knockdown efficiency, although this was not the case in knockdown of $G_{\alpha q/11}$.

Studies on stress fibre formation in fibroblasts have shown that LPA, bradykinin, and serotonin, act through $G_{\alpha 13}$ to induce this change (331). This study highlighted that there was a differential role of $G_{\alpha 12}$

and $G_{\alpha 13}$ in stress fibre formation in response to a variety of agonists (331). As there was no knockdown of $G_{\alpha 13}$ achieved in this experiment the question remains open as to whether it is involved in stretch-induced pSmad2. However, is also possible that RhoA activation in response to stretch does not occur in a paracrine or receptor mediated fashion. Indeed, a study that applied force directly to integrins on the surface of fibroblasts showed that the RhoGEFs LARG and GEF-H1 were activated in response to force (333). Moreover, both of these RhoGEFs were able to increase RhoA activation (333). This raises the possibility that stretch-induced TGFβ activation may be GPCR-independent and involve a feedback loop that starts with integrin activating RhoA, which in turn activates integrin and thus TGFβ activation. What is clear from this thesis is that ROCKI/II are essential for stretch-induced TGFβ activation, but $G_{\alpha q/11}$ and $G_{\alpha 12}$ are not required.

In this thesis, LPA-induced pSmad2 in ASM cells was not abrogated by either $G_{\alpha q/11}$ inhibition with a small molecule inhibitor, $G_{\alpha q/11}$ siRNA, or $G_{\alpha 12/13}$ siRNA. With genetic knockdown in particular, there can be indirect effects on other G-protein family members. In HeLa cells, both $G_{\alpha i1}$ and $G_{\alpha 12}$ expression was increased in cells that had undergone siRNA knockdown of $G_{\alpha q/11}$ (296). Further, $G_{\alpha q/11}$ and $G_{\alpha 12/13}$ are both able to activate p63-RhoGEF and LARG, which in turn activate RhoA in some cell types (143, 144). Although this hasn't been analysed in ASM cells it leaves open the possibility that there is crosstalk between these pathways. Moreover, LPA receptors have been shown to couple to $G_{\alpha i/0}$, $G_{\alpha q/11}$, $G_{\alpha 12/13}$, and $G_{\alpha s}$ (271). It was therefore important to rule out this possibility by knocking down both $G_{\alpha q/11}$ and $G_{\alpha 12/13}$.

Knockdown of $G_{\alpha q}$, $G_{\alpha 11}$, and $G_{\alpha 12}$ was successful, however there was no knockdown of $G_{\alpha 13}$. LPA induced an increase in pSmad2 that was

of a similar magnitude to knockdown $G_{\alpha 12/13}$ alone. These data suggest that LPA-induced pSmad2 may be acting via $G_{\alpha 13}$. Alternatively, it is possible that neither $G_{\alpha q/11}$ nor $G_{\alpha 12/13}$ are required for LPA-induced TGFβ activation in ASM cells. Earlier in this chapter, knockdown of $G_{\alpha 12/13}$ was shown to inhibit RhoA activation. Although RhoA activation was not measured in this experiment, it would not be unreasonable to hypothesise that RhoA is being inhibited and therefore suggest that RhoA may not be required for LPA-induced TGFβ activation. Indeed, knockdown of $G_{\alpha q/11}$ and $G_{\alpha 12/13}$, or $G_{\alpha 12/13}$ alone did not inhibit LPA-induced pSmad2, however RhoA was inhibited by the latter. Moreover, inhibition of ROCKI/II in chapter 4 did block LPA-induced pSmad2. These data would suggest that ROCKI/II but not RhoA are required for LPA-induced pSmad2. This hypothesis was in the process of being tested directly by using a C3-exoenzyme that inhibits RhoA, however was cut short due to the COVID-19 pandemic.

RhoA does not exclusively control ROCKI/II activation. Arachidonic acid is able to activate ROCKI/II by binding to its auto-inhibitory PH domain and induce contraction of smooth muscle fibres (298). Moreover, extracellular addition of arachidonic acid to rabbit artery strips has been shown to inhibit MLC phosphatase, a key effect of ROCKI/II activation (334). LPA has been shown to increase arachidonic acid in monocytes, but this has not been analysed in smooth muscle cells (335). ROCKI activation can also be induced by (phosphoinositide-dependent kinase-1) PDK1 binding in competition with its negative regulator RhoE (299). Moreover, LPA is able to induced PDK1 activation and stimulate cell growth via the AKT pathway in cancer cell lines (336).

The final possibility is that there is a different heterotrimeric G-protein family that is regulating TGFβ activation in ASM cells. LPA

receptors 1 to 5 are able to activate $G_{\alpha i/0}$, $G_{\alpha q/11}$, $G_{\alpha 12/13}$, and $G_{\alpha s}$, however an analysis of which LPA receptors were expressed in ASM cells was not conducted in this thesis (271). LPA has been shown to induce cytoskeletal reorganisation in ASM cells via RhoA (279). Further, this effect was inhibited when both $G_{\alpha q}$ and $G_{\alpha i2}$ were knocked down by siRNA, indicating that there is a level of crosstalk between these G-proteins (279). $G_{\alpha i2}$ and $G_{\alpha i3}$ expression has been shown to increase in the ASM of a murine and rat model of asthma respectively (160, 161). This raises the possibility of an involvement of the $G_{\alpha i/0}$ family of G-proteins and perhaps a combination of families that contribute to TGFβ activation in ASM cells.

In conclusion, this chapter has shown for the first time that $G_{\alpha 12/13}$, but not $G_{\alpha q/11}$ are required for LPA-induced RhoA activation in ASM cells. Furthermore, $G_{\alpha 12/13}$ or $G_{\alpha q/11}$ knockdown alone, nor $G_{\alpha q/11}$ and $G_{\alpha 12}$ knockdown blocked LPA-induced pSmad2. $G_{\alpha 13}$ knockdown wasn't sufficient to comment on its potential role. Knockdown of $G_{\alpha 12}$ did not inhibit stretch-induced pSmad2. This chapter raises the possibility that there are other heterotrimeric G-protein families, or even a combination of G-proteins, regulate LPA-induced pSmad2 in ASM cells. Moreover, results in this thesis cannot conclude whether there is a role for heterotrimeric G-proteins in stretch-induced pSmad2, however it is clear that $G_{\alpha q/11}$ or $G_{\alpha 12}$ alone are not responsible.

7 Chapter 8: Conclusion and Future Direction

7.1 Conclusions

Asthma is a chronic inflammatory disease of the airways characterised by airway hyper-responsiveness, bronchoconstriction and inflammation, affecting 5.5 million people in the UK. Approximately 10% of asthmatics suffer from severe uncontrolled asthma, which induces structural changes in the lung. These changes are collectively termed airway remodelling and include, ASM hyperplasia and hypertrophy, subepithelial fibrosis, angiogenesis, epithelial shedding, and goblet cell hyperplasia (1). Airway remodelling is a progressive process that reduces lung function and restricts airflow. TGFβ is a pleiotropic cytokine that is central to airway remodelling and contributes to all of the structural changes outlined. It is therefore important to understand the precise mechanism by which TGFβ activation and therefore airway remodelling occur.

This thesis is focussed on ASM cells, the primary contractile cells within the lung, and looked to define whether there is a role for heterotrimeric G-proteins in TGFβ activation. If one family of heterotrimeric G-proteins exclusively regulates TGFβ activation then it could be possible to develop inhibitors either targeting the G-protein, or narrow down candidate GPCRs to target, thereby reducing airway remodelling in asthmatic patients. The overall hypothesis was that the heterotrimeric G-proteins $G_{\alpha q/11}$ are responsible for initiating TGFβ activation in human ASM cells. The two methods for stimulating TGFβ activation were treating cells with LPA or subjecting them to a cyclical stretching regimen.

The first aim of this thesis was to generate a $G_{\alpha q/11}$ knockout ASM cells line. Tracheal ASM cells were isolated from $G_q^{fl/fl}G_{11}^{-/-}$ mice with the intention of transducing them with a lentivirus encoding cre

recombinase and an antibiotic resistance gene. This would have created a stable $G_{\alpha q/11}$ knockout ASM cell line that could have been used as a tool to test the hypothesis is this thesis. Generation of cre-producing lentivirus was successful because some murine embryonic fibroblasts were positively selected after incubation with lentivirus. However, it was not possible to replicate this in murine ASM cells. Further optimisation was carried out using a lentivirus encoding GFP to allow rapid visualisation of successful transduction. This resulted in some improvement in transduction efficiency in easy-to-transfect HEK T293 cells, again however, there was minimal transduction when this was replicated in murine ASM cells.

Primary cells are more difficult to transduce than fast-growing commercially available cell lines. It is likely that the lentivirus yield was not high enough for transduction in primary ASM cells. One method that I would have liked to include in future studies is to maximise viral concentration and thus maximise the chance of transduction is centrifugation. In the past, concentrating virus required ultracentrifugation at 90,000xg for 1 hour, but this requires specialist equipment that isn't always directly accessible (267). More recently, however, a method of centrifuging lentiviral media at an RCF of 10,000xg for 4 hours across a 20% glucose gradient has been shown to increase lentiviral transduction by 3-fold compared to un-concentrated virus and 2-fold compared to ultracentrifugation (258). Despite optimisation of lentiviral transduction in murine ASM being unsuccessful, this method of concentrating lentivirus would be interesting to adopt in order to transduce primary ASM cells.

LPA was used as a stimulus because it is able to induce a strong TGFβ signal and is increased in the airways of asthmatic patients (133). Moreover, it is able to activate heterotrimeric G-proteins from the $G_{\alpha q/11}$, $G_{\alpha 12/13}$, $G_{\alpha s}$, and $G_{\alpha i/o}$ families, therefore it could be used to

analyse multiple signalling pathways. TGFβ1 mRNA expression has been shown to increase after uniaxial stretch in ASM cells, however TGFβ activation has not been shown in ASM cells subjected to a stretching regimen (183). Data from this thesis conclusively demonstrate, for the first time, that there is no role for the heterotrimeric G-protein family $G_{\alpha q/11}$ in LPA- or stretch-induced TGFβ activation. This finding is in contrast to evidence in murine embryonic fibroblasts, which showed LPA-induced TGFβ activation to occur through $G_{\alpha q}$ (128).

RhoA and its effector ROCKI/II have long been described as central to TGFβ activation in multiple cell types (128, 175, 183). This thesis showed that ROCKI/II are required for LPA-induced TGFβ activation in ASM cells. The $G_{\alpha 12/13}$ family have often been described as upstream of RhoA activation (337). Analysis of active RhoA after treatment with siRNA targeting $G_{\alpha q/11}$ or $G_{\alpha 12/13}$ showed that $G_{\alpha 12/13}$ and not $G_{\alpha q/11}$ are upstream of LPA-induced RhoA activation in ASM cells. These data suggested that $G_{\alpha 12/13}$ would be a good candidate to prevent LPA-induced TGFβ activation. Moreover, rats subjected to repeated allergen exposure had increased expression of $G_{\alpha 12}$ and $G_{\alpha 13}$ in bronchial smooth muscle (154). In this thesis, blocking $G_{\alpha 12/13}$ by siRNA had no effect on LPA-induced pSmad2, and therefore TGFβ activation. Moreover, targeting both $G_{\alpha q/11}$ and $G_{\alpha 12/13}$ did not prevent LPA-induced pSmad2. However, knockdown of $G_{\alpha 13}$ protein was not achieved in this experiment, therefore it is only possible to conclude that $G_{\alpha q/11}$ and $G_{\alpha 12}$ are not required for LPA-induced TGFβ activation.

Despite knockdown of $G_{\alpha 13}$ not being complete at the protein level, siRNA appeared to functionally inhibit RhoA activation. It is important to note, however, that neither $G_{\alpha 12}$ nor $G_{\alpha 13}$ protein expression was measured while analysing RhoA activation, so protein knockdown was not measured. If, as the data suggests, there was functional

inhibition of RhoA after $G_{\alpha 12/13}$ siRNA treatment, then it implies that RhoA is not required for LPA-induced TGFβ activation, but its effector ROCKI/II is. Indeed, this would be an interesting finding and set ASM cells apart from many other cell types that show RhoA to be central to integrin-dependent TGFβ activation (128, 175). This hypothesis was in the process of being tested by using a C3 exoenzyme to block RhoA, however experiments were halted by the onset of the COVID-19 pandemic.

There are a few proven mechanisms by which ROCKI/II can be activated independently of RhoA. Arachidonic acid has been shown to activate ROCKI/II by binding to its autoinhibitory PH domain and inducing contraction of smooth muscle fibres (298). LPA is able to increase arachidonic acid in monocytes, but this has not been shown in ASM cells (335). Another mechanism of RhoA-independent ROCK activation requires PDK1. ROCKI activation can be induced by PDK1 binding in competition with its negative regulator RhoE (299). Many studies analysing ROCK focus on inhibiting both isoforms with the inhibitor Y27623. However, there are subtle differences between the roles of ROCKI and ROCKII. Analysis of the ROCKI/II in fibroblasts showed that siRNA depletion of ROCKI abrogated formation of stress fibres and focal adhesions, despite abundant ROCKII and active RhoA (338). Another study in vascular smooth muscle cells showed that ROCKII, but not ROCKI, was involved in cell contractility (339). Indeed, it would be interesting to inhibit ROCKI and ROCKII individually using small molecule inhibitors or siRNA to determine if one isoform regulates LPA-induced TGFβ in ASM cells. This could open up new avenues and narrow down the number of possible upstream activators that initiate TGFβ signalling.

Another possible avenue that was not explored during this PhD was the possibility of LPA-induced TGFβ activation acting via the $G_{\alpha i/o}$ G-

protein family. In a mouse and rat model of asthma both $G_{\alpha i2}$ and $G_{\alpha i3}$ expression was shown to be increased (160, 161). Moreover, LPA has been shown to activate RhoA and induce cytoskeletal reorganisation by a combination of $G_{\alpha q}$ and $G_{\alpha i2}$ in ASM cells (279). It would have been interesting to test whether there is a role for the $G_{\alpha i/o}$ family of heterotrimeric G-proteins in LPA-induced TGFβ activation. Indeed, it is possible that inhibiting $G_{\alpha i/o}$ alone would not inhibit LPA-induced TGFβ because there is crosstalk and redundancy built in to G-protein signalling. However, it would be interesting to investigate in the future using both genetic approaches and pertussis toxin, which is a potent inhibitor of $G_{\alpha i/0}$ (340).

It is possible that a single heterotrimeric G-protein family is not responsible for LPA-induced TGFβ signalling. Initially, the fact that LPA receptors can couple to all of the heterotrimeric G-protein families seemed like an advantage. However, the inherent drawback of using such multisystem stimuli is that if there is a web of crosstalk built into the signalling pathways then trying to delineate a specific pathway becomes far more complex. Moreover, knockdown of heterotrimeric G-proteins using siRNA can alter expression of other G-proteins. For example, knockdown of $G_{\alpha q/11}$ in HeLa cells caused an increase in expression of $G_{\alpha i1}$ and $G_{\alpha 12}$ (296).

Perhaps an alternative way of tackling the TGFβ signalling pathway would have been to adopt a top down approach. This could have involved analysing which LPA receptors were expressed in the human ASM cells used for experiments in this thesis. Subsequently, genetic knockdown of LPA receptors using siRNA or CRISPR could have been carried out to determine if a specific receptor was exclusively responsible for LPA-induced TGFβ activation. Then, a literature search of which heterotrimeric G-proteins are known to be coupled to the identified LPA receptor could have been carried out to identify

candidates. Of course, this method may have faced exactly the same challenges because LPA receptors often couple to multiple classes of heterotrimeric G-proteins (271).

As for stretch-induced TGFβ activation in human ASM cells less conclusions can be drawn. 15% cyclical mechanical stretch is able to induce TGFβ signalling after 4 hours of stretch, and it appears that ASM cells from asthmatic patients activate more TGFβ than cells from non-asthmatics. This was expected because asthmatic ASM have been shown to activate more TGFβ than non-asthmatic ASM cells in response to methacholine and LPA (133). It is clear from data presented in this thesis that $G_{\alpha q/11}$ alone are not responsible for stretch-induced TGFβ activation. Moreover, knockdown of $G_{\alpha 12}$ by siRNA showed that this heterotrimeric G-protein was also not responsible for stretch-induced TGFβ activation alone. Knockdown of $G_{\alpha 13}$ protein by siRNA was not successful in any stretch experiments, so the role of this protein remains unknown.

RhoA activation was not assessed in response to stretch in this thesis. However, RhoA activation has been shown to increase after 1 minute and peak after 5 minutes of 12% uniaxial stretch in human ASM cells (183). Inhibiting stretch-induced RhoA with a C3 exonezyme abrogates TGFβ1 mRNA expression (183). In this thesis, inhibiting ROCKI/II abrogated a stretch-induced increase in pSmad2. These data suggest that the RhoA/ROCKI/II axis is important in ASM cells.

This thesis hypothesised stretch-induced TGFβ activation in ASM cells was initiated by the release of a paracrine factor during stretch that binds to a GPCR. This was based on the observation that forced high-pressure ventilation increased total lung TGFβ in mice, which was abrogated by epithelial knockout of $G_{\alpha q/11}$ (127). This thesis neither proved nor disproved this hypothesis but did indicate that $G_{\alpha q/11}$ nor

$G_{\alpha 12}$ are required for stretch-induced TGFβ activation. Many factors are released from cells during stretch including angiotensin II, TGFβ1, endothelin-I, and matrix metalloproteinases (312-314, 322). MMP-9 has been shown to activate TGFβ in human lung fibroblasts cultured in collagen gels (341). Indeed this molecule was not specifically analysed in this thesis, however it may be interesting to see if inhibition of MMP-9 by siRNA reduced TGFβ signalling in ASM cells. The challenge with determining whether a paracrine factor released from cells activates TGFβ is that stretch itself induces the release of TGFβ. This makes media transfer experiments redundant because the TGFβ in the media would directly activate its receptor. Moreover, it isn't possible to treat conditioned media with proteases or heat shock due to the presence of TGFβ. There are too many factors within the media to design a clearly defined experiment, without a panel of candidates, to determine which released mediator actives TGFβ. A possible option to determine a panel of candidates could be to use mass spectrometry and compare the constituents of media from stretched versus unstretched ASM cells.

It is possible that stretch-induced TGFβ activation may occur directly in response to force. Integrins in focal adhesion complexes that are bound to the collagen coated plates will transduce force directly to the cytoskeleton during a stretching regimen. This may then activate integrins that are able to liberate active TGFβ from its latent associated peptide. Therefore, it is possible that no GPCR is involved in stretch-induced TGFβ activation. There have been several studies in smooth muscle cells that have shown stretch to activate RhoA and therefore ROCKI/II (342-344). Moreover, RhoA/ROCKI/II pathway has been described as essential to the formation of stress fibres in response to stretch (344). Growth of focal adhesions have been shown to occur in response to force, which are able to activate TGFβ

via cell surface integrins (345). This thesis concludes that ROCKI/II, but not $G_{\alpha q/11}$ nor $G_{\alpha 12}$, are required for stretch-induced TGFβ activation in ASM cells. It is therefore possible that cyclical stretch induced the activation of RhoA, ROCKI/II, and formation of focal adhesions, which are able to activate TGFβ through integrins.

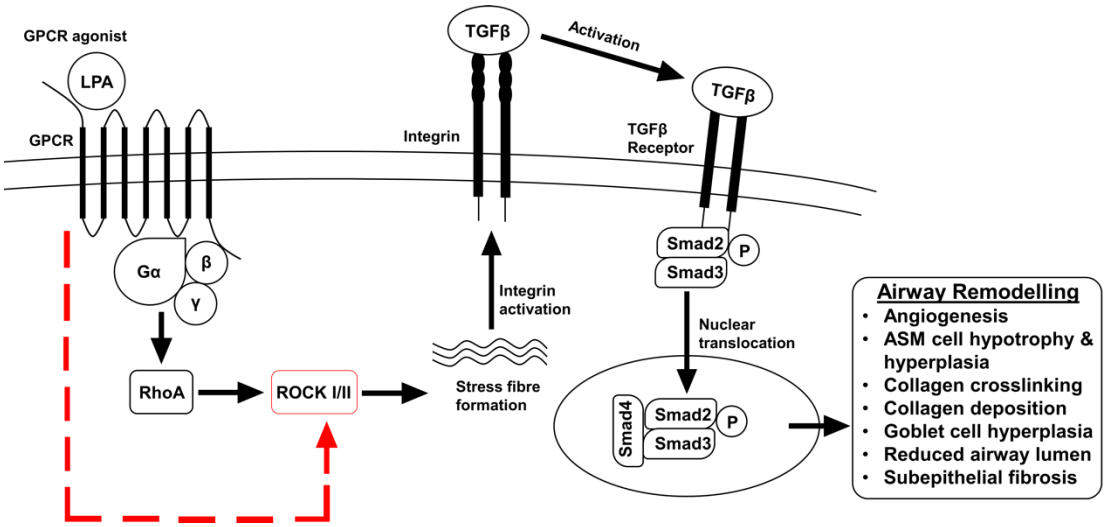

Figure 7.1. *Working hypothesis of LPA-induced TGFβ activation action pathway in human ASM cells.* Results in this thesis have shown the importance of ROCKI/II in LPA-induced TGFβ activation. Moreover, inhibition of RhoA activation through knockdown of $G_{\alpha 12/13}$ by siRNA did not inhibit pSmad2. This suggests that ROCKI/II activation may occur independently of RhoA in human ASM cells. Thus the working hypothesis is that LPA activates a single or multiple heterotrimeric G-proteins that ultimately lead to ROCKI or ROCKII activation and TGFβ activation.

7.2 Concluding Remarks

This thesis was designed to test the hypothesis that the heterotrimeric G-proteins $G_{\alpha q/11}$ are required for TGFβ activation in ASM cells. Data presented clearly demonstrated for the first time that there is no role for $G_{\alpha q/11}$ in LPA- or stretch-induced TGFβ activation in ASM cells. Collectively, ROCKI/II have been shown to be central to TGFβ activation and further delineation of the individual roles of ROCKI and ROCKII would be interesting. LPA-induced RhoA activation has been shown, for the first time, to be regulated by $G_{\alpha 12/13}$ heterotrimeric G-proteins in ASM cells. Data in this thesis suggests that there is no role for $G_{\alpha 12}$ in LPA-induced TGFβ activation and hints that RhoA may not be required for LPA-induced TGFβ activation. If correct this could be essential to further delineate asthma pathogenesis and explore opportunities for drug development.

8 Appendix

8.1 Appendix 1: figures referred to in main text

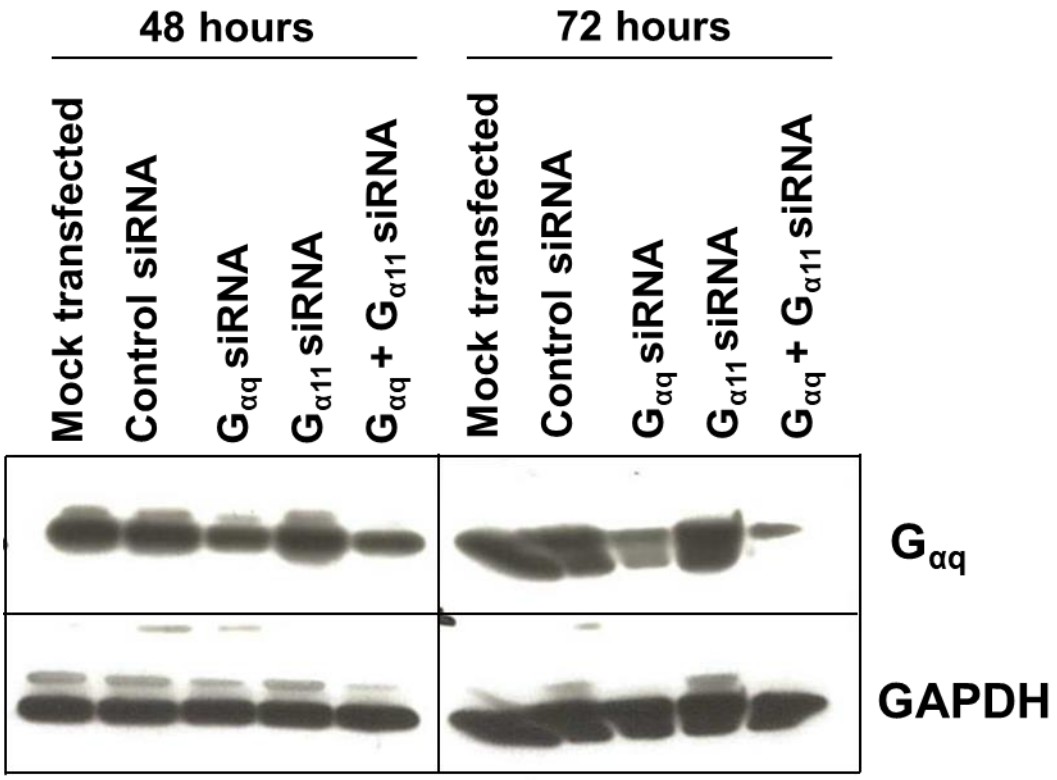

Appendix 1. Human asthmatic ASM cells mock transfected, transfected with control siRNA, $G_{\alpha q}$ siRNA, $G_{\alpha 11}$ siRNA, or $G_{\alpha q}$ and $G_{\alpha 11}$ (n=1 cell line). $G_{\alpha q}$ protein was measured by western blot 48 and 72 hours post-transfection. $G_{\alpha q}$ protein was reduced in $G_{\alpha q}$ and $G_{\alpha q}$ + $G_{\alpha 11}$ siRNA treated cells at 72 hours but not at 48 hours. Bands in the 72 hour western blot are smeared due to being moved during the transfer step.

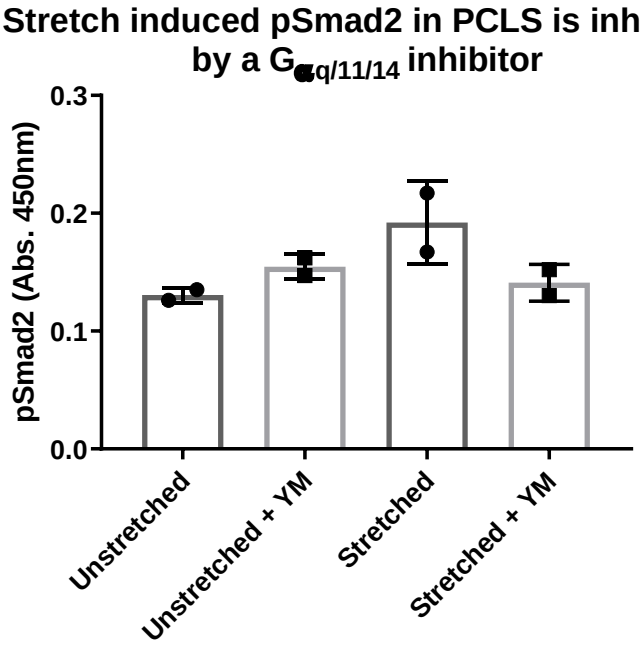

Appendix 2. This graph is from Amanda Tatler and is not my own work. Precision cut lung slices (PCLS) were taken from non-asthmatic human donors and attached to a Flexwell tissue culture plate. PCLS were subjected to 15% stretch for 48 hours at a frequency of 0.3Hz and pSmad2 was measured by ELISA (n=2 donors). PCLS were incubated with 10nM of the $G_{\alpha q/11/14}$ inhibitor YM254890 for 45 minutes prior to stretch. Stretch induced an increase in pSmad2, which was abrogated by the $G_{\alpha q/11/14}$ inhibitor YM254890.

8.2 Appendix 2: Buffer Recipes

8.2.1 Western Blot Buffers

Lysis Buffer:

50mM Tris-HCL pH 6.8, 150mM NaCl, 1% TritonX 100, 0.1% SDS, 0.5% deoxycholic acid, 10µl/ml NaVO4, and 0.01M EDTA.

Before use, 1µl/ml leupeptin, 20µl/ml PMSF, and 40µl/ml protease inhibitor cocktail and Phos-STOP were added.

4x Laemmli Buffer:

62.5mM Tris-HCL pH 6.8, 10% v/v glycerol, 1% w/v SDS, and 0.01% bromophenol blue.

Before use, 1% v/v β-mercaptoethanol was added.

10x Transfer Buffer:

50mM Tris base pH 8.3, 192mM glycine, and 20% v/v methanol.

Buffer 1:

1.5M Tris-HCL, 0.4% SDS, pH 8.8.

Buffer 2:

0.5M Tris-HCL, 0.4% SDS, pH 6.8.

Tris Buffered Saline, and Tween (TBST):

24.2g Tris Base, 87.6g NaCl, 1L dH_20, pH 7.4-7.6, 10ml Tween 20.

10% Resolving Gel:

6.66ml 30% Bis/acrylamide, 5.2ml buffer 1, 7.92ml dH_20.

Before use, 20µl tetramethylethylenediamine (temed) was added.

Stacking gel:

1.3ml 30% bis/acrylamide, 2.5ml buffer 2, 6.1ml dH_20.

Before use, 50µl 10% ammonium persulphate and 10µl temed was added.

8.2.2 Primer Sequences

Gene	**Primer sequence 5' -> 3'**
GNAQ	GGA CAG GAG AGA GTG GCA TGG GAT CTT GAG TGT GTC CA
GNA11	CCA CTG CTT TGA GAA CGT GA GCA GGT CCT TCT TGT TGA GG
GNA12	TTG AGG ACC GTG TTG TGT GT GCG TGC ACT GGA TGT CTA GA
GNA13	GAC TCC AGT GAG GGC TCA AG AGC AGG GAA GAA AAC TGC AA
PAI1	TCT GCA GAC CTG GTT CCC AC AGC CCC CGT AGT TCC ATC CTG
Cre	CGA GTG ATG AGG TTC GCA AG CCG GTA TTG AAA CTC GAG GG
β2-M	AAT CCA AAT GCG GCA TCT GAG TAT GCC TGC CGT GTG

8.2.3 Antibodies

Protein	**Antibody number**	**Company**	**Stock Concentration**	**Dilution**
pSmad2	3108S	Cell Signalling	1mg/ml	1:1000
Smad2/3	3102S	Cell Signalling	1mg/ml	1:1000
$G_{\alpha q}$	ab28060	Abcam	0.5mg/ml	1:1000

$G_{\alpha 11}$	ab192507	Abcam	1mg/ml	1:1000
$G_{\alpha 12}$	ab154004	Abcam	1mg/ml	1:1000
$G_{\alpha 13}$	ab227494	Abcam	1.29mg/ml	1:1000
Cre	ab24607	Abcam	1mg/ml	1:1000
GAPDH	ab181603	Abcam	1.485mg/ml	1:10,000

9 References

1. Makinde T, Murphy RF, Agrawal DK. The regulatory role of TGF-β in airway remodeling in asthma. Immunology & Cell Biology. 2007;85(5):348-56.
2. AsthmaUK. Asthma facts and statistics: AsthmaUK; 2016 [updated 2016/2017. Available from: https://www.asthma.org.uk/about/media/facts-and-statistics/.
3. Pearce N, Ait-Khaled N, Beasley R, Mallol J, Keil U, Mitchell E, et al. Worldwide trends in the prevalence of asthma symptoms: phase III of the International Study of Asthma and Allergies in Childhood (ISAAC). Thorax. 2007;62(9):758-66.
4. Lambrecht BN, Hammad H. The immunology of asthma. Nat Immunol. 2015;16(1):45-56.
5. Anderson GP. Endotyping asthma: new insights into key pathogenic mechanisms in a complex, heterogeneous disease. Lancet. 2008;372(9643):1107-19.
6. Daher S, Santos LM, Sole D, De Lima MG, Naspitz CK, Musatti CC. Interleukin-4 and soluble CD23 serum levels in asthmatic atopic children. Journal of investigational allergology & clinical immunology. 1995;5(5):251-4.
7. Gauvreau GM, El-Gammal AI, O'Byrne PM. Allergen-induced airway responses. Eur Respir J. 2015;46(3):819-31.
8. Robinson D, Hamid Q, Bentley A, Ying S, Kay AB, Durham SR. Activation of Cd4+ T-Cells, Increased T(H2)-Type Cytokine Messenger-Rna Expression, and Eosinophil Recruitment in Bronchoalveolar Lavage after Allergen Inhalation Challenge in Patients with Atopic Asthma. J Allergy Clin Immun. 1993;92(2):313-24.
9. Nabe T, Zindl CL, Jung YW, Stephens R, Sakamoto A, Kohno S, et al. Induction of a late asthmatic response associated with airway inflammation in mice. Eur J Pharmacol. 2005;521(1-3):144-55.
10. Ohtomo T, Kaminuma O, Kitamura N, Suko M, Kobayashi N, Mori A. Murine Th clones confer late asthmatic response upon antigen challenge. Int Arch Allergy Immunol. 2009;149 Suppl 1:2-6.
11. Reuter S, Stassen M, Taube C. Mast cells in allergic asthma and beyond. Yonsei Med J. 2010;51(6):797-807.
12. Bradding P, Roberts JA, Britten KM, Montefort S, Djukanovic R, Mueller R, et al. Interleukin-4, -5, and -6 and tumor necrosis factor-alpha in normal and asthmatic airways: evidence for the human mast cell as a source of these cytokines. Am J Respir Cell Mol Biol. 1994;10(5):471-80.
13. Amin K, Janson C, Boman G, Venge P. The extracellular deposition of mast cell products is increased in hypertrophic airways smooth muscles in allergic asthma but not in nonallergic asthma. Allergy. 2005;60(10):1241-7.

14. Brightling CE, Bradding P, Symon FA, Holgate ST, Wardlaw AJ, Pavord ID. Mast-cell infiltration of airway smooth muscle in asthma. The New England journal of medicine. 2002;346(22):1699-705.
15. Carroll NG, Mutavdzic S, James AL. Distribution and degranulation of airway mast cells in normal and asthmatic subjects. European Respiratory Journal. 2002;19(5):879.
16. Woodman L, Siddiqui S, Cruse G, Sutcliffe A, Saunders R, Kaur D, et al. Mast cells promote airway smooth muscle cell differentiation via autocrine up-regulation of TGF-beta 1. J Immunol. 2008;181(7):5001-7.
17. Kim Y-S, Ko H-M, Kang N-I, Song C-H, Zhang X, Chung W-C, et al. Mast cells play a key role in the developmentof late airway hyperresponsiveness through TNF-αin a murine model of asthma. Eur J Immunol. 2007;37(4):1107-15.
18. Méndez-Enríquez E, Hallgren J. Mast Cells and Their Progenitors in Allergic Asthma. Front Immunol. 2019;10(821).
19. Holgate S, Smith N, Massanari M, Jimenez P. Effects of omalizumab on markers of inflammation in patients with allergic asthma. Allergy. 2009;64(12):1728-36.
20. Paul WE, Seder RA. Lymphocyte responses and cytokines. Cell. 1994;76(2):241-51.
21. Hsieh CS, Macatonia SE, Tripp CS, Wolf SF, O'Garra A, Murphy KM. Development of TH1 CD4+ T cells through IL-12 produced by Listeria-induced macrophages. Science. 1993;260(5107):547-9.
22. Romagnani S. T-cell subsets (Th1 versus Th2). Annals of allergy, asthma & immunology : official publication of the American College of Allergy, Asthma, & Immunology. 2000;85(1):9-18; quiz , 21.
23. Wills-Karp M. Immunologic basis of antigen-induced airway hyperresponsiveness. Annual review of immunology. 1999;17:255-81.
24. Wills-Karp M, Luyimbazi J, Xu X, Schofield B, Neben TY, Karp CL, et al. Interleukin-13: central mediator of allergic asthma. Science. 1998;282(5397):2258-61.
25. Cohn L, Homer RJ, Marinov A, Rankin J, Bottomly K. Induction of airway mucus production By T helper 2 (Th2) cells: a critical role for interleukin 4 in cell recruitment but not mucus production. J Exp Med. 1997;186(10):1737-47.
26. Doherty TA, Soroosh P, Broide DH, Croft M. CD4+ cells are required for chronic eosinophilic lung inflammation but not airway remodeling. Am J Physiol Lung Cell Mol Physiol. 2009;296(2):L229-35.
27. Chang JT, Wherry EJ, Goldrath AW. Molecular regulation of effector and memory T cell differentiation. Nat Immunol. 2014;15(12):1104-15.
28. Hirose M, Horiguchi T. Asthma phenotypes. J Gen Fam Med. 2017;18(5):189-94.
29. Arron JR, Choy DF, Scheerens H, Matthews JG. Noninvasive biomarkers that predict treatment benefit from biologic therapies in asthma. Annals of the American Thoracic Society. 2013;10 Suppl:S206-13.
30. Young JD, Peterson CG, Venge P, Cohn ZA. Mechanism of membrane damage mediated by human eosinophil cationic protein. Nature. 1986;321(6070):613-6.
31. Weller PF. Human eosinophils. J Allergy Clin Immunol. 1997;100(3):283-7.

32. Trautmann A, Schmid-Grendelmeier P, Kruger K, Crameri R, Akdis M, Akkaya A, et al. T cells and eosinophils cooperate in the induction of bronchial epithelial cell apoptosis in asthma. J Allergy Clin Immunol. 2002;109(2):329-37.
33. Piliponsky AM, Pickholtz D, Gleich GJ, Levi-Schaffer F. Human eosinophils induce histamine release from antigen-activated rat peritoneal mast cells: a possible role for mast cells in late-phase allergic reactions. J Allergy Clin Immunol. 2001;107(6):993-1000.
34. Walker C, Bode E, Boer L, Hansel TT, Blaser K, Virchow JC. Allergic and Nonallergic Asthmatics Have Distinct Patterns of T-Cell Activation and Cytokine Production in Peripheral-Blood and Bronchoalveolar Lavage. American Review of Respiratory Disease. 1992;146(1):109-15.
35. Gonzalo JA, Lloyd CM, Kremer L, Finger E, Martinez AC, Siegelman MH, et al. Eosinophil recruitment to the lung in a murine model of allergic inflammation. The role of T cells, chemokines, and adhesion receptors. The Journal of clinical investigation. 1996;98(10):2332-45.
36. Woodruff PG, Modrek B, Choy DF, Jia G, Abbas AR, Ellwanger A, et al. T-helper type 2-driven inflammation defines major subphenotypes of asthma. Am J Respir Crit Care Med. 2009;180(5):388-95.
37. Wenzel S, Ford L, Pearlman D, Spector S, Sher L, Skobieranda F, et al. Dupilumab in persistent asthma with elevated eosinophil levels. The New England journal of medicine. 2013;368(26):2455-66.
38. Albers FC, Papi A, Taille C, Bratton DJ, Bradford ES, Yancey SW, et al. Mepolizumab reduces exacerbations in patients with severe eosinophilic asthma, irrespective of body weight/body mass index: meta-analysis of MENSA and MUSCA. Respir Res. 2019;20(1):169.
39. Ortega HG, Liu MC, Pavord ID, Brusselle GG, FitzGerald JM, Chetta A, et al. Mepolizumab treatment in patients with severe eosinophilic asthma. The New England journal of medicine. 2014;371(13):1198-207.
40. Bullone M, Carriero V, Bertolini F, Folino A, Mannelli A, Di Stefano A, et al. Elevated serum IgE, oral corticosteroid dependence and IL-17/22 expression in highly neutrophilic asthma. European Respiratory Journal. 2019;54(5):1900068.
41. Simpson JL, Scott R, Boyle MJ, Gibson PG. Inflammatory subtypes in asthma: assessment and identification using induced sputum. Respirology. 2006;11(1):54-61.
42. Al-Ramli W, Prefontaine D, Chouiali F, Martin JG, Olivenstein R, Lemiere C, et al. T(H)17-associated cytokines (IL-17A and IL-17F) in severe asthma. J Allergy Clin Immunol. 2009;123(5):1185-7.
43. Kudo M, Melton AC, Chen C, Engler MB, Huang KE, Ren X, et al. IL-17A produced by αβ T cells drives airway hyper-responsiveness in mice and enhances mouse and human airway smooth muscle contraction. Nature medicine. 2012;18(4):547-54.
44. Nakae S, Komiyama Y, Nambu A, Sudo K, Iwase M, Homma I, et al. Antigen-specific T cell sensitization is impaired in IL-17-deficient mice, causing suppression of allergic cellular and humoral responses. Immunity. 2002;17(3):375-87.
45. Wang YH, Voo KS, Liu B, Chen CY, Uygungil B, Spoede W, et al. A novel subset of CD4(+) T(H)2 memory/effector cells that produce

inflammatory IL-17 cytokine and promote the exacerbation of chronic allergic asthma. J Exp Med. 2010;207(11):2479-91.
46. Manni ML, Trudeau JB, Scheller EV, Mandalapu S, Elloso MM, Kolls JK, et al. The complex relationship between inflammation and lung function in severe asthma. Mucosal Immunol. 2014;7(5):1186-98.
47. Wang F, He XY, Baines KJ, Gunawardhana LP, Simpson JL, Li F, et al. Different inflammatory phenotypes in adults and children with acute asthma. European Respiratory Journal. 2011;38(3):567-74.
48. Busse WW, Holgate S, Kerwin E, Chon Y, Feng J, Lin J, et al. Randomized, double-blind, placebo-controlled study of brodalumab, a human anti-IL-17 receptor monoclonal antibody, in moderate to severe asthma. Am J Respir Crit Care Med. 2013;188(11):1294-302.
49. Pascual RM, Peters SP. Airway remodeling contributes to the progressive loss of lung function in asthma: an overview. J Allergy Clin Immunol. 2005;116(3):477-86; quiz 87.
50. Lange P, Parner J, Vestbo J, Schnohr P, Jensen G. A 15-year follow-up study of ventilatory function in adults with asthma. The New England journal of medicine. 1998;339(17):1194-200.
51. Mascia K, Haselkorn T, Deniz YM, Miller DP, Bleecker ER, Borish L, et al. Aspirin sensitivity and severity of asthma: evidence for irreversible airway obstruction in patients with severe or difficult-to-treat asthma. J Allergy Clin Immunol. 2005;116(5):970-5.
52. Fehrenbach H, Wagner C, Wegmann M. Airway remodeling in asthma: what really matters. Cell Tissue Res. 2017;367(3):551-69.
53. Temann UA, Geba GP, Rankin JA, Flavell RA. Expression of interleukin 9 in the lungs of transgenic mice causes airway inflammation, mast cell hyperplasia, and bronchial hyperresponsiveness. J Exp Med. 1998;188(7):1307-20.
54. Lee JJ, McGarry MP, Farmer SC, Denzler KL, Larson KA, Carrigan PE, et al. Interleukin-5 expression in the lung epithelium of transgenic mice leads to pulmonary changes pathognomonic of asthma. J Exp Med. 1997;185(12):2143-56.
55. Rankin JA, Picarella DE, Geba GP, Temann UA, Prasad B, DiCosmo B, et al. Phenotypic and physiologic characterization of transgenic mice expressing interleukin 4 in the lung: lymphocytic and eosinophilic inflammation without airway hyperreactivity. Proc Natl Acad Sci U S A. 1996;93(15):7821-5.
56. Zhu Z, Homer RJ, Wang Z, Chen Q, Geba GP, Wang J, et al. Pulmonary expression of interleukin-13 causes inflammation, mucus hypersecretion, subepithelial fibrosis, physiologic abnormalities, and eotaxin production. The Journal of clinical investigation. 1999;103(6):779-88.
57. Temann UA, Ray P, Flavell RA. Pulmonary overexpression of IL-9 induces Th2 cytokine expression, leading to immune pathology. The Journal of clinical investigation. 2002;109(1):29-39.
58. Atherton HC, Jones G, Danahay H. IL-13-induced changes in the goblet cell density of human bronchial epithelial cell cultures: MAP kinase and phosphatidylinositol 3-kinase regulation. Am J Physiol Lung Cell Mol Physiol. 2003;285(3):L730-9.

59. Amin K, Ludviksdottir D, Janson C, Nettelbladt O, Bjornsson E, Roomans GM, et al. Inflammation and structural changes in the airways of patients with atopic and nonatopic asthma. BHR Group. Am J Respir Crit Care Med. 2000;162(6):2295-301.
60. Jeffery PK, Wardlaw AJ, Nelson FC, Collins JV, Kay AB. Bronchial biopsies in asthma. An ultrastructural, quantitative study and correlation with hyperreactivity. Am Rev Respir Dis. 1989;140(6):1745-53.
61. Trautmann A, Kruger K, Akdis M, Muller-Wening D, Akkaya A, Brocker EB, et al. Apoptosis and loss of adhesion of bronchial epithelial cells in asthma. Int Arch Allergy Immunol. 2005;138(2):142-50.
62. Heijink IH, van Oosterhout A, Kapus A. Epidermal growth factor receptor signalling contributes to house dust mite-induced epithelial barrier dysfunction. Eur Respir J. 2010;36(5):1016-26.
63. Puddicombe SM, Polosa R, Richter A, Krishna MT, Howarth PH, Holgate ST, et al. Involvement of the epidermal growth factor receptor in epithelial repair in asthma. Faseb J. 2000;14(10):1362-74.
64. Undevia NS, Dorscheid DR, Marroquin BA, Gugliotta WL, Tse R, White SR. Smad and p38-MAPK signaling mediates apoptotic effects of transforming growth factor-beta1 in human airway epithelial cells. Am J Physiol Lung Cell Mol Physiol. 2004;287(3):L515-24.
65. Hackett TL, Warner SM, Stefanowicz D, Shaheen F, Pechkovsky DV, Murray LA, et al. Induction of epithelial-mesenchymal transition in primary airway epithelial cells from patients with asthma by transforming growth factor-beta1. Am J Respir Crit Care Med. 2009;180(2):122-33.
66. Stevens PT, Kicic A, Sutanto EN, Knight DA, Stick SM. Dysregulated repair in asthmatic paediatric airway epithelial cells: the role of plasminogen activator inhibitor-1. Clin Exp Allergy. 2008;38(12):1901-10.
67. Grainge CL, Davies DE. Epithelial injury and repair in airways diseases. Chest. 2013;144(6):1906-12.
68. Carroll N, Elliot J, Morton A, James A. The structure of large and small airways in nonfatal and fatal asthma. Am Rev Respir Dis. 1993;147(2):405-10.
69. Little SA, Sproule MW, Cowan MD, Macleod KJ, Robertson M, Love JG, et al. High resolution computed tomographic assessment of airway wall thickness in chronic asthma: reproducibility and relationship with lung function and severity. Thorax. 2002;57(3):247.
70. Boulet LP, Laviolette M, Turcotte H, Cartier A, Dugas M, Malo JL, et al. Bronchial subepithelial fibrosis correlates with airway responsiveness to methacholine. Chest. 1997;112(1):45-52.
71. Chakir J, Shannon J, Molet S, Fukakusa M, Elias J, Laviolette M, et al. Airway remodeling-associated mediators in moderate to severe asthma: effect of steroids on TGF-beta, IL-11, IL-17, and type I and type III collagen expression. J Allergy Clin Immunol. 2003;111(6):1293-8.
72. Huang J, Olivenstein R, Taha R, Hamid Q, Ludwig M. Enhanced proteoglycan deposition in the airway wall of atopic asthmatics. Am J Respir Crit Care Med. 1999;160(2):725-9.
73. Pini L, Hamid Q, Shannon J, Lemelin L, Olivenstein R, Ernst P, et al. Differences in proteoglycan deposition in the airways of moderate and severe asthmatics. European Respiratory Journal. 2007;29(1):71.

74. Batra V, Musani AI, Hastie AT, Khurana S, Carpenter KA, Zangrilli JG, et al. Bronchoalveolar lavage fluid concentrations of transforming growth factor (TGF)-β1, TGF-β2, interleukin (IL)-4 and IL-13 after segmental allergen challenge and their effects on α-smooth muscle actin and collagen III synthesis by primary human lung fibroblasts. Clinical & Experimental Allergy. 2004;34(3):437-44.
75. Roche WR, Beasley R, Williams JH, Holgate ST. Subepithelial fibrosis in the bronchi of asthmatics. Lancet. 1989;1(8637):520-4.
76. Weitoft M, Andersson C, Andersson-Sjöland A, Tufvesson E, Bjermer L, Erjefält J, et al. Controlled and uncontrolled asthma display distinct alveolar tissue matrix compositions. Respiratory Research. 2014;15(1):67.
77. Brewster CEP, Howarth PH, Djukanovic R, Wilson J, Holgate ST, Roche WR. Myofibroblasts and Subepithelial Fibrosis in Bronchial Asthma. Am J Resp Cell Mol. 1990;3(5):507-11.
78. Brewster CE, Howarth PH, Djukanovic R, Wilson J, Holgate ST, Roche WR. Myofibroblasts and subepithelial fibrosis in bronchial asthma. Am J Respir Cell Mol Biol. 1990;3(5):507-11.
79. Michalik M, Pierzchalska M, Legutko A, Ura M, Ostaszewska A, Soja J, et al. Asthmatic bronchial fibroblasts demonstrate enhanced potential to differentiate into myofibroblasts in culture. Medical science monitor : international medical journal of experimental and clinical research. 2009;15(7):Br194-201.
80. Khalil N, Xu YD, O'Connor R, Duronio V. Proliferation of pulmonary interstitial fibroblasts is mediated by transforming growth factor-beta1-induced release of extracellular fibroblast growth factor-2 and phosphorylation of p38 MAPK and JNK. J Biol Chem. 2005;280(52):43000-9.
81. Gizycki MJ, Adelroth E, Rogers AV, O'Byrne PM, Jeffery PK. Myofibroblast involvement in the allergen-induced late response in mild atopic asthma. Am J Respir Cell Mol Biol. 1997;16(6):664-73.
82. Silva PL, Passaro CP, Cagido VR, Bozza M, Dolhnikoff M, Negri EM, et al. Impact of lung remodelling on respiratory mechanics in a model of severe allergic inflammation. Respiratory physiology & neurobiology. 2008;160(3):239-48.
83. Mattos W, Lim S, Russell R, Jatakanon A, Chung KF, Barnes PJ. Matrix metalloproteinase-9 expression in asthma: effect of asthma severity, allergen challenge, and inhaled corticosteroids. Chest. 2002;122(5):1543-52.
84. Wiggs BR, Bosken C, Pare PD, James A, Hogg JC. A model of airway narrowing in asthma and in chronic obstructive pulmonary disease. Am Rev Respir Dis. 1992;145(6):1251-8.
85. Carroll N, Elliot J, Morton A, James A. The Structure of Large and Small Airways in Nonfatal and Fatal Asthma. American Review of Respiratory Disease. 1993;147(2):405-10.
86. Kuwano K, Bosken CH, Paré PD, Bai TR, Wiggs BR, Hogg JC. Small Airways Dimensions in Asthma and in Chronic Obstructive Pulmonary Disease. American Review of Respiratory Disease. 1993;148(5):1220-5.
87. Ebina M, Takahashi T, Chiba T, Motomiya M. Cellular Hypertrophy and Hyperplasia of Airway Smooth Muscles Underlying Bronchial Asthma:

A 3-D Morphometric Study. American Review of Respiratory Disease. 1993;148(3):720-6.
88. Woodruff PG, Dolganov GM, Ferrando RE, Donnelly S, Hays SR, Solberg OD, et al. Hyperplasia of Smooth Muscle in Mild to Moderate Asthma without Changes in Cell Size or Gene Expression. Am J Resp Crit Care. 2004;169(9):1001-6.
89. Regamey N, Ochs M, Hilliard TN, Mühlfeld C, Cornish N, Fleming L, et al. Increased Airway Smooth Muscle Mass in Children with Asthma, Cystic Fibrosis, and Non-Cystic Fibrosis Bronchiectasis. Am J Resp Crit Care. 2008;177(8):837-43.
90. James AL, Elliot JG, Jones RL, Carroll ML, Mauad T, Bai TR, et al. Airway Smooth Muscle Hypertrophy and Hyperplasia in Asthma. Am J Resp Crit Care. 2012;185(10):1058-64.
91. Johnson PR, Roth M, Tamm M, Hughes M, Ge Q, King G, et al. Airway smooth muscle cell proliferation is increased in asthma. Am J Respir Crit Care Med. 2001;164(3):474-7.
92. McKay S, de Jongste JC, Saxena PR, Sharma HS. Angiotensin II induces hypertrophy of human airway smooth muscle cells: expression of transcription factors and transforming growth factor-beta1. Am J Respir Cell Mol Biol. 1998;18(6):823-33.
93. Goldsmith AM, Bentley JK, Zhou L, Jia Y, Bitar KN, Fingar DC, et al. Transforming growth factor-beta induces airway smooth muscle hypertrophy. Am J Resp Cell Mol. 2006;34(2):247-54.
94. Liu L, Zhai C, Pan Y, Zhu Y, Shi W, Wang J, et al. Sphingosine-1-phosphate induces airway smooth muscle cell proliferation, migration, and contraction by modulating Hippo signaling effector YAP. Am J Physiol-Lung C. 2018;315(4):L609-L21.
95. Berger P, Perng DW, Thabrew H, Compton SJ, Cairns JA, McEuen AR, et al. Tryptase and agonists of PAR-2 induce the proliferation of human airway smooth muscle cells. J Appl Physiol (1985). 2001;91(3):1372-9.
96. Black PN, Young PG, Skinner SJ. Response of airway smooth muscle cells to TGF-beta 1: effects on growth and synthesis of glycosaminoglycans. Am J Physiol. 1996;271(6 Pt 1):L910-7.
97. Parameswaran K, Cox G, Radford K, Janssen LJ, Sehmi R, O'Byrne PM. Cysteinyl leukotrienes promote human airway smooth muscle migration. Am J Respir Crit Care Med. 2002;166(5):738-42.
98. Jendzjowsky NG, Kelly MM. The Role of Airway Myofibroblasts in Asthma. Chest. 2019;156(6):1254-67.
99. Wang CH, Huang CD, Lin HC, Lee KY, Lin SM, Liu CY, et al. Increased circulating fibrocytes in asthma with chronic airflow obstruction. Am J Respir Crit Care Med. 2008;178(6):583-91.
100. Saunders R, Siddiqui S, Kaur D, Doe C, Sutcliffe A, Hollins F, et al. Fibrocyte localization to the airway smooth muscle is a feature of asthma. The Journal of allergy and clinical immunology. 2009;123(2):376-84.
101. Schmidt M, Sun G, Stacey MA, Mori L, Mattoli S. Identification of circulating fibrocytes as precursors of bronchial myofibroblasts in asthma. J Immunol. 2003;171(1):380-9.
102. Dunnill MS. THE PATHOLOGY OF ASTHMA, WITH SPECIAL REFERENCE TO CHANGES IN THE BRONCHIAL MUCOSA. Journal of Clinical Pathology. 1960;13(1):27.

103. Li X, Wilson JW. Increased vascularity of the bronchial mucosa in mild asthma. Am J Respir Crit Care Med. 1997;156(1):229-33.
104. Tanaka H, Yamada G, Saikai T, Hashimoto M, Tanaka S, Suzuki K, et al. Increased airway vascularity in newly diagnosed asthma using a high-magnification bronchovideoscope. Am J Respir Crit Care Med. 2003;168(12):1495-9.
105. Li XUN, Wilson JW. Increased Vascularity of the Bronchial Mucosa in Mild Asthma. Am J Resp Crit Care. 1997;156(1):229-33.
106. Dvorak HF, Brown LF, Detmar M, Dvorak AM. Vascular permeability factor/vascular endothelial growth factor, microvascular hyperpermeability, and angiogenesis. Am J Pathol. 1995;146(5):1029-39.
107. Hoshino M, Takahashi M, Aoike N. Expression of vascular endothelial growth factor, basic fibroblast growth factor, and angiogenin immunoreactivity in asthmatic airways and its relationship to angiogenesis. J Allergy Clin Immunol. 2001;107(2):295-301.
108. Hoshino M, Nakamura Y, Hamid QA. Gene expression of vascular endothelial growth factor and its receptors and angiogenesis in bronchial asthma. J Allergy Clin Immunol. 2001;107(6):1034-8.
109. Kobayashi T, Liu X, Wen F-Q, Fang Q, Abe S, Wang XQ, et al. Smad3 mediates TGF-β1 induction of VEGF production in lung fibroblasts. Biochem Bioph Res Co. 2005;327(2):393-8.
110. Wen F-Q, Liu X, Manda W, Terasaki Y, Kobayashi T, Abe S, et al. TH2 Cytokine-enhanced and TGF-β-enhanced vascular endothelial growth factor production by cultured human airway smooth muscle cells is attenuated by IFN-γ and corticosteroids. J Allergy Clin Immun. 2003;111(6):1307-18.
111. Lee KS, Min KH, Kim SR, Park SJ, Park HS, Jin GY, et al. Vascular endothelial growth factor modulates matrix metalloproteinase-9 expression in asthma. Am J Respir Crit Care Med. 2006;174(2):161-70.
112. Lee SH, Eren M, Vaughan DE, Schleimer RP, Cho SH. A Plasminogen Activator Inhibitor-1 Inhibitor Reduces Airway Remodeling in a Murine Model of Chronic Asthma. Am J Resp Cell Mol. 2012;46(6):842-6.
113. Aikawa T, Shimura S, Sasaki H, Ebina M, Takishima T. Marked goblet cell hyperplasia with mucus accumulation in the airways of patients who died of severe acute asthma attack. Chest. 1992;101(4):916-21.
114. Bateman JR, Pavia D, Sheahan NF, Agnew JE, Clarke SW. Impaired tracheobronchial clearance in patients with mild stable asthma. Thorax. 1983;38(6):463-7.
115. Ordonez CL, Khashayar R, Wong HH, Ferrando R, Wu R, Hyde DM, et al. Mild and moderate asthma is associated with airway goblet cell hyperplasia and abnormalities in mucin gene expression. Am J Respir Crit Care Med. 2001;163(2):517-23.
116. Bonser LR, Zlock L, Finkbeiner W, Erle DJ. Epithelial tethering of MUC5AC-rich mucus impairs mucociliary transport in asthma. The Journal of clinical investigation. 2016;126(6):2367-71.
117. Chu HW, Balzar S, Seedorf GJ, Westcott JY, Trudeau JB, Silkoff P, et al. Transforming growth factor-beta2 induces bronchial epithelial mucin expression in asthma. Am J Pathol. 2004;165(4):1097-106.
118. McMillan SJ, Xanthou G, Lloyd CM. Manipulation of allergen-induced airway remodeling by treatment with anti-TGF-beta antibody: effect on the Smad signaling pathway. J Immunol. 2005;174(9):5774-80.

119. Powell RJ, Cronenwett JL, Fillinger MF, Wagner RJ, Sampson LN. Endothelial cell modulation of smooth muscle cell morphology and organizational growth pattern. Annals of vascular surgery. 1996;10(1):4-10.
120. Halayko AJ, Salari H, Ma X, Stephens NL. Markers of airway smooth muscle cell phenotype. Am J Physiol. 1996;270(6 Pt 1):L1040-51.
121. Chamley-Campbell J, Campbell GR, Ross R. The smooth muscle cell in culture. Physiological Reviews. 1979;59(1):1-61.
122. Dekkers BGJ, Schaafsma D, Nelemans SA, Zaagsma J, Meurs H. Extracellular matrix proteins differentially regulate airway smooth muscle phenotype and function. Am J Physiol-Lung C. 2007;292(6):L1405-L13.
123. Katoh K, Kano Y, Amano M, Onishi H, Kaibuchi K, Fujiwara K. Rho-kinase--mediated contraction of isolated stress fibers. J Cell Biol. 2001;153(3):569-84.
124. Park D, Jhon DY, Lee CW, Ryu SH, Rhee SG. Removal of the carboxyl-terminal region of phospholipase C-beta 1 by calpain abolishes activation by G alpha q. J Biol Chem. 1993;268(5):3710-4.
125. Wynne BM, Chiao C-W, Webb RC. Vascular Smooth Muscle Cell Signaling Mechanisms for Contraction to Angiotensin II and Endothelin-1. J Am Soc Hypertens. 2009;3(2):84-95.
126. Kozasa T, Jiang X, Hart MJ, Sternweis PM, Singer WD, Gilman AG, et al. p115 RhoGEF, a GTPase activating protein for Galpha12 and Galpha13. Science. 1998;280(5372):2109-11.
127. John AE, Stavrou A, Tatler AL, Porte J, Habgood A, Knox AJ, et al. Loss Of Epithelial Gq/11 Signaling In The Lung Leads To Il-33 Mediated M2 Macrophage Polarization And Loss Of Tgf beta-Mediated Suppression Of Macrophage Mmp12. Am J Resp Crit Care. 2015;191.
128. Xu MY, Porte J, Knox AJ, Weinreb PH, Maher TM, Violette SM, et al. Lysophosphatidic Acid Induces alpha v beta 6 Integrin-Mediated TGF-beta Activation via the LPA2 Receptor and the Small G Protein G alpha(q). Am J Pathol. 2009;174(4):1264-79.
129. Nakagawa O, Fujisawa K, Ishizaki T, Saito Y, Nakao K, Narumiya S. ROCK-I and ROCK-II, two isoforms of Rho-associated coiled-coil forming protein serine/threonine kinase in mice. FEBS Lett. 1996;392(2):189-93.
130. Kimura K, Ito M, Amano M, Chihara K, Fukata Y, Nakafuku M, et al. Regulation of myosin phosphatase by Rho and Rho-associated kinase (Rho-kinase). Science. 1996;273(5272):245-8.
131. Tojkander S, Gateva G, Lappalainen P. Actin stress fibers – assembly, dynamics and biological roles. Journal of Cell Science. 2012;125(8):1855.
132. Gingras AR, Vogel KP, Steinhoff HJ, Ziegler WH, Patel B, Emsley J, et al. Structural and dynamic characterization of a vinculin binding site in the talin rod. Biochemistry. 2006;45(6):1805-17.
133. Tatler AL, John AE, Jolly L, Habgood A, Porte J, Brightling C, et al. Integrin alphavbeta5-mediated TGF-beta activation by airway smooth muscle cells in asthma. J Immunol. 2011;187(11):6094-107.
134. Ohashi K, Nagata K, Maekawa M, Ishizaki T, Narumiya S, Mizuno K. Rho-associated kinase ROCK activates LIM-kinase 1 by phosphorylation at threonine 508 within the activation loop. J Biol Chem. 2000;275(5):3577-82.

135. Ammit AJ, Armour CL, Black JL. Smooth-muscle myosin light-chain kinase content is increased in human sensitized airways. Am J Respir Crit Care Med. 2000;161(1):257-63.
136. Fish JE. Calcium channel antagonists in the treatment of asthma. J Asthma. 1984;21(6):407-18.
137. Janssen LJ, Tazzeo T, Zuo J. Enhanced myosin phosphatase and Ca(2+)-uptake mediate adrenergic relaxation of airway smooth muscle. Am J Respir Cell Mol Biol. 2004;30(4):548-54.
138. Pierce KL, Premont RT, Lefkowitz RJ. Seven-transmembrane receptors. Nature Reviews Molecular Cell Biology. 2002;3(9):639-50.
139. Ballesteros JA, Jensen AD, Liapakis G, Rasmussen SG, Shi L, Gether U, et al. Activation of the beta 2-adrenergic receptor involves disruption of an ionic lock between the cytoplasmic ends of transmembrane segments 3 and 6. J Biol Chem. 2001;276(31):29171-7.
140. Zhang L, Shi G. Gq-Coupled Receptors in Autoimmunity. J Immunol Res. 2016;2016:3969023-.
141. Lyon AM, Tesmer VM, Dhamsania VD, Thal DM, Gutierrez J, Chowdhury S, et al. An autoinhibitory helix in the C-terminal region of phospholipase C-β mediates Gαq activation. Nature Structural & Molecular Biology. 2011;18(9):999-1005.
142. Rhee SG. Regulation of phosphoinositide-specific phospholipase C. Annu Rev Biochem. 2001;70:281-312.
143. Lutz S, Freichel-Blomquist A, Yang Y, Rumenapp U, Jakobs KH, Schmidt M, et al. The guanine nucleotide exchange factor p63RhoGEF, a specific link between Gq/11-coupled receptor signaling and RhoA. J Biol Chem. 2005;280(12):11134-9.
144. Booden MA, Siderovski DP, Der CJ. Leukemia-associated Rho guanine nucleotide exchange factor promotes G alpha q-coupled activation of RhoA. Mol Cell Biol. 2002;22(12):4053-61.
145. Vogt S, Grosse R, Schultz G, Offermanns S. Receptor-dependent RhoA activation in G12/G13-deficient cells: genetic evidence for an involvement of Gq/G11. J Biol Chem. 2003;278(31):28743-9.
146. Tang H, Sun Y, Shi Z, Huang H, Fang Z, Chen J, et al. YKL-40 Induces IL-8 Expression from Bronchial Epithelium via MAPK (JNK and ERK) and NF-κB Pathways, Causing Bronchial Smooth Muscle Proliferation and Migration. The Journal of Immunology. 2013;190(1):438-46.
147. Kozasa T, Hajicek N, Chow CR, Suzuki N. Signalling mechanisms of RhoGTPase regulation by the heterotrimeric G proteins G12 and G13. Journal of biochemistry. 2011;150(4):357-69.
148. Fukuhara S, Murga C, Zohar M, Igishi T, Gutkind JS. A novel PDZ domain containing guanine nucleotide exchange factor links heterotrimeric G proteins to Rho. J Biol Chem. 1999;274(9):5868-79.
149. Fukuhara S, Chikumi H, Gutkind JS. Leukemia-associated Rho guanine nucleotide exchange factor (LARG) links heterotrimeric G proteins of the G(12) family to Rho. FEBS Lett. 2000;485(2-3):183-8.
150. Hart MJ, Jiang X, Kozasa T, Roscoe W, Singer WD, Gilman AG, et al. Direct stimulation of the guanine nucleotide exchange activity of p115 RhoGEF by Galpha13. Science. 1998;280(5372):2112-4.

151. Bhattacharyya R, Wedegaertner PB. Characterization of G alpha 13-dependent plasma membrane recruitment of p115RhoGEF. Biochem J. 2003;371(Pt 3):709-20.
152. Gohla A, Schultz G, Offermanns S. Role for G(12)/G(13) in agonist-induced vascular smooth muscle cell contraction. Circ Res. 2000;87(3):221-7.
153. Diviani D, Soderling J, Scott JD. AKAP-Lbc anchors protein kinase A and nucleates Galpha 12-selective Rho-mediated stress fiber formation. J Biol Chem. 2001;276(47):44247-57.
154. Chiba Y, Misawa M. Increased expression of G12 and G13 proteins in bronchial smooth muscle of airway hyperresponsive rats. Inflammation research : official journal of the European Histamine Research Society [et al]. 2001;50(6):333-6.
155. Hanoune J, Defer N. Regulation and Role of Adenylyl Cyclase Isoforms. Annual Review of Pharmacology and Toxicology. 2001;41(1):145-74.
156. Gerthoffer WT. Calcium dependence of myosin phosphorylation and airway smooth muscle contraction and relaxation. Am J Physiol. 1986;250(4 Pt 1):C597-604.
157. Morgan SJ, Deshpande DA, Tiegs BC, Misior AM, Yan H, Hershfeld AV, et al. β-Agonist-mediated relaxation of airway smooth muscle is protein kinase A-dependent. The Journal of biological chemistry. 2014;289(33):23065-74.
158. Rabe KF, Hurd S, Anzueto A, Barnes PJ, Buist SA, Calverley P, et al. Global strategy for the diagnosis, management, and prevention of chronic obstructive pulmonary disease: GOLD executive summary. Am J Respir Crit Care Med. 2007;176(6):532-55.
159. Nino G, Hu A, Grunstein JS, Grunstein MM. Mechanism regulating proasthmatic effects of prolonged homologous beta2-adrenergic receptor desensitization in airway smooth muscle. American journal of physiology Lung cellular and molecular physiology. 2009;297(4):L746-L57.
160. Chiba Y, Sakai H, Misawa M. Possible involvement of G(i3) protein in augmented contraction of bronchial smooth muscle from antigen-induced airway hyperresponsive rats. Biochem Pharmacol. 2001;61(7):921-4.
161. McGraw DW, Elwing JM, Fogel KM, Wang WCH, Glinka CB, Mihlbachler KA, et al. Crosstalk between Gi and Gq/Gs pathways in airway smooth muscle regulates bronchial contractility and relaxation. The Journal of clinical investigation. 2007;117(5):1391-8.
162. Alcorn JF, Rinaldi LM, Jaffe EF, van Loon M, Bates JH, Janssen-Heininger YM, et al. Transforming growth factor-beta1 suppresses airway hyperresponsiveness in allergic airway disease. Am J Respir Crit Care Med. 2007;176(10):974-82.
163. Sime PJ, Xing Z, Graham FL, Csaky KG, Gauldie J. Adenovector-mediated gene transfer of active transforming growth factor-beta1 induces prolonged severe fibrosis in rat lung. The Journal of clinical investigation. 1997;100(4):768-76.
164. Frank S, Madlener M, Werner S. Transforming growth factors beta1, beta2, and beta3 and their receptors are differentially regulated during normal and impaired wound healing. J Biol Chem. 1996;271(17):10188-93.

165. Kubiczkova L, Sedlarikova L, Hajek R, Sevcikova S. TGF-β – an excellent servant but a bad master. Journal of Translational Medicine. 2012;10(1):183.
166. Dubois CM, Laprise MH, Blanchette F, Gentry LE, Leduc R. Processing of transforming growth factor beta 1 precursor by human furin convertase. J Biol Chem. 1995;270(18):10618-24.
167. Miyazono K, Hellman U, Wernstedt C, Heldin CH. Latent high molecular weight complex of transforming growth factor beta 1. Purification from human platelets and structural characterization. J Biol Chem. 1988;263(13):6407-15.
168. Yu Q, Stamenkovic I. Cell surface-localized matrix metalloproteinase-9 proteolytically activates TGF-beta and promotes tumor invasion and angiogenesis. Genes & development. 2000;14(2):163-76.
169. Khalil N, Corne S, Whitman C, Yacyshyn H. Plasmin regulates the activation of cell-associated latent TGF-beta 1 secreted by rat alveolar macrophages after in vivo bleomycin injury. Am J Respir Cell Mol Biol. 1996;15(2):252-9.
170. Annes JP, Munger JS, Rifkin DB. Making sense of latent TGFβ activation. Journal of Cell Science. 2003;116(2):217-24.
171. Jullien P, Berg TM, Lawrence DA. Acidic cellular environments: Activation of latent tgf-β and sensitization of cellular responses to tgf-β and egf. International Journal of Cancer. 1989;43(5):886-91.
172. Brown PD, Wakefield LM, Levinson AD, Sporn MB. Physicochemical activation of recombinant latent transforming growth factor-beta's 1, 2, and 3. Growth factors (Chur, Switzerland). 1990;3(1):35-43.
173. Wipff PJ, Rifkin DB, Meister JJ, Hinz B. Myofibroblast contraction activates latent TGF-beta1 from the extracellular matrix. J Cell Biol. 2007;179(6):1311-23.
174. Asano Y, Ihn H, Yamane K, Jinnin M, Mimura Y, Tamaki K. Involvement of alphavbeta5 integrin-mediated activation of latent transforming growth factor beta1 in autocrine transforming growth factor beta signaling in systemic sclerosis fibroblasts. Arthritis Rheum. 2005;52(9):2897-905.
175. Jenkins RG, Su X, Su G, Scotton CJ, Camerer E, Laurent GJ, et al. Ligation of protease-activated receptor 1 enhances alpha(v)beta6 integrin-dependent TGF-beta activation and promotes acute lung injury. The Journal of clinical investigation. 2006;116(6):1606-14.
176. Mu D, Cambier S, Fjellbirkeland L, Baron JL, Munger JS, Kawakatsu H, et al. The integrin alpha(v)beta8 mediates epithelial homeostasis through MT1-MMP-dependent activation of TGF-beta1. J Cell Biol. 2002;157(3):493-507.
177. Klapholz B, Brown NH. Talin – the master of integrin adhesions. Journal of Cell Science. 2017;130(15):2435.
178. Horwitz A, Duggan K, Buck C, Beckerle MC, Burridge K. Interaction of plasma membrane fibronectin receptor with talin--a transmembrane linkage. Nature. 1986;320(6062):531-3.
179. Dekkers BG, Bos IS, Gosens R, Halayko AJ, Zaagsma J, Meurs H. The integrin-blocking peptide RGDS inhibits airway smooth muscle remodeling in a guinea pig model of allergic asthma. Am J Respir Crit Care Med. 2010;181(6):556-65.

180. Yang Z, Mu Z, Dabovic B, Jurukovski V, Yu D, Sung J, et al. Absence of integrin-mediated TGFbeta1 activation in vivo recapitulates the phenotype of TGFbeta1-null mice. J Cell Biol. 2007;176(6):787-93.
181. Munger JS, Huang X, Kawakatsu H, Griffiths MJ, Dalton SL, Wu J, et al. The integrin alpha v beta 6 binds and activates latent TGF beta 1: a mechanism for regulating pulmonary inflammation and fibrosis. Cell. 1999;96(3):319-28.
182. O'Callaghan CJ, Williams B. Mechanical strain-induced extracellular matrix production by human vascular smooth muscle cells: role of TGF-beta(1). Hypertension. 2000;36(3):319-24.
183. Mohamed JS, Boriek AM. Stretch augments TGF-beta1 expression through RhoA/ROCK1/2, PTK, and PI3K in airway smooth muscle cells. Am J Physiol Lung Cell Mol Physiol. 2010;299(3):L413-24.
184. Arora PD, Narani N, McCulloch CA. The compliance of collagen gels regulates transforming growth factor-beta induction of alpha-smooth muscle actin in fibroblasts. Am J Pathol. 1999;154(3):871-82.
185. Li Q, Muragaki Y, Hatamura I, Ueno H, Ooshima A. Stretch-induced collagen synthesis in cultured smooth muscle cells from rabbit aortic media and a possible involvement of angiotensin II and transforming growth factor-beta. J Vasc Res. 1998;35(2):93-103.
186. Sato Y, Rifkin DB. Inhibition of endothelial cell movement by pericytes and smooth muscle cells: activation of a latent transforming growth factor-beta 1-like molecule by plasmin during co-culture. J Cell Biol. 1989;109(1):309-15.
187. Verrecchia F, Mauviel A. Transforming growth factor-beta signaling through the Smad pathway: role in extracellular matrix gene expression and regulation. J Invest Dermatol. 2002;118(2):211-5.
188. Lyons RM, Keski-Oja J, Moses HL. Proteolytic activation of latent transforming growth factor-beta from fibroblast-conditioned medium. J Cell Biol. 1988;106(5):1659-65.
189. Frazier WA. Thrombospondins. Current opinion in cell biology. 1991;3(5):792-9.
190. Wight TN, Raugi GJ, Mumby SM, Bornstein P. Light microscopic immunolocation of thrombospondin in human tissues. Journal of Histochemistry & Cytochemistry. 1985;33(4):295-302.
191. Border WA, Ruoslahti E. Transforming growth factor-beta in disease: the dark side of tissue repair. The Journal of clinical investigation. 1992;90(1):1-7.
192. Murphy-Ullrich JE, Schultz-Cherry S, Höök M. Transforming growth factor-beta complexes with thrombospondin. Mol Biol Cell. 1992;3(2):181-8.
193. Schultz-Cherry S, Murphy-Ullrich JE. Thrombospondin causes activation of latent transforming growth factor-beta secreted by endothelial cells by a novel mechanism. J Cell Biol. 1993;122(4):923-32.
194. Ribeiro SM, Poczatek M, Schultz-Cherry S, Villain M, Murphy-Ullrich JE. The activation sequence of thrombospondin-1 interacts with the latency-associated peptide to regulate activation of latent transforming growth factor-beta. J Biol Chem. 1999;274(19):13586-93.

195. Crawford SE, Stellmach V, Murphy-Ullrich JE, Ribeiro SM, Lawler J, Hynes RO, et al. Thrombospondin-1 is a major activator of TGF-beta1 in vivo. Cell. 1998;93(7):1159-70.
196. Weiss A, Attisano L. The TGFbeta superfamily signaling pathway. Wiley interdisciplinary reviews Developmental biology. 2013;2(1):47-63.
197. Esparza-Lopez J, Montiel JL, Vilchis-Landeros MM, Okadome T, Miyazono K, Lopez-Casillas F. Ligand binding and functional properties of betaglycan, a co-receptor of the transforming growth factor-beta superfamily. Specialized binding regions for transforming growth factor-beta and inhibin A. J Biol Chem. 2001;276(18):14588-96.
198. Tsukazaki T, Chiang TA, Davison AF, Attisano L, Wrana JL. SARA, a FYVE domain protein that recruits Smad2 to the TGFbeta receptor. Cell. 1998;95(6):779-91.
199. Pierreux CE, Nicolás FJ, Hill CS. Transforming Growth Factor β-Independent Shuttling of Smad4 between the Cytoplasm and Nucleus. Mol Cell Biol. 2000;20(23):9041-54.
200. Moustakas A, Souchelnytskyi S, Heldin C-H. Smad regulation in TGF-β signal transduction. Journal of Cell Science. 2001;114(24):4359-69.
201. Nakao A, Afrakhte M, Morn A, Nakayama T, Christian JL, Heuchel R, et al. Identification of Smad7, a TGFβ-inducible antagonist of TGF-β signalling. Nature. 1997;389(6651):631-5.
202. Kavsak P, Rasmussen RK, Causing CG, Bonni S, Zhu HT, Thomsen GH, et al. Smad7 binds to Smurf2 to form an E3 ubiquitin ligase that targets the TGF beta receptor for degradation. Mol Cell. 2000;6(6):1365-75.
203. Shi W, Sun C, He B, Xiong W, Shi X, Yao D, et al. GADD34–PP1c recruited by Smad7 dephosphorylates TGFβ type I receptor. J Cell Biol. 2004;164(2):291-300.
204. Lin X, Duan XY, Liang YY, Su Y, Wrighton KH, Long JY, et al. PPM1A functions as a Smad phosphatase to terminate TGF beta signaling. Cell. 2006;125(5):915-28.
205. Kulkarni AB, Karlsson S. Transforming growth factor-beta 1 knockout mice. A mutation in one cytokine gene causes a dramatic inflammatory disease. The American journal of pathology. 1993;143(1):3-9.
206. Dickson MC, Martin JS, Cousins FM, Kulkarni AB, Karlsson S, Akhurst RJ. Defective haematopoiesis and vasculogenesis in transforming growth factor-beta 1 knock out mice. Development. 1995;121(6):1845-54.
207. Christ M, McCartney-Francis NL, Kulkarni AB, Ward JM, Mizel DE, Mackall CL, et al. Immune dysregulation in TGF-beta 1-deficient mice. J Immunol. 1994;153(5):1936-46.
208. Sanford LP, Ormsby I, Gittenberger-de Groot AC, Sariola H, Friedman R, Boivin GP, et al. TGFbeta2 knockout mice have multiple developmental defects that are non-overlapping with other TGFbeta knockout phenotypes. Development. 1997;124(13):2659-70.
209. Kaartinen V, Voncken JW, Shuler C, Warburton D, Bu D, Heisterkamp N, et al. Abnormal lung development and cleft palate in mice lacking TGF–β3 indicates defects of epithelial–mesenchymal interaction. Nature genetics. 1995;11(4):415-21.
210. Taya Y, O'Kane S, Ferguson MW. Pathogenesis of cleft palate in TGF-beta3 knockout mice. Development. 1999;126(17):3869-79.

211. Redington AE, Madden J, Frew AJ, Djukanovic R, Roche WR, Holgate ST, et al. Transforming growth factor-beta 1 in asthma. Measurement in bronchoalveolar lavage fluid. Am J Respir Crit Care Med. 1997;156(2 Pt 1):642-7.
212. Minshall EM, Leung DY, Martin RJ, Song YL, Cameron L, Ernst P, et al. Eosinophil-associated TGF-beta1 mRNA expression and airways fibrosis in bronchial asthma. Am J Respir Cell Mol Biol. 1997;17(3):326-33.
213. Vignola AM, Chanez P, Chiappara G, Merendino A, Pace E, Rizzo A, et al. Transforming growth factor-beta expression in mucosal biopsies in asthma and chronic bronchitis. Am J Resp Crit Care. 1997;156(2):591-9.
214. Sagara H, Okada T, Okumura K, Ogawa H, Ra C, Fukuda T, et al. Activation of TGF-beta/Smad2 signaling is associated with airway remodeling in asthma. J Allergy Clin Immunol. 2002;110(2):249-54.
215. Ojiaku CA, Yoo EJ, Panettieri RA, Jr. Transforming Growth Factor β1 Function in Airway Remodeling and Hyperresponsiveness. The Missing Link? Am J Resp Cell Mol. 2017;56(4):432-42.
216. Magnan A, Frachon I, Rain B, Peuchmaur M, Monti G, Lenot B, et al. Transforming growth factor beta in normal human lung: preferential location in bronchial epithelial cells. Thorax. 1994;49(8):789-92.
217. Kelley J, Kovacs EJ, Nicholson K, Fabisiak JP. Transforming growth factor-beta production by lung macrophages and fibroblasts. Chest. 1991;99(3 Suppl):85s-6s.
218. de Boer WI, van Schadewijk A, Sont JK, Sharma HS, Stolk J, Hiemstra PS, et al. Transforming growth factor beta1 and recruitment of macrophages and mast cells in airways in chronic obstructive pulmonary disease. Am J Respir Crit Care Med. 1998;158(6):1951-7.
219. Lee KY, Ho SC, Lin HC, Lin SM, Liu CY, Huang CD, et al. Neutrophil-derived elastase induces TGF-beta1 secretion in human airway smooth muscle via NF-kappaB pathway. Am J Respir Cell Mol Biol. 2006;35(4):407-14.
220. Flood-Page P, Menzies-Gow A, Phipps S, Ying S, Wangoo A, Ludwig MS, et al. Anti-IL-5 treatment reduces deposition of ECM proteins in the bronchial subepithelial basement membrane of mild atopic asthmatics. The Journal of clinical investigation. 2003;112(7):1029-36.
221. Cho JY, Miller M, Baek KJ, Han JW, Nayar J, Lee SY, et al. Inhibition of airway remodeling in IL-5-deficient mice. The Journal of clinical investigation. 2004;113(4):551-60.
222. Leivonen SK, Chantry A, Hakkinen L, Han J, Kahari VM. Smad3 mediates transforming growth factor-beta-induced collagenase-3 (matrix metalloproteinase-13) expression in human gingival fibroblasts. Evidence for cross-talk between Smad3 and p38 signaling pathways. J Biol Chem. 2002;277(48):46338-46.
223. Kenyon NJ, Ward RW, McGrew G, Last JA. TGF-beta1 causes airway fibrosis and increased collagen I and III mRNA in mice. Thorax. 2003;58(9):772-7.
224. Moir LM, Burgess JK, Black JL. Transforming growth factor beta 1 increases fibronectin deposition through integrin receptor alpha 5 beta 1 on human airway smooth muscle. J Allergy Clin Immunol. 2008;121(4):1034-9.e4.

225. Chen G, Khalil N. TGF-beta1 increases proliferation of airway smooth muscle cells by phosphorylation of map kinases. Respir Res. 2006;7:2.
226. Coutts A, Chen G, Stephens N, Hirst S, Douglas D, Eichholtz T, et al. Release of biologically active TGF-beta from airway smooth muscle cells induces autocrine synthesis of collagen. Am J Physiol Lung Cell Mol Physiol. 2001;280(5):L999-1008.
227. Frazier K, Williams S, Kothapalli D, Klapper H, Grotendorst GR. Stimulation of fibroblast cell growth, matrix production, and granulation tissue formation by connective tissue growth factor. J Invest Dermatol. 1996;107(3):404-11.
228. Xie S, Sukkar MB, Issa R, Oltmanns U, Nicholson AG, Chung KF. Regulation of TGF-beta 1-induced connective tissue growth factor expression in airway smooth muscle cells. Am J Physiol Lung Cell Mol Physiol. 2005;288(1):L68-76.
229. Burgess JK, Johnson PR, Ge Q, Au WW, Poniris MH, McParland BE, et al. Expression of connective tissue growth factor in asthmatic airway smooth muscle cells. Am J Respir Crit Care Med. 2003;167(1):71-7.
230. Johnson PR, Burgess JK, Ge Q, Poniris M, Boustany S, Twigg SM, et al. Connective tissue growth factor induces extracellular matrix in asthmatic airway smooth muscle. Am J Respir Crit Care Med. 2006;173(1):32-41.
231. Kobayashi T, Liu X, Wen FQ, Fang Q, Abe S, Wang XQ, et al. Smad3 mediates TGF-beta1 induction of VEGF production in lung fibroblasts. Biochem Biophys Res Commun. 2005;327(2):393-8.
232. Wen FQ, Liu X, Manda W, Terasaki Y, Kobayashi T, Abe S, et al. TH2 Cytokine-enhanced and TGF-beta-enhanced vascular endothelial growth factor production by cultured human airway smooth muscle cells is attenuated by IFN-gamma and corticosteroids. J Allergy Clin Immunol. 2003;111(6):1307-18.
233. Jenkins HA, Cool C, Szefler SJ, Covar R, Brugman S, Gelfand EW, et al. Histopathology of severe childhood asthma: a case series. Chest. 2003;124(1):32-41.
234. Naylor B. The shedding of the mucosa of the bronchial tree in asthma. Thorax. 1962;17:69-72.
235. Naveed S-u-n, Clements D, Jackson DJ, Philp C, Billington CK, Soomro I, et al. Matrix Metalloproteinase-1 Activation Contributes to Airway Smooth Muscle Growth and Asthma Severity. Am J Resp Crit Care. 2016;195(8):1000-9.
236. Slater M, Torr E, Harrison T, Forrester D, Knox A, Shaw D, et al. The differential effects of azithromycin on the airway epithelium in vitro and in vivo. Physiol Rep. 2016;4(18).
237. Abe M, Harpel JG, Metz CN, Nunes I, Loskutoff DJ, Rifkin DB. An assay for transforming growth factor-beta using cells transfected with a plasminogen activator inhibitor-1 promoter-luciferase construct. Anal Biochem. 1994;216(2):276-84.
238. Wettschureck N, Rütten H, Zywietz A, Gehring D, Wilkie TM, Chen J, et al. Absence of pressure overload induced myocardial hypertrophy after conditional inactivation of Gαq/Gα11 in cardiomyocytes. Nature Medicine. 2001;7(11):1236-40.

239. Weglarz L, Molin I, Orchel A, Parfiniewicz B, Dzierzewicz Z. Quantitative analysis of the level of p53 and p21(WAF1) mRNA in human colon cancer HT-29 cells treated with inositol hexaphosphate. Acta biochimica Polonica. 2006;53(2):349-56.
240. Bergeron C, Tulic MK, Hamid Q. Airway remodelling in asthma: from benchside to clinical practice. Can Respir J. 2010;17(4):e85-93.
241. Mendonça NT, Kenyon J, LaPrad AS, Syeda SN, O'Connor GT, Lutchen KR. Airway resistance at maximum inhalation as a marker of asthma and airway hyperresponsiveness. Respiratory Research. 2011;12(1):96.
242. Xie S, Sukkar MB, Issa R, Khorasani NM, Chung KF. Mechanisms of induction of airway smooth muscle hyperplasia by transforming growth factor-beta. American journal of physiology Lung cellular and molecular physiology. 2007;293(1):L245-L53.
243. Davies DE. The role of the epithelium in airway remodeling in asthma. ProcAmThoracic Soc. 2009;6(8):678-82.
244. Moir LM, Burgess JK, Black JL. Transforming growth factor beta 1 increases fibronectin deposition through integrin receptor alpha 5 beta 1 on human airway smooth muscle. J Allergy Clin Immunol. 2008;121(4):1034-9 e4.
245. Bartlett DW, Davis ME. Insights into the kinetics of siRNA-mediated gene silencing from live-cell and live-animal bioluminescent imaging. Nucleic acids research. 2006;34(1):322-33.
246. Karginov FV, Hannon GJ. The CRISPR system: small RNA-guided defense in bacteria and archaea. Mol Cell. 2010;37(1):7-19.
247. Marraffini LA, Sontheimer EJ. CRISPR interference: RNA-directed adaptive immunity in bacteria and archaea. Nat Rev Genet. 2010;11(3):181-90.
248. Hsu PD, Scott DA, Weinstein JA, Ran FA, Konermann S, Agarwala V, et al. DNA targeting specificity of RNA-guided Cas9 nucleases. Nature Biotechnology. 2013;31(9):827-32.
249. Thyme SB, Akhmetova L, Montague TG, Valen E, Schier AF. Internal guide RNA interactions interfere with Cas9-mediated cleavage. Nat Commun. 2016;7(1):11750.
250. Cockrell AS, Kafri T. Gene delivery by lentivirus vectors. Mol Biotechnol. 2007;36(3):184-204.
251. Kobiler O, Drayman N, Butin-Israeli V, Oppenheim A. Virus strategies for passing the nuclear envelope barrier. Nucleus. 2012;3(6):526-39.
252. Naldini L. Lentiviruses as gene transfer agents for delivery to non-dividing cells. Current opinion in biotechnology. 1998;9(5):457-63.
253. Kafri T, Blomer U, Peterson DA, Gage FH, Verma IM. Sustained expression of genes delivered directly into liver and muscle by lentiviral vectors. Nature genetics. 1997;17(3):314-7.
254. Nasri M, Karimi A, Allahbakhshian Farsani M. Production, purification and titration of a lentivirus-based vector for gene delivery purposes. Cytotechnology. 2014;66(6):1031-8.
255. Manceur AP, Kim H, Misic V, Andreev N, Dorion-Thibaudeau J, Lanthier S, et al. Scalable Lentiviral Vector Production Using Stable HEK293SF Producer Cell Lines. Hum Gene Ther Method. 2017;28(6):330-9.

256. Offermanns S, Zhao LP, Gohla A, Sarosi I, Simon MI, Wilkie TM. Embryonic cardiomyocyte hypoplasia and craniofacial defects in G alpha q/G alpha 11-mutant mice. Embo j. 1998;17(15):4304-12.
257. Geraerts M, Willems S, Baekelandt V, Debyser Z, Gijsbers R. Comparison of lentiviral vector titration methods. BMC Biotechnol. 2006;6:34-.
258. Jiang W, Hua R, Wei M, Li C, Qiu Z, Yang X, et al. An optimized method for high-titer lentivirus preparations without ultracentrifugation. Scientific Reports. 2015;5(1):13875.
259. Zhang B, Metharom P, Jullie H, Ellem KAO, Cleghorn G, West MJ, et al. The significance of controlled conditions in lentiviral vector titration and in the use of multiplicity of infection (MOI) for predicting gene transfer events. Genet Vaccines Ther. 2004;2(1):6-.
260. Lavnikova N, Lakhotia A, Patel N, Prokhorova S, Laskin DL. Cytostasis is required for IL-1 induced nitric oxide production in transformed hamster fibroblasts. J Cell Physiol. 1996;169(3):532-7.
261. Boussif O, Lezoualch F, Zanta MA, Mergny MD, Scherman D, Demeneix B, et al. A Versatile Vector for Gene and Oligonucleotide Transfer into Cells in Culture and in-Vivo - Polyethylenimine. P Natl Acad Sci USA. 1995;92(16):7297-301.
262. Longo PA, Kavran JM, Kim M-S, Leahy DJ. Transient mammalian cell transfection with polyethylenimine (PEI). Methods Enzymol. 2013;529:227-40.
263. Chuck AS, Clarke MF, Palsson BO. Retroviral infection is limited by Brownian motion. Human Gene Therapy. 1996;7(13):1527-34.
264. Chuck AS, Palsson BO. Consistent and high rates of gene transfer can be obtained using flow-through transduction over a wide range of retroviral titers. Human Gene Therapy. 1996;7(6):743-50.
265. Davis HE, Rosinski M, Morgan JR, Yarmush ML. Charged polymers modulate retrovirus transduction via membrane charge neutralization and virus aggregation. Biophys J. 2004;86(2):1234-42.
266. Davis HE, Morgan JR, Yarmush ML. Polybrene increases retrovirus gene transfer efficiency by enhancing receptor-independent virus adsorption on target cell membranes. Biophysical chemistry. 2002;97(2-3):159-72.
267. Segura MM, Kamen AA, Garnier A. Overview of current scalable methods for purification of viral vectors. Methods Mol Biol. 2011;737:89-116.
268. Van Campenhout C, Cabochette P, Veillard AC, Laczik M, Zelisko-Schmidt A, Sabatel C, et al. Guidelines for optimized gene knockout using CRISPR/Cas9. Biotechniques. 2019;66(6):295-302.
269. Alvarez-Curto E, Inoue A, Jenkins L, Raihan SZ, Prihandoko R, Tobin AB, et al. Targeted Elimination of G Proteins and Arrestins Defines Their Specific Contributions to Both Intensity and Duration of G Protein-coupled Receptor Signaling. The Journal of biological chemistry. 2016;291(53):27147-59.
270. Lin M-E, Herr DR, Chun J. Lysophosphatidic acid (LPA) receptors: signaling properties and disease relevance. Prostaglandins & other lipid mediators. 2010;91(3-4):130-8.

271. Ishii I, Fukushima N, Ye X, Chun J. Lysophospholipid receptors: signaling and biology. Annu Rev Biochem. 2004;73:321-54.
272. Georas SN, Berdyshev E, Hubbard W, Gorshkova IA, Usatyuk PV, Saatian B, et al. Lysophosphatidic acid is detectable in human bronchoalveolar lavage fluids at baseline and increased after segmental allergen challenge. Clin Exp Allergy. 2007;37(3):311-22.
273. He D, Natarajan V, Stern R, Gorshkova IA, Solway J, Spannhake EW, et al. Lysophosphatidic acid-induced transactivation of epidermal growth factor receptor regulates cyclo-oxygenase-2 expression and prostaglandin E(2) release via C/EBPbeta in human bronchial epithelial cells. Biochem J. 2008;412(1):153-62.
274. Cummings R, Zhao Y, Jacoby D, Spannhake EW, Ohba M, Garcia JG, et al. Protein kinase Cdelta mediates lysophosphatidic acid-induced NF-kappaB activation and interleukin-8 secretion in human bronchial epithelial cells. J Biol Chem. 2004;279(39):41085-94.
275. Knowlden SA, Hillman SE, Chapman TJ, Patil R, Miller DD, Tigyi G, et al. Novel Inhibitory Effect of a Lysophosphatidic Acid 2 Agonist on Allergen-Driven Airway Inflammation. Am J Resp Cell Mol. 2015;54(3):402-9.
276. Emo J, Meednu N, Chapman TJ, Rezaee F, Balys M, Randall T, et al. Lpa2 is a negative regulator of both dendritic cell activation and murine models of allergic lung inflammation. J Immunol. 2012;188(8):3784-90.
277. Yung YC, Stoddard NC, Chun J. LPA receptor signaling: pharmacology, physiology, and pathophysiology. J Lipid Res. 2014;55(7):1192-214.
278. Toews ML, Ustinova EE, Schultz HD. Lysophosphatidic acid enhances contractility of isolated airway smooth muscle. J Appl Physiol (1985). 1997;83(4):1216-22.
279. Hirshman CA, Emala CW. Actin reorganization in airway smooth muscle cells involves Gq and Gi-2 activation of Rho. Am J Physiol. 1999;277(3):L653-61.
280. Chrzanowska-Wodnicka M, Burridge K. Rho-stimulated contractility drives the formation of stress fibers and focal adhesions. J Cell Biol. 1996;133(6):1403-15.
281. Xu MY, Porte J, Knox AJ, Weinreb PH, Maher TM, Violette SM, et al. Lysophosphatidic acid induces alphavbeta6 integrin-mediated TGF-beta activation via the LPA2 receptor and the small G protein G alpha(q). Am J Pathol. 2009;174(4):1264-79.
282. Leung T, Manser E, Tan L, Lim L. A novel serine/threonine kinase binding the Ras-related RhoA GTPase which translocates the kinase to peripheral membranes. J Biol Chem. 1995;270(49):29051-4.
283. Riento K, Ridley AJ. ROCKs: multifunctional kinases in cell behaviour. Nature Reviews Molecular Cell Biology. 2003;4(6):446-56.
284. Maekawa M, Ishizaki T, Boku S, Watanabe N, Fujita A, Iwamatsu A, et al. Signaling from Rho to the actin cytoskeleton through protein kinases ROCK and LIM-kinase. Science. 1999;285(5429):895-8.
285. Khalil N. TGF-beta: from latent to active. Microbes and infection. 1999;1(15):1255-63.
286. Puthawala K, Hadjiangelis N, Jacoby SC, Bayongan E, Zhao ZC, Yang ZW, et al. Inhibition of integrin alpha v beta 6, an activator of latent

transforming growth factor-beta, prevents radiation-induced lung fibrosis. Am J Resp Crit Care. 2008;177(1):82-90.
287. John AE, Wilson MR, Habgood A, Porte J, Tatler AL, Stavrou A, et al. Loss of epithelial Gq and G11 signaling inhibits TGFbeta production but promotes IL-33-mediated macrophage polarization and emphysema. Sci Signal. 2016;9(451):ra104.
288. Takasaki J, Saito T, Taniguchi M, Kawasaki T, Moritani Y, Hayashi K, et al. A novel Galphaq/11-selective inhibitor. J Biol Chem. 2004;279(46):47438-45.
289. Htwe SS, Cha BH, Yue K, Khademhosseini A, Knox AJ, Ghaemmaghami AM. Role of Rho-Associated Coiled-Coil Forming Kinase Isoforms in Regulation of Stiffness-Induced Myofibroblast Differentiation in Lung Fibrosis. Am J Respir Cell Mol Biol. 2017;56(6):772-83.
290. Uehata M, Ishizaki T, Satoh H, Ono T, Kawahara T, Morishita T, et al. Calcium sensitization of smooth muscle mediated by a Rho-associated protein kinase in hypertension. Nature. 1997;389(6654):990-4.
291. Becky Kelly EA, Busse WW, Jarjour NN. A comparison of the airway response to segmental antigen bronchoprovocation in atopic asthma and allergic rhinitis. J Allergy Clin Immunol. 2003;111(1):79-86.
292. Nalli AD, Wang H, Bhattacharya S, Blakeney BA, Murthy KS. Inhibition of RhoA/Rho kinase pathway and smooth muscle contraction by hydrogen sulfide. Pharmacol Res Perspect. 2017;5(5).
293. Zhang W, Huang Y, Gunst SJ. The small GTPase RhoA regulates the contraction of smooth muscle tissues by catalyzing the assembly of cytoskeletal signaling complexes at membrane adhesion sites. The Journal of biological chemistry. 2012;287(41):33996-4008.
294. Kureishi Y, Kobayashi S, Amano M, Kimura K, Kanaide H, Nakano T, et al. Rho-associated kinase directly induces smooth muscle contraction through myosin light chain phosphorylation. J Biol Chem. 1997;272(19):12257-60.
295. He WC, Tan RY, Dai CS, Li YJ, Wang D, Hao S, et al. Plasminogen Activator Inhibitor-1 Is a Transcriptional Target of the Canonical Pathway of Wnt/beta-Catenin Signaling. J Biol Chem. 2010;285(32):24665-75.
296. Krumins AM, Gilman AG. Targeted Knockdown of G Protein Subunits Selectively Prevents Receptor-mediated Modulation of Effectors and Reveals Complex Changes in Non-targeted Signaling Proteins. J Biol Chem. 2006;281(15):10250-62.
297. Matsui T, Amano M, Yamamoto T, Chihara K, Nakafuku M, Ito M, et al. Rho-associated kinase, a novel serine/threonine kinase, as a putative target for small GTP binding protein Rho. Embo j. 1996;15(9):2208-16.
298. Araki S, Ito M, Kureishi Y, Feng J, Machida H, Isaka N, et al. Arachidonic acid-induced Ca2+ sensitization of smooth muscle contraction through activation of Rho-kinase. Pflugers Archiv : European journal of physiology. 2001;441(5):596-603.
299. Pinner S, Sahai E. PDK1 regulates cancer cell motility by antagonising inhibition of ROCK1 by RhoE. Nat Cell Biol. 2008;10(2):127-37.
300. Chikumi H, Vazquez-Prado J, Servitja JM, Miyazaki H, Gutkind JS. Potent activation of RhoA by G alpha(q) and G(q)-coupled receptors. J Biol Chem. 2002;277(30):27130-4.

301. Siehler S. Regulation of RhoGEF proteins by G12/13-coupled receptors. Brit J Pharmacol. 2009;158(1):41-9.
302. Bian D, Mahanivong C, Yu J, Frisch SM, Pan ZK, Ye RD, et al. The G12/13-RhoA signaling pathway contributes to efficient lysophosphatidic acid-stimulated cell migration. Oncogene. 2006;25(15):2234-44.
303. Fukuhara S, Chikumi H, Gutkind JS. RGS-containing RhoGEFs: the missing link between transforming G proteins and Rho? Oncogene. 2001;20(13):1661-8.
304. Zhong H, Wade SM, Woolf PJ, Linderman JJ, Traynor JR, Neubig RR. A spatial focusing model for G protein signals. Regulator of G protein signaling (RGS) protien-mediated kinetic scaffolding. J Biol Chem. 2003;278(9):7278-84.
305. Lee CH, Park D, Wu D, Rhee SG, Simon MI. Members of the Gq alpha subunit gene family activate phospholipase C beta isozymes. J Biol Chem. 1992;267(23):16044-7.
306. Momotani K, Somlyo AV. p63RhoGEF: a new switch for G(q)-mediated activation of smooth muscle. Trends Cardiovasc Med. 2012;22(5):122-7.
307. Takashima S, Sugimoto N, Takuwa N, Okamoto Y, Yoshioka K, Takamura M, et al. G12/13 and Gq mediate S1P2-induced inhibition of Rac and migration in vascular smooth muscle in a manner dependent on Rho but not Rho kinase. Cardiovasc Res. 2008;79(4):689-97.
308. Kozasa T, Jiang X, Hart MJ, Sternweis PM, Singer WD, Gilman AG, et al. p115 RhoGEF, a GTPase Activating Protein for Gα₁₂ and Gα₁₃. Science. 1998;280(5372):2109-11.
309. Ruwhof C, van Wamel AET, Egas JM, van der Laarse A. Cyclic stretch induces the release of growth promoting factors from cultured neonatal cardiomyocytes and cardiac fibroblasts. Mol Cell Biochem. 2000;208(1):89-98.
310. Sakata R, Ueno T, Nakamura T, Ueno H, Sata M. Mechanical stretch induces TGF-beta synthesis in hepatic stellate cells. European journal of clinical investigation. 2004;34(2):129-36.
311. Joki N, Kaname S, Hirakata M, Hori Y, Yamaguchi T, Fujita T, et al. Tyrosine-kinase dependent TGF-beta and extracellular matrix expression by mechanical stretch in vascular smooth muscle cells. Hypertens Res. 2000;23(2):91-9.
312. Froese AR, Shimbori C, Bellaye PS, Inman M, Obex S, Fatima S, et al. Stretch-induced Activation of Transforming Growth Factor-beta1 in Pulmonary Fibrosis. Am J Respir Crit Care Med. 2016;194(1):84-96.
313. van Wamel AJ, Ruwhof C, van der Valk-Kokshoom LE, Schrier PI, van der Laarse A. The role of angiotensin II, endothelin-1 and transforming growth factor-beta as autocrine/paracrine mediators of stretch-induced cardiomyocyte hypertrophy. Mol Cell Biochem. 2001;218(1-2):113-24.
314. Forrester SJ, Booz GW, Sigmund CD, Coffman TM, Kawai T, Rizzo V, et al. Angiotensin II Signal Transduction: An Update on Mechanisms of Physiology and Pathophysiology. Physiological reviews. 2018;98(3):1627-738.
315. Nishida M, Sato Y, Uemura A, Narita Y, Tozaki-Saitoh H, Nakaya M, et al. P2Y6 receptor-Galpha12/13 signalling in cardiomyocytes triggers pressure overload-induced cardiac fibrosis. Embo j. 2008;27(23):3104-15.

316. Vetter TR. Fundamentals of Research Data and Variables: The Devil Is in the Details. Anesthesia and analgesia. 2017;125(4):1375-80.
317. Swartz MA, Tschumperlin DJ, Kamm RD, Drazen JM. Mechanical stress is communicated between different cell types to elicit matrix remodeling. Proceedings of the National Academy of Sciences. 2001;98(11):6180-5.
318. Hughes JM, Hoppin FG, Jr., Mead J. Effect of lung inflation on bronchial length and diameter in excised lungs. J Appl Physiol. 1972;32(1):25-35.
319. Pitcher JA, Inglese J, Higgins JB, Arriza JL, Casey PJ, Kim C, et al. Role of beta gamma subunits of G proteins in targeting the beta-adrenergic receptor kinase to membrane-bound receptors. Science. 1992;257(5074):1264-7.
320. Wilkie TM, Scherle PA, Strathmann MP, Slepak VZ, Simon MI. Characterization of G-protein alpha subunits in the Gq class: expression in murine tissues and in stromal and hematopoietic cell lines. Proc Natl Acad Sci U S A. 1991;88(22):10049-53.
321. Ho MK, Yung LY, Chan JS, Chan JH, Wong CS, Wong YH. Galpha(14) links a variety of G(i)- and G(s)-coupled receptors to the stimulation of phospholipase C. Brit J Pharmacol. 2001;132(7):1431-40.
322. Hasaneen NA, Zucker S, Cao J, Chiarelli C, Panettieri RA, Foda HD. Cyclic mechanical strain-induced proliferation and migration of human airway smooth muscle cells: role of EMMPRIN and MMPs. The FASEB Journal. 2005;19(11):1507-9.
323. Takahara N, Ito S, Furuya K, Naruse K, Aso H, Kondo M, et al. Real-Time Imaging of ATP Release Induced by Mechanical Stretch in Human Airway Smooth Muscle Cells. Am J Resp Cell Mol. 2014;51(6):772-82.
324. Damera G, Panettieri RA, Jr. Does airway smooth muscle express an inflammatory phenotype in asthma? Brit J Pharmacol. 2011;163(1):68-80.
325. Iizuka K, Yoshii A, Samizo K, Tsukagoshi H, Ishizuka T, Dobashi K, et al. A major role for the rho-associated coiled coil forming protein kinase in G-protein-mediated Ca2+ sensitization through inhibition of myosin phosphatase in rabbit trachea. Br J Pharmacol. 1999;128(4):925-33.
326. Kume H, Takeda N, Oguma T, Ito S, Kondo M, Ito Y, et al. Sphingosine 1-phosphate causes airway hyper-reactivity by rho-mediated myosin phosphatase inactivation. J Pharmacol Exp Ther. 2007;320(2):766-73.
327. Pellegrin S, Mellor H. Actin stress fibres. Journal of Cell Science. 2007;120(20):3491-9.
328. Cramer LP, Siebert M, Mitchison TJ. Identification of Novel Graded Polarity Actin Filament Bundles in Locomoting Heart Fibroblasts: Implications for the Generation of Motile Force. J Cell Biol. 1997;136(6):1287-305.
329. Sah VP, Seasholtz TM, Sagi SA, Brown JH. The Role of Rho in G Protein-Coupled Receptor Signal Transduction. Annual Review of Pharmacology and Toxicology. 2000;40(1):459-89.
330. Klages B, Brandt U, Simon MI, Schultz G, Offermanns S. Activation of G12/G13 Results in Shape Change and Rho/Rho-Kinase–mediated Myosin Light Chain Phosphorylation in Mouse Platelets. J Cell Biol. 1999;144(4):745-54.

331. Gohla A, Offermanns S, Wilkie TM, Schultz G. Differential involvement of Galpha12 and Galpha13 in receptor-mediated stress fiber formation. J Biol Chem. 1999;274(25):17901-7.
332. Hirshman CA, Emala CW. Actin reorganization in airway smooth muscle cells involves Gq and Gi-2 activation of Rho. Am J Physiol-Lung C. 1999;277(3):L653-L61.
333. Guilluy C, Swaminathan V, Garcia-Mata R, Timothy O'Brien E, Superfine R, Burridge K. The Rho GEFs LARG and GEF-H1 regulate the mechanical response to force on integrins. Nature Cell Biology. 2011;13(6):722-7.
334. Gong MC, Fuglsang A, Alessi D, Kobayashi S, Cohen P, Somlyo AV, et al. Arachidonic acid inhibits myosin light chain phosphatase and sensitizes smooth muscle to calcium. J Biol Chem. 1992;267(30):21492-8.
335. D'Aquilio F, Procaccini M, Izzi V, Chiurchiu' V, Giambra V, Carotenuto F, et al. Activatory Properties of Lysophosphatidic Acid on Human THP-1 Cells. Inflammation. 2007;30(5):167-77.
336. Bhola NE, Freilino ML, Joyce SC, Sen M, Thomas SM, Sahu A, et al. Antitumor mechanisms of targeting the PDK1 pathway in head and neck cancer. Mol Cancer Ther. 2012;11(6):1236-46.
337. Jin J, Mao Y, Thomas D, Kim S, Daniel JL, Kunapuli SP. RhoA downstream of G(q) and G(12/13) pathways regulates protease-activated receptor-mediated dense granule release in platelets. Biochemical pharmacology. 2009;77(5):835-44.
338. Yoneda A, Multhaupt HAB, Couchman JR. The Rho kinases I and II regulate different aspects of myosin II activity. The Journal of cell biology. 2005;170(3):443-53.
339. Wang Y, Zheng XR, Riddick N, Bryden M, Baur W, Zhang X, et al. ROCK isoform regulation of myosin phosphatase and contractility in vascular smooth muscle cells. Circulation research. 2009;104(4):531-40.
340. Mangmool S, Kurose H. G(i/o) protein-dependent and -independent actions of Pertussis Toxin (PTX). Toxins (Basel). 2011;3(7):884-99.
341. Kobayashi T, Kim H, Liu X, Sugiura H, Kohyama T, Fang Q, et al. Matrix metalloproteinase-9 activates TGF-β and stimulates fibroblast contraction of collagen gels. American journal of physiology Lung cellular and molecular physiology. 2014;306(11):L1006-L15.
342. Numaguchi K, Eguchi S, Yamakawa T, Motley ED, Inagami T. Mechanotransduction of rat aortic vascular smooth muscle cells requires RhoA and intact actin filaments. Circ Res. 1999;85(1):5-11.
343. Ito S, Kume H, Oguma T, Ito Y, Kondo M, Shimokata K, et al. Roles of stretch-activated cation channel and Rho-kinase in the spontaneous contraction of airway smooth muscle. Eur J Pharmacol. 2006;552(1):135-42.
344. Kaunas R, Nguyen P, Usami S, Chien S. Cooperative effects of Rho and mechanical stretch on stress fiber organization. P Natl Acad Sci USA. 2005;102(44):15895-900.
345. Galbraith CG, Yamada KM, Sheetz MP. The relationship between force and focal complex development. J Cell Biol. 2002;159(4):695-705.